An Investigation into the Mechanism by which Cholesterol Induces Interleukin-1 Secretion from the Vascular Endothelium

Author: Dr Majid Almansouri

Supervised by: Professor Sheila Francis & Dr Janet Chamberlain

A thesis submitted in partial fulfilment of the requirements for the degree of Doctor of Philosophy.

The Department of Infection Immunity & Cardiovascular Disease

The Faculty of Medicine and Dentistry

The University of Sheffield

Acknowledgments

Author's Declaration

I declare that solely I have composed this thesis and that it has not been submitted in whole or in part, in any previous submission for any other degree. Except where it is stated otherwise by reference, the work presented is entirely my own.

List of Contents

5

List of Figures:

Table of Abbreviations:

ABCG1: ATP-binding cassette G1	MI Myocardial infarction
ACAT Acetyl coenzyme A acyltransferase	MMP Matrix metalloproteinase
Acyl-CoA Acetyl coenzyme A AcLDL Acetylated Low Density Lipoprotien	NALP3 NACHT, LRR and PYD domains-containing protein 3
ACS Acute coronary syndrome	NE Neutrophil elastase
ApoE Apolipoprotein E	NF-κB Nuclear factor-kappa B
CHD Coronary heart disease	NLRP3 Nucleotide-binding domain leucine-rich repeat containing (NLR) family pyrin domain containing 3
CRP C-reactive protein	OxLDL Oxidised low density lipoprotein
CTB Cholera toxin subunit	PBMC Peripheral blood mononuclear cells
EDTA Ethylenediaminetetraacetic acid	ROS Reactive oxygen species

ELISA Enzyme-linked immunosorbent assay	GSDMD Gasdermin D
HCAECs Human coronary artery endothelial cells	SMC Smooth muscle cells
HUVECs Human umbilical vein endothelial cells	TCFA Thin cap fibroatheroma
HMG-CoA 3-hydroxy-3-methyl-glutaryl-coenzyme A	TNF Tumour necrosis factor
HVSMs Human vascular smooth muscle cells	TNF-α Tumour necrosis factor alpha
ICAM-1 Intracellular adhesion molecule 1	VCAM-1 Vascular cell adhesion molecule 1
IHD Ischaemic Heart Disease	VEGF Vascular endothelial growth factor
IL-1 Interleukin 1	WGA Wheat Germ Agglutinin
IL-1R1 Interleukin-1 receptor type I	IL-1R1 Interleukin-1 receptor type I
IL-1ra Interleukin-1 receptor antagonist	IL-1ra Interleukin-1 receptor antagonist
IL-6 Interleukin 6	IL-6 Interleukin 6

IL-1β Interleukin 1 beta	CCTA Coronary computed tomography angiography
IL-1α Interleukin 1 alpha	
IPP Isopentenylpyrophosphate	
LDL Low density lipoprotein	
LDL-C Low density lipoprotein cholesterol	
LPS Lipopolysaccharide	
MβCD Methyl-β-cyclodextrin	
MCP-1 Monocyte chemoattractant protein 1	

Abstract

Background: Atherosclerosis is a chronic vascular inflammatory disease characterised by disturbed blood flow due to an atheromatous plaque build-up within arterial layers. These plaques contain various forms of modified cholesterol, such as oxidised low-density lipoprotein (OxLDL). OxLDL enters vascular cells, contributing towards foam cell formation and initiating over exuberant repair processes, leading to arterial occlusion and life threatening myocardial infarction or stroke. Endothelial cells, by producing pro-inflammatory cytokines, such as interleukin-1 beta (IL-1β), are also strongly involved in the pathogenesis of atherosclerosis. However, little is known of the link between OxLDL and endothelial cell actions. Hypothesis: I hypothesised that OxLDL enters the arterial endothelium and induces IL-1β secretion, potentially via a caspase-1/NLRP3 mechanism. **Methods:** Human coronary artery endothelial cells (HCAEC), isolated from different donors, were cultured and stimulated with pro-inflammatory cytokines TNFα and IL-1α (10 ng/ml each, for 48 hours), followed by incubation with native human OxLDL cholesterol at multiple concentrations (10-200 ug/ml) for 6 hours. Inhibitors of Caspase-1 (YVAD), NLRP3 (MCC950) and P2X7 receptor (A438079 HCl) were also used. Cell lysates and culture supernatants were collected and analysed for IL-1β using ELISA and Western Blot. Cell viability and caspase-1 activity were also measured. **Results:** Brightfield microscopy imaging showed OxLDL enters HCAECs, and forms particles. However,

uptake of OxLDL was not seen following inhibition of the P2X7 receptor. OxLDL induced the release of IL-1β from stimulated HCAECs with maximum release at concentration of 50 ug/ml compared to control. This release was not caused by toxicity of the OxLDL: cell viability was confirmed by lactate dehydrogenase cell viability assay. Inhibition of either NLRP3 or Caspase-1 significantly reduced the release of extracellular IL-1β (4-fold, $p<0.0001$; 14-fold, $p<0.0001$, respectively). Release of IL-1β was associated with expression of active GSDMD, suggesting the release via a pyroptosis mechanism. **Conclusion:** HCAEC uptake of OxLDL occurs via the P2X7 receptor. OxLDL elicits IL-1β release in activated HCAECs by a Caspase-1/NLRP3 mechanism, without causing toxicity. The released IL-1β probably exits the cells via a GSDMD-induced membrane pore. These data show that the study of modified lipids linked to the release of inflammatory cytokines such as IL-1 from endothelial cells could lead to the discovery and development of a useful strategy for the prevention/reduction of atherosclerosis.

(Chapter 1) Introduction

1.1 What is Atherosclerosis and Why Study it?

In 1755, the Latin term "atheroma" was used, for the first time, to describe deposited plaque on the innermost layer of arterial walls by Albrecht von Halles (Li and Fang, 2004, DUFF, 1951). However, since the development of atheroma was reported to be accompanied with abnormal arterial wall hardening "sclerosis", in 1940, Félix Marchand devised the term "atherosclerosis" (Benditt, 1977).

Atherosclerosis is a chronic inflammatory lipoprotein-driven disease, that develops in the inner layer of arteries as a result of the pathological production of a lipid heavy plaque contained within a fibrous cap known as an "atheroma" (Adams et al., 2000). The pathological development of atherosclerosis takes decades to occur (stages shown in Figure 1.1), and is diagnosed clinically as a life-threatening condition underlying the cause of many acute coronary syndromes (ACS) including myocardial infarction (MI), ischemic heart disease (IHD), ischemic stroke and coronary heart disease (CHD) (Libby, 2013, Nabel and Braunwald, 2012). CHD is considered the leading cause of death worldwide, with reduced coronary blood flow at atherosclerotic lesion sites being the causative agent in 90% of CHD cases (Herrington et al., 2016, Lung et al., 2014).

Risk factors for developing atherosclerosis include ageing and smoking, in addition to a medical history of diabetes mellitus, hypertension and hyperlipidaemia, all of which play a role in causing inflammation and vascular injury to the endothelial layer of the arterial wall (Messner and Bernhard, 2014, van Rooy and Pretorius, 2014).

19
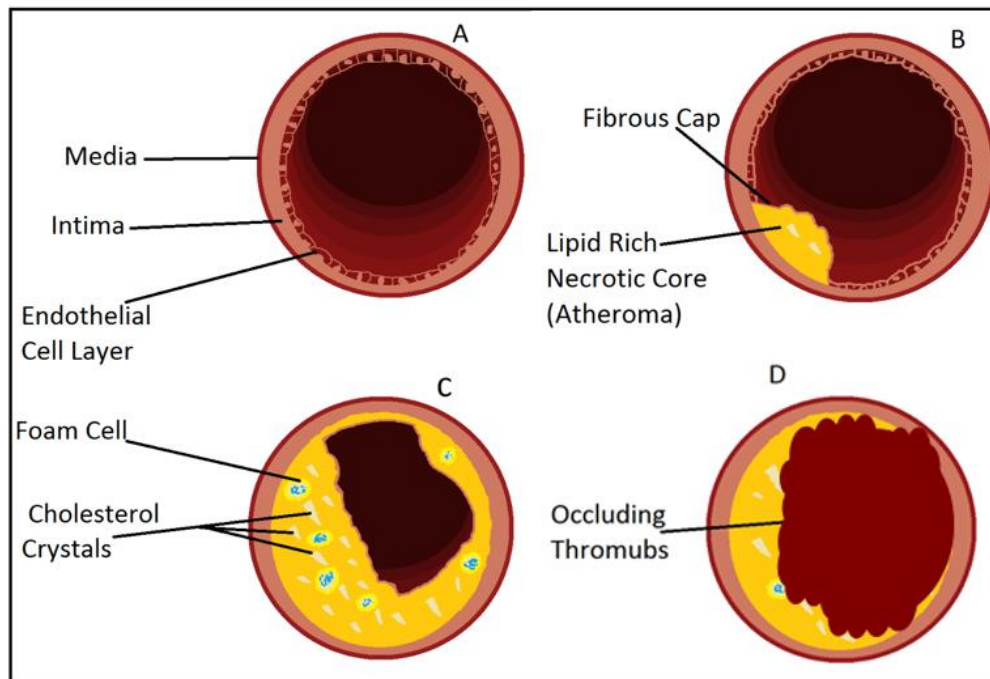
(Figure 1.1) Development of an Atherosclerotic Plaque and Progression into a Lesion: (A) Healthy artery, free from any plaque accumulation or development on its endothelial cell layer, compared to a developed atheroma surrounded by a fibrous cap (B). This necrotic core is composed of apoptotic smooth muscle cells (SMC) and is rich in lipids which contain foam cells and cholesterol crystals. The collagen released from smooth muscle cells forms the fibrous cap. In the late stage of an atheroma, more atheromatous plaque has been deposited (C), surrounding the majority of the vessel lumen, allowing a limited amount of blood to pass through i.e. decreased blood flow. The plaque protrudes through the surrounding fibrous cap, causing a plaque rupture. Plaque rupture can be seen in cardiac patients of MI and ACS and is composed of necrotic tissue that in many cases can form a large thrombus that may occlude the vessel (D), causing a cerebrovascular stroke.

Studies have concluded that hyperlipidaemia causes both inflammation and endothelial dysfunction, which are the major events in developing atherosclerosis (Ross, 1999b, Shimokawa, 1999, Morton et al., 2015). Investigating the disease pathways and the inflammatory markers involved, as well as identifying the molecules and mechanisms that cause vascular injury relevant to atherosclerosis development, will help enhance and improve the current therapeutic agents and drugs used to treat the disease. However, despite the advances and the clinical effectiveness of hypolipidemic agents as treatment and prevention agents for CVDs [statins (simvastatin and lovastatin) (Yebyo et al., 2019), cholesterol absorption inhibitors (Ezetimibe) (Bach et al., 2019), PCSK9 inhibitors (Evolocumab and Alirocomab) (Tomkin and Owens, 2017), nicotinic acid (Romani et al., 2019), fibric acids (Gemfibrozil and Bezafibrate) (Millan et al., 2018) and omega-3 fatty acids (Abdelhamid et al., 2018)], CVDs are still the global leading cause of death with an uncontrolled, increasing, prevalence in the developing world (Thirunavukkarasu and Khader, 2019, Mc Namara et al., 2019).

This continued, increasing, prevalence has triggered a renewed interest in studying and investigating the inflammatory processes associated with the early development of atherosclerosis and CVD. Recently, a growing number of studies were dedicated to investigating the major inflammatory markers, in particular, interleukin-1 (IL-1) and its production and release from vascular cells involved in the disease process, which is the goal of this project.

1.2 Pathophysiology of Atherosclerosis

The process of atheroma development, referred to as "atherogenesis", is a complicated process involving the interaction and signalling between different molecules and often takes years to develop (Steffen et al., 2015). Clinically, it has always been a challenge to investigate and diagnose patients at an early stage before the appearance of symptoms (Wierzbicki, 2013). Initially, it is thought that the innermost endothelial layer of the artery wall becomes injured due to contact with blood circulation with a stream of laminar and turbulent physical force applied to the surface (Ross and Agius, 1992). However, some regions along the vascular tree, called sites of predilection, are known to be more prone to atherosclerosis development than others (Gu et al., 1998). These regions are exposed to different haemodynamic stress conditions which experience alterations in shear stress with a reverse cyclical direction of flow known as oscillatory flow (Malek et al., 1999).

There is a well-established understanding that oscillatory flow promotes endothelial dysfunction, inflammation, and leukocyte adhesion and migration, primarily by increasing the expression of adhesion molecules such as intracellular adhesion molecule-1 (ICAM-1) and vascular adhesion molecule-1 (VCAM-1), which contribute towards leukocyte recruitment, creating an atherogenic inflammatory environment (Chappell et al., 1998). Additionally, areas with high shear stress that can be found in major curves, such as the aortic arch and areas near branch points, are more prone to develop an atherosclerotic lesion (Wara et al., 2008, Garcia-Herrera and

Celentano, 2013). However, in the presence of hyperlipidaemia, the disturbed blood flow in these regions causes endothelial dysfunction (Xu, 2000, Foteinos et al., 2008). This injury of the endothelial cell layer, together with the subendothelial precipitation of low-density lipoprotein cholesterol (LDL-C), are considered the first alterations of the vasculature (shown in Figure 1.2A) (Palinski et al., 1989). A complex process then starts as lymphocytes and monocytes adhere to the endothelial surface of the artery wall (Figure 1.2B), involving adhesion molecules and their receptors (predominantly ICAM-1 and VCAM-1), which further enable leukocytes to invade into blood vessels (Jang et al., 1994, Kirii et al., 2003).
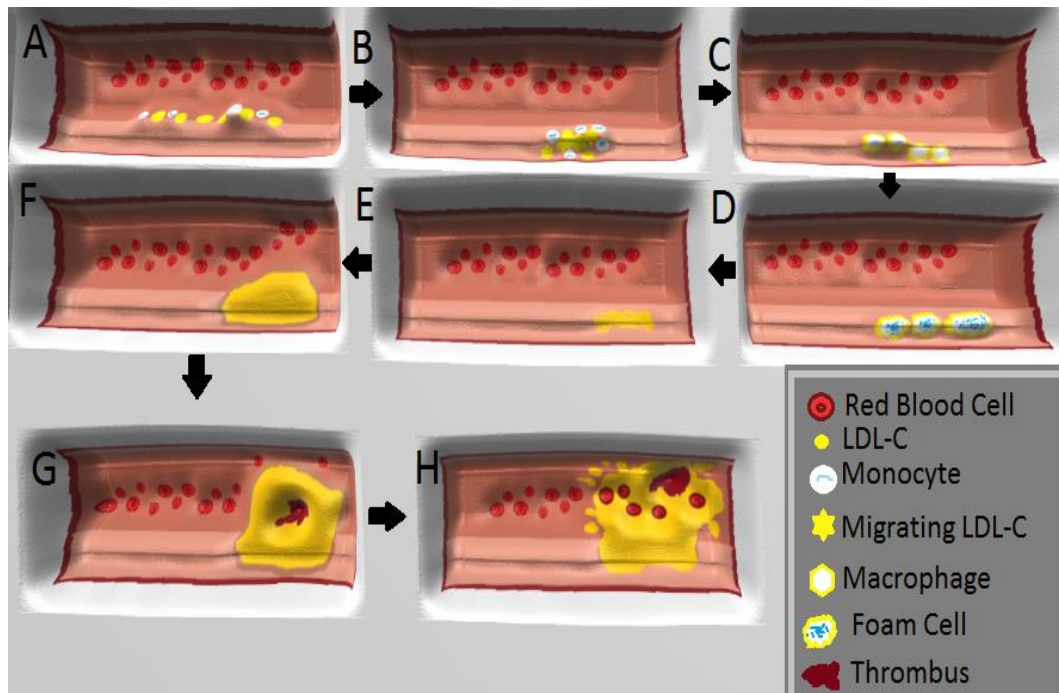
(Figure 1.2) Transverse 3D Illustration of the Pathophysiology of Atherosclerosis within an Artery During Different Stages of Lesion Development: (A) Molecules of LDL-C start to precipitate along the dysfunctional endothelial layer of the vessel. (B) Monocytes adhere together along the endothelial layer, and start migrating through the endothelial layer into the subendothelial layer and differentiate into macrophages (C). Due to the dysfunctional endothelium more circulating cholesterol molecules and lipoproteins can enter the subendothelial space where they can be digested by the newly differentiated macrophages. As a result of this digestion they are transformed into foam cells (D), which become fatty streaks along the vessel wall (E) that start to build up together and form an immature atheroma. Continuous precipitation of lipoprotein molecules and its digestion by macrophages increases the amount of plaque built up which increases the size of the atheroma (F). When a mature atheroma is formed (G) it is more vulnerable to rupture. Plaque rupture (H) allows the plaque to forcefully exit the fibrous cap and diffuse into the blood stream, where severe cardiovascular and cerebrovascular complications may occur.

The role of ICAM-1 is evidenced by the fact that low concentrations are found in endothelial cells and leukocyte membranes, with increased concentrations upon cytokine stimulation. Interleukin-1 (IL-1) and tumour necrosis factor alpha (TNF-α), expressed by macrophages, lymphocytes and vascular endothelium, both induce ICAM-1 expression (Kim et al., 2008).

VCAM-1 is known to mediate adhesion of monocytes and lymphocytes to the vascular endothelium. In addition, its upregulation by cytokines is induced by IL-1 and TNF-α, and regulation of both pro-inflammatory cytokines is via the transcription factor known as nuclear factor kappa-light-chain-enhancer of activated B cells (NF-κB) (Kim et al., 2001). NF-κB, a pivotal mediator for adaptive and innate immunity, is known to induce the expression of many genes that encode inflammatory molecules, which play key roles in the pathological development and maintenance of an atherosclerotic lesion. These inflammatory molecules include: cytokines (IL-1, IL-2, IL-6, IL-8 and TNF-α)(Sun et al., 2013, Hayden and Ghosh, 2011), chemokines (MCP-1 and IL-18)(Liu et al., 2017), adhesion molecules (ICAM-1, VCAM-1 and matrix metalloproteinases (MMPs)) (Kim et al., 2008, Tak and Firestein, 2001), and participate in inflammasome regulation including the NLRP3 inflammasome (Bauernfeind et al., 2009).

Furthermore, monocytes are known to migrate into the subendothelial intimal space, with the aid of chemoattractant molecules such as monocyte chemoattractant protein-1 (MCP-1) (Gu et al., 1998), which attracts both leukocytes and cytokines to the site of inflammation (Kirii et al., 2003). After

their migration, monocytes differentiate into macrophages (Ross, 1993) (Figure 1.2C). This differentiation is associated with increased expression of the antigen CD68 (which is mainly found on lysosomes of macrophages), with the main regulator of this process being macrophage colony stimulating factor (M-CSF) ((Clinton et al., 1992, Smith et al., 1995)).

Additionally, the dysfunctional endothelium allows the continued entry of an excess of circulating lipoprotein and cholesterol molecules (Davignon and Ganz, 2004), including cholesterol crystals that have crystalized from a liquid form, which pierce the intimal layer and the plaque, making it more vulnerable to plaque rupture (Abela, 2010). Some of the LDL-C molecules undergo oxidized modification and become inflammatory molecules due to oxidation enzymes and free radicals such as reactive nitrogen species (RNS) and reactive oxygen species (ROS) (Singh et al., 2015).

Studies report that these radicals are generated *in vivo*, mainly in vascular cells, by different endogenous systems secondary to the human body's exposure to pathological conditions (such as diabetes mellitus (Giacco and Brownlee, 2010) and hyperlipidaemia (Onody et al., 2003)) and physiochemical conditions (such as smoking (Dikalov et al., 2019) and exposure to ionizing radiation (Bucci et al., 2006, Baselet et al., 2019)). ROS-induced oxidative stress occurs when the equilibrium between generation of ROS and the ability to initiate antioxidant responses (mainly mitochondrial antioxidants, specifically mitochondrial targeted vitamin E) is disrupted, which has the ability to alter proteins, DNA and lipids (Singh et al.,

2015). ROS-induced oxidative stress exerted on modified LDL-C molecules in the intima, results in the formation of oxidized LDL (OxLDL) (Leonarduzzi et al., 2012) a major contributor to atherosclerosis development and key player in my study. Furthermore, oscillatory shear stress induces an increased production of ROS in endothelial cells, and LDL molecules are generally only oxidised in cells containing excess ROS (Cunningham and Gotlieb, 2005, Hwang et al., 2003).

These modified LDLs are prone to be ingested by macrophages, as their scavenger receptors are expressed by macrophages, e.g. the LOX-1 scavenger receptor (Qiao et al., 1997, Dai et al., 2013) allowing their transformation to foam cells (Figure 1.2D), which eventually contribute to fatty streaks in the arterial wall (Figure 1.2E) with the aid of T lymphocytes (Abela, 2010, Bobryshev, 2006). The continued insult to smooth muscle cells and the endothelium of artery walls triggers intense fibro-proliferative inflammatory responses that act together to develop an atheroma, through continued build-up of fatty streaks, lipoprotein molecules and cholesterol crystals (Figure 1.2F). Continued build-up and increased expression of regulatory molecules enhances the destabilisation of the plaque and increases the size of the atheroma making it vulnerable to rupture (Figure 1.2G).

1.2.1 Plaque rupture, erosion and the role of cholesterol crystals

There a is well-established understanding that plaque rupture is a life threatening clinical event (Shah and Lecis, 2019, Friedman, 1975). It exposes the blood circulation with high platelets to areas of the vessel wall that are

27

rich in necrotic core material (Figure 1.2H), leading to coronary thrombosis (Miller, 2016). There are two contrasting mechanisms allowing the release of this thrombogenic material. Often, a thin cap fibroatheroma (TCFA) is formed, allowing direct rupture of the cap and subsequent release of the plaque constituents (Vengrenyuk et al., 2006). Alternatively, plaque erosion can occur, permitting thrombi formation on lesion surfaces without complete plaque rupture (Spagnoli et al., 2007). Both plaque rupture and erosion are considered to be the two leading causes for ACS (Abela and Aziz, 2005) (Thondapu et al., 2020). Furthermore, sudden coronary death, the most abrupt clinical form of reported ACS, has been shown by coronary computed tomography angiography (CCTA) to have the presence of luminal thrombosis in the form of plaque rupture or plaque erosion which is a hallmark of sudden coronary death cases (van den Hoogen et al., 2019).

There is distinct fundamental difference between rupture and erosion of plaque (Farb et al., 1996). Plaque rupture takes place in a "vulnerable plaque". A classical rupture-vulnerable plaque is composed of a large lipid core, which is filled with macrophages that engulf modified LDL particles and became foam cells, or dead macrophages that result in debris accumulation (Ouweneel et al., 2019, Virmani et al., 2006). The surrounding extracellular matrix molecules (mainly interstitial collagen) creates the TCFA, which encapsulates this lipid core and its contents (Libby and Aikawa, 2002).

Conversely, plaque erosion classically occurs in a plaque that is lipid-poor and has little macrophage-foam cell accumulation, but is rich in matrix

(Libby, 2015, Libby et al., 2019, Pasterkamp et al., 2017). Furthermore, fibrinous clots, which complicate plaque rupture, have fewer platelets when compared with the platelet-rich thrombi that complicate erosion (Libby et al., 2019, Quillard et al., 2017, Badimon et al., 2012).

Although many molecular mechanisms of plaque rupture have been described (Bentzon et al., 2014), a few recent studies have highlighted the potential role of cholesterol crystals in causing physical plaque rupture as the crystalized shape can make it easy for these to pierce through the intima and the fibrous cap, causing a plaque explosion (Abela, 2010). Abela demonstrated that atherosclerotic plaques of patients who died from ACS, have cholesterol crystals perforating the cap and the surface of the intima. This supports previous work that showed that the process of cholesterol crystallization from liquid forms (which are also present within the arterial walls (Lundberg, 1985)), to solid crystals, increases cholesterol volume in the vessel wall and that this crystallization process is the trigger for atherosclerotic lesion core expansion (Abela and Aziz, 2006). This results in more pressure directed towards the fibrous cap, which can lead to overlying intima and plaque cap disruption leading to a thrombosis that blocks the artery (Dai et al., 2016).

Several lipid-lowering agents (such as aspirin, ethanol and statins) have also been shown to have an effect on dissolving cholesterol crystals, suggesting that this mechanism may be how these agents exert their immediate effects,

however the exact mechanism is not fully understood (Bentzon et al., 2014, Dai et al., 2016, Abela, 2010).

1.3 The role of Inflammation in Atherosclerosis

Until relatively recently (1990s), there was a long-established understanding that the occurrence of atherosclerosis was primarily due to a metabolic disorder rather than an inflammatory condition, and many studies hypothesised it as no more than a monotonous lipid storage disorder and accumulation of lipid debris (Libby et al., 2002). However, investigation of the link between inflammation, lipoprotein metabolism and atherosclerosis began in the 1950's and continues to the present day. Early studies reported inflammatory changes such as elevated levels of pro-inflammatory mediators, including C-reactive protein (CRP), a representative marker for the pro-inflammatory cytokine IL-1 and other cytokines, which play a key inflammatory role in atherosclerosis (Enos et al., 1953, Kushner et al., 1978).

Clinical studies on ACS patients have shown that levels of the acute phase reactant serum CRP are elevated in association with disease progression and development of cardiovascular complications (Ridker et al., 2005). That high sensitivity CRP measurement is an indicator of ACS severity and plays a role in risk stratification and patient prognosis prediction, has also been shown recently, in a study conducted on more than 10,000 ACS patients (Liu et al., 2020). The importance of inflammation in atherosclerotic progression is also indicated by studies using therapies that aim to lower serum lipid levels through changes in diet and lifestyle alone. These were not effective, with the risk of death from CHD still markedly high, as the inflammatory pathway

30

of the disease has not been altered (Pearson et al., 2003, Grundy et al., 2004, Ridker, 2018). The drug class of statins, which are now routinely prescribed (and have been used effectively for LDL cholesterol lowering, for more than 30 years), are known to have pleiotropic effects especially upon inflammation (Oesterle et al., 2017). These are cardiovascular protective effects that are independent of LDL cholesterol lowering (further explained in section 1.4).

1.3.1 The Role of the Pro-Inflammatory Cytokine IL-1 in Atherosclerosis

IL-1 is an inflammatory cytokine that is mainly released from macrophages and monocytes during the innate response to inflammation, transducing signals through activation of a complement pattern recognition receptor and TNF alpha (Dinarello et al., 2012). In atherosclerosis, IL-1 is crucially involved in the inflammatory process of vessel walls and is recognised as a potential target presenting a manageable therapeutic system, as it is highly expressed in arteries of patients with atherosclerosis and CHDs (Satterthwaite et al., 2005).

The production of the cytokine interleukin 6 (IL-6) is promoted by IL-1 via NF-kB (Yi et al., 2014), and together these play a role in stimulating the liver to produce CRP (Schindler et al., 1990). High serum levels of IL-6 are observed in ACS patients (Nijm et al., 2005), and high levels of CRP alone are considered a major clinical sign of increased mortality in ACS patients (Biasucci et al., 1999, Liu et al., 2020). Furthermore, *in vivo* experimental studies have reported a reduction in the formation of neointima in mouse models that underwent IL-1 inhibition (Chamberlain et al., 2006). In this

31

study, *IL-1β−/−* mice experienced a fourfold increased lumen area and a fourfold reduction in neointima/media, compared to wild-type mice.

Studies on the genetically modified Apolipoprotein E (ApoE) deficient mice, which are more vulnerable to developing atherosclerotic lesions (Kolovou et al., 2008), have shown that interleukin-1 receptor antagonist (IL-1ra), which blocks the interleukin-1 receptor 1 (IL-1R1) has an inhibitory effect on the intimal development of fatty streaks (Elhage et al., 1998), while complete genetic deletion of IL-1R1 reduces the development of atherosclerosis as a result of a fatty diet (Chamberlain et al., 2009). Clinical trials on ACS patients have also shown that treatment with recombinant human (IL-1ra) had an effective role in reducing markers of inflammation e.g. CRP over the treatment period (Morton et al., 2015). The CANTOS (Anti-inflammatory Thrombosis Outcome Study) trial, which used cankinumab, a monoclonal therapeutic antibody that targets IL-1β, investigated the clinical effectiveness of IL-1β inhibiting agents. The study was conducted on 10,061 patients with previous MI and high hs-CRP level (2 mg or more per litre), and showed that inhibition of IL-1β resulted in better patient prognosis with significant reduction in rates of adverse clinical events (Ridker et al., 2017).

All these previous studies emphasise the key role of IL-1 as a target to reduce the development of atherosclerosis and thus reduce clinical cardiovascular manifestations.

Interleukin 1 beta (IL-1β) and interleukin 1 alpha (IL-1α), both have been studied heavily in the context of inflammation in atherosclerosis

(Satterthwaite et al., 2005). Both cytokinescomplexc are synthesised as precursor proteins and their signalling effects are exerted by activation of IL-1R1 as well as inhibited by IL-1ra (Dinarello, 2005). IL-1β is initially produced as pro-IL-1β, an inactive form that can be activated into a mature IL-1β by cleaving enzymes such caspase-1 (Burns et al., 2003) (section 1.5). IL-1α stays bound to the plasma membrane and associated with local inflammation, and is released from necrotic cells (such as necrotic human aortic vascular smooth muscle cells (Clarke et al., 2010)) while IL-1β is secreted completely, making it a circulatory isoform (Dinarello, 2009, Dinarello, 1991). This attributes to IL-1β having both paracrine and endocrine effects, and it is, therefore, a potentially better target of study than IL-1α (Rader, 2012). Furthermore, it has been reported *in vivo* and *in vitro* that IL-1β has important roles in different stages of atherogenesis (Van Tassell et al., 2013).

1.3.2 IL-1β is an Important Target for Atherosclerosis Development and Progression

IL-1β plays a major role in endothelial activation by promoting adhesion molecule expression and eliciting the production of chemokines, causing infiltration and recruitment of inflammatory cells into the sub-intimal space during atherogenesis (Szmitko et al., 2003). IL-1β also enhances vascular endothelial growth factor (VEGF) expression, which then promotes endothelial cell reactivity, through increasing vascular leakiness which further aggravates inflammation and infiltration of immune cells (Lange et al., 2016).

33

The level of plaque inflammation is directly related to the extent of plaque formation (Van Tassell et al., 2013). Expression of IL-1β correlates with the progress of the atherosclerotic lesion, where very high levels of IL-1β expression were seen in complicated lesions and less expression in stable lesions. Low expression was reported in coronary arteries of healthy individuals (Dewberry et al., 2000). Furthermore, levels of plasma IL-1β are elevated in patients with more severe atherosclerotic complications (Ikonomidis et al., 2005) and this elevation was a precursor for less favourable ACS prognosis (Orn et al., 2012).

In addition, IL-1β has a crucial role in plaque destabilisation as it up-regulates MMPs' expression and over production in macrophages, endothelial cells and SMCs, all of which are components that build up to form the plaque during atherogenesis. This elevated expression leads to degradation of the subendothelial collagen matrix and exposure of the contents of the vessel wall to flowing blood, increases the chance of plaque rupture, leading to acute coronary syndrome (Newby, 2016).

This central role of IL-1β is supported in experimental models where ApoE deficient mice also lacking IL-1β exhibit smaller atherosclerotic lesions, in response to reduced VCAM-1 and MCP-1 expression in blood vessels (Kirii et al., 2003, Libby, 2008).Given the central and proven role of IL-1β, it is clear that release of IL-1β has to be carefully controlled within the body, and there are several levels of regulation possible (Brough et al., 2011, Folco et al., 2014, Latz et al., 2013). In monocytes, the mechanisms are well understood

but this is not the case for vascular wall cells like endothelium. One recently discovered mechanism is that vessel wall proteases e.g. neutrophil elastase lead to IL-1β release inside lysosomally derived extracellular vesicles (Alfaidi et al., 2015). There are also suggestions that cholesterol crystals may promote processing and release of IL-1β from macrophages (Rajamaki et al., 2010). In monocytes, the mechanism to enable this is via the NLRP3 (nucleotide-binding domain leucine-rich repeat containing (NLR) family, pyrin domain containing 3) inflammasome (Duewell et al., 2010), but no data are available from vessel wall cells such as endothelium and this, therefore, is the main aim of my study.

1.4 The Role of Cholesterol and Cholesterol Crystals

Cholesterol is an organic lipid molecule, biosynthesized by all human and animal cells (80% synthesised in the liver) and is a vital cellular component that maintains cellular fluidity and provides structural integrity for membranes (Chang et al., 2006). Owing to its chemical and physical characteristics as a low aqueous soluble molecule, it cannot be transported in blood without lipoprotein carriers, such as LDL (Phillips, 2014). The main route for cholesterol settlement into cellular membranes is through LDL receptor mediated endocytosis (Le May et al., 2013).

In the cell, excess free cholesterol undergoes esterification by acetyl coenzyme A (acyl-CoA) cholesterol acyltransferase (ACAT) (see Figure 1.3), which turns it into cholesterol esters that are deposited as droplets of lipid (Walther and Farese, 2012).
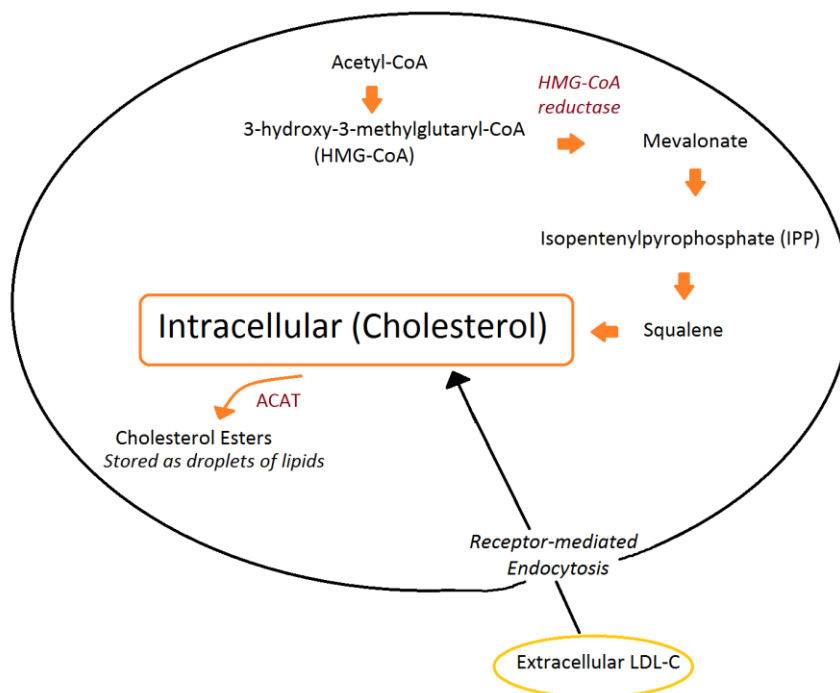
(Figure 1.3) Cellular Cholesterol Biosynthesis: Cholesterol synthesis is initiated by the transportation of Acetyl-CoA from mitochondria to cytoplasm. Acetyl-CoA is converted into HMG-CoA by HMG-CoA synthase which is encoded by the HMGCS1 gene. The conversion into mevalonate is by the action of HMG-CoA reductase (HMGR) which is an endoplasmic reticulum bound enzyme. Mevalonate is activated by phosphorylation into mevalonate 5-diphosphate which undergoes an ATP-dependent decarboxylation. As a result, an activated isoprenoid molecule known as isopentenylpyrophosphate (IPP) is synthesized. Squalene is then synthesised from IPP with the action of the squalene synthase enzyme. Cyclisation of squalene yields lanosterol, which is converted into cholesterol through a process of 19 reactions.

It has long been known that the accumulation of cholesterol in both ester and crystal forms are widely present in atherosclerotic plaques (Katz et al., 1976, Katz and Small, 1980). Recently, however, cholesterol has been implicated in other areas. A complicated clinical syndrome, with a challenging management approach and poor prognosis, called CCE (Cholesterol crystal embolic) syndrome, was described in 2017 (Ghanem et al., 2017). This syndrome occurs as the result of plaque rupture accompanied by cholesterol crystal release into the circulation, embolizing into multiple tissue organs, initiating systemic and local inflammation, which eventually leads to vascular obstruction, and fibrosis, causing symptoms mimicking vasculitic conditions.

In cultured human macrophages, it has been reported that the collection of non-esterified cellular excess free cholesterol (Figure 1.3) is transformed eventually to cholesterol crystals (Geng et al., 2003). Macrophages undergo an adaptive mechanism, which promotes sterol crystallization, in response to the oxidative products of cholesterol. However, crystallization and nucleation of free cholesterol only takes place during the onset of plaque formation, when cholesterol esterification is diminished and membrane cholesterol is supersaturated.

Studies using SMCs showed that the accumulation of free cholesterol itself in SMC is not inflammatory, as it did not alter MCP-1 or VCAM-1 (Rong et al., 2003). However, cellular free cholesterol did promote smooth muscle cell differentiation into macrophage foam cells, a major event in the

37

pathophysiology of atheroma development (Feil et al., 2014, Giannotti et al., 2019). In addition, SMC showed elevated production of ROS in addition to mitochondrial dysfunction when overloaded with free cholesterol (Kedi et al., 2009).

Surprisingly, however, there are no definitive studies on the effects of cholesterol crystals in cultured endothelial cells, despite that these cells express receptors for oxidized lipoproteins, and have the biochemical pathways for sterol synthesis and receptor-mediated endocytosis of lipoproteins (Hassan et al., 2006).

Pathology studies on coronary arteries of ACS patients showed that, at the sites of plaque rupture, there were usually dense clusters of cholesterol crystals (Abela et al., 2009). Electron microscopy, used to visualise cholesterol within tissue prepared without the use of solvents also showed that *in vitro* statins and aspirin could dissolve cholesterol crystals, due to their lipophilic properties and their anti-inflammatory and pleiotropic effects (Abela, 2010). This observation may well be connected to the success of clinical trials that have used statins to prevent and reduce the occurrence of cardiovascular events (Ridker et al., 2008). Statins could act as solvents of cholesterol crystals thereby preventing the volume expansion that leads to plaque rupture and development of clinical coronary symptoms (Ioannou et al., 2015).

1.4.1 Modified LDL cholesterol in atherosclerosis

There is well established understanding that the process of atherosclerosis development is mainly caused by LDL modification (in particular oxidative changes) in the arterial wall by ROS (Aviram, 1993, Lepedda and Formato, 2020). There is also a suggestion that smoking, a common risk factor of atherosclerosis, exerts its effects, by increasing ROS production from cells, in particular endothelial cells, and therefore increasing the chances of LDL alterations (Miao et al., 2019). Studies reported that circulating modified LDL has a direct effect on inducing damage to the endothelium and cause endothelial dysfunction (Paoletti et al., 2004), while extensive modification of LDL causes oxidative stress and accelerates endothelial cell senescence, two key atherosclerosis leading events (Yang et al., 2019, Ehara et al., 2001).

Several modified LDL forms have been identified since the 1970s, these include: Oxidised LDL (OxLDL) (Schuh et al., 1978), Acetylated LDL (AcLDL) (Goldstein et al., 1979) and Aggregated LDL (AgLDL) (Dyerberg et al., 1978).

1.4.1.1 OxLDL

The oxidative modification of proteins and lipids is commonly seen in several pathophysiological processes *in vivo*, such as inflammation-related gut diseases, diabetes and CVD (Sottero et al., 2018, Randle et al., 1994).

Lipid molecules containing native LDL are easily oxidized under oxidative stress, such as hydroperoxides, lipooxigneases and free radicals (Itabe, 1998, Di Pietro et al., 2016).

In addition to being the most studied form of modified LDL in context to atherosclerosis, OxLDL is considered an extensively modified, highly

39

inflammatory and proatherogenic form of modified LDL. The prothatherogenic properties of OxLDL are mainly driven by oxidised phospholipids, which are also the principal epitopes and the major structural feature making OxLDL recognisable by scavenger receptors as a ligand (Leitinger, 2005). Macrophages are known to take up OxLDL by scavenger receptors, which leads to their formation into lipid-laden foam cells, which is the hallmark of an early atherosclerotic lesion. Although there is almost no size difference between unmodified native LDL molecules (22-27.5 nm in diameter (Campos et al., 1992)) and OxLDL molecules (25-30 nm in diameter (Han and Pak, 1999)), OxLDL at only 50 µg/ml can induce foam cell formation, while the concentration needed in native LDL is at 2 mg/ml (40-fold greater)(Kruth et al., 2005).

1.4.1.2 AcLDL

Unlike OxLDL, AcLDL is an artificial model ligand that is used in variety of modified lipid studies and was never reported to be found in vivo (Steinberg, 2009). There are several methods of preparation of AcLDL, the most common is acetylation with excess acetic anhydride, which has been previously used been used as a targeted drug delivery mechanism reported to be taken up by cells via scavenger receptors (Limmon et al., 2008). AcLDL and OxLDL behave similarly as they are both degraded inside lysosomes and are taken up by macrophages via scavenger receptors at similar concentrations (Liu et al., 2015, Brown et al., 2000). Furthermore, the size of AcLDL in diameter is almost identical to that of OxLDL as measured by atomic force microscopy (Gan et al., 2018).

1.4.1.3 AgLDL

Although the molecular mechanisms of lipid droplet formation and retention of LDL in the subendothelial arterial space are not entirely understood, there is growing evidence supporting the fact that modified LDLs undergo fusion and aggregation, which limits their exit from the arterial wall and contributes to atherogenesis (Hurt-Camejo et al., 2000, Camejo et al., 1998, Zhao et al., 2004), thus forming AgLDL molecules.

AgLDL has been reported to be found *in vivo* in arterial walls of CVD patients as well as ApoE deficient mice (Zhao et al., 2004, Aviram et al., 1995, Hoff and Morton, 1985, Maor et al., 2000). The exact mechanisms leading to AgLDL formation are also poorly understood, however, in contrast to native LDL, it has been reported that native LDL does not normally aggregate nor fuse under normal physiological conditions, highlighting the importance of LDL modification prior to aggregation (Goldstein et al., 1979, Lu and Gursky, 2013).

AgLDL is also taken up by macrophages (Haberland et al., 2001) and HVSMCs incubation with AgLDL *in vitro* induces foam cell formation (Costales et al., 2015).

Since AgLDL is formed via the fusion and aggregation of modified LDLs, it has been reported with variety of sizes. A study reported the formation of AgLDL molecules which ranged 40-200 nm in diameter (Zhang et al., 2000) while (Costales et al., 2015) reported AgLDL molecules as large as 600 nm in diameter.

41

1.4.2 Cholesterol Crystals Promote Endothelial Cell Activation

Although the role of cholesterol crystals in different stages of atherosclerosis development, including promoting inflammation and plaque rupture, is well established (Sections 1.2-1.4), questions arise as to if/how cholesterol crystals play a role in endothelial cell activation. Cholesterol crystals (at concentration of 2 mg/ml, prepared by dissolving and mixing free cholesterol with 1-propanol *in vitro* (Samstad et al., 2014)) can activate HUVECs only when co-incubated with whole blood (Nymo et al., 2014). These data could be explained by the presence of many activating factors in whole blood such as TNF and IL-1β or, perhaps, cellular vesicles arising from other cells such as neutrophils or monocytes. TNF has a key role in activating the endothelium following incubation with cholesterol crystals, demonstrated by use of an IL-1β specific inhibitor canakinumab which did not affect expression levels of adhesion molecules ICAM-1 or E selectin, while inhibition with the TNF inhibitor infliximab resulted in complete attenuation of their responses (Nymo et al., 2014). In addition, cholesterol crystals promoted the release of IL-1ra from the whole blood and inhibited signalling of IL-1β explaining the insufficient effect of IL-1β alone (Nymo et al., 2014).

1.4.3 The Link Between Cholesterol Crystals and IL-1β

The potential mechanistic link between the effects of cholesterol crystals and release of IL-1β is the NLRP3 inflammasome (Duewell et al., 2010), which is a cytoplasmic protein complex that encodes the gene NALP3 (NACHT, LRR

and PYD domains-containing protein 3), a gene that is mainly expressed in macrophages (Kunnas et al., 2015) (further details in section 1.5).

Macrophage uptake of oxidised LDL (OxLDL) via the CD36 scavenger receptor, leads to formation of intracellular cholesterol crystals that activate NLRP3 through lysosomal destabilisation (Moore et al., 2013, Oury, 2014). NLRP3 plays a major role in the cleavage of pro-IL-1β into a mature form via caspase-1 activation (Shenderov et al., 2014), and can be activated with cholesterol crystals in peripheral blood mononuclear cells (PBMCs) following lipopolysaccharide (LPS) priming as well as cytokine cell priming (Duewell et al., 2010).

There are little data on endothelial cells, but HUVECs primed with TNF-α have increased expression of adhesion molecule ICAM-1 and E-selectin, in addition to increased release of IL-1β, when also activated by cholesterol crystals (Samstad et al., 2014). However, human coronary artery endothelial cells (HCAECs) primed with TNF-α and LPS did not show increased IL-1β release upon incubating with cholesterol crystals (same concentration used by (Samstad et al., 2014) and (Nymo et al., 2014), 2 mg/ml) (Champaiboon et al., 2014). This was explained by the presence of hydrocortisone in the media of HCAECs, which is known to inhibit the release of IL-1.

1.5 The Caspase-1/NLRP3 inflammasome activation pathway of IL-1β secretion

1.5.1 Understanding the Caspase-1/NLRP3 mechanism

It is well established that the NLRP3 inflammasome is formed in the cytoplasm in response to danger associated molecular patterns (DAMPs) or

43

pathogen associated molecular patterns (PAMPs), and after its cytoplasmic formation, the NLRP3 inflammasome serves as the molecular platform for the activation of Caspase-1 and for the processing of proIL-1β (Martinon et al., 2002, Karasawa and Takahashi, 2017a). What distinguishes the NLRP3 inflammasome from others, is that the NLRP3 inflammasome can be activated by both endogenous or exogenous DAMPs which makes them involved in pathophysiological mechanisms of sterile inflammatory diseases (Lamkanfi and Dixit, 2014).

The protein structure of the NLRP3 inflammasome complex is composed mainly of three parts: 1) NOD-like receptor protein number 3 (NLRP3 protein); 2) an apoptosis associated speck-like protein containing a caspase-1 recruitment domain (ASC), which is occasionally referred to as the adaptor protein; 3) the cysteine protease caspase-1 (Martinon et al., 2002, Burns et al., 2003, Strowig et al., 2012). The NLRP3 protein is also composed of three domains: 1) NACHT, which is a central nucleotide domain; 2) C-terminal leucine-rich repeats (known as LRRs); 3) pyrin domain (PYD) which is an N-terminal effector domain. ASC also contains an N-terminal PYD and contains a caspase recruitment domain (CARD) C-terminal. Caspase-1, (which was previously known as IL-1 converting enzyme (ICE) (Black et al., 1989)), contains a CARD as well as two catalytic domains known as p10 and p20 (Duewell et al., 2010, Jiang et al., 2017).

When a cell is stimulated by DAMPs, the stimulation triggers the NLRP3 to assemble (Bauernfeind et al., 2009). This is initiated by the NACHT domain

44

which provides a scaffold for the oligomerization of ASC by the interacting PYDs. Due to the structure of NLRP3 protein, and because it lacks CARD, NLRP3 therefore cannot choose to recruit caspase-1, unless in the presence of ASC. After oligomerization of ASC, it interacts with caspase-1 via the homophilic interaction with CARD, which induces the auto-activation of caspase-1 allowing it to exercise its pro-inflammatory effects (Karasawa and Takahashi, 2017a, Karasawa and Takahashi, 2017b).

Studies have shown that cholesterol crystals and OxLDL are considered danger signals that can activate the NLRP3 inflammasome in macrophages (Rajamaki et al., 2010, Duewell et al., 2010, Abdul-Muneer et al., 2017), although the exact mechanisms of recognition and activation of NLRP3 by cholesterol crystals or LDL molecules are not understood. However, multiple upstream pathways have been reported to be essential for the activation of the NLRP3 inflammasome: 1) lysosomal destabilisation; 2) potassium ion (K+) efflux, which is mainly induced by the P2X7 receptor in macrophages; 3) production of mitochondrial ROS (Guo et al., 2015). It is well-established that among those three upstream pathways, lysosomal destabilisation, accompanied with a subsequent release of cathepsin B, is the most important pathway (Lima et al., 2013, Niemi et al., 2011, Karasawa and Takahashi, 2017a).

The most accepted understanding of IL-1β production and release is known as the "two-step process"(Wang et al., 2013), or the "two-signal process" (Cassel et al., 2009). The first step is the transcriptional synthesis of pro-IL-

1β, which is known as the priming step or first signal. This process is regulated by the NF-kB-mediated mRNA induction of NLRP3 and pro-IL-1β synthesis, and is mediated by cytokine receptors (such as the IL-1 receptor) or PRRs (such as TLRs). At this stage, both the cytosol accumulated pro-IL-1β and the NLRP3 are inactive and in standby mode, until a second signal is given. This second signal, known as the activation signal or oligomerization signal (Satoh et al., 2013), which could be the exposure and uptake of cholesterol crystals or OxLDL (as DAMPs) by the cell, results in activation of the NLRP3 and release of active caspase-1 (Zheng et al., 2013, Abdul-Muneer et al., 2017, Rajamaki et al., 2010). The NLRP3 inflammasome mediated activation of caspase-1 initiates the rapid processing of pro-IL-1β 31 kD (the precursor of IL-1β), cleaves the pro-IL-1β into a mature IL-1β (17 kD), causing the release of mature bioactive IL-1β outside the cell. Thus, to regulate and maintain inflammatory homeostasis of the potent inflammatory cytokine IL-1β, this two-signal process is crucial.

1.5.2 Activation of the Caspase-1/NLRP3 mechanism by cholesterol and release of IL-1β from macrophages

The first group to show the direct involvement of the NLRP3 inflammasome in atherosclerosis development and the importance of cholesterol in the process of the underlying NLRP3 activation mechanism were Duewell et al. 2010. Their study used IL-1α/β$^{-/-}$, NLRP3$^{-/-}$, or ASC$^{-/-}$ bone marrow cells transplanted into atherosclerosis-prone, LDL receptor-deficient mice (LDLR$^{-/-}$) and showed that absence of these inflammatory molecules dramatically decreased the development of atherosclerotic lesions. Focusing on

46

cholesterol crystals as an important candidate for NLRP3 activation, the study also reported the successful activation of NLRP3 inflammasome and release of IL-1β from macrophages. The release of IL-1β from LPS-primed macrophages, secondary to cholesterol crystal treatment was more than 60 fold greater than untreated LPS-primed only macrophages. This release was completely inhibited when a Caspase-1 inhibitor was used (YVAD). Interestingly, this study was also among the first to highlight the presence of OxLDL, which possesses highly inflammatory and atherogenic properties, leading to cholesterol crystallization and activation of the NLRP3 inflammasome mediated activation of caspase-1. Macrophages internalised OxLDL molecules, resulting in the formation of peri-nuclear crystals as early as one hour post incubation, with OxLDL treatment (200 µg/ml for 24 hours) inducing the release of almost 10-fold more IL-1β compared to untreated macrophages which did not release IL-1β (Duewell et al., 2010).

1.5.3 The pyroptosis theory of IL-1β exit from the cells
The mechanism by which IL-1β is released from cells is not fully elucidated. One possible mechanism is that IL-1β and other non-signal sequence protiens might exit cells via membrane pores. This is supported by the observation that activated caspase-1 is also capable of cleaving gasdermin D (GSDMD), which is known as the pore forming protein or the pyroptosis inducing protein (Evavold et al., 2018).

Pyroptosis is a form of highly inflammatory programmed cell death, which is accompanied by membrane pore formation, and increased permeability of the plasma membrane, allowing cells to dispose of inflammatory, damage or

47

danger molecules (Kayagaki et al., 2015, Shi et al., 2015). The association of GSDMD cleavage and caspase-1 activation in the pathway of mature IL-1β release from macrophages during atherosclerosis development, is evidenced by the fact that the pore formed after release of active GSDMD is the exit gate for active IL-1β (Evavold et al., 2018). However, the role of GSDMD and its association with the release of IL-1β from vascular endothelial cells has not been investigated.

Thus, because the mechanism of release of IL-1β is still unknown and the exocytosis of IL-1β has no signal sequence (Martín-Sánchez et al., 2016), understanding pyroptosis-mediated membrane pore formation and permeabilization in endothelial cells will add further understanding to the mechanism of IL-1β release.

1.6 Summary and Knowledge Gap

Cholesterol, cholesterol esters and cholesterol crystals are present in atherosclerotic plaques, including in endothelial cells. These are not usually seen histologically, because pathological processing of samples removes all these entities. However, cholesterol crystals have been shown to elicit IL-1β release from macrophages, and this is well known. However, the release of IL-1β from other cell types in the vessel wall, especially endothelial cells in response to cholesterol forms, is unknown.

1.7 Hypothesis, Aims and Relevance of the Study

I hypothesise that cholesterol enters the endothelium and induces IL-1β secretion via a caspase-1/NLRP-3 mechanism. Secondly, I hypothesise that cholesterol esters (lipid droplets) and cholesterol crystals stored in cells induce IL-1β secretion following priming of the cells with an inflammatory stimulus. Finally, that IL-1β secretion in response to the above stimuli can be inhibited by treatment with inhibitors of the NLRP3 inflammasome or inhibition of any of its up-/downstream factors.

The first aim of this project was to investigate whether cholesterol, in both the forms of free native cholesterol and modified cholesterol, induces the release of IL-1β from human coronary artery endothelial cells (HCAECs), and whether the release of IL-1β was secondary to uptake by vascular endothelial cells. A further aim was to investigate the mechanism of cholesterol uptake and IL-1β release by HCAECs using inhibitors of Caspase 1 and NLRP3.

Cholesterol crystals are common in atherosclerosis, and their point of entry to the vascular wall is the endothelium. Thus, identifying a cellular mechanism to prevent cholesterol-primed pro-inflammatory IL-1β release from endothelial cells could eventually lead to a new targeted therapeutic agent which may have a promising influence on the future of cardiovascular treatment regimes, and aid in reducing mortality rates.

(Chapter 2) Materials & Methods

2.1 Materials:

2.1.1 Reagents & Solutions:

Stock concentrations, working doses, sources of solutions and reagents used

are listed in appendices (I & II).

2.2 Methods:

2.2.1 Cell culture:

All cell culture experiments were carried out under a Class II sterile laminar

flow hood and all cells were incubated at 37°C with 95% air and 5% CO_2.

Strict sterile procedures were used at all times to prevent the development

of infections which might alter the interpretation of the results and interfere

with the quantification methods used.

2.2.1.1 Human umbilical venous endothelial cells (HUVECs):

HUVECs were used as an initial model to test the effect of cholesterol, due

to their cost effectiveness compared to HCAECs and their easy availability as

a fresh endothelial cell line, in addition to being responsive to cytokine

stimulation as previously reported (Alfaidi et al., 2015). HUVECs were

isolated from the fresh umbilical cords of babies born in the maternity unit

of Jessop Wing Sheffield Teaching Hospital (STH). The collection and use of

these cords/HUVECs was regulated by the ethical committee and registered

as ethical approval (STH15599, REC ref 10/H1308/25), see appendix (V) for

more details. The cords were collected from mothers whom have consented

and after following strict assessment measures. These measures ensure that

cords were only collected from normal, full term deliveries (pre-term and

caesarean section deliveries were excluded). Complete serology testing for

infectious diseases (Hepatitis and HIV) were taken, positive tested mothers were excluded from the study.

2.2.1.1.1 HUVECs isolation process:

Fresh umbilical cords stored within individual containers in minimum essential media (MEM) (see appendix II for composition) at 4°C and were ideally used within 24 hours of collection, for the isolation process. A total of 12 cords were used in the study.

The isolation was carried out in accordance with the established protocol by (Jaffe et al., 1973). Cords without clamp markings and with a minimum length of 10cm minimum were used during all isolations. Cords not matching these criteria were discarded.

Each cord was inspected for any damaged parts or any tears in its surface, and the outer layer was cleaned with Azo© wipes. Gentle massage was then applied to the cord towards one end, to expel any excess venous blood or blood clots. The vein was cannulated using a 14G cannula, and a tight bung was attached to the cannulated region to secure its place inside the vein. A long plastic needle sheath was first inserted into the vein, followed by a shorter needle, to allow the plastic part to be prominent. This also avoids the needle piercing through the vein wall. The needle was then clamped to secure it in place (Figure 2.1A). A 60ml syringe was attached to the needle inlet, and the vein was washed with 40 ml of pre-warmed serum free M199, by applying moderate pressure to remove traces of clots and blood. A second clamp was then applied to the other end of the cord, and the cord

was inflated with 10ml of 0.1% (w/v) collagenase solution (0.20 μm sterile filtered), prepared at room temperature in serum free M119 using collagenase from *clostridium histolyticum* (See Appendices I &II for all compositions). After observing moderate distention of the vein without any leaking, the cord was placed on a layer of Azo© wipes and left in the laminar flow hood at room temperature for exactly 12 minutes (Jaffe et al., 1973), allowing the detachment of venous endothelial cells by collagenase (Figure 2.1B).

The distal end of the cord was then placed in a 50ml falcon tube and was de-clamped, allowing the contents for the cord (which contain the detached endothelial cells) to be collected in the tube, with a gentle massage applied to the cord to flush the cells. The tube was centrifuged at 300g for 5 minutes at 24°C, the supernatants carefully discarded, and the pellet re-suspended in 10 ml of pre-warmed complete growth media CGM, ensuring complete disposal of the pellet into the media.

The cells were then transferred into a pre-coated 1% (w/v) gelatin T75 flask, and left to grow in the flow incubator at 37°C with 5% CO_2 and 95% air overnight.

The pre-coating of the flask was performed by adding 5 mL of 1% (w/v) gelatin to the flask and leaving it in the incubator at 37°C with 95% air and 5% CO_2 for at least 30 minutes, after which the gelatin was removed and the flask was washed once with 10 ml of PBS.

The next day, cells were observed under the microscope to make sure they were contamination free, and the flask was washed with PBS (pH 7.4) to remove any traces of blood and red blood cells. In addition to washing away non-adherent cells, media was replaced with fresh CGM; thereafter the media was changed every 2-3 days until the cells were observed under the microscope to be 80-90% confluent.

(Figure 2.1) Isolation of HUVECs: (A) Fixation of the needle sheath followed by needle inside the umbilical vein. (B) Distended umbilical vein after loading with 0.1% (w/v) collagenase.

In the first 24-36 hours after isolation, HUVECs look like small epithelioid clusters. However, after 48-72 hours, the clusters spread to the typical cobblestone monolayer appearance (Figure 2.2).
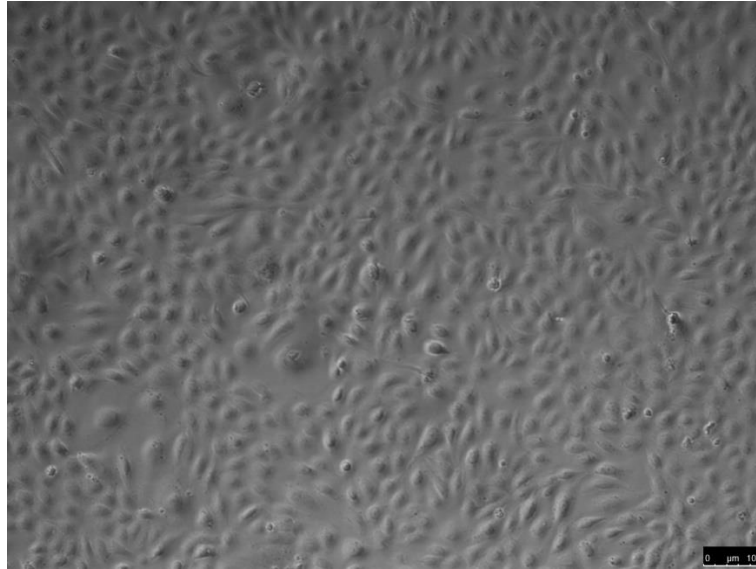
(Figure 2.2) Cobblestone appearance of HUVECs under microscope following isolation from cords: This image has been taken using bright field microscopy and image was managed by the software LAS AF Lite by Leica©. Scale bar = 100 μm.

2.2.1.1.2 Culture and sub culture of HUVECs

HUVECs were passaged when 80-90% confluent, (approximately every 4-5 days). HUVECs were always cultured in a 1% (w/v) gelatin coated T75 flask, and the CGM was changed once every 72 hours at a maximum. When the cells were ready to be passaged, the CGM media was discarded and the cells washed gently with 10 ml of PBS once. Pre-warmed Trypsin/EDTA (Ethylenediaminetetraacetic acid; EDTA, 0.2% v/v in PBS without Magnesium, Calcium or Phenol Red) was added to the flask (1 ml volume), and incubated for 3 minutes at 37°C with 5% CO_2 95% air.

Trypsin solution was applied to the cells as it dissolves the junctions between the cells, the trypsin exposure period was not exceeded by 3 minutes as to avoid the risk dissolving the cellular lipid bilayer. The flask was then gently tapped and checked under the microscope to confirm the detachment of cells. CGM (5 ml volume) was then added to the flask to neutralise the trypsin, and the contents of the flask were transferred to a 50 ml falcon tube, which was then centrifuged at 300g for 5 minutes at 24°C.

The supernatant was gently discarded leaving a pellet at the bottom of the tube which was re-suspended into 24 ml of CGM, pre-warmed to 37°C. The cell solution was then transferred to two gelatin pre-coated T75 flasks (12 ml each), and left to grow in the incubator.

All HUVECs experiments were performed using cells at passage 2-3 and each stated n number represents HUVECs from a different donor.

The volume of medium to surface area ratio was; 1ml per 5 cm2 (5 ml per a T25 flask or 15ml per a T75 flask), and 1 ml per well in a 12-well plate.

2.2.1.1.3 HUVECs seeding density in a 12 well plate:

HUVECs were seeded in a 12 well plate at 10,000 cells/cm^2 and left to grow in the incubator for 48 hours after which they were viewed under the microscope for determination of confluence by eye.

2.2.1.2 Human Coronary Artery Endothelial cells (HCAECs):

Three vials of cryopreserved HCAECs from three different biological donors (supplied at passage 2) were bought from PromoCell (Product code C-12221)

and were received in a dry ice filled container. The lot numbers for the three cell orders are 440Z021.1, 424Z011.1 and 411Z027.

2.2.1.2.1 HCAECs Culture:

Upon receipt of the cells and according to the supplier's instructions, MV2 supplemented media (composition of media in appendix II) was prepared and 9 ml of this prepared MV2 media was pre-warmed in a T75 flask to 37°C with 5% CO_2 / 95% air for 30 minutes to be used for culturing the cells. The vial containing the cryopreserved cells was removed from the dry ice and a quarter twist to the cap was applied under the laminar flow hood to relieve the pressure, then it was re-sealed tightly. The vial was thawed quickly in a waterbath (30 seconds), thereafter the cells were transferred immediately from the vial into the pre-warmed T75 flask and returned to the incubator and left to grow. The media was changed and replaced with fresh MV2 media 24 hours later, after which it was changed every 48 hours until the cells were 80-90% confluent.

When the cells were confluent they were sub cultured (to passage 3) into four T25 flasks according to the protocol below. At this step the cells were either used to seed an experimental plate or stored frozen in liquid nitrogen until used. The cell density used in all experiments when cells were confluent was approximately 5,000 cells/cm^2.

2.2.1.2.2 HCAECs sub-culture:

To maintain continuous healthy cell growth, the cells were passaged 1:3 when 80-90% confluent. This was to avoid the cells from becoming over-confluent, exhausting the media and nutrients, allowing cells to easily

58

detach from the flask surface and die. Over-confluent cells also have a high possibility of suppressing the production of IL-1β (Jung et al., 2001), and therefore giving false data in the study. When the confluence level was reached, media was removed from the flask, and cells washed once with sterile PBS (pH 7.4). Afterwards, 3 ml of pre-warmed (37°C) trypsin solution was added to the cells and the flask was left for 3 minutes in the incubator to aid detachment of cells. When the cells were viewed detaching under the microscope, the trypsin was diluted by adding 10 ml of CGM into the flask, and the contents were transferred into a 50 ml tube and centrifuged at 300g at 24°C for 5 minutes. The supernatants were then discarded gently and the pellet was re-suspended in 1ml of CGM.

The appropriate amount of CGM was then added to the 1 ml cell solution, to enable seeding into flasks to maintain growth, or experimental plates.

The volume of culture medium to surface area ratio was; 1ml per 5 cm2 (5 ml per a T25 flask or 15ml per a T75 flask), and 1 ml per well in a 12-well plate.

All flasks were placed in the incubator and the media was changed with fresh CGM every 48 hours until cells became confluent. Endothelial cells at high passage numbers have been reported to have slower growth rates, loss of their surface markers and reduced stimulation response (King et al., 2003). Therefore, HCAECs at passages from 2 until passage 6 maximum were used for all experiments.

2.2.1.3 Human Coronary Artery Smooth Muscle Cells (HCASMCs):

Adult HCASMCs were bought from Sigma-Aldrich© and were supplied via Cell Applications INC.©. They arrived as a cryopreserved vial of half a million HCASMCs in their 2nd passage, frozen in basal smooth muscle cell media 10% v/v FBS and 10% v/v DMSO. This type of vascular smooth muscle cells (350-05A) was previously used in studying signalling pathways which regulate differentiation of smooth muscle cells (Zhou et al., 2010) and the atherosclerotic leading pathways of the OxLDL induced inflammatory responses (Kiyan et al., 2014).

2.2.1.3.1 HCASMCs culture:

Cells were thawed as per the manufacturer's instructions in 15ml of HCASMCs growth media (composition of media in appendix II) in a pre-incubated T75 flask (the process of removing the cryopreserved vial from dry ice is identical to the steps in section 2.2.1.2.1).

Similarly, to HCAECs, the media was changed and replaced with fresh HCASMCs growth media 24 hours later, after which it was changed every 48 hours until the cells have become 80-90% confluent.

When the cells became confluent they were sub cultured (to passage 3) into four T25 flasks according to the protocol below. At this step the cells were either used to seed into an experimental plate or stored frozen in liquid nitrogen until used.

2.2.1.3.2 HCASMCs sub-culture:

HCASMCs were sub-cultured following the same protocol as for HCAECs in section 2.2.1.2.2 with the exception that sub-culturing was performed every

60

48 hrs due to the faster growth of HCASMCs. HCASMCs were also washed with Hanks' Balanced Salt Solution (composition in appendix II) instead of PBS.

The medium to surface area ratio was also identical to that in HCAECs and HUVECS; 1ml per 5 cm2 (5 ml per a T25 flask or 15ml per a T75 flask), and 1 ml per well in a 12-well plate. The cell density used in all experiments when cells were confluent was 10,000 cells/cm^2.

2.2.2 Cytokine stimulation of Vascular Cells

Complete growth medium (CGM) (see appendix A.2.1.3) was used in all stimulation experiments and through all steps, except during treatment with cholesterol or NE, where the treatment was delivered in serum free media (SFM).

To upregulate maximal endogenous proIL-1β production within endothelial cells (HUVECs and HCAECs) and HCASMCs, a combination of the cytokines IL-1α and TNF-α was used, both at working concentrations of 10 ng/ml, which has been previously reported to upregulate high levels of IL-1β production (Alfaidi et al., 2015).

Cells at 80-90% confluency were trypsinised (as per protocol in section 2.2.1.2.2) and centrifuged to collect a pellet of cells which was re-suspended in 1 ml of CGM, after which the cells were counted using a haemocytometer. HUVECs were seeded on a 1% (w/v) (gelatin) pre-coated 12-well plate at a density of $2x10^4$ cells/well. HCAECs and HCASMCs were seeded directly on

61

the 12 well flat bottom plate in an identical approach between different repeats of experiments. No pre-treatment of the plate was required.

After seeding the cells, the plate was incubated at 37°C with 5% CO_2 for 48 hours allowing cells to grow until they were 80-90% confluent. The cells were then washed once with PBS (pH 7.4) and the media replaced with 1 ml CGM containing both pro-inflammatory cytokines TNF-α and IL-1α at concentrations of 10 ng/ml each (further details of the pro-inflammatory cytokines used to upregulate and induce IL-1β synthesis and release are stated in appendix I). Cells were incubated with the pro-inflammatory cytokines for 48 hours, afterwhich the media was discarded from the plate and the cells were washed three times with either sterile PBS (pH 7.4) (endothelial cells) or Hanks' Balanced Salt Solution (HCASMCs), to remove any debris, remaining IL-1β or any traces of serum from the CGM. This cytokine treatment ensures the cells are stimulated, free of any exogenous cytokine and activated to produce IL-1.

2.2.3 Preparation of NE for use in cell culture

NE cleaves proIL-1β in endothelial cells and causes significant secretion of mature IL-1β into the cell culture supernatants (Alfaidi et al., 2015). Therefore, NE was used as a maximum release control (positive control) for experiments in both endothelial cell types in my study.

NE was purchased from Sigma-Aldrich© as lyophilised powder, reconstituted in 1ml of sterile deionised water, and stored in 10 μl aliquots at -20°C to be used at final concentration of 1 μg/ml in each experimental

plate as positive control. NE incubation in HCAECs and HUVECs was carried out in SFM for a period of 6 hours.

2.2.4 Preparation of cholesterol as endothelial and smooth muscle cell treatments

2.2.4.1 Water-soluble cholesterol

Water-soluble cholesterol was delivered to the cells via a complex of cholesterol and methyl-beta-cyclodextrin (MβCD), purchased from Sigma-Aldrich©. The use of this cholesterol complex has been previously reported in several endothelial cell models *in vitro*, including HUVECs (Fang et al., 2013), human pulmonary artery endothelial cells HPAECs (Yamamoto et al., 2007), bovine artery endothelial cells BAECs (Byfield et al., 2004, Romanenko et al., 2002, Levitan et al., 2000) and mouse aortic smooth muscle cells (MASMs) (Rong et al., 2003).

Each gram of this complex contains approximately 40 mg of cholesterol, with MβCD being the balance. The complex was reconstituted by adding 3 ml of sterile de-ionised water to make a stock solution of 10 mg/ml, which was mixed gently until completely dissolved. The stock was then divided into 200 µl aliquots and stored at -20°C, to be used fresh in each experiment. Treatments of water-soluble cholesterol was carried out in SFM in all experiments. Cells were incubated with cholesterol for 6 hours at 37°C with 5% CO_2/ 95% air in both HUVECs and HCAECs experiments. Several concentrations were used throughout the study (50, 100, 250 and 500 µg/ml). To test the effect of MβCD alone on the cells, endothelial cells were incubated with same concentrations of MβCD were used as controls in

parallel to water-soluble cholesterol treatment. An example of a typical

assay plate layout is shown below (Figure 2.3).
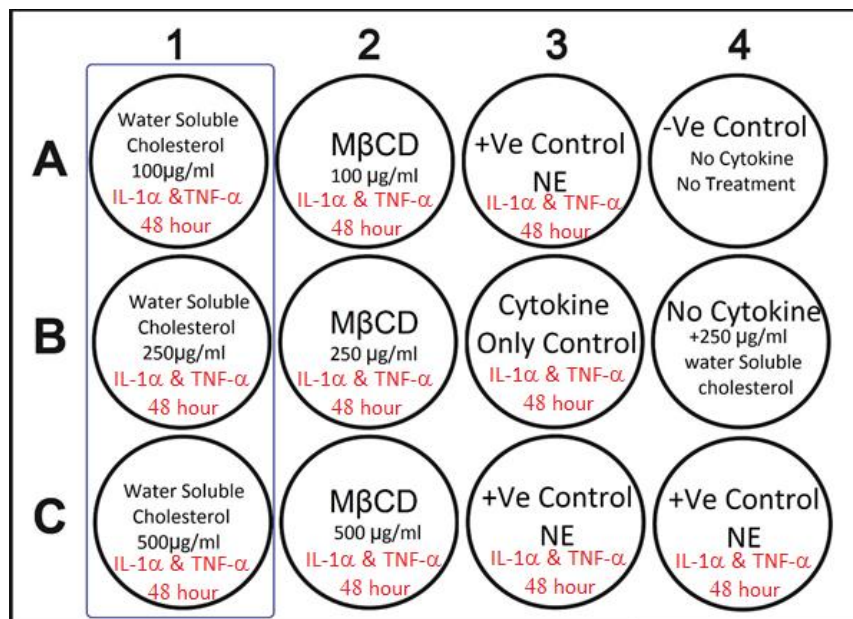
(Figure 2.3) 12-Well plate layout used in HUVECs and HCAECs water-soluble

cholesterol treatment experiments: The first three wells in column 1 (within blue box) represent endothelial cells (either HUVECs or HCAECs) treated with concentrations of 100, 250 and 500 µg/ml water-soluble cholesterol (conjugated with MβCD) for 6 hours, after being stimulated with cytokines TNF-α and IL-1α for 48 hours. The next 3 wells in column 2 are used as control for water-soluble cholesterol, as they are treated with same concentrations with MβCD alone. Three wells have been used as positive controls for IL-1β release, as they were incubated with 1 µg/ml of NE for 6 hours following 48 hours of cytokine stimulation. A cytokine only well was set to test the effect of cytokine stimulation alone on IL-1β release. In addition, a treatment with 250 µg/ml of water-soluble cholesterol has been applied with non-cytokine stimulation to test the effects of the treatment alone on IL-1β levels. Finally, a non-cytokine stimulated, non-treated well has been used as an assay negative control. Each plate represents n=1 per treatment.

2.2.4.2 Aggregated LDL

Human plasma derived low density lipoprotein (LDL) was purchased from

Sigma-Aldrich as a lyophilized powder. Aggregated LDL (AgLDL) was

generated by full speed vortexing of 1 mg/ml LDL in PBS for 4 minutes at

room temperature. AgLDL was then centrifuged at 10,000 g for 10 min and

stored immediately in 500 μl aliquots at -20°C until used fresh for experiments. Before each experiment, the AgLDL was vortexed for 10 minutes at full speed until the contents were completely mixed. This vortexing process forms the correct ultrastructure of AgLDL similar to the structure of the veriscan modified LDL, which is one of the primary chondroitin sulphate proteoglycans of the arterial intima (Costales et al., 2015).

This method of preparing and using AgLDL has been used in human vascular smooth muscle cell (HVSM) *in vitro*, showing the activation of the receptor-related protein 1 (LRP1), a critical receptor for aggregated LDL-induced foam cell formation from HVSMCs (Costales et al., 2015, Llorente-Cortés et al., 2002).

Similar to NE and water-soluble cholesterol treatments, AgLDL treatment was carried out for 6 hours in SFM, with different doses used (25, 50, 75, 100, 125, 200 and 250 μg/ml). The experimental plate layout for both HUVECs and HCAECs treated with AgLDL is shown in (Figure 2.4).
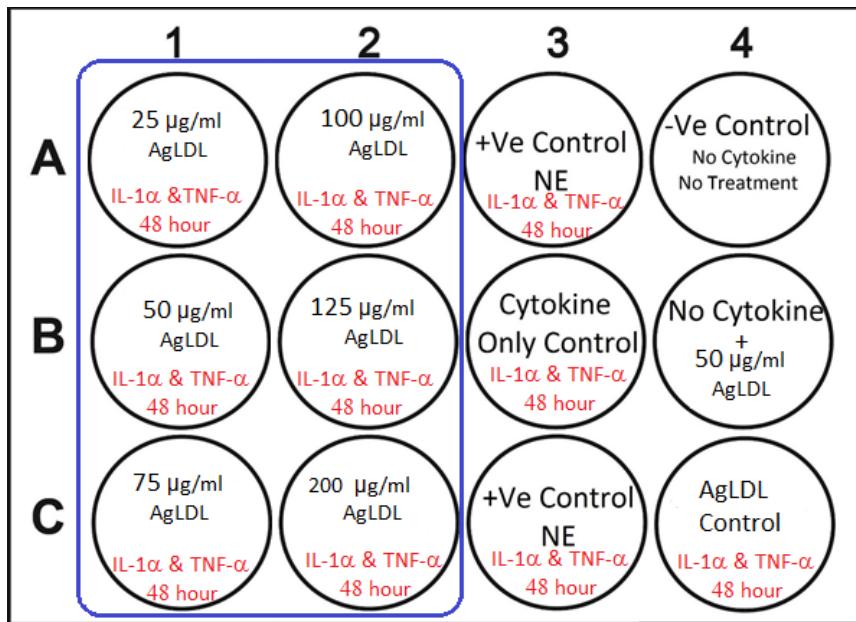
(Figure 2.4) 12-Well plate layout used in HUVECs and HCAECs Aggregated

LDL treatment experiments: The first six wells in columns 1&2 highlighted with blue represent endothelial cells (either HUVECs or HCAECs) treated with concentrations of 25, 50, 75, 100, 125 and 200 µg/ml of AgLDL for 6 hours, after being stimulated with cytokines (TNF-α and IL-1α) for 48 hours. A well with 50 µl of sterile distilled water has been used as an AgLDL control. Two wells have been used as positive controls for IL- 1β release, as they were incubated with 1 µg/ml of NE for 6 hours following 48 hours of cytokine stimulation. A cytokine only well was set to test the effect of cytokine stimulation alone on IL-1β release. In addition, a treatment with 50 µg/ml of AgLDL has been applied to a well with non-cytokine stimulation to test the effects of the treatment alone on IL-1β levels. As an assay negative control a non-cytokine stimulated, non-treated well has been used. During this study one assay was repeated by using one positive control well instead of two and a well was treated with 250 µg/ml of AgLDL to further investigate the effect of this concentration on IL-1β levels.

2.2.4.3 Acetylated LDL

Native Human Acetylated Low Density Lipoprotein (AcLDL) was purchased from Bio-Rad Laboratories Inc. as 2 mg of purified protein at concentration of 2 mg/ml. This form of LDL has been ultracentrifuged and purified to homogeneity and underwent the acetylation process with excess acetic anhydride. This has been previously used in the process of specific cell type depletion when combined with a ribosome inactivating protein such as saporin (Roy et al., 2017), and been used as a targeted drug delivery mechanism reported to be taken up by cells via scavenger receptors (Limmon et al., 2008). Interestingly, AcLDL and oxidised LDL behave similarly as they are both degraded inside lysosomes (Liu et al., 2015, Brown et al., 2000). AcLDL was used at different concentrations throughout my study (25, 50, 75, 100, 125 and 200 µg/ml).

2.2.4.4 Oxidized LDL

Native oxidized Human Low Density Lipoprotein (OxLDL) was purchased from Bio-Rad Laboratories Inc. as 2 mg powder of purified protein from human plasma. Reconstitution was performed according to manufacturer's instructions in 1 ml of sterile deionised water. Similar to Acetylated LDL (Section 2.2.4.3) this form has also undergone ultracentrifugation and purification to homogeneity. Oxidation was carried out using 20 µM cupric sulphate in PBS at 37°C for 24 hours, and was terminated with excess EDTA. The level of oxidation was measured by TBARS (Thiobarbituric acid reactive substances) and determined via a Malondialdehyde (MDA) standard. The oxidation levels were batch specific as informed by the supplier, the

oxidation levels of the batches I received were 24.6 nmoles/mg protein and 38.9 nmoles/mg. In addition to its contribution in the overall cholesterol accumulation during the development of atherosclerosis, OxLDL molecules are favourably engulfed by macrophages, a process resulting in the macrophage-foam cell differentiation, an important step in the pathophysiology of an atheromatous plaque formation (Zhang et al., 2017). Due to their reported presence in atheromatous plaques and because of their vital role in the pathophysiology of atherosclerosis, it was important to investigate their potential to influence the activity of IL-1β. OxLDL was used at different concentrations throughout my study (25, 50, 75 and 100µg/ml).

2.2.4.5 Native Human Free LDL Cholesterol

Human plasma derived low density lipoprotein was purchased from Sigma-Aldrich as a lyophilized powder. Native LDL was generated at concentration of 1 mg/ml LDL in PBS and stored immediately in 500 µl aliquots at -20°C until used fresh prior each experiment. Native LDL was used at different concentrations throughout my study (25, 50, 75 and 100µg/ml).

2.2.5 Collection of Cell Lysates and Culture Supernatants

After incubation with cholesterol, the culture supernatants of each well were collected and transferred to a set of ice-cold Eppendorf tubes. Cell debris was removed by centrifugation at 300g for 5 minutes, and the supernatant transferred to a new ice cold Eppendorf tube and immediately stored in -20°C until analysed by ELISA.

The cells in each well were then washed twice with 1 ml of ice cold PBS (or Hanks' Balanced Salt Solution in HCASMCs) with the plate placed on ice

68

throughout. Cell lysates were collected via scraping the cells with a disposable cell scraper for each well, in 500µl ice-cold lysis buffer composed of 0.1% (v/v) Triton-X100 in PBS. Triton X was used as a detergent as it can gently detach the cells and has the ability to dissolve cellular membranes (Birdwell et al., 1978). To ensure complete lysis of cells, the lysate suspension was pipetted 4-5 times of the contents against the bottom of each well before transferring into an ice-cold Eppendorf tube. To prevent degradation of IL-1, lysates were stored immediately at -20°C and analysed within 48 hours, or stored at -80°C if immediate analysis wasn't possible.

2.2.6 IL-1β Quantification Using ELISA

A quantitative sandwich enzyme linked immunosorbent assay (ELISA) kit (DLB50 by R&D Systems©, UK) was used to directly measure the levels of mature IL-1β (17 kDa). Investigating the effect of cholesterol on the release of IL-1β in the culture supernatants and the production of IL-1β within the cells lysates is a vital aim of the study, therefore both culture supernatants and cell lysates were analysed.

The ELISA was performed following the manufacturer's instructions. Briefly, a standard curve was generated from IL-1β standards at concentrations of 3.9, 7.8, 15.6, 31.2, 62.5, 125, and 250 pg/ml in duplicate samples. Samples (test, standards and controls) were added to the ELISA plate, covered by a covering lid and incubated at room temperature for 2 hours. The plate was then washed three times with a supplied wash buffer. After the last wash the plate was inverted against a clean paper towel and blotted to ensure complete removal of buffer. IL-1β conjugated antibody was then added to

69

each well and the plate incubated for 1 hour at room temperature. The plate was then washed as before, and a supplied substrate solution (stabilized hydrogen peroxide plus stabilized chromogen tetramethylbenzidine) was added to each well. The plate was protected from light by foil covering and incubated for 20 minutes at room temperature. The reaction was then stopped using the supplied stop solution (2N sulphuric acid). To ensure thorough mixing of the stop solution, the plate was gently tapped and/or gently mixed using a 10 μl pipette tip.

The plate was then read using a Varioskan© Flash microplate reader from Thermo Scientific©, at OD of 450nm. A standard curve was constructed using a four parameter logistic (4-PL) curve-fit using Skanit RE for Varioskan Flash 2.4.5 software. The average concentrations of IL-1β in pg/ml of all samples were than calculated using the four parameter logistic curve.

The data were then analysed using the GraphPad prism for windows software, version 8.0.

2.2.7 Lactate Dehydrogenase Cytotoxicity Assay

A LDH cytotoxixity assay was performed to ensure that the quantified levels of IL-1β detected within cells and supernatants were due to stimulation by cholesterol and not secondary to cell death caused by toxicity. Lactate dehydrogenase (LDH) is an intracellular enzyme present in almost all cell types which acts as a mediator to the enzymatic oxidation of lactate to pyruvate (Sekine et al., 1994). It is released rapidly to the extracellular area when the cells are damaged by injury, chemicals or stress. Therefore, LDH

70

measurement is an *in vitro* method that is commonly used as a cell death indicator (Abe and Matsuki, 2000).

HUVECs and HCAECs (80-90% confluent), were seeded into 12 well experimental plates in CGM (see section 2.2.1 for protocol and seeding densities) and were incubated at 37°C with 5% CO_2 for 48 hours. The media was then changed into CGM with the pro-inflammatory cytokine combination TNF-α and IL-1α (10 ng/ml, each) and incubated for a further 48 hours. As negative control, two wells were incubated in CGM alone. The media was then changed into SFM and cholesterol or NE added.

Cells were treated with either water-soluble cholesterol (100, 250 and 500 µg/ml), MβCD (100, 250 and 500 µg/ml) as negative control, AgLDL (25, 50, 75, 100, 125 and 200 µg/ml) or NE (1 µg/ml). As controls, some wells were incubated with media +/- cytokines. All incubations were for 6 hours at 37°C with 5% CO_2.

Cell cytotoxicity (viability) was measured using a LDH cytotoxicity assay (G1780 from Promega©, USA) performed fresh on supernatants collected immediately after incubation (with NE or cholesterol).

Following manufacturer's instructions, each sample was loaded into an assay plate and substrate solution was added. The plate was then covered by foil to protect from light, and incubated for 30 minutes at room temperature. To stop the reaction, 50µl of the supplied stop solution was added to all wells, and the plate was placed immediately in the chamber of a Varioskan© Flash microplate reader, where the absorbance was recorded

71

at 490nm within 30 minutes. The percentage of LDH released into the supernatant was then calculated.

2.2.8 Caspase-1 Activity Assay

A Caspase-Glo® 1 Activity Assay was purchased from Promega® (Catalogue number G9951). This assay is specific for the use with a 96-well plate and does not require any form of sample preparation, allowing the assay to perform high throuput screening of the activity of caspase-1 and the inflammasome activation.

Following the manufacturer's instructions, cells were seeded into a 96-well plate (30,000 cells/100 µl) and equal volumes of the Caspase-Glo® 1 reagent were added to each well (1:2). The plate was left incubated at room temperature and covered with foil for one hour. Luminescence was then measured using the plate-reading luminometer.

2.2.9 Inhibition of Caspase-1, NLRP3 and the P2X7 receptor

To determine the mechanism of IL-1 release/cholesterol uptake in cells, inhibitors of Caspase-1, NLRP3 and the P2X7 receptor were used. All inhibitors were delivered in SFM for 1 hour prior to cholesterol treatment (following the protocol in section 2.2.4).

For inhibition of Caspase-1 YVAD (50 µM (27 µg/ml)) was used. Studies showed that YVAD provides an irreversible cell-permeable and selective inhibition of caspase-1 (Garcia-Calvo et al., 1998, Zhang et al., 2014, Alfaidi et al., 2015).

MCC950 (10 µM (4.04 µg/ml)) was used as an inhibitor of the NLRP3 inflammasome. MCC95O is a selective and potent inhibitor, which prevents the oligomerization of the NLRP3 inflammasome adaptor protein ASC (apoptosis-associated speck-like protein), blocking the release IL 1β induced by the inflammasome activators such as nigericin and ATP (Coll et al., 2015, Swanson et al., 2019, Guo et al., 2015).

The chemical A438079 hydrochloride (2.5 µM (0.8565 µg/ml)), a competitive P2X7 receptor antagonist, was used to challenge the P2X7 receptor in my study. Studies have shown that this compound inhibits phagocytosis and mediates the NLRP3 inflammasome-dependent IL-1β secretion from neutrophils (Braganhol et al., 2015, Karmakar et al., 2016, Jiang et al., 2017).

Further details regarding the inhibitors' concentrations, compositions and sources are listed in appendix (I).

2.2.10 Western Blotting Analysis of IL-1β Isoform

2.2.10.1 Collection of culture supernatants and cell lysates for western blots

Western blotting was performed on samples prepared following protocols described in sections (2.2.1 - 2.2.5). At the end of each experiment, supernatants were collected. The cells were then washed with ice cold PBS while the plates placed on ice. Each well was then treated with 100 µl of newly prepared ice cold RIPA buffer (see appendix for components) in 12-well plates or 200 µl of buffer in 6-well plates. Cell lysates were collected (see section 2.2.5) and centrifuged at 500 g at 4 degrees for 10 minutes.

Supernatants were collected and the pellet was discarded. Both supernatants and lysates were stored at -80 until analysed.

2.2.10.2 Acetone precipitation and preparation of samples for electrophoresis

In some experiments when assessing low levels of protein by western blot it was necessary to use alternative methods. Acetone precipitation was performed as per the protocol described by (Mambwe et al., 2019). Ice cold acetone (4 ml per ml of media collected) was added to samples and incubated at -20°C for one hour. The solution was then centrifuged at 1500 rpm for 15 minutes. The supernatant was discarded and the pellet was air-dried in a fume hood for 20 minutes. The pellets were then re-suspended in equal volumes of laemmlli buffer (100-150 µl) and boiled using a heat block at 95°C for 5 minutes.

Following boiling, the samples were loaded into a NuPAGE™ 4-12% Bis-Tris Protein Gel (30 µl/well), and run at 200V for 30 minutes. The gel was then extracted from its plastic cassette to prepare it for blotting.

2.2.10.3 Western Blotting using iBlot 2™

The extracted gel from section 2.2.10.2 was soaked in 20% v/v ethanol to activate it prior to blotting on the iBlot 2™ machine (See Appendix as per the manufacturer's recommendation). The gel was placed gently against a nitrocellulose membrane provided in each cassette of the iBlot™ 2 nitrocellulose transfer stacks. The cassette was enclosed following manufacturer's instructions (20 volt using 0.9A current), and blotted for 7 minutes.

Following blotting, the cassette was discarded and the membrane placed in a tray with 10 ml of Odyssey® Blocking Buffer in TBS for one hour. After blocking the membrane was placed on a rotating tray and washed three times for 5 minutes with 0.01% v/v TBS-Tween (Tween20 from VWR chemicals see appendix A.2.4 for details and composition).

The membrane was treated with the primary antibody of choice diluted in the blocking buffer and incubated overnight at 4°C (See appendix (I) for list of all primary antibodies used, their concentrations, sources and dilutions).

The membrane was then washed three times for 5 minutes each in TBS-Tween and incubated with the secondary antibody in room temperature for 1 hour. The washing process was then repeated and the membrane placed on the Licor machine for measurements to be taken (See appendix (I) for list of all secondary antibodies used, their concentrations, sources and dilutions).

2.2.11 Microscopic Imaging of LDL molecules
2.2.11.1 Acetylated LDL and Plasma membrane labelling with CtB and WGA in HCAECs

To determine uptake of cholesterol into cells, HCAECs were stained for the presence of acetylated LDL (AcLDL) molecules as previously described (Singh et al., 2016). A directly conjugated LDL was used (AcLDL Alexa Fluor™ 488 Conjugate, see appendix (I) for details).

Three glass bottom dishes (35 mm dish with No. 1.5 coverslip with a glass diameter of 14 mm, supplied from MatTek Corporation©, United States) were coated with 1% w/v gelatin and incubated for 10 minutes at 37°C with

95% air/5% CO_2 to enhance cell adherence to the glass surface. HCAECs were trypsinised and seeded (see section 2.2.1 for protocol and seeding density) into each dish. Dishes were then incubated for 48 hours.

Cells were then cytokine stimulated (see section 2.2.2 for protocol) and then incubated with LDL (10 and 100 μg/ml) for 6 hours in serum free MV media (Appendix II). As control, one dish was incubated with media alone.

After 5 hours of LDL treatment and for the last hour, all three dishes were treated with AcLDL Alexa Fluor™ 488 Conjugate (10 μg/ml). After the 6-hour incubation, cells were washed gently with PBS (pH 7.4) and the dishes were placed on ice. Cells were then labelled with Cholera Toxin Subunit B (CTB), Alexa Fluor™ 555 (CTB-555) conjugate (10 μg/ml) for 5 minutes on ice. CTB staining was used for labelling the plasma membrane and cell surface.

The media was discarded and the cells were washed gently with PBS and fixed immediately with 4% w/v paraformaldehyde (PFA) and 0.5% v/v glutaraldehyde in PBS (pH 7.4) at 1 ml/dish for 45 minutes in room temperature, then washed with PBS. Glutaraldehyde was added to the fixation solution due to block diffusion of lipid-linked proteins (Perez et al., 2017, Singh et al., 2016).

Finally, cells were labelled with Wheat Germ Agglutinin (WGA), Alexa Fluor™ 647 Conjugate (1 μg/ml in PBS) for 10 minutes in room temperature. The aim of WGA labelling was to allow visualisation of the compartments which contain LDL molecules inside the cells. Cells imaging was done using a Zeiss LSM 510 confocal fluorescent microscope.

2.2.11.2 Imaging of LDL Uptake by HCAECs

After treating HCAECs with LDL (Either OxLDL, AcLDL or Native LDL, see sections 2.2.4 & 2.2.5 for protocol), cells were washed with ice cold PBS three times and immediately fixed at room temperature with 10% Buffered Formalin solution (see appendix (II) section A.2.5 for composition). The fixation process with the formalin solution was carried under a ventilated fume hood for 15 minutes. The experimental plate was taken then to a bright field microscope and imaged.

2.2.12 Statistical Analysis

All statistical analyses were done using GraphPad prism for windows software, version 8.0.2. To check whether or not the data sets presented were normally or not normally distributed, Shapiro–Wilk's test was used to confirm that my data were not normally distributed prior to running statistical analysis with Anova or student independent T-Test. Below is an example of data analysed by Shapiro-Wilk test using a normality and lognormality QQ plot (Figure 2.5).

All experiments were repeated on three different biological donors at least, or three technical repeats as mentioned. One way Anova with corrections for multiple comparisons by Bonferroni post hoc test was used in all data containing more than two groups (with one variable being quantified levels of IL-1β by ELISA) and multiple experimental assay controls. In experiments that had two groups only, student T-Test was used.
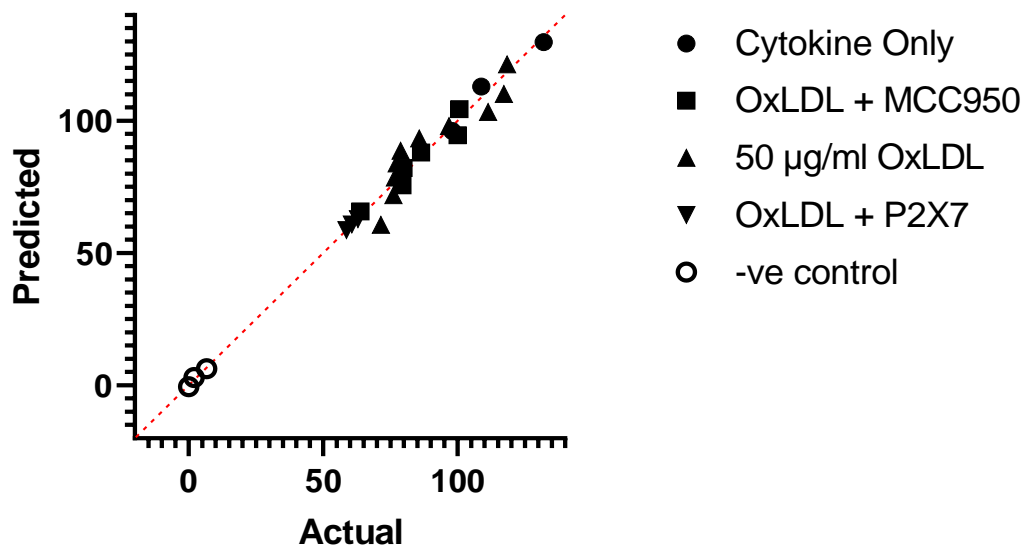
(Figure 2.5) Normality and lognormality test for all data sets: QQ plot showing the linear distribution of data. In addition to the linear distribution and passing the normality test on GraphPad prism, Shapiro-Wilk test was also used to confirm that the data are normally distributed. This test example was carried on the graph in Chapter 5 (Figure 5.4A), n=3.

(Chapter 3) Optimisation of the Experimental Conditions for the Release of IL-1β, Including Type of Vascular Cell and Lipid Formulation

3.1 Introduction

Inflammation is involved in all phases of coronary artery disease (Kleemann et al., 2008, Randolph, 2014). The role of active inflammation in atherosclerotic plaques increases vulnerability and can lead to plaque rupture (Sakaguchi et al., 2017, Shah, 2003), which is a significant clinical event with life threatening manifestations such as MI and stroke (Bentzon et al., 2014).

As a consequence of inflammation, activation of the endothelium occurs (Gimbrone and García-Cardeña, 2016). The activated endothelium within a highly inflammatory environment of an atherosclerotic lesion causes endothelial cells and macrophages to produce high levels of pro-inflammatory cytokines, such as IL-1β, which maintains the inflammatory process, through the induction of an adhesion cascade (Gomez et al., 2017, Ceneri et al., 2017).

Cholesterol is present in atherosclerotic lesions from early stages, in the form of lipoprotein particles and lipid droplets containing free circulatory cholesterol. Due to oxidative, acidic and enzymatic modifications, some non-inflammatory plasma lipoprotein molecules transform into crystallised particles, forming cholesterol crystals (Grebe and Latz, 2013, Abdul-Muneer et al., 2017). It has recently been shown that both cholesterol in the form of crystals and free LDL molecules induce the release of IL-1β from macrophages and monocytes *in vitro*, but the role of cholesterol in promoting the production and release of IL-1β from endothelial cells

remains to be elucidated (Estruch et al., 2015, Samstad et al., 2014, Duewell et al., 2010).

This project focuses on investigating the role of cholesterol in inducing the release of IL-1β from the vascular endothelium. Specifically, the experiments presented in this chapter aim to identify the most effective form of cholesterol with respect to promoting IL-1β release from vascular cells, to be used in future experiments to elucidate the molecular mechanism of release (Chapter 5), and to optimise experimental conditions using HUVEC prior to using more clinically relevant, but also more expensive HCAECs (Chapter 4). In this chapter, two types of cholesterol were studied: water-soluble cholesterol and aggregated LDL (AgLDL).

3.2 Brief Materials and Methods

All materials and methods used in the experimental approaches in this chapter are detailed in (Chapter 2), briefly: HUVECs were seeded at passages 2-5 into 12 well plates and were allowed to grow until they were 80-90% confluent (approximately 48 hrs incubation). Cells were then stimulated by the cytokines IL-1α and TNF-α at a concentration of 10 ng/ml for each, for 48 hrs. After thorough washing with PBS, cholesterol treatment (with either water-soluble cholesterol or AgLDL) was applied to the cells for 6 hrs in serum free media. Cells were harvested and samples stored until analysis. Supernatant media was also collected and analysed for cytotoxicity using a LDH toxicity assay. IL-1β ELISA was performed to measure the amounts of produced and released IL-1β in response to cholesterol treatment and pro-inflammatory cytokine stimulation. Bright-field microscopic images were

81

taken to investigate the uptake of LDL molecules by vascular endothelial cells and the changes of cell morphology in response to stimulation and/or treatment.

3.3 Results

3.3.1 IL-1α and TNF-α in combination promote production, but only minimal release, of IL-1β in HUVECs.

In this initial experiment, I investigated whether HUVECs could produce and release IL-1β without needing a second stimulus. As stimulation with a combination of IL-1α and TNF-α has previously been reported to upregulate intracellular levels of pro-IL-1β (Wilson et al., 2007, Alfaidi et al., 2015) to a detectable level, HUVECs were stimulated with a combination of these pro-inflammatory cytokines prior to incubating with cholesterol or NE (as positive control). NE has previously been shown to induce IL-1β release from endothelial cells; hence, it is a suitable positive control for the assay. Observing cells under phase contrast and bright-field microscopy showed that the morphology of stimulated cells was changed. HUVECs appeared elongated in comparison to unstimulated cells, which had a cobblestone appearance (Figure 3.1B compared with Figure 3.1A).
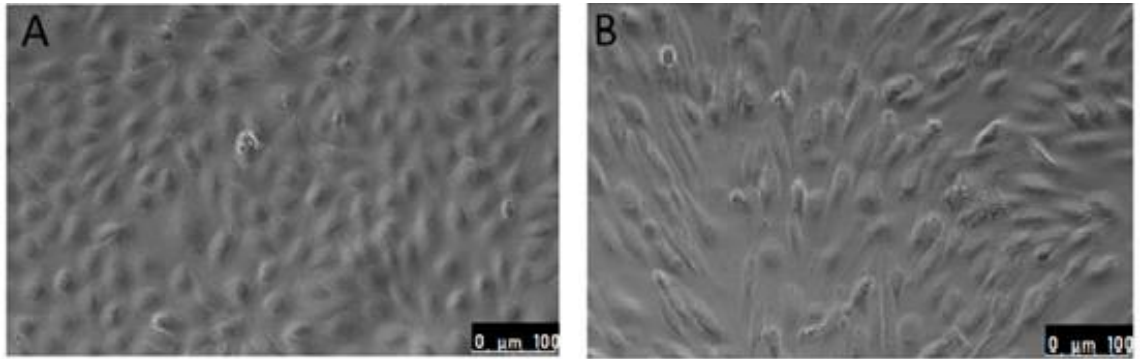
(Figure 3.1) Morphologic change of HUVECs in response to cytokine stimulation: A and B are representative images of HUVECs seeded at passage 2 in a 6-well plate and allowed to grow until confluent at 37°C with 95% air/5% CO_2. In (A), the control cells were left in CGM and not stimulated. The cobblestone shape of HUVECs appears to be maintained. In (B) (stimulated cells with 10 ng/ml of IL-1α and TNF-α) the elongated appearance of cells suggests their successful priming. Images are representative and were recorded at 48 hours post incubation with the cytokines after fixing the cells with 2% w/v PFA. Images were taken using a bright-field phase contrast Leica© microscope x100 eyepiece. Scale Bar = 100 μm.

Next, HUVECs from 3 different donors were seeded into experimental plates and stimulated with cytokines TNF-α and IL-1α as described in section 2.2.2. Cells in 'plain' CGM with no cytokine stimulation were used as controls. IL-1β, measured by ELISA, showed 35-fold elevated levels of IL-1β in the lysates (125.4 ± 11.51 pg/ml) compared to unstimulated control cells (3.68 ± 0.65 pg/ml) (Figure 3.2A), indicating the successful stimulation and upregulation of IL-1β intracellularly.

In supernatants from these experiments, there was a consistent very low release of IL-1β (>15 pg/ml) into cell supernatants as shown in (Figure 3.2B).
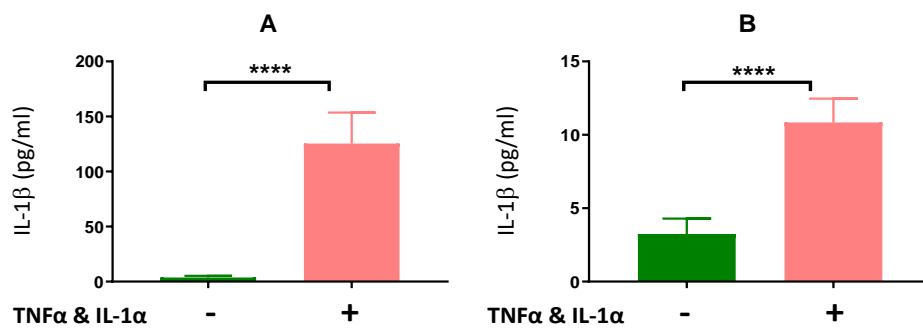
(Figure 3.2) TNF-α and IL-1α upregulate the production intracellularly (A) and release (B) of IL-1β in stimulated HUVECs. HUVECs from three different cords were seeded and stimulated with both TNFα and IL-1α for 48 hours at concentrations of 10 ng/ml each. (A) cell lysates and (B) cell culture supernatants. Values are presented as mean ± SEM, unpaired t-test was used for comparison between both samples, ****p<0.0001, n=3.

3.3.2 NE induces the release of IL-1β from HUVECs

Next, to augment the release of IL-1β from HUVECs, I tested a known positive control, neutrophil elastase (NE) (Alfaidi et al., 2015). Three different biological donors of HUVECs were stimulated with the cytokine combination used in the previous section (section 3.3.1) and then either left stimulated with cytokines (incubated with CGM) as controls or treated with NE for 6 hours, after thorough PBS washing. Culture supernatants and cell lysates were collected and assayed for IL-1β by ELISA. Treatment with NE did not alter IL-1β production in the lysates (130.1 ± 4.1 pg/ml) when compared with untreated controls (125.4 ± 11.51 pg/ml) (Figure 3.3A). However, released IL-1β detected in response to NE treatment of HUVECs was significantly increased, compared to cytokines stimulated alone, although absolute levels were relatively low (13.86 ± 0.6 pg/ml) (Figure 3.3B).
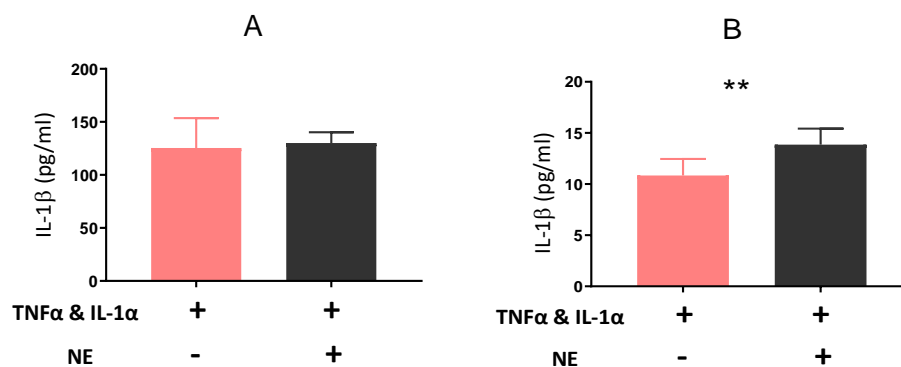
(Figure 3.3) HUVECs release IL-1β extracellularly following 6-hour incubation with NE: Quantification of IL-1β production in lysates (A), followed by release of IL-1β in supernatants (B). Values are presented as mean ± SEM, unpaired t-test was used for comparison between both samples, **$p < 0.01$ in supernatants, n=3.

3.3.3 Water-soluble cholesterol promotes the release of IL-1β in HUVECs

Having established experimental conditions that will reliably induce IL-1β production and release in response to a second stimuli, I examined the effects of different forms of cholesterol upon IL-1β generation and release. Cultured HUVECs from three different donors were seeded into 12-well plates, stimulated with cytokines, and then treated with water-soluble cholesterol at different concentrations as shown in (Figure 2.3, methods). Cell culture lysates and supernatants were assayed for IL-1β using ELISA.

Figures 3.4 and 3.5 show that water-soluble cholesterol led to a decrease in IL-1β inside cells compared to cells treated with only MβCD (the solubilising agent, control). Conversely, an increased release of IL-1β was detected in the supernatant of cholesterol-treated cells when compared with both the MβCD control and with the cytokine only treated control (Figure 3.5).

Levels of IL-1β in cell lysates of cholesterol treated cells were an average of (28.1 ± 3.3), (27.4 ± 2.1) and (23.6 ± 3.7) pg/ml in samples with treatment concentrations of 100, 250 and 500 µg/ml respectively (Figure 3.4). IL-1β production in MβCD treated cells was highest following 250 µg/ml treatment (116.6 ± 10.5 pg/ml). Non-cytokine stimulated, water-soluble cholesterol treated cells had an almost undetectable level of IL-1β of 2.5 ± 0.5 pg/ml. It is clear, therefore, that cells need a pre-treatment with cytokines, in order to upregulate IL-1β inside cells.

TNF & IL-1	+	-	+	-	+	+	+	+	+	+
WSC + MßCD (µg/ml)	-	250	-	-	100	-	250	-	500	-
MßCD (µg/ml)	-	-	-	-	-	100	-	250	-	500
NE	+	-	-	-	-	-	-	-	-	-
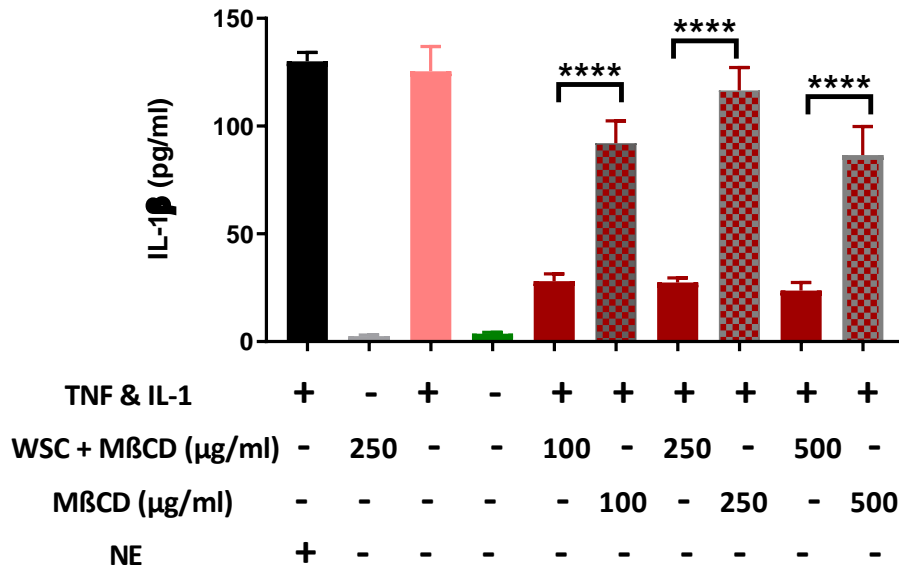
(Figure 3.4) Intracellular levels of IL-1β are lower in water-soluble cholesterol treated HUVECs: Cell lysates of water-soluble cholesterol treated cells and controls were analysed by ELISA for quantification of IL-1β production. Data are expressed as mean ± SEM, n=3 independent donors. Data are analysed by one-way ANOVA with correction for multiple comparisons by Bonferroni post hoc test, ****$p < 0.0001$.

For supernatants from these same experiments, increased release of IL-1β occured with water-soluble cholesterol compared to MβCD alone (Figure 3.5). Average IL-1β release was (16.24 ± 2.3), (22.2 ± 2.3) and (20.4 ± 2.9) pg/ml for the doses 100, 250 and 500 µg/ml cholesterol, respectively.

As a proportion of IL-1 inside HUVECs, approximately 10% was released in response to MβCD and 50% in response to water-soluble cholesterol.
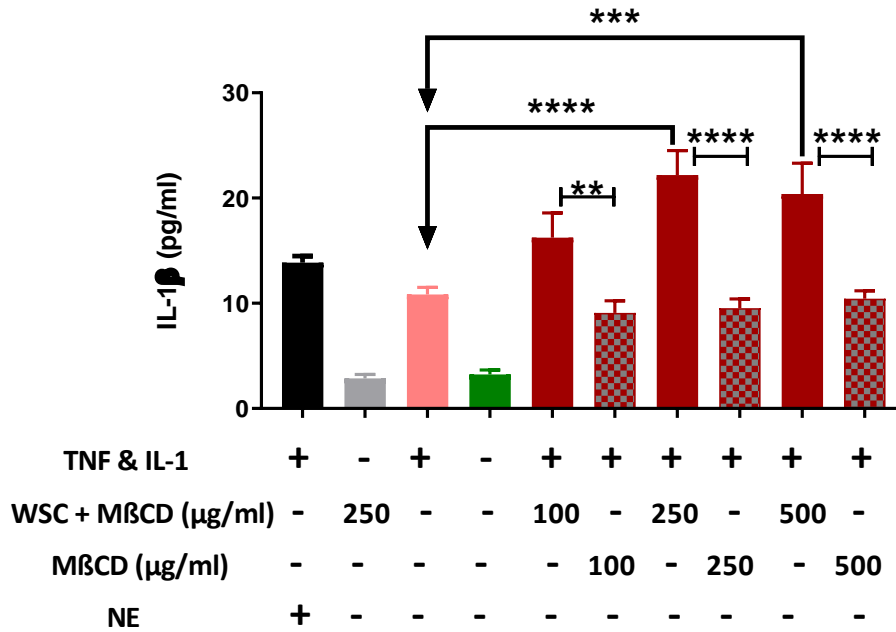
(Figure 3.5) Water-soluble cholesterol promotes the release of IL-1β from HUVECs into culture supernatants: Release of IL-1β was induced from HUVECs treated with water-soluble cholesterol for 6 hours after cytokine stimulation. Data are obtained from cell culture supernatants collected from three sets of experiments using HUVECs each from a different donor (n=3). Data are expressed as mean ± SEM, analysis done by one-way ANOVA followed by Bonferroni post hoc test, **p<0.01 and ***p<0.001, ****p<0.0001.

3.3.4 Water-soluble cholesterol induces the release of lactate dehydrogenase in HUVECs in a dose dependent manner:

To determine whether the IL-1β release seen following cholesterol treatment was due to stimulation of release by, or toxicity of, cholesterol, I measured levels of LDH in supernatants of stimulated cells. LDH release from cells indicates various forms of cell death (den Hartigh and Fink, 2018).

High levels of LDH were released from HUVECs in response to incubation with water-soluble cholesterol in a dose dependent manner (Figure 3.6).

Incubation with the solubilising carrier, MβCD (negative control), had no adverse effects upon LDH release over and above the control (cytokines stimulated only). Specifically, the basal LDH release in CGM was 11%. This was increased 3 fold with cholesterol treatment (100 μg/ml, 250 μg/ml and 500 μg/ml showed a LDH release of 32.9%, 42.9% and 43.2% respectively compared to the positive control).

	Maximum LDH	No Cell Control									
TNF & IL-1			+	-	+	-	+	+	+	+	+	+
WSC + MßCD (μg/ml)			-	250	-	-	100	-	250	-	500	-
MßCD (μg/ml)			-	-	-	-	-	100	-	250	-	500
NE			+	-	-	-	-	-	-	-	-	-
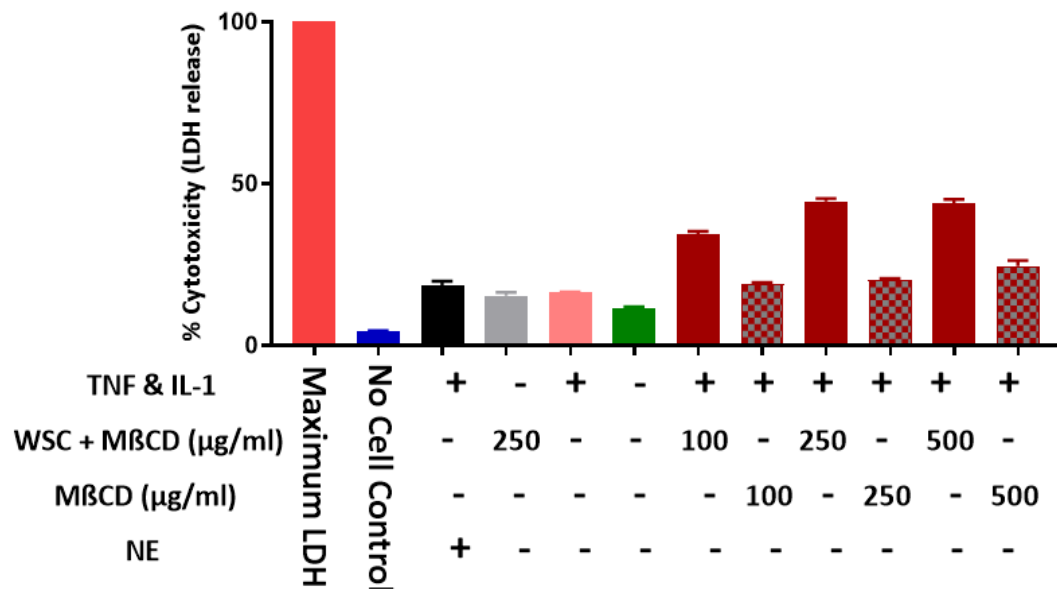
(Figure 3.6) Water-soluble cholesterol treated HUVECs exhibit induced LDH release: Culture supernatants of samples were used for analysis of LDH release by the LDH cytotoxicity assay. Levels of LDH were increased following incubation with water-soluble cholesterol, compared to control, n=3, data are expressed as mean ± SD.

3.3.5 Aggregated LDL is not toxic to HUVECs and does not induce LDH release

It has been widely known that there are multiple forms of cholesterol present in the vessel wall in the setting of atherosclerosis (Stocker and Keaney, 2004, Brown and Goldstein, 1983, Orekhov and Sobenin, 2018). As water-soluble cholesterol is not biologically present, I continued my investigation using AgLDL, a form that has been previously reported to be both present in atherosclerotic plaques of human cardiovascular patients and has been widely studied in *in vitro* models of atherosclerosis (Badimon and Vilahur, 2012, Marathe et al., 1998, Westhorpe et al., 2012). The aim of introducing AgLDL was to see if this form of modified LDL could also potentially induce the release of IL-1β from HUVECs.

Given the previous data on cholesterol toxicity using water-soluble cholesterol (Figure 3.6), I first performed an AgLDL cytotoxicity assay (as described in section 2.2.7), to rule out the possibility that AgLDL was toxic to endothelial cells. The percentage of LDH release in AgLDL treated HUVECs was similar to that of the untreated controls (Figure 3.7), indicating that AgLDL has no toxic effect on HUVECs regardless of the concentrations used.
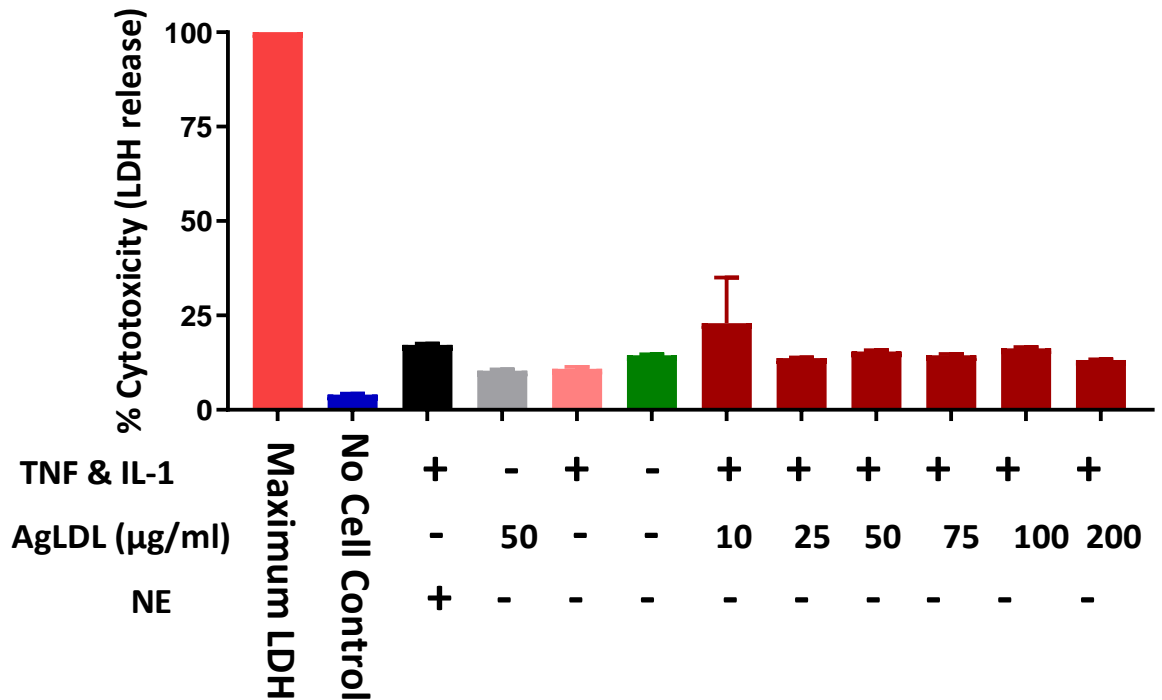
(Figure 3.7) Cytotoxicity assay on HUVECs treated with AgLDL shows no cytotoxicity: An LDH cytotoxicity assay was used to analyse the culture supernatants of cells treated with AgLDL and controls. No significant difference between control and AgLDL treated samples with multiple concentrations (10-200 µg/ml) was seen. Three technical repeats from two different biological donors are presented data are expressed as mean ± SD.

3.3.6 Investigating the Potential Roles of AgLDL Treatment on HUVECs

Once the non-toxicity of AgLDL was confirmed (Section 3.3.5), the potential

role on IL-1β signalling intracellularly and extracellularly was investigated.

After incubation with AgLDL (section 2.2.4.2 for details), HUVECs culture

supernatants and cell lysates were analysed for IL-1β using ELISA.

3.3.6.1 AgLDL does not induce the production IL-1β in HUVECs

AgLDL treated HUVECs showed only low levels of intracellular IL-1β

production (Figure 3.8).

IL-1β quantification of cell lysates showed IL-1β in the AgLDL treated samples was no different to the cytokine-only stimulated controls, with very low IL-1 production in non-cytokine stimulated cells (Figure 3.8). ELISA quantification of lysates from AgLDL treated HUVEC show the quantified levels of IL-1β to be less than 40 pg/ml in each condition (29.2 ± 1.4, 39.4 ± 2.0, 39.4 ± 2.3, 32.7 ± 0.9, 36.3 ± 5.4 and 37.2 ± 3.6 pg/ml, respectively), which is very low compared with previous water-soluble cholesterol data (section 3.3.4). The cytokine only treated samples and the NE treated samples generated 33.8 ± 3.6 and 34.7 ± 3.5 pg/ml IL-1 respectively. Both the assay negative control and the non-cytokine stimulated control treated with 50 μg/ml had approximately 1.4 ± 0.6 pg/ml of IL-1β (which is below the detection limit of the assay at 3.9 pg/ml).

IL-1β (pg/ml)									
TNF & IL-1	+	-	+	-	+	+	+	+	+	+
AgLDL (µg/ml)	-	50	-	-	10	25	50	75	100	200
NE	+	-	-	-	-	-	-	-	-	-
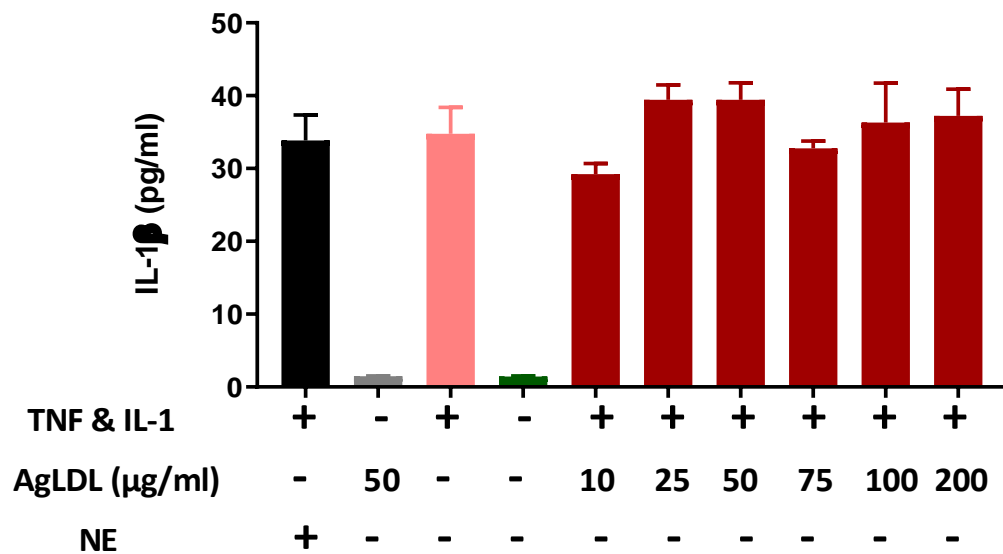
(Figure 3.8) AgLDL has no effect on IL-1β production in HUVECs: HUVECs were treated with different concentrations of AgLDL (10-200 µg/ml) after cytokine stimulation. Cell lysates of AgLDL treated cells and controls were analysed by ELISA for intracellular quantification of IL-1β. Despite multiple concentrations used, AgLDL had no effect on inducing IL-1β production in stimulated or non stimulated HUVECs in comparison with controls. Data are expressed as mean ± SEM, three technical repeats from two different biological donors.

3.3.6.2 AgLDL does not induce the release of IL-1β from HUVECs

IL-1β in cell culture supernatants from samples treated with all different concentrations of AgLDL (except 10 µg/ml), was found to be lower or equal to the levels measured in the cytokine only treated samples (Figure 3.9).

These data strongly suggest that AgLDL does not induce HUVECs to release IL-1β.

TNF & IL-1	+	-	+	-	+	+	+	+	+	+
AgLDL (µg/ml)	-	50	-	-	10	25	50	75	100	200
NE	+	-	-	-	-	-	-	-	-	-
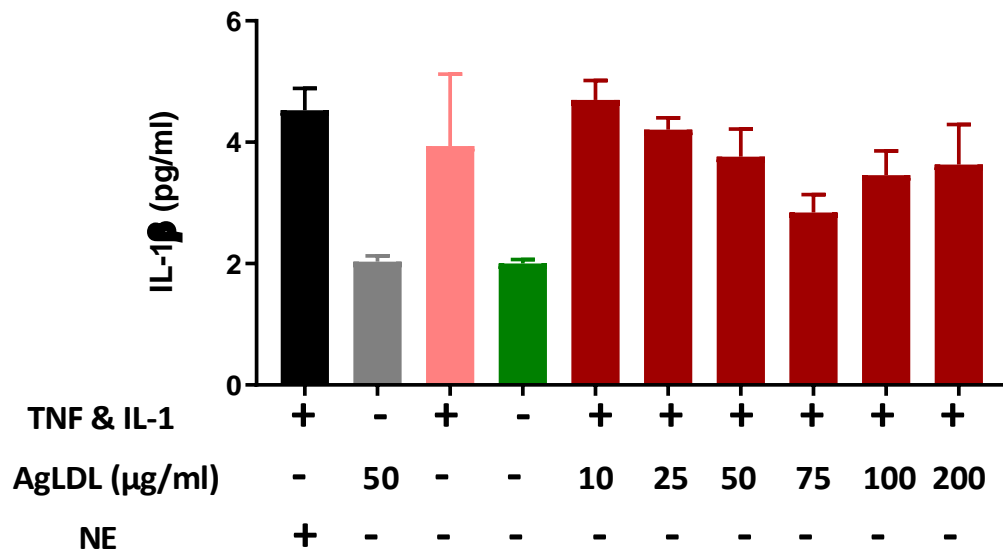
(Figure 3.9) AgLDL has no effect on the release of IL-1β by HUVECs into culture supernatants: ELISA quantification of IL-1β for supernatants showed very low release of IL-1β from all AgLDL treated cells and controls. Data are expressed as mean ± SEM, three technical repeats from two different biological donors.

3.3.7 Summary of Results

In this chapter, I demonstrate, the ability of HUVECs to release IL-1β in response to incubation with water-soluble cholesterol. Optimising this *in vitro* model was necessary before proceeding with more costly cells (HCAECs) and different forms of LDL. Water-soluble cholesterol has successfully shown its capability of being a second signal inducer of mature IL-1β from primed HUVECs, as measured by high sensitivity ELISA, unlike AgLDL. The data obtained from this chapter provide several lines of evidence to support this:

94

- Pro-inflammatory cytokine stimulated (Primed) HUVECs, produce significant high levels of intracellular IL-1β.

- HUVECs require priming, in order to release IL-1β in response to water-soluble cholesterol treatment.

- Un-primed HUVECs, do not release IL-1β in response to water-soluble cholesterol treatment.

- The quantified release of IL-1β from primed HUVECs, in response to water-soluble cholesterol treatment, is higher than the release in response to NE (the positive control).

- The water-soluble cholesterol-induced release of IL-1β is associated with LDH release suggesting cytotoxicity, however this has been investigated in the next two chapters.

3.4 Discussion

HUVECs were stimulated with the cytokine combination TNF-α and IL-1α, a regime that results in priming of endothelial cells and upregulation of the production of intracellular proIL-1β (Alfaidi et al., 2015, Wilson et al., 2007). This combination was chosen, as it induces the activation of Caspase-1 (Furuoka et al., 2016), transcription upregulation of both the NLRP3 inflammasome and proIL-1β (McGeough et al., 2017) and promotes endothelial cell adhesion molecules expression such as E-selectin (Wyble et al., 1997) and ICAM-1 (Thichanpiang et al., 2014). Many cytokines and mediators have been widely used for stimulating vascular smooth muscle cells, macrophages and endothelial cells (in particular INF-γ, TNF-α, IL-1α and LPS), in combinations or alone (Wilson et al., 2007, Masters et al., 2010,

Mullen et al., 2010, Burzynski et al., 2015, Basatemur et al., 2019). However, the work by (Alfaidi et al., 2015) showed that this combination in particular, for the specified duration (IL-1α and TNF-α at a concentration of 10 ng/ml for each, for 48 hrs.) resulted in maximum proIL-1β production in primary vascular endothelial cells.

Upregulation of proIL-1β inside cells is necessary in order to detect the release of mature IL-1β in response to a stimulus (Chan and Schroder, 2020, Andrei et al., 1999). Therefore, successful cytokine stimulation of HUVECs was crucial in all experiments. Incubation with NE was used as a positive control for IL-1β release, as this has previously been reported to significantly enhance release in cytokine stimulated endothelial cells (Alfaidi et al., 2015). Alfaidi, showed that NE cleaved and induced the release of bioactive IL-1β via a vesicular-mediated caspase-1-independent release process.

My data show a morphological change by HUVECs in response to cytokine stimulation, indicating that the cells are successfully primed and this agrees with published reports that the morphological change of HUVECs from cobblestone appearance to elongated indicates that the cells are stimulated (Mason et al., 1997). Interestingly, this appearance is also seen in cells subjected to abnormal high shear stress (DeStefano et al., 2017). Additionally, ELISA analysis confirmed the presence of high levels of IL-1β within the lysate of HUVECs when stimulated with cytokines, which was not seen in lysates of unstimulated control cells. This is in agreement with a study reporting that stimulation with this combination of cytokines

upregulates the production of proIL-1β and unstimulated HUVECs fail to produce constitutive levels of IL-1β (Wilson et al., 2007). Furthermore, the average levels of proIL-1β detected inside the cells was similar to the levels reported in the study by Wilson et al., 2007. This change of morphology together with the IL-1β ELISA data confirmed the successful stimulation of HUVECs.

Although, in HUVECs, cytokine stimulation alone induced low release of IL-1β into supernatants, this release was minimal because the cells were only primed and there was no second signal to induce the maximal release of IL-1β. These findings are supported by the study of Rajamäki et al., (2010), which showed that *IL1A* and *TNFA* mRNAs were both highly and equally induced in primary macrophages that were stimulated with LPS alone or stimulated and treated with cholesterol crystals. However, the study also showed that cholesterol crystal treatment secondary to LPS priming markedly increased the expression of *NLRP3, CASP1* and *IL1B* mRNAs, and only minimal expression was seen in LPS only primed cells. Unsurprisingly, *IL1A, TNFA, IL1B, NLRP3* and *CASP1* mRNAs were not expressed in the non-primed cholesterol crystals-treated macrophages in the same study. Although these data are from primary macrophages, this explains why in my data only limited amounts of IL-1β were secreted into culture supernatants of cytokine only primed cells, and therefore no robust release of IL-1β was detected due to the absence of a second signal that cleaves the proIL-1β into a mature form.

The potential role of water-soluble cholesterol as a secondary signal for inducing the release of proIL-1β in cytokine stimulated HUVECs was investigated, for the first time. Cholesterol is a primary structural component that maintains cellular membrane integrity and fluidity, therefore it is structured to be insoluble in blood and in aqueous medium (Roy et al., 2006). However, free cholesterol can be conjugated with a compound such as methyl-β-cyclodextrin to mimic solubility (Rong et al., 2003). This water-soluble cholesterol compound was used previously in an atherosclerosis *in vitro* model of a lipid uptake study using mouse vascular SMCs (Xu et al., 2010). This study showed the water-soluble cholesterol treatment caused SMCs to undergo a complex mode of cell death and organelle damage, which activated SMCs autophagy of cholesterol as a survival process to prevent water-soluble cholesterol induced cell death.

In my work, unstimulated HUVECs treated with water-soluble cholesterol alone was found not to have increased intracellular production of IL-1β, further indicating that cytokine stimulation is crucial in this experimental protocol. Stimulated HUVECs treated with water-soluble cholesterol showed decreased IL-1β inside cells in contrast to the 'control' MβCD (the solubilising agent). This suggested that water-soluble cholesterol did not enter the cell, or that water-soluble cholesterol inhibited the production of intracellular IL-1β, that water-soluble cholesterol induces cell death and/or that the produced levels of IL-1β were released out of the cell into the medium.

It has been previously shown that water-soluble cholesterol is taken up by SMCs (Xu et al., 2010), ruling this out as a possible reason. Furthermore, MβCD only treated cells showed high levels of intracellular IL-1β, indicating that MβCD does not inhibit IL-1β production. Interestingly, there was a statistically significant increased release of IL-1β by water-soluble cholesterol in HUVECs compared to MβCD only treated controls, which was higher than that from cells treated with NE (the positive control). Therefore, it seemed possible that water-soluble cholesterol treated cells have decreased IL-1β, due to the successful high release of IL-1β from the cells.

My data, however, showed that water-soluble cholesterol, at the concentrations used in this project, might have potentially caused endothelial cell toxicity (which was further investigated in the next two chapters). This occurred despite the cells appearing to be physically intact by phase contrast microscopy. The percentage LDH that was released appeared to be correlated with the concentration of water-soluble cholesterol used. These data indicate that the IL-1β released into the culture supernatant is either because of the stimulation of active release in response to water-soluble cholesterol treatment, because of cell death induced by the water-soluble cholesterol. Cell toxicity is unlikely; as despite LDH release, the cells remain attached and appear healthy microscopically. LDH release is also associated with pyroptosis (Evavold et al., 2018), which is discussed in detail in chapter 5 and is a more likely explanation of the LDH release. These findings support a previous study that showed smooth muscle cell induced LDH release following incubation with doses higher than 20 μg/ml of water-

soluble cholesterol (Rong et al., 2003). However, in that study the incubation period was 72 hours, rather than 6-hours. Since the treatment of MβCD alone did not cause cell death, nor increased LDH, I conclude that it is the water-soluble cholesterol conjugated to MβCD at the concentrations studied that caused endothelial cell induced LDH release which was associated with the release of IL-1β.

Since the overall aim of my project was to investigate the effects of cholesterol with its multiple forms on IL-1β induced release from the vascular endothelium, and after finding the data above, I proceeded to investigate a more clinically relevant form of cholesterol that is the major carrier of cholesterol in lesions (Kruth, 2001). One such form is aggregated LDL, which is believed to be formed *in vivo* (Persson et al., 2006) and has been found in early lesions and the subendothelial space (Frank and Fogelman, 1989, Tamminen et al., 1999) and found in plaques of ApoE knockout mice (Maor et al., 2000). In addition, other studies have shown that HVSMCs incubation with AgLDL *in vitro* can induce foam cell formation (Costales et al., 2015) a major pathological milestone in early atherosclerotic lesion formation (Clinton et al., 1992, Yahagi et al., 2016). Costales et al., (2015) also showed the internalisation and uptake of AgLDL molecules by HVSMCs after a 4 hour incubation (at concentration of 75 and 100 μg/ml) using AgLDL staining viewed by confocal laser microscopy.

My data revealed no cytotoxicity of AgLDL on HUVECS at the concentrations studied, in agreement with studies that showed that the process of

aggregation of OxLDL reduced OxLDL cytotoxicity (Asmis et al., 2005). Surprisingly, however, AgLDL led to a low amount of IL-1β production in HUVECs and therefore was no appreciable and measurable release of mature IL-1β in these experiments. This was further investigated in HCAECs in the next chapter.

3.4.1 Limitations and future work

HUVECs were used as an initial model of vascular endothelial cells, due to their cost effectiveness compared to HCAECs. Although HUVECs are venous endothelial cells, and the focus of my project is on arterial endothelial cells (HCAECs), which are prone to develop atherosclerotic lesions (Mestas and Ley, 2008) , HUVECs are still widely used in studies as an *in vitro* model of atherosclerosis. However, due to the project timeframe and the specific focus of this project on HCAECs, the work conducted on HUVECs was not continued.

A next step to take the work from this chapter forward is to investigate the uptake of AgLDL by HUVECs. One such way is using oil red O staining of cholesterol (Kubo et al., 1997). Also investigating the effects of other modified LDLs (such as OxLDL and AcLDL) on the release of IL-1 and other pro-inflammatory cytokines. Recent studies highlighted the relationship between atherosclerosis development and venous thrombosis (Reich et al., 2006, Prandoni et al., 2006). During atherosclerosis development in patients, both blood coagulation and platelets are activated in addition to increased turnover of fibrin, which leads to developing thrombotic complications (Prandoni et al., 2003). However, it is not fully understood how

101

atherosclerosis contributes towards increasing the risk of venous thromboembolism (Arenas de Larriva et al., 2019).

Investigating the mechanism of IL-1 release from HUVECs and comparing the mechanism of release, from venous, with that from arterial endothelial cells, will add to the understanding of atherosclerosis development and its association with cardiovascular diseases.

3.5 Conclusions and Summary of Chapter

In this chapter, I optimised an *in vitro* model of studying the IL-1β induced release from human vascular endothelial cells using HUVECs. This model will be used in more expensive and more biological relevant vascular endothelial cells in the next chapters (HCAECs). The data collected from the experiments conducted in this chapter showed the potential of modified cholesterol as a second stimulus to induce the release of IL-1β, secondary to pro-inflammatory cytokine stimulation. The results also increased my attention towards a possible relationship between LDH release (while cells appear microscopically viable and intact) and the release of IL-1β from cells, which will be further investigated in the upcoming chapters.

(Chapter 4) Modified LDL Cholesterol Induces IL-1β Release from Primed Human Coronary Artery Endothelial Cells

4.1 Introduction

Having established the optimal conditions for an *in vitro* model of cholesterol-induced IL-1β release from HUVECs, I extended my studies into a more biologically relevant endothelial cell type: human coronary artery endothelial cells (HCAECs). These cells are more representative of the microenvironment of atherosclerosis, making the findings more clinically relevant, an important factor in my study.

Although it has been widely shown that macrophages take up some forms of modified LDL, in particular OxLDL (Ooi et al., 2017), there are multiple other forms of LDL reported to be present in atherosclerotic lesions, such as AgLDL (Tamminen et al., 1999), electronegative LDL (Sobal et al., 2000) and glycated LDL (Sobal et al., 2000).

During the process of atherosclerosis development, and due to the combined effect of certain oxidants (ROS, free radicals, myeloperoxidase, lipoxygenase) as well as lipolytic (phospholipase A2, sphingomyelinase, phospholipase C), hydrolytic (esterase), and proteolytic enzymes (thrombin, tryptase, kinase, metalloproteinases), LDL molecules undergo modification processes. These modifications, which are either chemical, structural, or both, result in the generation of different types of modified LDL molecules, with OxLDL and AgLDL being the most commonly found, and the most widely studied (Badimon and Vilahur, 2012, Westhorpe et al., 2012, Marathe et al., 1998).

Previous studies showed that macrophages take up molecules of acetylated LDL (AcLDL) *in vitro*, and this increases the expression of inflammatory molecules such as ICAM-1 and MMP9 in addition to causing apoptosis (Han et al., 2009, Virella et al., 1995), promoting release of IL-1β (Akeson et al., 1991, Wakabayashi et al., 2018).

The surfaces of vascular cell walls (smooth muscle cells, endothelial cells and macrophages) have several scavenger receptors such as CD36, LOX-1 and TLRs, which all promote the internalisation of OxLDL and mediate its cellular effects (Di Pietro et al., 2016, Kiyan et al., 2014). OxLDL also plays a major role in inducing the release of IL-1β from macrophages by activating the NLRP3 inflammasome (Liu et al., 2014), secondary to its uptake, which is mainly by the scavenger receptor CD36 (Kuda et al., 2013, Stewart et al., 2005).

These studies suggest AcLDL and OxLDL may be potential stimulants of cytokine release in endothelial cells. OxLDL has already been found in human coronary atherosclerotic plaques (Hasanally et al., 2017, Nishi et al., 2002). AcLDL, however, although widely used as a modified LDL and a lipid model, is not biologically available and has not been reported *in vivo* (Steinberg, 2009).

Recent studies have also raised attention towards the importance of native (unmodified) LDL in the early stages of inflammation, endothelial dysfunction and atherosclerotic lesion formation by interacting with ROS leading to oxidation and transformation into OxLDL (Lubrano and Balzan,

2014). ROS upregulates LOX-1 with or without the presence of Native LDL, although the extent of upregulation of LOX-1 is increased when ROS interacts with Native LDL, resulting in OxLDL formation. In view of this, and to investigate the role of unmodified LDL and to further understand the effect on endothelial cells between modified vs un-modified LDL, I studied free native human LDL in my study.

In this chapter, therefore, HCAECs were stimulated with pro-inflammatory cytokines and water-soluble cholesterol was used as a potential release stimulus. Then, the effect of AgLDL, AcLDL, OxLDL and unmodified native human low-density lipoprotein (Native LDL) were tested for their ability to potentiate release of IL-1β from endothelial cells.

The first part of my project hypothesis was to identify whether or not vascular endothelial cells take up cholesterol. Since the endothelium is the innermost layer of the vascular wall, there is a high potential for the inflamed and damaged endothelial cell layer to engulf modified LDL molecules, or act as a gateway for their entry during the pathological development of an atherosclerotic lesion. Published studies have shown microscopic images illustrating macrophage uptake of LDL (Roy et al., 2019, Haberland et al., 2001). However, very few studies have examined endothelial cellular uptake of modified LDL. Therefore, I examined the change of morphology and behaviour of HCAECs in response to incubation with modified and unmodified LDL molecules.

106

The second part of my hypothesis was to investigate if endothelial cells would release IL-1β secondary to the uptake of LDL, and whether or not IL-1β release is dependent on LDL entering the vascular endothelial cells, providing a second signal to activate proteins able to cleave and release mature IL-1β from the cells.

After setting a solid experimental infrastructure for my project with the optimisation of the *in vitro* model (Chapter 3), this chapter illustrates the experimental work that I conducted to address the first two parts of my hypothesis.

4.2 Materials and Methods

Detailed materials and methods used in this chapter are explained in (Chapter 2). Concentrations, sources and lot numbers of all reagents used, can be found in Appendices (I) and (II). Briefly, HCAECs were cultured as per protocol (section 2.2.1.2). Modified and non-modified cholesterol treatments were applied to the cells (section 2.2.4). HCAECs culture samples were used for quantification of IL-1β by ELISA (section 2.2.6), LDH toxicity assay (section 2.2.7) and western blotting (section 2.2.10). HCAECs were imaged by fluorescent and bright-field microscopy as per protocols (section 2.2.11).

4.3 Results

4.3.1 IL-1α and TNF-α in combination promote production and release of IL-1β in HCAECs.

HCAECs were seeded and stimulated with TNF-α and IL-1α, as described in

(section 2.2.2). Similar to HUVECs, bright field microscopic imaging of

stimulated HCAECs show a changed morphology from round cells to long

string-shaped cells (Figure 4.1B compared with Figure 4.1A). This indicated

that the cells were successfully stimulated, which was later confirmed by

ELISA.
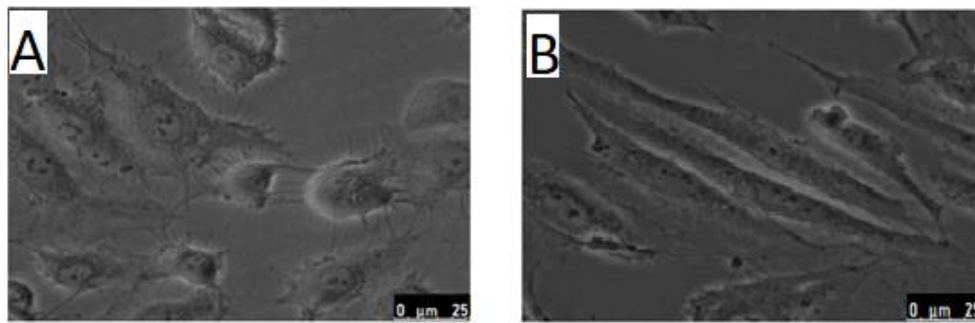
(Figure 4.1) Morphology changes of HCAECs in response to stimulation with the pro-inflammatory cytokines TNF-α and IL-α: A and B represent HCAECs seeded at passage 3 in a 12-well plate. HCAECs stimulated with the combination of pro-inflammatory cytokines shown in image B appear elongated and stretched, in comparison to the non-stimulated HCAECs shown in A. Images A and B taken using a bright field phase contrast Leica© microscope x75 lens.

For the cell culture lysates and supernatants, quantification of IL-1β by ELISA showed high levels of IL-1β production in the cytokine-stimulated cell lysates compared with non-stimulated control cell lysates, as expected (Figure 4.2). There was an approximate 47-fold increase in IL-1β production from stimulated cells (163.2 ± 23.33 pg/ml) compared with cell lysates of non-stimulated controls (3.51 ± 1.62 pg/ml).

IL-1β was also significantly increased in the supernatants of the cytokine-stimulated cells (37.27 ± 1.01 pg/ml) when compared with supernatant samples of non-stimulated controls (6.21 ± 0.55 pg/ml). However, although significant, this was still minimal at < 40 pg/ml (Figure 4.2B).
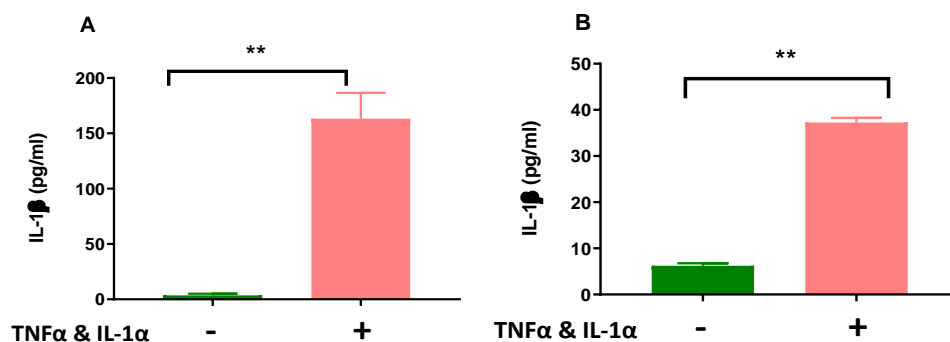
(Figure 4.2) TNF-α and IL-1α upregulate the intracellular production (A) and release (B) of IL-1β significantly in stimulated HCAECS: HCAECs from three different donors were seeded and stimulated with both TNF-α and IL-1α for 48 hours at concentrations of 10 ng/ml each. (A) Represents cell lysates while (B) represents cell culture supernatants. Values are presented as mean ± SEM, unpaired t test was used for comparison between both samples, **p<0.01, n=3.

4.3.2 NE induces the release of IL-1β from HCAECs

NE was reported to induce the release of high amounts (exceeding 100pg/ml) of IL-1β from cytokine-stimulated HCAECs (Alfaidi et al., 2015)

and this, therefore, was a potential positive control for my work. To test this, HCAECs from three different biological donors were stimulated with pro-inflammatory cytokines (10 ng/ml of TNF-α and IL-1α as per protocol in (section 2.2.2)). After washing, cells were then treated with NE at concentration of 1 μg/ml for 6 hours.

NE treatment enhanced the release of IL-1β in cytokine-stimulated HCAECs (Figure 4.3), although there was some release of IL-1β after cytokine-stimulation alone. Comparing HUVECs to HCAECs, the absolute levels of released IL-1β were higher in HCAECs (49.45± 2.9 pg/ml) (Figure 4.3) compared with HUVECs (section 3.3.2) from previous chapter. Following NE treatment, IL-1β release was 3-fold higher in HCAECs than HUVECs.

As a percentage of the total IL-1β inside the cells, under the conditions tested, HCAECs released 14.91%, which is 40% higher than the percentage of release from HUVECs (10.65%) (Figure 3.3).
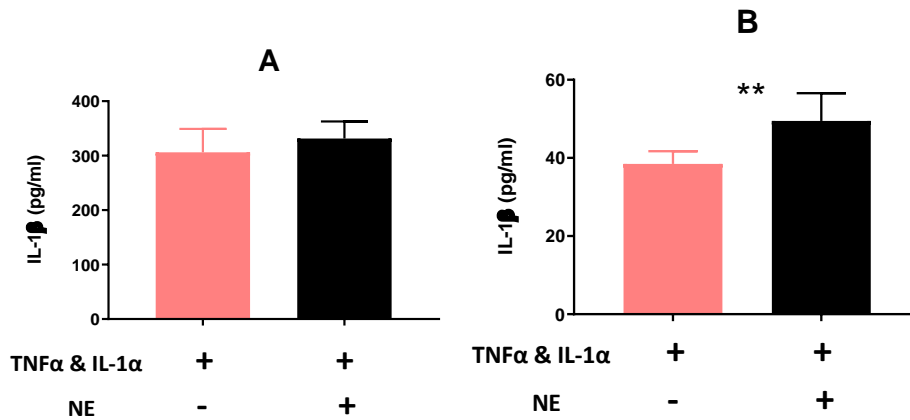
(Figure 4.3) Stimulated HCAECs release IL-1β extracellularly following a 6-hour incubation with NE: (A) IL-1β in lysates shows levels are unchanged within the cell. (B) IL-1β in supernatants shows NE increased release of IL-1β. Values are presented as mean ± SEM, unpaired T test was used for comparison between both samples, **p<0.01 in supernatants, n=3.

In terms of IL-1β production, there was a difference in the overall amount of IL-1β produced inside HCAECs, compared to HUVECs, under identical conditions (130.1 ± 4.1 pg/ml in HUVECs compared with 331.6 ± 22.04 pg/ml in HCAECs) (Figure 3.3A versus Figure 4.3A).

4.3.3 Water-soluble cholesterol induces the release of LDH from stimulated HCAECs

In an earlier section (section 3.3.4), water-soluble cholesterol led to LDH release in HUVECs, therefore, this "cytotoxicity" assay was performed first to determine if the cells released LDH. Unsurprisingly, for HCAECs, the basal release of LDH was similar to HUVECs. However, HCAECs treated with 100 µg/ml, 250 µg/ml and 500 µg/ml exhibited LDH release 20.5%, 27.9% and 47.5% LDH respectively (solid red bars in figure 4.4), in direct proportion with

the concentration of water-soluble cholesterol (Figure 4.4). The conjugation

agent MβCD led to minimal LDH release (as figure 3.6 for HUVECs).

TNF & IL-1	+	-	+	-	+	+	+	+	+	+
WSC + MßCD (µg/ml)	-	250	-	-	100	-	250	-	500	-
MßCD (µg/ml)	-	-	-	-	-	100	-	250	-	500
NE	+	-	-	-	-	-	-	-	-	-
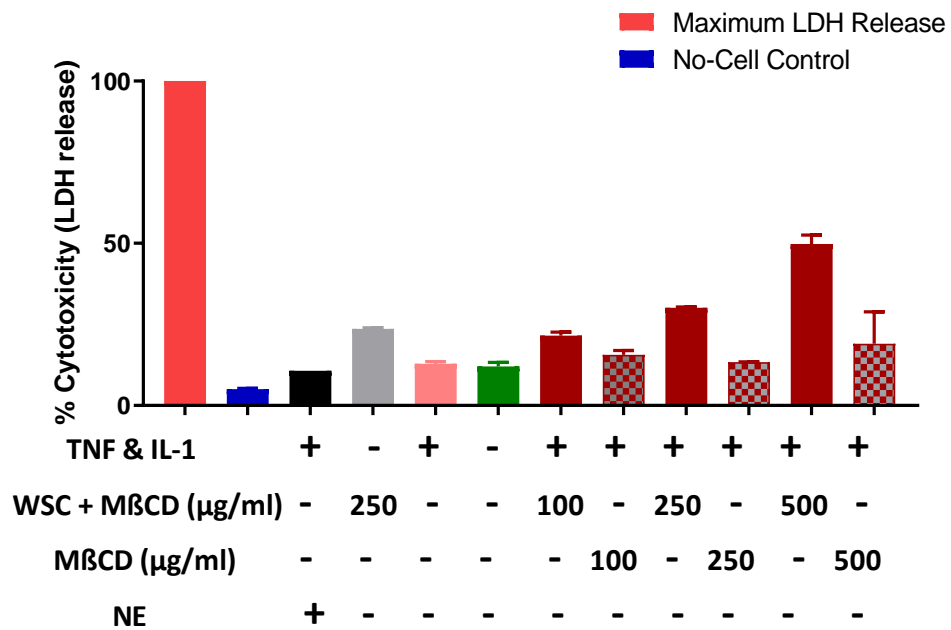
(Figure 4.4) LDH assay on HCAECs treated with water-soluble cholesterol shows induced LDH release: The percentage of LDH released is shown in relation to the maximum LDH release control of the assay (100%). HCAEC treated with water-soluble cholesterol show increased LDH release compared to control. Values are presented as means of three technical replicates ± SD.

4.3.4 AgLDL does not induce LDH release from HCAECs

AgLDL was also tested for its ability to cause potential cell death. HCAECs in

CGM, without any treatment, showed 17% LDH release after 6 hours, which

is similar to that of the different doses of AgLDL treatments (10,25, 50, 75,

100 and 200 µg/ml) showing 13.6%, 16.6%, 13.9%, 15.8%, 13.6% and 14.3%

respectively. Thus, AgLDL does not have an LDH inducing effect on HCAECs.

NE treated cells showed 19% LDH release after 6-hour incubation. The non-

cytokine stimulated AgLDL treated cells exhibited 15.3% LDH release (Figure

4.5).

TNF & IL-1	+	-	+	-	+	+	+	+	+	+
AgLDL (µg/ml)	-	-	-	-	10	25	50	75	100	200
NE	+	-	-	-	-	-	-	-	-	-
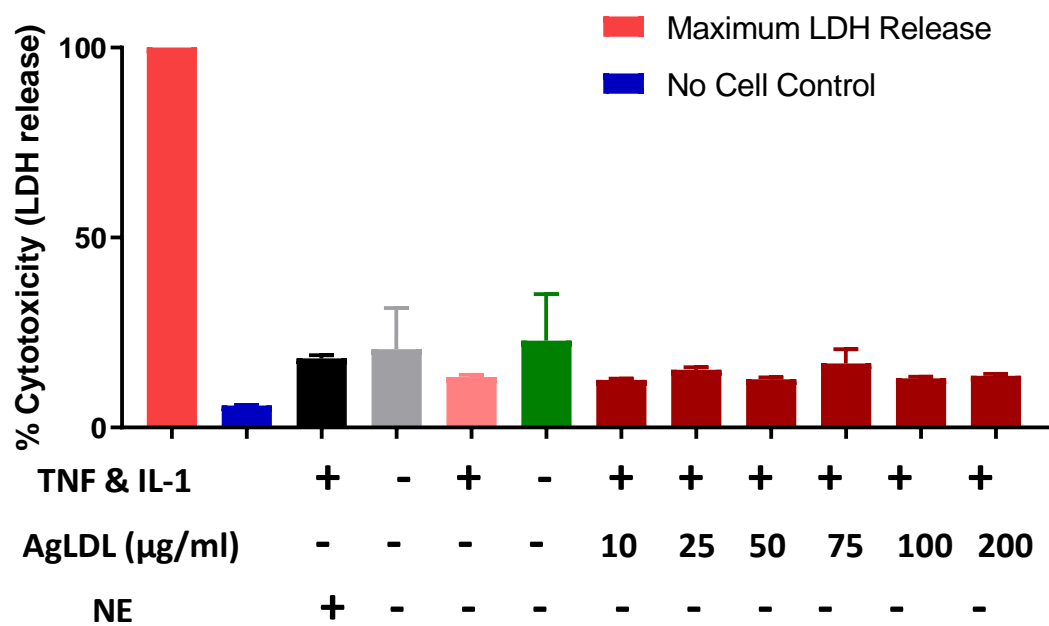
(Figure 4.5) LDH assay on HCAECs with AgLDL shows no release: The percentage of LDH released in relation to the maximum LDH release control of the assay (100%) does not differ between samples. Triplicate samples of two separate biological donors ± SD.

4.3.5 AgLDL does not induce the release of IL-1β from HCAECs

AgLDL occurs *in vivo*, in the vessel wall as well as in the blood (Singh et al., 2019, Tamminen et al., 1999) and may theoretically provide a physical stimulus for IL-1β release. Cytokine release was therefore measured after exposure of HCAECs to AgLDL. HCAEC lysate samples from cells treated with AgLDL at concentrations of 10, 25, 50, 75, 100 and 200 µg/ml produced IL-1β quantified at concentrations of 379.6, 374.8, 330.4, 323.3, 253.5 and 373.8 pg/ml, respectively within cells (Figure 4.6). NE treated samples (positive controls) and cytokine only treated control produced 331.6 ± 22 and 333.8 ± 15.1 pg/ml IL-1β inside cells. Together and alongside the controls, these data show AgLDL is not inducing IL-1β production inside HCAECs (Figure 4.6).

Although there were high levels of intracellular IL-1β consistent between cytokine-stimulated samples, there was low release in culture supernatants. ELISA quantification of IL-1β in culture supernatants (Figure 4.7) showed release of IL-1β in AgLDL treated samples to be comparable to the cytokine only treated control, but less than the NE treated positive control of the assay (Figure 4.7). IL-1β release into culture supernatants of samples treated with AgLDL (at concentrations of 10, 25, 50, 75, 100 and 200 µg/ml) were an average of (11.5 ± 2.2, 12.3 ± 2.6, 9.8 ± 1.8, 9.6 ± 1.9, 11.97 ± 2.5 and 8.4 ± 0.8 pg/ml) respectively (Figure 4.7). NE treated cells (positive control) released 17.3 ± 2.1 pg/ml and 9.3 ± 1.2 pg/ml in cytokine only stimulated controls. Both negative controls released 1.9 pg/ml. Findings from this assay

suggest that AgLDL is not a successful promoter of IL-1β release from
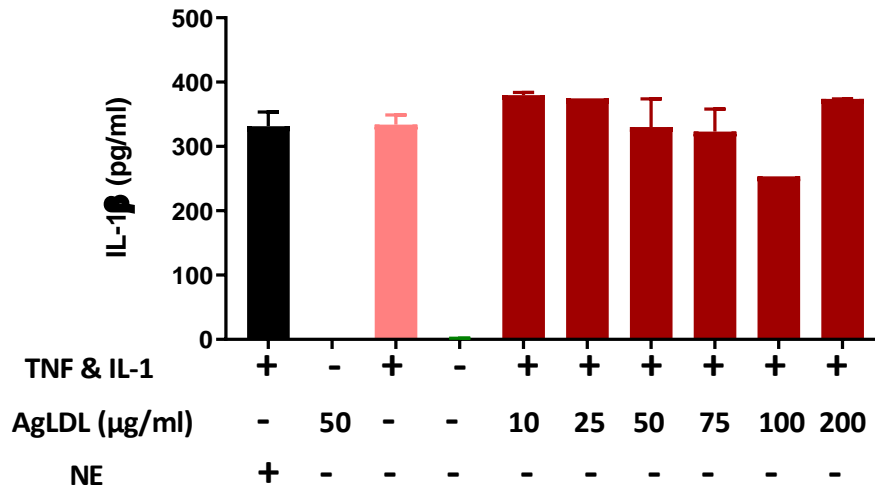
HCAECs.

(Figure 4.6) AgLDL treatment and intracellular production of IL-1β in HCAEC: No difference in intracellular IL-1β levels is seen between samples. n=3, data are expressed as mean ± SEM, Data are analysed by ordinary one-way ANOVA with multiple comparisons.
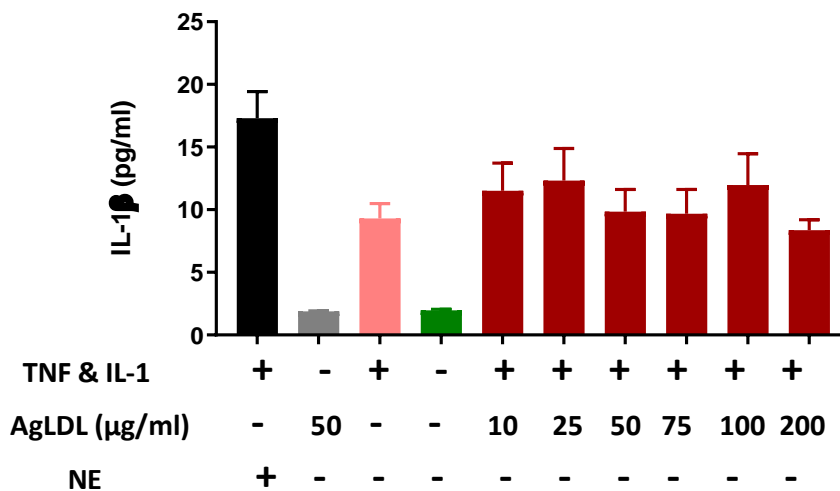
(Figure 4.7) AgLDL does not appear to induce release of IL-1β from HCAEC into culture supernatants: n=3, data are expressed as mean ± SEM, Data are analysed by ordinary one-way ANOVA with multiple comparisons.

4.3.6 AcLDL molecules reside within cellular perinuclear and cytoplasmic compartments that maintain surface connectivity in HCAECs with limited access to the extracellular space.

To investigate whether LDL was entering the cells, I used imaging to investigate uptake of AcLDL by HCAECs. A pre-labelled acetylated LDL (AcLDL) was used for those studies (as per protocol in section 2.2.11.1).

Results obtained from confocal fluorescent microscopy, showed minimal uptake of AcLDL molecules inside HCAECs after 6 hours, mostly in the perinuclear area (Figures 4.8 and 4.9).
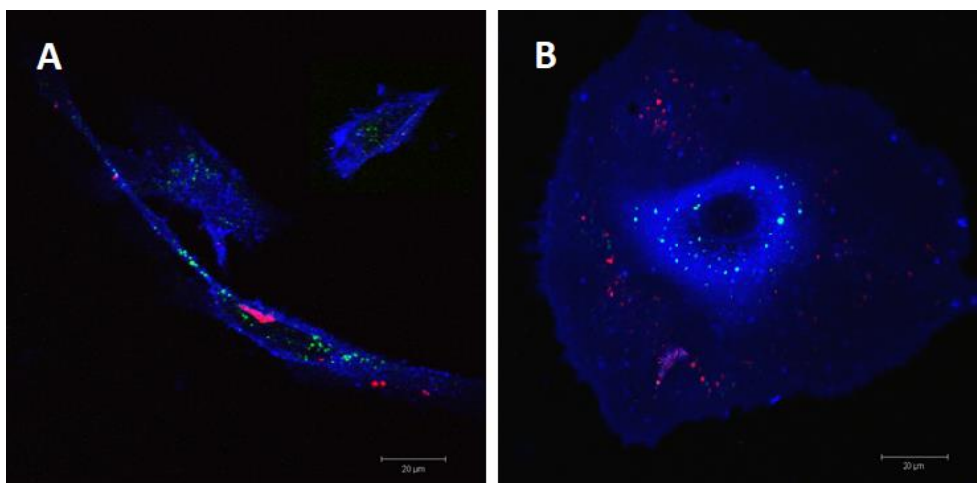
(Figure 4.8) AcLDL resides intracellularly around the nucleus in HCAECs after a 6-hour incubation: In this condensed Z stack image, LDL molecules appear to be residing in perinuclear area and in the cytoplasm of HCAECs both A and B. AcLDL Alexa Fluor™ 488 Conjugate shown in green, Alexa Fluor™ 555 (CTB-555) conjugate staining was used for labelling the plasma membrane and cell surface, shown in blue. Finally, cells were labelled with Wheat Germ Agglutinin (WGA), Alexa Fluor™ 647 Conjugate shown in red, which binds to cell surface glycoproteins.
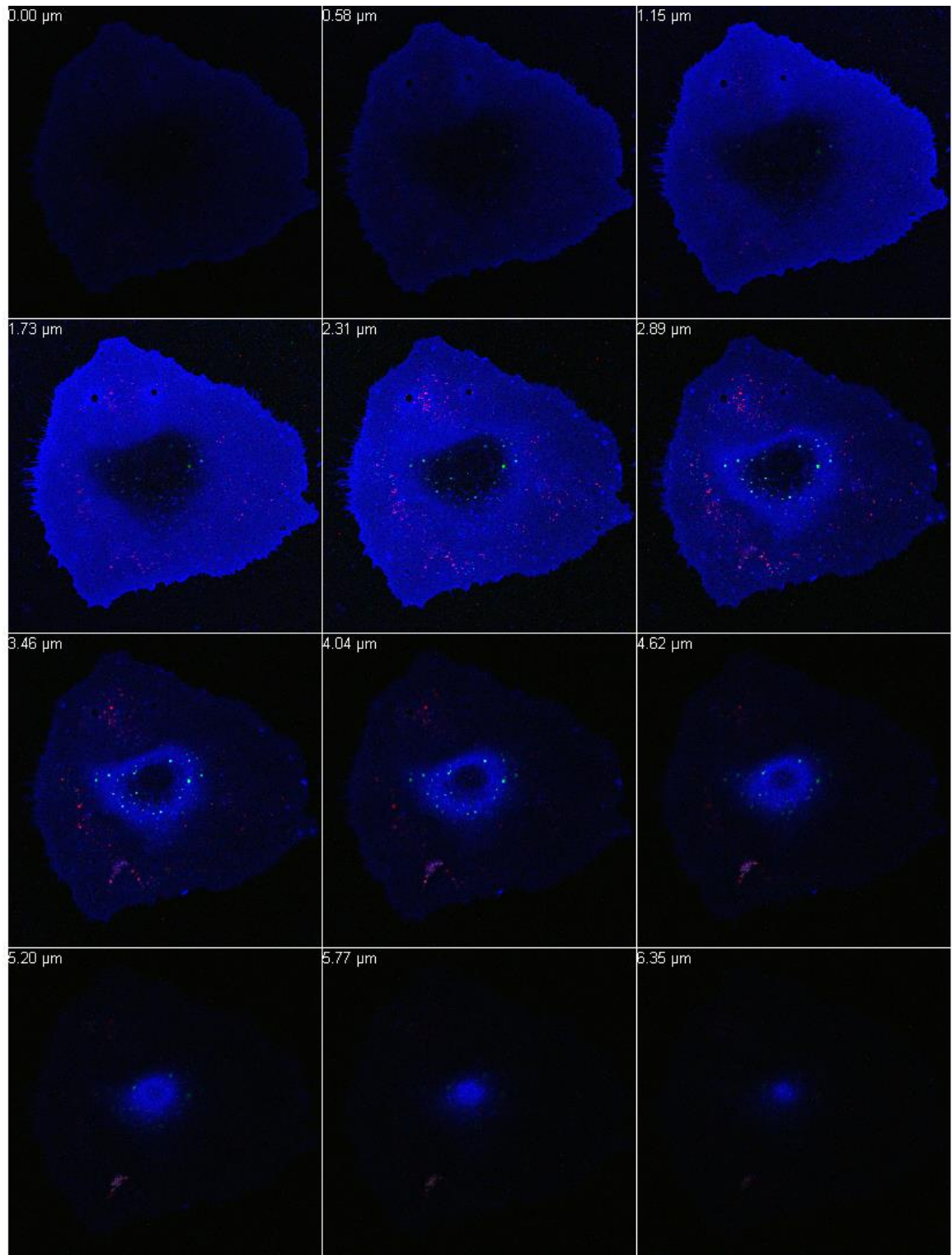
(Figure 4.9) Montage of individual slices from a z stack confocal imaging of a Human coronary artery endothelial cell showing AcLDL molecules residing around the nucleus after incubation with AcLDL: The numbers in μm in top left hand panel show the distance between the slices through the cell.

4.3.7 Investigating the Potential Roles of AcLDL Treatment on IL-1β activity in HCAECs

4.3.7.1 HCAECs incubation with AcLDL does not induce cell death

After determining uptake of AcLDL molecules by HCAECs, the effect of AcLDL incubation with HCAECs and production and release of IL-1β was tested. First, toxic effects of AcLDL on the cells or any possibility of induced cell death was excluded. Experiments using HCAECs incubated for 6 hours with different concentrations of AcLDL, were analysed for cytotoxicity by using the LDH cytotoxicity assay described in section (2.2.7).

LDH assay data showed variations and no pattern of LDH release in proportion to AcLDL concentration (Figure 4.10), indicating the non-toxicity of AcLDL, especially at high concentrations. The highest release of LDH was recorded in cells treated with 50 μg/ml of AcLDL, which had 267% more LDH release compared to cytokine only stimulated control.

Bright-field microscopy images were taken at the end of the 6th hour of incubation with 50 μg/ml of AcLDL and were compared with both cytokine only stimulated and non-treated non-stimulated HCAECs as controls (Figure 4.11). These showed that cells were thriving and attached to the experimental plate, with no loss of cells or cell death after incubation with AcLDL.
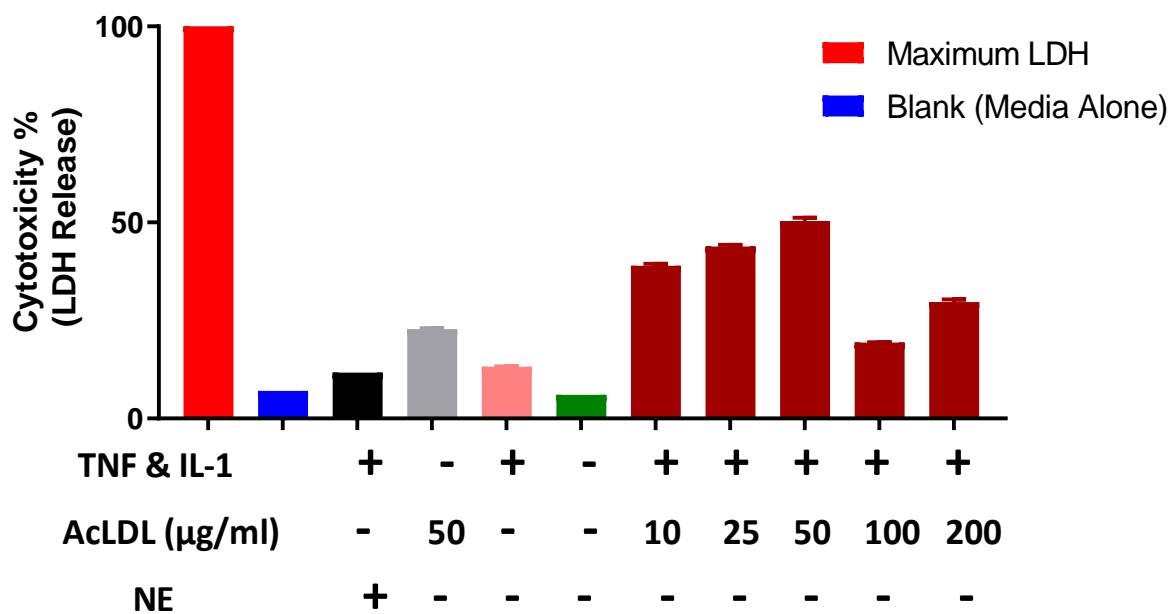
(Figure 4.10) AcLDL incubation with HCAECs induces LDH release at low concentrations: Triplicate samples of HCAECs culture supernatants treated with AcLDL in different concentrations (10, 25, 50, 100, 200 µg/ml) and assayed for LDH (following the protocol in section 2.2.7). Results showed the release of LDH in variable manner in relation to the concentration of AcLDL. LDH release was high in low concentrations (10-50 µg/ml) and low release was measured at high concentrations of AcLDL. Data are represented as mean ± SD, three technical replicates.
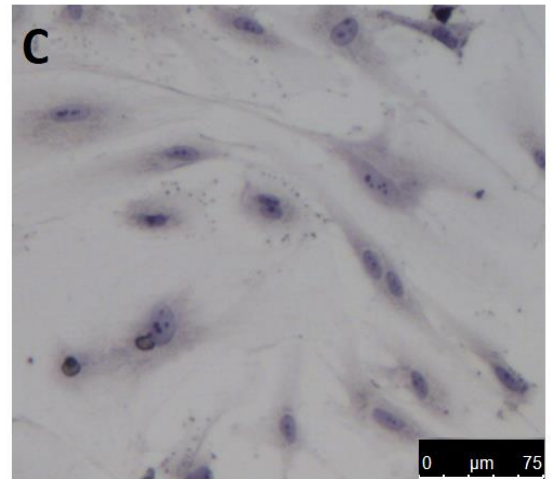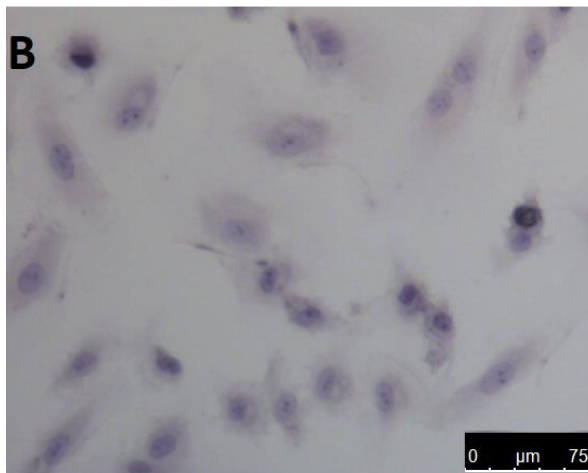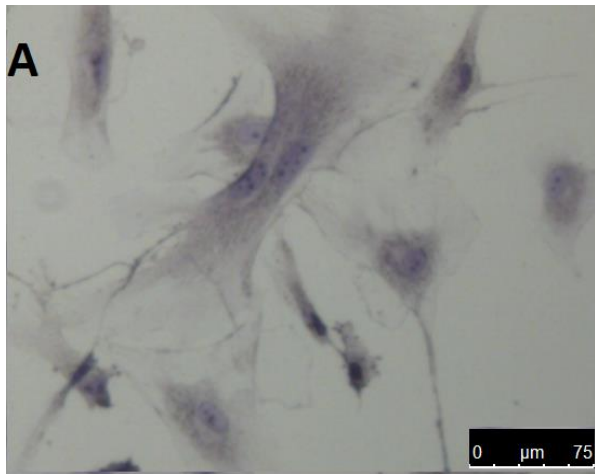
(Figure 4.11) AcLDL incubation with HCAECs is not inducing cell death: Cytokine stimulated (10 ng/ml of TNF-α and IL-1α for 48 hours) and AcLDL treated (50 µg/ml of AcLDL for 6 hours) HCAECs (A), appear to have larger size with dilated cytoplasm compared to cytokine only treated cells (C). Untreated, unstimulated HACECs (B) maintain their round shape. Images were taken by bright-field phase contrast Leica© microscope x75 lens, scale bar 75 µm. Treatment with AcLDL and or cytokine stimulation did not affect the viability of cells for the duration tested.

4.3.7.2 AcLDL does not induce the production of intracellular IL-1β in stimulated HCAECs

AcLDL was non-toxic to HCAECs by LDH assay and by microscopic evaluation (section 4.3.7.1), and its ability to promote IL-1β release from HCAECs was investigated next.

HCAECs isolated from three different donors (n=3) were cultured (sections 2.2.1 - 2.2.2) and incubated with AcLDL using a range of concentrations (50, 100, 200 µg/ml) delivered in serum free MV2 media (see appendix for media composition) for 6 hours. After the incubation period, the levels of produced IL-1β were quantified by ELISA (section 2.2.6). As expected, AcLDL treatment had no direct effect on increasing the production of IL-1β intracellularly when compared with cytokine stimulated only and NE treated controls. (Figure 4.12).
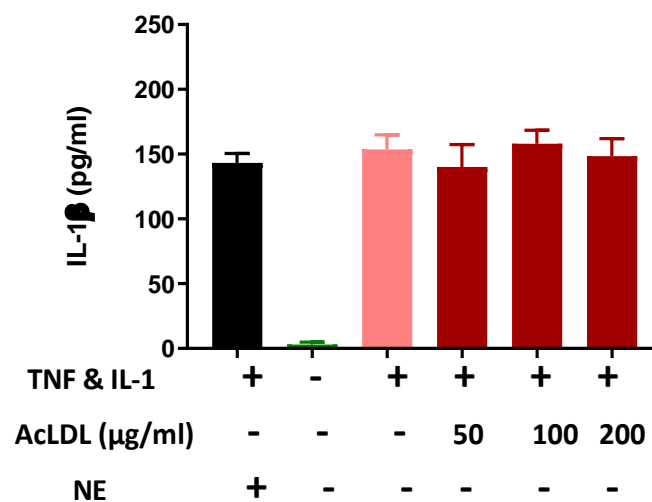
(Figure 4.12) AcLDL treatment does not induce production of IL-1β inside HCAECs: n=3 independent donors, data are expressed as mean ± SEM, Data are analysed by one-way ANOVA followed by Bonferroni post hoc test, ****p<0.0001.

121

4.3.7.3 AcLDL induces IL-1β release from stimulated HCAECs

Next, IL-1β release was studied. HCAECs were stimulated by TNF-α and IL-1α

for 48 hours (section 2.2.2) followed by a 6-hour incubation with AcLDL. The

results of IL-1β quantification in culture supernatants showed significant

increase in IL-1β release compared to cytokine only stimulated and NE

treated controls (Figure 4.13). Separate experiments using high (50-200

µg/ml) and low (10-20 µg/ml) concentrations of AcLDL revealed the peak of

this induction of IL-1β release was at the 50 µg/ml concentration of AcLDL

(Figures 4.13 and 4.14).
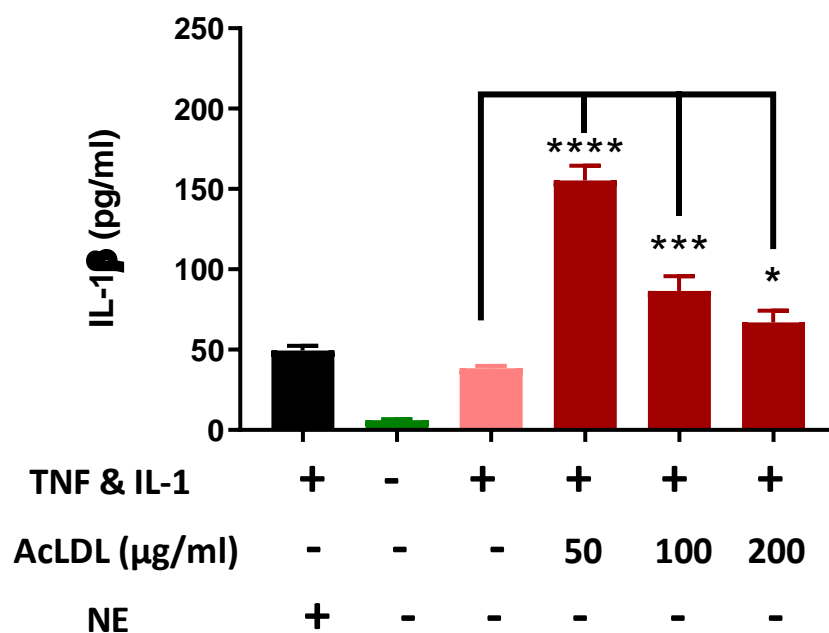
(Figure 4.13) AcLDL induces the release of IL-1β from HCAECs: ELISA showing high levels of IL-1β released in culture supernatants of cells treated with AcLDL. Cells treated with 50 µg/ml AcLDL appear to have the highest released IL-1β levels. Samples were compared to cytokine only treated cells as a control, n=3 independent donors, data are expressed as mean ± SEM, analysed by one-way ANOVA followed by Bonferroni post hoc test, ****p<0.0001, ***P<0.001 and *p<0.05.

To investigate this I repeated the same experiment with lower concentrations of AcLDL using HCAECs from a different biological donor (Figure 4.14).
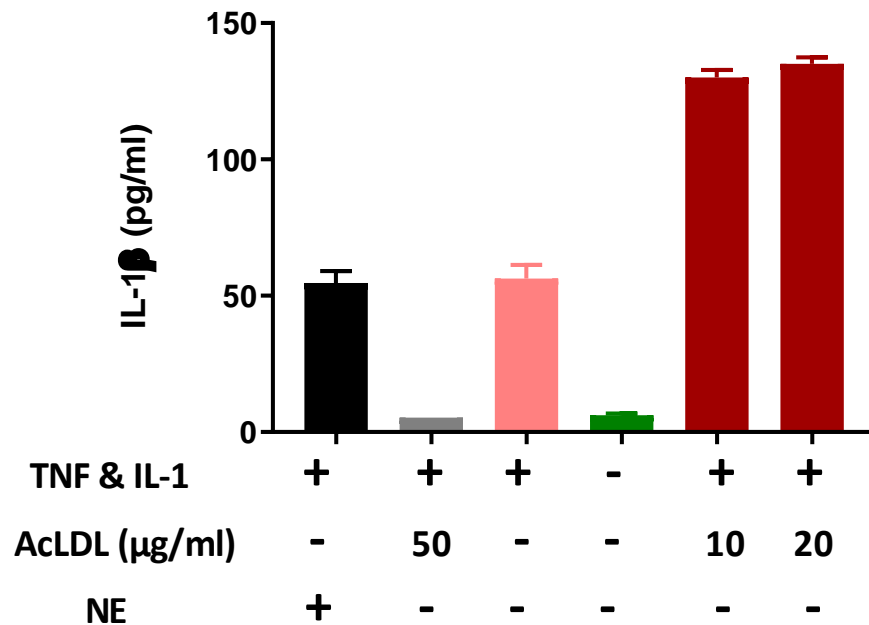
(Figure 4.14) AcLDL induces IL-1β release from HCAECs at low concentrations and is concentration dependent: Low concentrations of AcLDL (10 and 20 µg/ml) results in induced release of IL-1β from stimulated HCAECs. Data are presented as mean ± SEM, n=3.

4.3.7.4 HCAECs only release LDH during AcLDL incubation

On comparing results of LDH release (section 4.3.7.1) with IL-1β release (section 4.3.7.3) I noticed the LDH release increased in cells that also had higher IL-1β release. As I showed that AcLDL is not toxic to the cells, I wanted to investigate if it damaged the HCAECs, and whether or not the cells eventually die or continue to survive after the AcLDL is removed. For this experiment, HCAECs were incubated with concentrations of 10, 20 and 50

µg/ml AcLDL for 6 hours (section 2.2.4), and then the media was replaced with complete growth media for 12 hours. Cells were then analysed for LDH release (using the cytotoxicity assay described in section 2.2.7).

Results showed no difference in LDH release between all samples after 12 hours of incubation in complete growth media post AcLDL treatment (Figure 4.15). Both AcLDL treated and non-treated cells released levels of LDH within the same range (Figure 4.15). Thus, the AcLDL treatment of 6 hours before changing the media had no permanent damaging effect on cells nor did it induce cell death.
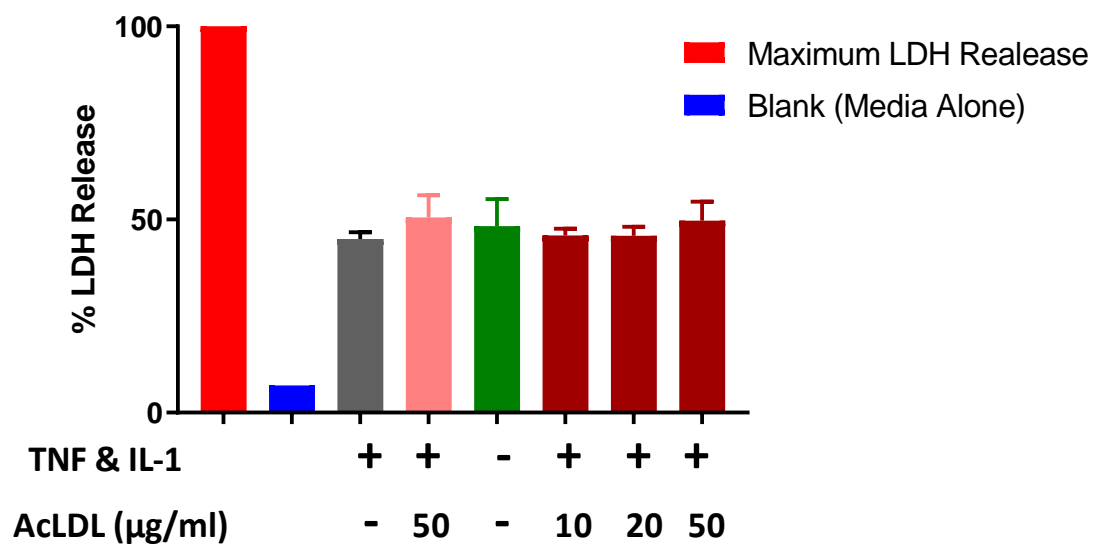
(Figure 4.15) HCAECs treated with AcLDL release similar LDH levels compared to non-treated controls after 12 hours post treatment: HCACEs treated with different concentrations of AcLDL (10, 20 and 50 µg/ml) for 6 hours followed by washing with PBS and incubation in complete growth media for 12 hours. Results show the almost identical levels of LDH release between all samples (AcLDL treated and non AcLDL treated) regardless of the concentration used. Mean +/- SEM, n=3, from the same biological donor.

4.3.8 Investigating the role of OxLDL treatment on HCAECs
4.3.8.1 OxLDL molecules are taken up by stimulated HCAECs

To determine whether OxLDL is taken up by HCAECs, I incubated cytokine-stimulated and non-stimulated HCAECs with OxLDL (50 µg/ml) and imaged the cells at 6 and 24 hours post incubation using bright-field microscopy (section 2.2.11.2).

Results showed the presence of OxLDL within the cytoplasm of cytokine-stimulated HCAECs (Figure 4.16) with the majority being in the perinuclear site (similar to AcLDL uptake seen in section 4.3.6). The build-up of OxLDL appears to take a needle shape similar to cholesterol crystals seen in macrophages (Rajamaki et al., 2010).

To determine whether non-cytokine-stimulated cells would eventually take up OxLDL following longer incubation, cells were exposed to OxLDL for 24 hours (Figure 4.17). Prolonged treatment did not result in uptake of OxLDL in unstimulated cells, but did increase the amount of visible OxLDL build-up of residual particles in cytokine-stimulated cells (Figure 4.17).
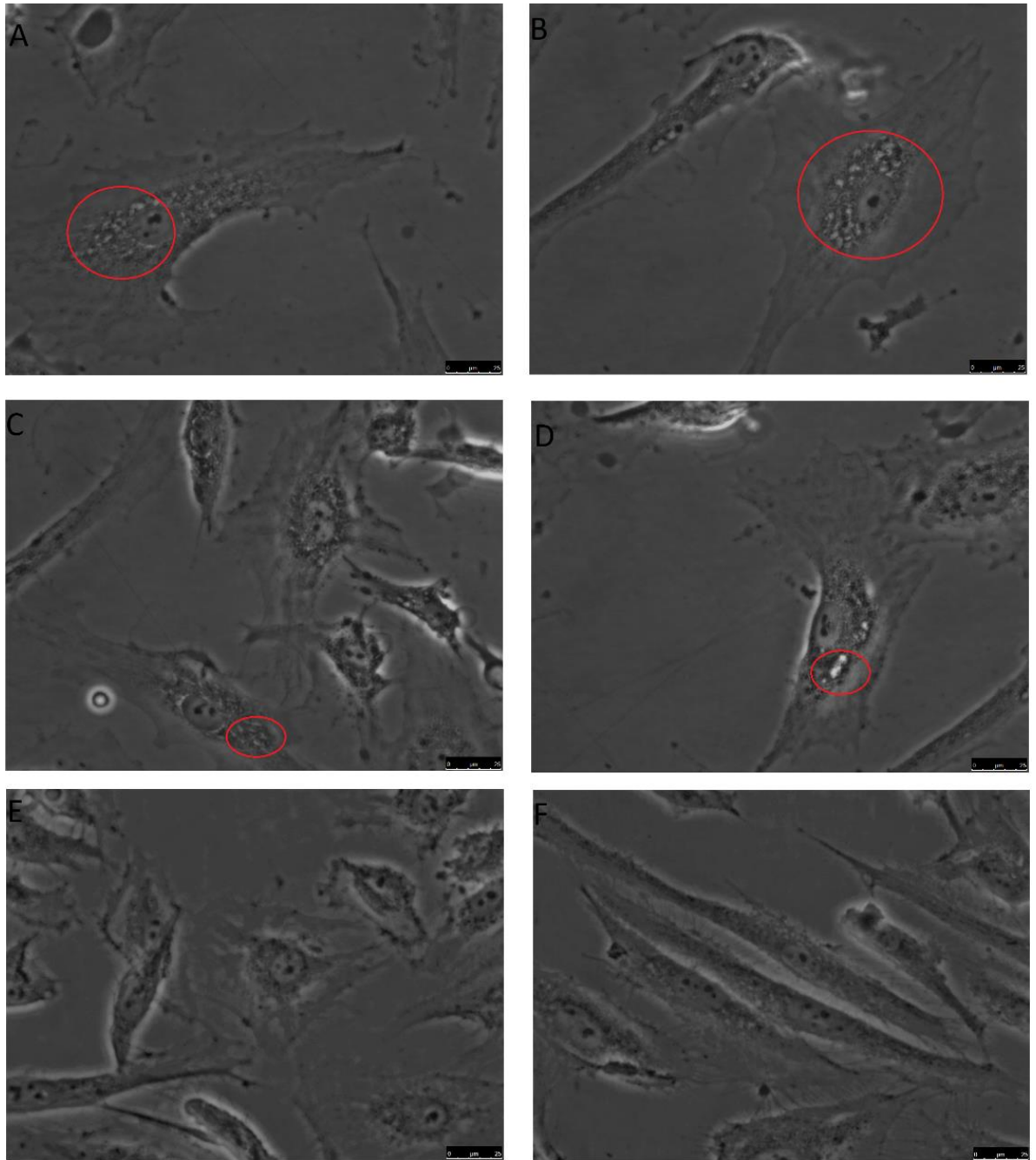
(Figure 4.16) OxLDL is seen in the perinuclear region of OxLDL treated HCAECs: (A,B,C and D) Four different cell samples of HCAECs stimulated with pro-inflammatory cytokines IL-1α and TNF-α (10 ng/ml for 48 hours), then treated with OxLDL (50 µg/ml for 6 hours). The intracellular build-up of OxLDL can be seen taking a crystallised shape highlighted in red. Cytokine stimulated non OxLDL-treated cells (F) have an elongated appearance consistent with previously shown images. Non-cytokine stimulated, OxLDL treated cells in (E) are rounded in shape and do not take up OxLDL. Images were taken by bright-field phase contrast Leica© microscope, scale bar 25 µm. Higher resolution and larger size images can be found in Appendix (III).

126
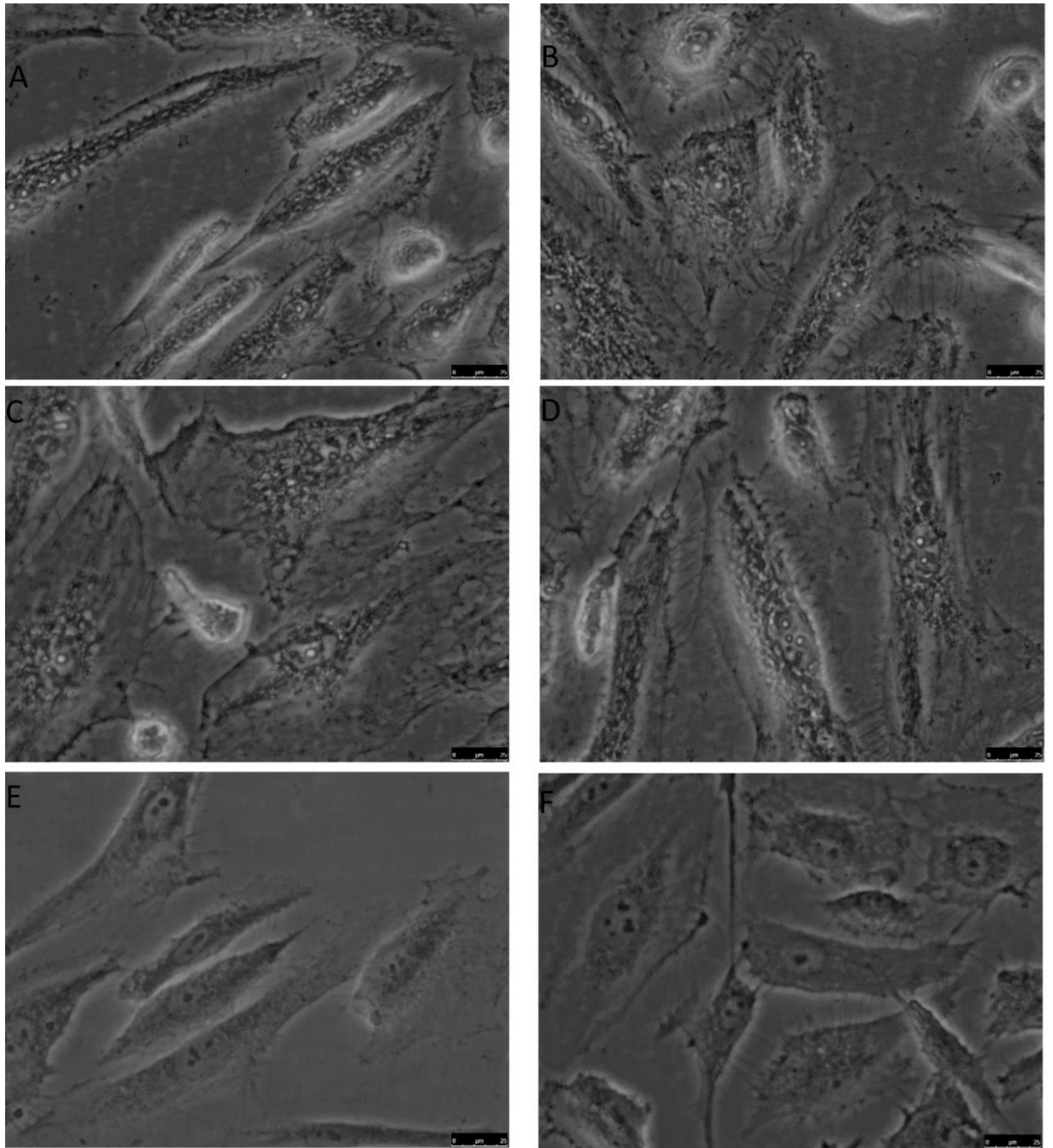
(Figure 4.17) Build-up of OxLDL in the perinuclear region of HCAECs following a 24-hour OxLDL incubation: (A,B,C and D) Four different cell samples of HCAECs stimulated with pro-inflammatory cytokines IL-1α and TNF-α (10 ng/ml for 48 hours), then treated with OxLDL (50 µg/ml for 24 hours). OxLDL treated cells show an increased intracellular build-up of OxLDL compared to 6 hours (Figure 4.16). Cytokine only stimulated cells (E) appear mainly elongated. Non-cytokine stimulated, OxLDL treated HCAECs show no uptake of OxLDL. Images were taken by bright-field phase contrast Leica© microscope, scale bar 25 µm. Higher resolution and larger size images can be found in Appendix (III).

4.3.8.2 OxLDL incubation does not induce production of cellular IL-1β in HCAECs

As AcLDL is not fully biologically relevant and referred to as a "model lipid".

I then investigated whether OxLDL has the same effect on HCAECs. Three different biological donors of HCAECs were stimulated (section 2.2.2) and treated with OxLDL (section 2.2.4.4) for 6 hours. As expected, IL-1β levels did not show a significant change in the amount of produced IL-1β inside the cells, indicating that OxLDL does not induce the production of IL-1β by stimulated HCAECs. This was consistent with results seen with AcLDL in the previous section. OxLDL also did not have an effect on IL-1β production in unstimulated HCAECs (Figure 4.18).

| TNF & IL-1 | - | + | + | + | + | - |
| OxLDL (µg/ml) | - | - | 10 | 20 | 50 | 50 |
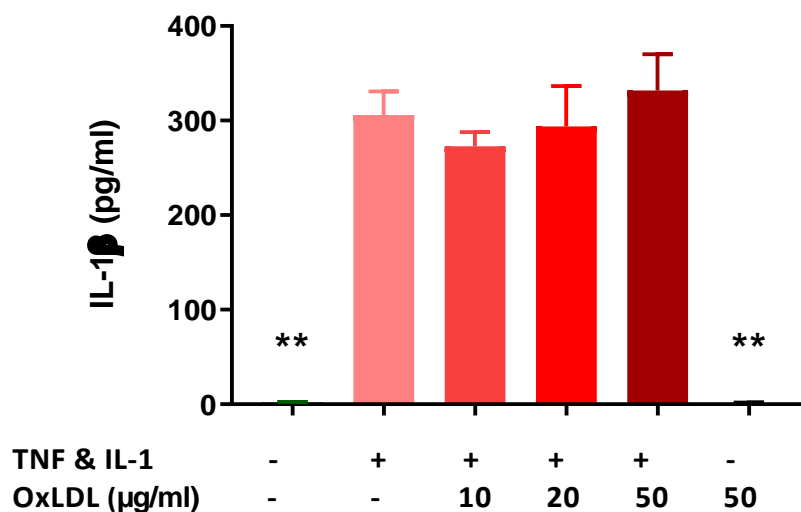
(Figure 4.18) OxLDL does not induce IL-1β production in HCAECs: ELISA analysis showing OxLDL (10,20 and 50 µg/ml) treatment for 6 hours did not affect production of IL-1β inside cytokine stimulated or non-stimulated HCAECs. n=3 independent donors, data are expressed as mean ± SEM, analysed by one-way ANOVA followed by Bonferroni post hoc test, **P<0.01.

4.3.8.3 OxLDL Induces the Release of IL-1β from HCAECs

The culture supernatant of the cells treated in (section 4.3.8.2) were analysed by ELISA to determine levels of IL-1β release. Results showed a significant increase in released IL-1β from cells treated with 50 µg/ml (Figure 4.19). The released levels of IL-1β were 2.4 fold that of cytokine only controls. Cells treated with 10 and 20 µg/ml of OxLDL did not release IL-1β above levels detected in cytokine only stimulated controls or in unstimulated cells.

TNF & IL-1	-	+	+	+	+	-
OxLDL (µg/ml)	-	-	10	20	50	50
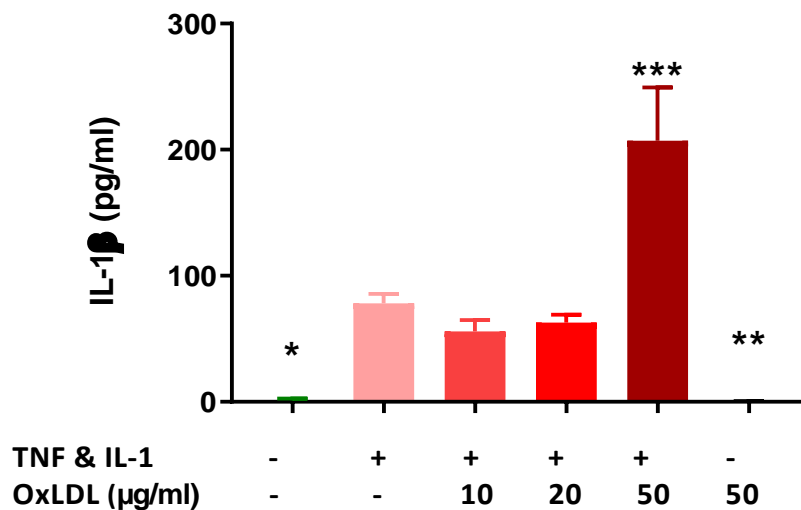
(Figure 4.19) OxLDL induces the release from HCAECs in a concentration dependent manner: HCAECs released high amounts of IL-1β after treatment with 50 µg/ml compared to cytokine only stimulated controls. n=3 independent donors, data are expressed as mean ± SEM, analysed by one-way ANOVA followed by Bonferroni post hoc test, **P<0.01.

4.3.8.4 The OxLDL induced release of IL-1β from HCAECs is accompanied by LDH release

To ensure that cells were not harmed by OxLDL treatment, bright-field microscopic imaging of the OxLDL treated cells was performed to determine whether the cells were intact and thriving.

The cells remained viable and attached to the experimental plate after thorough washing with PBS. However, cells incubated with OxLDL (50 μg/ml), looked larger in size compared with both the untreated cells and the cytokine-stimulated controls (Figure 4.20). The OxLDL treated cells also appear to have engulfed particles of OxLDL as a result of the 6-hour incubation (as they appear larger in size compared to control cells in figure 4.20). A few cells also appeared with an abnormal morphology and had a thinner cytoplasm compared to healthy control cells. These changes to the treated cells were further investigated in the current and final chapters.

To further determine this effect of OxLDL, LDH release was investigated as per protocol (Section 2.2.7). Cells were treated with 50 μg/ml OxLDL, for 6 hours to cause IL-1β release prior to LDH assessment. There was a 55.3% increase in LDH release in OxLDL treated cells compared to cytokine only stimulated controls (Figure 4.21).
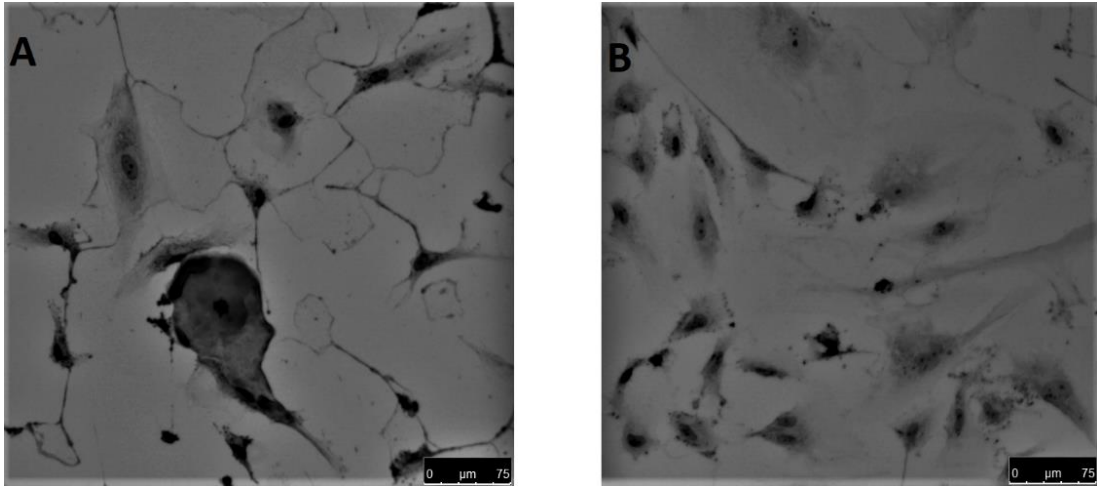
(Figure 4.20) OxLDL treated HCAECs appear to have a fatty dilated cytoplasm suggesting OxLDL uptake: Proinflammatory cytokine stimulated (10 ng/ml of TNF-α and IL-1α for 48 hours) HCAECs were treated with OxLDL (50 µg/ml) for 6 hours (A), while (B) were left without OxLDL as stimulation only controls. Treated cells had a fatty cytoplasm appearance and were significantly larger in size than untreated controls. Some cells appear abnormal and have a thin cytoplasm maybe suggesting that those cells released and secreted pro-inflammatory cytokines.
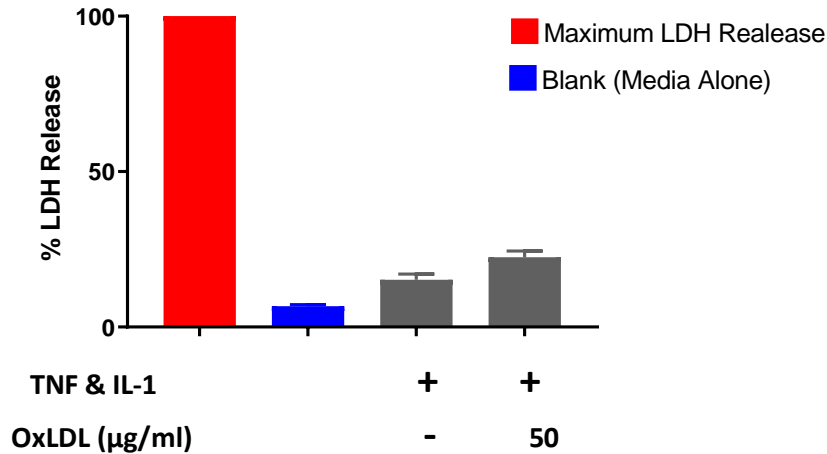
(Figure 4.21) OxLDL at the IL-1β inducing concentration promote the release of LDH: HCAECs incubated with OxLDL (50 µg/ml) released 55.3% more LDH than cytokine-stimulated controls. Samples from three different biological donors n=3, data expressed as mean ± SD. Red bar represents the maximum LDH released from positive control. Positive control value was as 100% release. Vehicle only negative control (contains media only) displayed in blue bar.

4.3.9 Investigating the effects of Native human LDL treatment on HCAECs

To determine whether LDL has to be modified (for example oxidised) before it can exert an effect on HCAECs, I investigated the effects of native LDL treatment on cytokine-stimulated HCAECs. HCAECs were treated with three different concentrations of native LDL (10, 25 and 50 μg/ml) for 6 hours, prior to analysis. Culture supernatants showed that native LDL has no effect of inducing IL-1β release from cytokine-stimulated HCACEs (Figure 4.22).
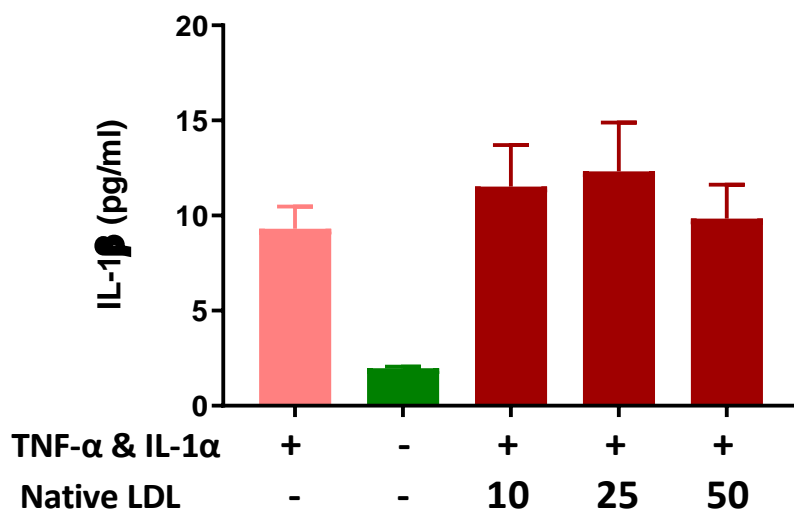
(Figure 4.22) Native LDL does not induce the release of IL-1β from stimulated HCAECs: HCAECs were stimulated with proinflammatory cytokines IL-1α and TNF-α (10 ng/ml for 48 hours), then treated with native LDL (10, 25 and 50 μg/ml for 6 hours). No difference in IL-1β release was seen between LDL-treated and control cells, n=3.

HCAECs treated with native LDL also showed very low release of LDH (Figure

4.23).
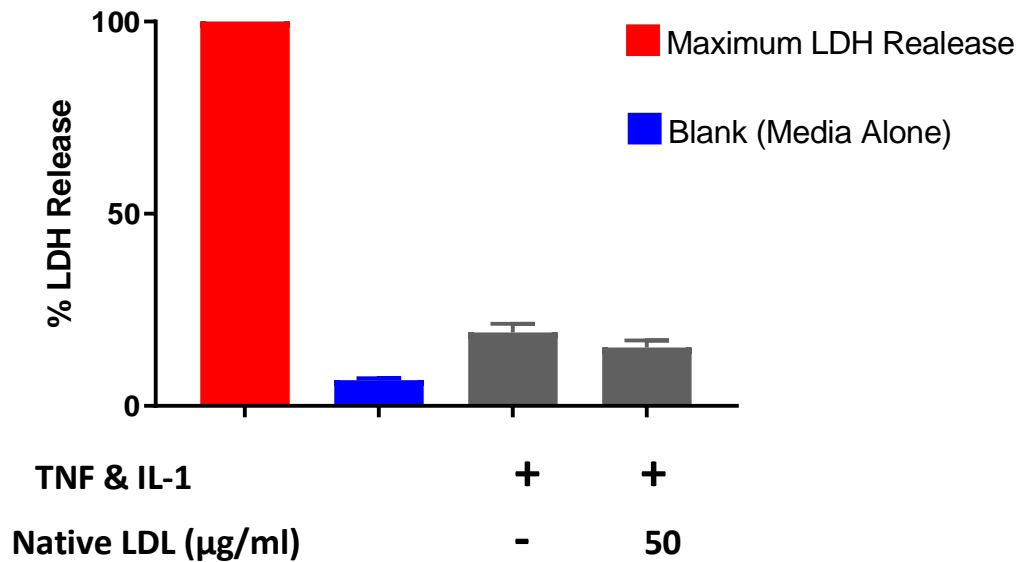
(Figure 4.23) Native LDL treatment does not induce the release of LDH from HCAECs: HCAECs were stimulated with pro-inflammatory cytokines IL-1α and TNF-α (10 ng/ml for 48 hours), then treated with native LDL (50 μg/ml for 6 hours). No significant release of LDH was seen in either group. Red bar represents the maximum LDH released from positive control. Positive control value was as 100% release. Vehicle only negative control (contains media only) displayed in blue bar, n=3 data expressed as mean ± SD.

Representative bright-field microscopy of these cells showed that the cytokine only stimulated cells appeared almost identical to cells treated with native LDL secondary to cytokine stimulation, with no evidence of LDL uptake compared to OxLDL treated cells (Figure 4.24).
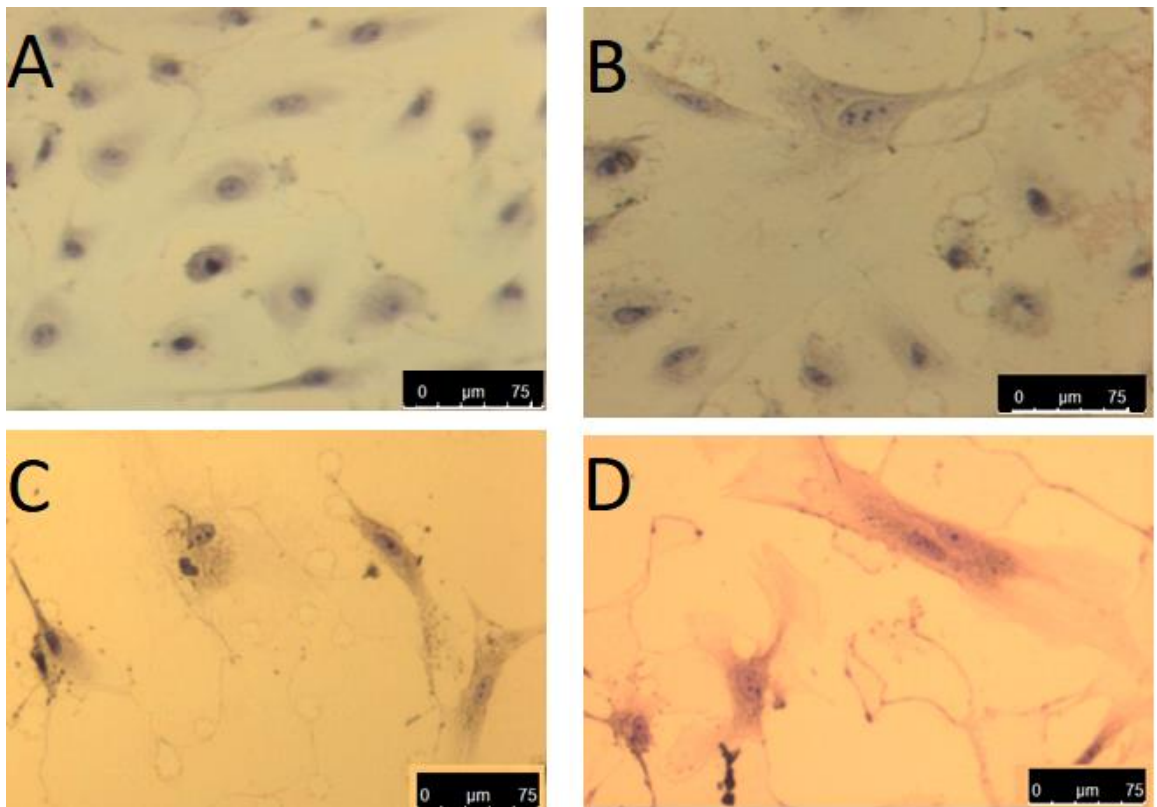
(Figure 4.24) HCAECs do not engulf native LDL after 6 hours of treatment: HCAECs without stimulation or treatment (A) and HCAECs stimulated with Pro-inflammatory cytokines IL-1α and TNF-α (10 ng/ml for 48 hours) (B) as controls. Stimulated HCAECs treated with native LDL (50 μg/ml for 6 hours) (C) and finally OxLDL treated (50 μg/ml for 6 hours) stimulated HCAECs (D).

4.3.10 Summary of Results

The response of HCAECs to the pro-inflammatory cytokine combination in producing intracellular IL-1β was greater than that seen in HUVECs. Primed HCAECs also released high levels of IL-1β in response to NE, in agreement with findings from (Alfaidi et al., 2015). The key findings of this chapter in the context of the cholesterol induced IL-1β release from HCAECs are:

- HCAECs release IL-1β when incubated with modified LDLs (OxLDL and AcLDL) only when the cells are cytokine stimulated (primed).

- AgLDL does not induce IL-1β release from primed HCAECs.

- AcLDL is taken up by cells and induces the release of IL-1β from primed HCAECs.

- OxLDL is taken up by cells and induces the release of IL-1β from primed HCAECs.

- HCAECs release IL-1β in response to uptake of modified LDLs.

- The release of IL-1β from HCAECs is associated with release of LDH.

4.4 Discussion

This chapter investigates the effect of LDLs on HCAECs, a relevant cell type for the investigation of atherosclerosis. In a similar pattern to HUVECs, HCAECs are successfully activated by cytokines, as confirmed by the change in morphology and stimulated to release IL-1β, in agreement with previous studies (Alfaidi et al., 2015). Although lysates in both cytokine-stimulated HCAECs and HUVECs contain high levels of IL-1β, HCAECs produced more than two-fold higher levels of IL-1β. This indicates that HCAECs are more

135

responsive to cytokine-stimulation than HUVECs. This also agrees with published work showing that coronary artery ECs are substantially different to HUVECs in terms of the cytokines and interleukins they produce (Krishnaswamy et al., 1999, Dewberry et al., 2000, Francis et al., 1999).

Due to water-soluble cholesterol being not biologically relevant, I tested the effects of AgLDL treatment on HCAECs. However, AgLDL failed to release IL-1β into the culture supernatant of HCAECs similar to that seen in HUVECs. This may be because the aggregates of LDL are so large that they cannot enter the cells. Indeed, some investigators have suggested that cholesterol retention in AgLDL results mainly from surface attachment of AgLDL and that it does not enter cellular compartments (Zhao et al., 2004). Zhao et al., showed uptake of AgLDL by macrophages, but only minimal surface retention and incomplete internalisation in HCAECs. This non-entry would explain the lack of IL-1β release seen in my AgLDL experiments and indicates that the release of IL-1β from HCAECs in response to LDL is contingent on the mechanism of cellular LDL uptake.

Experiments conducted using AcLDL, the model lipid ligand, added more evidence supporting the LDL uptake theory of IL-1β release. Low doses of AcLDL induced high amounts of IL-1β release compared to high doses (100 and 200 µg/ml), with the highest quantified levels of IL-1β release seen in samples treated with AcLDL at concentration of 50 µg/ml, although all concentrations used successfully released high levels of IL-1β compared to the cytokine only stimulated control samples. A possible explanation for this,

is that HCAECs take up small molecules of AcLDL, and therefore release IL-1β proportionally in response to the uptake. However, high concentrations may be harder take up by endothelial cells, since AcLDL can aggregate at high concentrations (Okaji et al., 2004, Zhang et al., 1997, Ruuth et al., 2018).

Confocal imaging with fluorescently labelled AcLDL showed the cellular uptake of AcLDL by HCAECs, especially in the perinuclear region of the cells. This uptake, however, was only seen in cells treated with 50 μg/ml, which was the maximum IL-1β releasing concentration from treated cells. Higher concentrations of AcLDL were not taken up by cells. This adds further support to why lower concentrations of AcLDL (10,20 and 50 μg/ml) caused higher IL-1β release compared to higher concentrations which were not taken up by HCAECs. To clarify that these results were not caused by the thorough washing and chemical treatment used in the imaging protocol resulting in partial cell loss and creating a high risk of LDL denaturation, I conducted bright-field microscopy imaging following a direct formalin fixing protocol. This altered protocol also showed uptake of AcLDL at concentration of 50 μg/ml.

Although AcLDL is a common form of modified LDLs that has been widely used in LDL uptake studies of vascular cells and macrophages (Doran et al., 2008, D'Elios et al., 2017), it was considered not to be a biologically relevant candidate for my study. AcLDL is a laboratory-prepared artificial tool for modified LDL studies and has never been reported to be found *in vivo* (Steinberg, 2009).

137

Conversely, several studies showed the presence of OxLDL in multiple phases of atherosclerosis development in human atherosclerotic lesions and within macrophages and foam cells, confirmed by electron microscopy, radionuclide microscopy and fluorescent tagging of OxLDL (Steinberg, 1997, Ross, 1999a, Parthasarathy et al., 2000, Davies et al., 2006, Stacy, 2019, Nishi et al., 2002). Furthermore, OxLDL has been used in multiple atherosclerotic modelling studies *in vitro* as well as on human and *in vivo* studies of macrophages and vascular cells (Ahsan et al., 2015, Asmis et al., 2005, Brown et al., 2000, Hasanally et al., 2017, Kiyan et al., 2014, Stewart et al., 2005, Thum and Borlak, 2008). These studies have shown many roles that OxLDL plays during the process of atherosclerosis development and lesion formation, from endothelial injury to recruiting monocytes and macrophages and inducing platelet aggregation, and also show that OxLDL plays a role in inducing growth factors, increase the macrophage LDL uptake, increase the production of ROS and the creation of OxLDL autoantibodies, which all contribute towards increasing inflammation, thrombosis and plaque disruption. Furthermore, OxLDL induces metabolic dysfunction, oxidative stress and oxidative DNA damage (Thum and Borlak, 2008, Mondal et al., 2013).

During atherosclerotic lesion formation, LDL molecules that infiltrate to the subendothelial space undergo further oxidation and modification, transforming the infiltrated LDL molecules into OxLDL (Davignon and Ganz, 2004, de Nigris et al., 2003, Steinberg, 2009, Stewart et al., 2005). This has a clinical relevance as it has been shown that the plaque vulnerability to

138

rupture is correlated with high levels of OxLDL in both plaque and plasma (Nishi et al., 2002), which increases the risks of developing acute coronary syndromes and stroke (Packer, 2000, Rioufol et al., 2002).

Thus, OxLDL was a great candidate for my study. Indeed, OxLDL induced high levels of IL-1β release from stimulated HCAECs in my experiments. This is in agreement with studies that report that OxLDL activates the NLRP3 inflammasome, inducing release of IL-1β from other cells such as THP-1 macrophages (Liu et al., 2014). There is no published work, that I am aware of, on activated HCAECs that showed the OxLDL induced release of IL-1β.

OxLDL, at the concentration of 50 μg/ml, induced the maximum release of IL-1β from HCAECs, matching release with the highest studied concentration of AcLDL (the model ligand), and confirming that the effect is concentration dependent. OxLDL had also the highest IL-1β inducing effect of all the different modified LDLs studied. AcLDL, at 50 μg/ml, induced a recorded average of 155.38 pg/ml of IL-1β in supernatants, while OxLDL at the same concentration induced an average of 185.6 pg/ml, suggesting that OxLDL has a more inflammatory role than AcLDL.

 Studies have shown the uptake of OxLDL by macrophages was accompanied with increased expression of both the LOX-1 and CD36 scavenger receptors, a significant event in the process of foam cell formation (Xie et al., 2018, Rios et al., 2012, Cerletti et al., 2010). However, the uptake of OxLDL and the association between the uptake and the release of IL-1β has never been investigated in HCAECs. My data show the accumulation and build up of

139

OxLDL molecules within the cytoplasm of stimulated HCAECs. Non-stimulated HCAECs did not uptake OxLDL particles which adds further validation to the theory of LDL infiltration only after dysfunctional and inflamed endothelium, and that normal healthy (uninjured) endothelium does not allow infiltration (or uptake) of LDL molecules at high and low concentrations. These findings highlight the ability of HCAECs to internalise and uptake OxLDL, and the potential of OxLDL molecules for clustering inside the cell and potentially creating OxLDL crystal-like particles. This uptake consequently provides a secondary danger signal that cleaves ProIL-1β into a mature IL-1β, which was detected in culture supernatants of these cells.

This project aims to understand the effect of LDL on the release of IL-1β from HCAECs. Thus, it was important to study and monitor the LDH release in response to treatment with the different LDLs. Although no cell death was seen following treatment with all modified and non-modifed LDLs used in my study, I found LDH release associated with cells that have released IL-1β. HCAEC samples that did not release a significant amount of IL-1β did not release a significant amount of LDH either. In OxLDL treated HCAECs the increase in LDH release is less than that seen in AcLDL treated HCAECs with the same concentration, which had a 2.7 fold increased release of LDH compared to cytokine only stimulated control (section 4.7.1). This suggests that LDH release is associated with the mechanism of release and not the amount of IL-1β released, which will be further investigated in the next chapter. However, the idea of cell death and the release of IL-1 is not new. Researchers have been puzzled that IL-1 does not have a signal sequence

and cannot exit the cell. It had been thought that IL-1 is passively released from dead cells, but recently new mechanisms have been proposed including pyroptosis (discussed in chapter 5).

Finally, native LDL did not release a significant amount of IL-1β from treated HCAECs. Microscopically, it was clear that the reason for this was that inflamed and non-inflamed HCAECs did not take up native LDL. This is in agreement with a recent study that reported that OxLDL but not native LDL induced vascular inflammation (Daub et al., 2010). In this study, only OxLDL but not native LDL, induced foam cell formation in human CD34^{+} progenitor cells and induced ICAM-1 expression in the differentiated endothelial cells. Furthermore in the same study, activated platelets (20 µM adenosine diphosphate (ADP)), treated with OxLDL (10 µg/ml for 4 hours) showed uptake and internalisation of OxLDL by fluorescent microscopy, and this internalisation caused endothelial activation and inhibited endothelium regeneration. However, this was not seen after incubation with native LDL.

In my data, HCAECs treated with Native LDL experienced very low release of LDH. This further emphasises the role of LDH release from endothelial cells that was seen accompanied with all the modified cholesterol-induced IL-1β release mechanisms.

4.4.1 Limitations and future work
Although AcLDL molecules were seen inside the cells (section 4.3.6), in the perinuclear region by fluorescent microscopy, the protocol used (section 2.2.11.1) was complicated and required multiple washing and exposure to

different chemicals in order to fix the cells and stain the AcLDL. In addition, there was also a suggestion that the cells appeared senescent. Vascular endothelial cells and HCAECs in particular are known to become senescent in response to ageing as well as during inflammation and inflammatory markers expression (Olivieri et al., 2013). Therefore, uptake of AcLDL and OxLDL imaging was done by a formalin fixing protocol (section 2.2.11.2), which required less cell exposure to chemicals, and imaged by Brightfield microscopy. Although Brightfield microscopy was less specific than fluorescent tagging of OxLDL and AcLDL, the OxLDL internalisation was clear.

The accumulation of OxLDL particles/droplets was a very interesting finding in my work, however, a specified evaluation method was needed to further identify the chemical and physical properties of these internalised particles, and to investigate whether they were crystalized intracellularly. Many studies were able to image cholesterol crystals using electron microscopy (Abela and Aziz, 2006), polarized microscopy (Baumer et al., 2019) and optical coherence tomography (Katayama et al., 2020, Toutouzas et al., 2016, Koide et al., 2017) thus, this may be a future research direction.

4.5 Conclusions and Summary of Chapter

OxLDL is a key player in the pathophysiology of atherosclerosis and is present during all stages of atherosclerotic lesion formation. In this chapter, I have shown for the first time, that OxLDL induces the release of IL-1β from stimulated HCAECs. This release is secondary to HCAECs' uptake of OxLDL. OxLDL builds up in the perinuclear area in HCAECs and forms OxLDL crystal-like particles that accumulate over time and were seen from 6 hours of

incubation until 24 hours. OxLDL induces the release of LDH but does not cause typical cell death within 6 hours of treatment. Native LDL on its own is not inflammatory, nor does it induce an inflammatory response.

(Chapter 5) Unravelling the Mechanism Leading to IL-1β Release from Primed and OxLDL Treated Human Coronary Artery Endothelial Cells

5.1 Introduction

My project, and in particular this chapter, was based on the well-established understanding in macrophages that the NLRP3 inflammasome needs two signals to activate (Karasawa and Takahashi, 2017a) and, without this activation, IL-1β cannot be secreted (Rajamaki et al., 2010).

The first signal, referred to as the "priming signal", initiates via the NF-κB signalling pathway, which detects several TLRs, PAMPs and DAMPs (such as OxLDL (Duewell et al., 2010)) that trigger the activation of NF-κB, leading to the intracellular regulation of proIL-1β. At this stage, proIL-1β is produced, but remains within the cell until a second signal, known as the "oligomerization signal", is established (Dinarello and van der Meer, 2013). This signal comprises the oligomerization of the NLRP3 inflammasome activation components, phosphorylation of ASC and Caspase-1, which allow the external secretion of IL-1β from the cell (Mezzasoma et al., 2016).

Recent studies have identified multiple other upstream pathways that lead to NLRP3 inflammasome activation, such as the potassium ion efflux which is induced by the P2X7 receptor, acting as an agonist to the NLRP3 inflammasome (Tschopp and Schroder, 2010). Moreover, the release of cathepsin B is essential for cholesterol crystal induced activation of the NLRP3 inflammasome and release of IL-1β via lysosomal destabilisation in macrophages (Schroder et al., 2010, Niemi et al., 2011).

To determine whether the mechanism of OxLDL induced IL-1β release from HCAECs, which I demonstrated in my work in the previous chapters, is via a

Caspase-1/NLRP3 inflammasome dependent pathway, as hypothesised, I used inhibitors of Caspase-1 (Ac-YVAD-cmk) and the NLRP3 inflammasome (MCC950). Since the P2X7 receptor is highly involved in the early stages of the molecular pathway of IL-1β secretion (Section 1.5), I also conducted experiments using a P2X7 receptor inhibitor (A-438079-Hydrochloride). Lysosomal destabilisation is proposed as the most effective upstream pathway leading to activation of the NLRP3 inflammasome (Section 1.5), and release of active cathepsin B is a hallmark of lysosomal destabilisation, therefore studying the expression of cathepsin B was also included in my investigation.

Pyroptosis has recently been shown to be associated with Caspase-1/NLRP3 activation leading to IL-1β release from macrophages (Evavold et al., 2018, Kayagaki et al., 2015). These studies have identified a pyroptosis formed membrane pore as the gateway of IL-1β exit from the cell, and identified active GSDMD (cleaved GSDMD by active caspase-1) as the pyroptosis effector protein. Therefore, I also investigated GSDMD protein expression in HCAECs to further understand the mechanism of OxLDL-induced IL-1β release from these cells.

5.2 Materials & Methods

Detailed materials and methods used in this chapter are explained in (Chapter 2). Briefly, HCAECs were cultured as per protocol (section 2.2.1.2). Cells were treated with inhibitors of either Caspase-1, the NLRP3 inflammasome, or the P2X7 receptor inhibitor as described in (section 2.2.9). After the treatment with inhibitors, OxLDL treatments were applied to the

cells as described in (section 2.2.4). The produced and secreted levels of IL-1β were quantified by ELISA (section 2.2.6). Lysates and supernatants were also analysed for Caspase-1 activity (section 2.2.8).

The cells were imaged after incubation with OxLDL in the presence of each inhibitor by bright-field and phase contrast microscopy as described (section 2.2.11). Cell lysates and culture supernatants were also analysed by western blotting (section 2.2.10) to investigate expression of IL-1β, cathepsin B and GSDMD.

5.3 Results
5.3.1 OxLDL induces the release of IL-1β from HCAECs via a Caspase-1/NLRP3 dependent pathway
Having shown that OxLDL was an effective second stimulus to release IL-1β from cytokine-stimulated HCAECs and given the biological relevance of OxLDL (Section 4.3.8), I used OxLDL (50 µg/ml for 6 hours) as the main second stimulus in investigating all inhibitor effects for modulating the release of IL-1β.

5.3.1.1 Caspase-1 inhibition does not inhibit intracellular production of IL-1β, but significantly reduces OxLDL induced IL-1β release
Cytokine stimulated HCAECs (section 2.2.2) treated with OxLDL both with and without the presence of the potent caspase-1 inhibitor YVAD, showed no significant difference between intracellular production levels of IL-1β inside the cells (Figure 5.1A). However, the supernatants showed a significant reduction in IL-1β release (approximately 2.5 fold) from the cells, (Figure 5.1B), suggesting that the release of IL-1β from HCAECs is via a Caspase-1 dependent activation pathway.

147

Given that the level of IL-1β release from OxLDL and YVAD treated, stimulated cells, was not different to cytokine only stimulated cells (Figure 5.1B), this indicates that the caspase-1 pathway has a dominant effect.

(A)

TNF & IL-1	-	+	+	+	-
OxLDL	-	-	+	+	-
YVAD	-	-	-	+	+

(B)

TNF & IL-1	-	+	+	+	-
OxLDL	-	-	+	+	-
YVAD	-	-	-	+	+
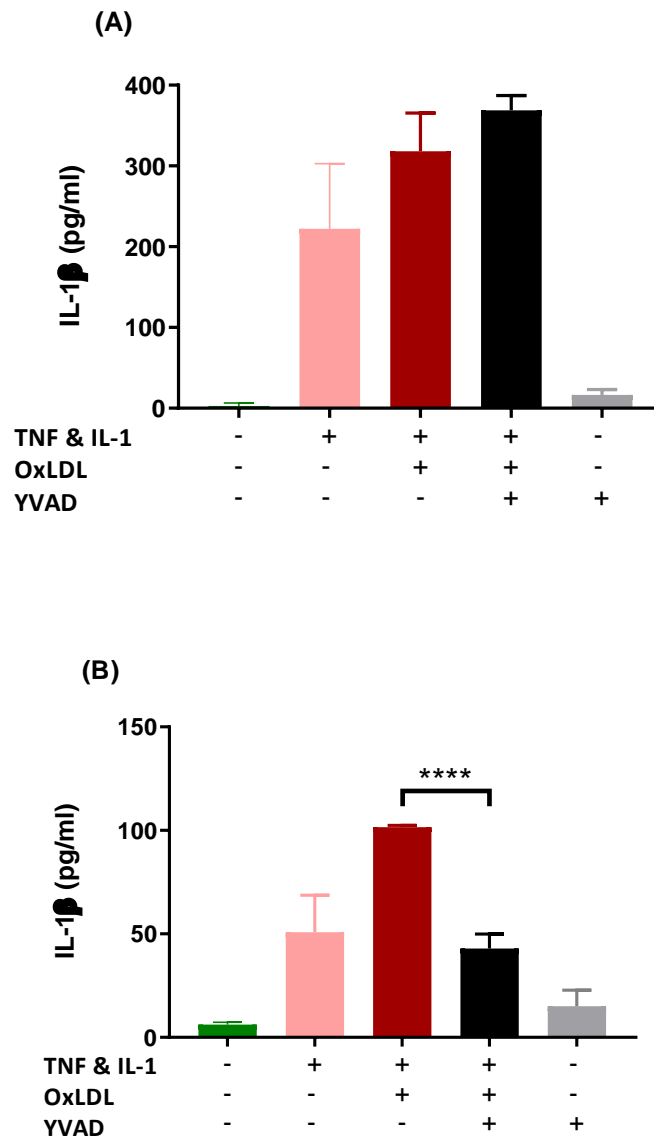
(Figure 5.1) YVAD inhibits OxLDL induced IL-1β release from HCAECs with no effect on production: HCAECs stimulated with pro-inflammatory cytokines IL-1α and TNF-α (10 ng/ml for 48 hours) and treated with OxLDL (50 µg/ml for 6 hours) with and without the presence of YVAD (50 µM) showed no significant difference between production in cell lysates (A), while in supernatants (B) significant inhibition of IL-1β release was observed. n=3 independent donors, data are expressed as mean ± SEM, analysed by one-way ANOVA followed by Bonferroni post hoc test, ****P<0.0001.

5.3.1.2 Inhibition of Caspase-1 causes ProIL-1β leakage from primed HCAECs following OxLDL treatment

Western blot analysis of cell lysates (Figure 5.2A) and culture supernatants

(Figure 5.2B), showed proIL-1β is expressed in all lysates. However, only the

supernatants of primed cells (stimulated with pro-inflammatory cytokines

IL-1α and TNF-α (10 ng/ml each) for 48 hours), that have undergone OxLDL

treatment (50 μg/ml for 6 hours) following Caspase-1 inhibition shows the

presence of proIL-1β (Figure 5.2). This surprising result suggests that proIL-

1β is somehow being released from cells, even when OxLDL is present, if

processing to mature IL-1β is inhibited (due to presence of YVAD).
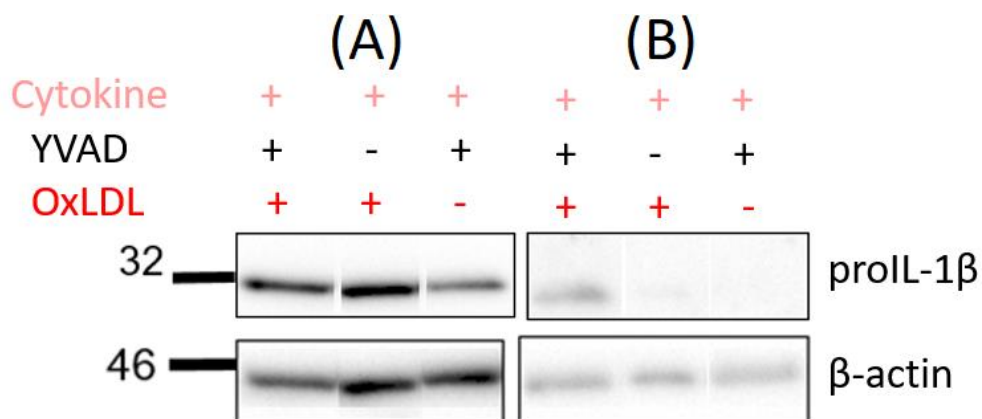
(Figure 5.2) Caspase-1-inhibited, OxLDL-treated, primed HCAECs leak ProIL-1β into culture supernatant: HCAECs stimulated with pro-inflammatory cytokines IL-1α and TNF-α (10 ng/ml for 48 hours) and treated with OxLDL (50 μg/ml for 6 hours) with and without the presence of YVAD (50 μM) showed ProIL-1β expressed in all cell lysates (A), but ProIL-1β was only detected in the supernatant (B), of the YVAD and OxLDL-treated, primed HCAECs. The western blots were repeated 4 times. This figure is a representative blot. B-actin was used as a house keeping protein to ensure equal loading of samples. For more details and for full blot see Appendix (VI).

5.3.1.3 Inhibition of the NLRP3 Inflammasome, inhibits IL-1β release

Having confirmed that inhibition of Caspase-1 reduces the release of mature IL-1β into supernatants from OxLDL treated HCAECs, and to further investigate whether the Caspase-1/NLRP3 activation pathway of OxLDL induced release of IL-1β, the NLRP3 inflammasome activation inhibitor MCC950 was used in the next set of experiments. Inhibiting the NLRP3 inflammasome in OxLDL treated, cytokine stimulated HCAECs, does not affect IL-1β production (Figure 5.3A), but results in complete inhibition of the OxLDL induced IL-1β release from stimulated HCAECs (Figure 5.3B). The level of release is lower than that measured in cytokine only stimulated cells, which is in contrast to the previous YVAD data (Figure 5.1).

(A)

TNF & IL-1	-	+	+	+	+	-
OxLDL	-	-	+	+	-	-
MCC950	-	-	-	+	+	+

(B)

TNF & IL-1	-	+	+	+	+	-
OxLDL	-	-	+	+	-	-
MCC950	-	-	-	+	+	+
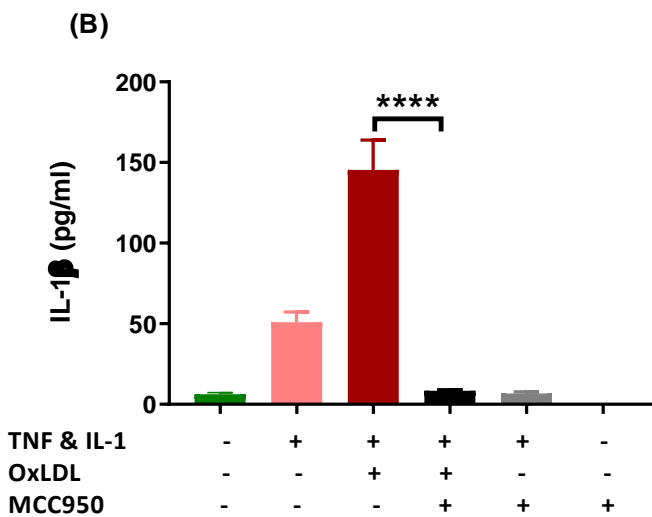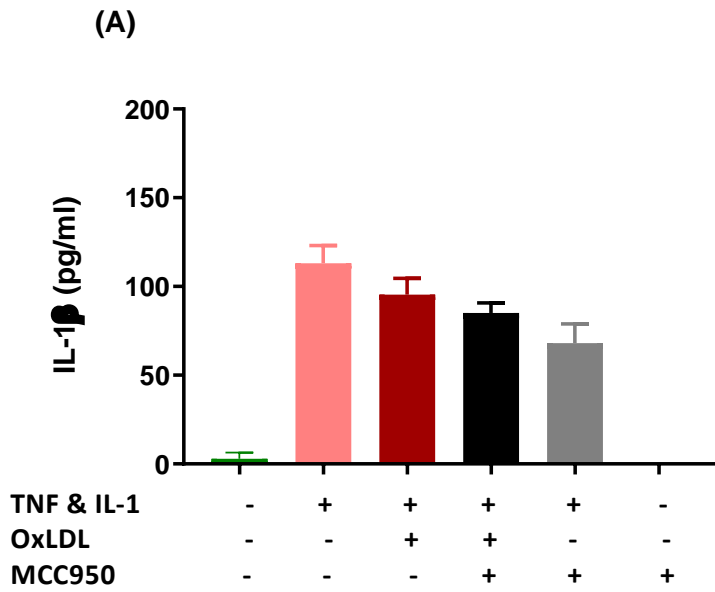
(Figure 5.3) MCC950 inhibits OxLDL induced IL-1β release from HCAECs with no significant effect on production: HCAECs stimulated with pro-inflammatory cytokines IL-1α and TNF-α (10 ng/ml for 48 hours) and treated with OxLDL (50 μg/ml for 6 hours) with and without the presence of MCC950 (10 μM) showed no significant difference in IL-1β production in cell lysates (A), while complete inhibition of IL-1β release was observed in supernatants (B). n=3 independent donors, data are expressed as mean ± SEM, analysed by one-way ANOVA followed by Bonferroni post hoc test, ****P<0.0001.

5.3.1.4 Caspase-1 is activated in HCAECs by OxLDL

Having shown that the mechanism of OxLDL induced IL-1β release from HCAECs is via Caspase-1/NLRP3 (Sections 5.3.1.1 - 5.3.1.3); I investigated the role of OxLDL on HCAECs in relation to caspase-1 activation, to further validate my findings. This approach is important as it indicates the dynamic nature of the system, and is therefore preferable to the western blot technique. Application of a caspase-1 bioluminescent substrate (Caspase-Glo 1, see section 2.2.8 for details) showed that OxLDL induced the activity of intracellular caspase-1, increasing it by approximately 75% in cytokine-stimulated cells and more than 100% in OxLDL treated cells only, compared to caspase-1 inhibited cells. As expected, inhibition of the NLRP3 inflammasome resulted in the lowest Caspase-1 activity (Figure 5.4A).

Released Caspase-1 activity (in the supernatant) followed the same trend of produced caspase-1, except that the lowest released caspase-1 activity was detected from the NLRP3 inhibited cells (Figure 5.4B).

(A)

(B)
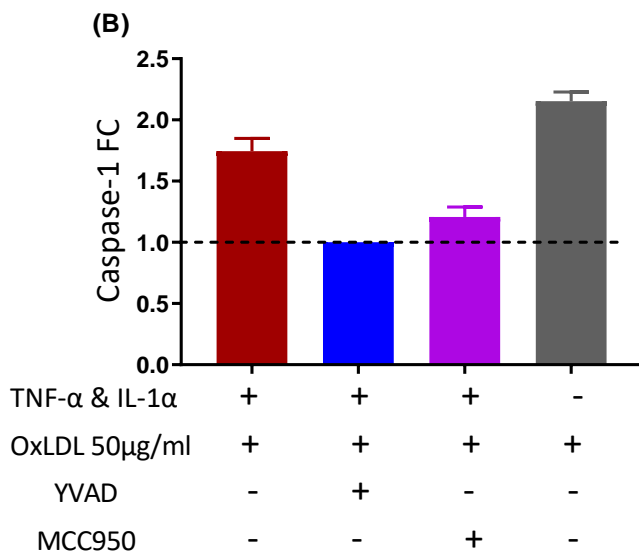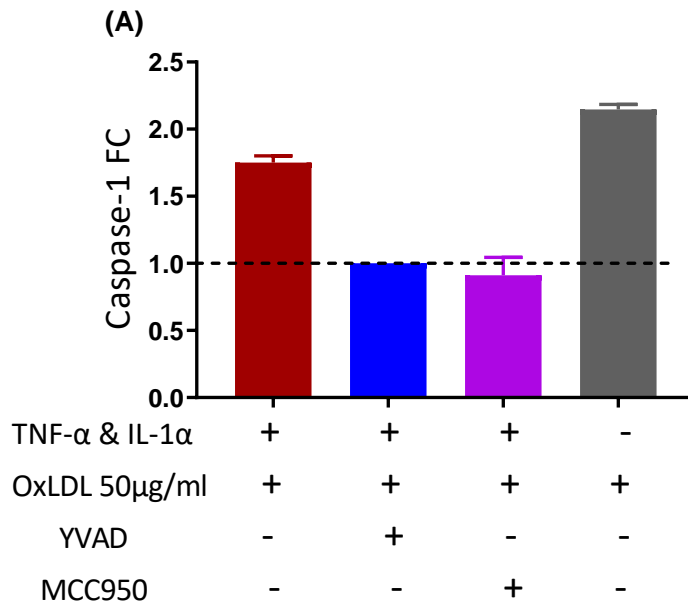
(Figure 5.4) OxLDL increases Caspase-1 activity in HCAECs: HCAECs stimulated with pro-inflammatory cytokines IL-1α and TNF-α (10 ng/ml for 48 hours) and treated with OxLDL (50 µg/ml for 6 hours) showed nearly 75% increase in capsase-1 activity intracellularly as shown in lysates (A), and in released active caspase-1 in supernatants (B). OxLDL without cytokine stimulation induced the highest Caspase-1 activity, with nearly two folds in both released and produced active caspase-1. n=3 independent donors, data are expressed as fold-change (FC) normalised to the assay negative control (cells treated with YVAD as per the manufacturer's instructions).

5.3.2 The P2X7 receptor facilitates OxLDL uptake

Next, the P2X7 receptor was investigated, because it was known to modulate an important upstream pathway that leads to the NLRP3 inflammasome activation in monocytes (Sections 1.5 and 5.1). The competitive P2X7 receptor antagonist A438079 hydrochloride (P2X7Ri) was used as per protocol (section 2.2.9).

5.3.2.1 Inhibition of the P2X7 receptor inhibits the OxLDL induced release of IL-1β

P2X7 inhibition resulted in partial but non-significant inhibition of IL-1β production inside the cells, as measured in lysates (Figure 5.5A). However, complete inhibition of IL-1β release was observed in cell culture supernatants following P2X7 receptor inhibition (Figure 5.5B).

Thus, P2X7 receptor appears to be involved in the mechanism of OxLDL induced release of IL-1β from HCAECs.

(A)

TNF & IL-1	-	+	+	+
OxLDL	-	-	+	+
P2X7Ri	-	-	-	+

(B)

TNF & IL-1	-	+	+	+
OxLDL	-	-	+	+
P2X7Ri	-	-	-	+
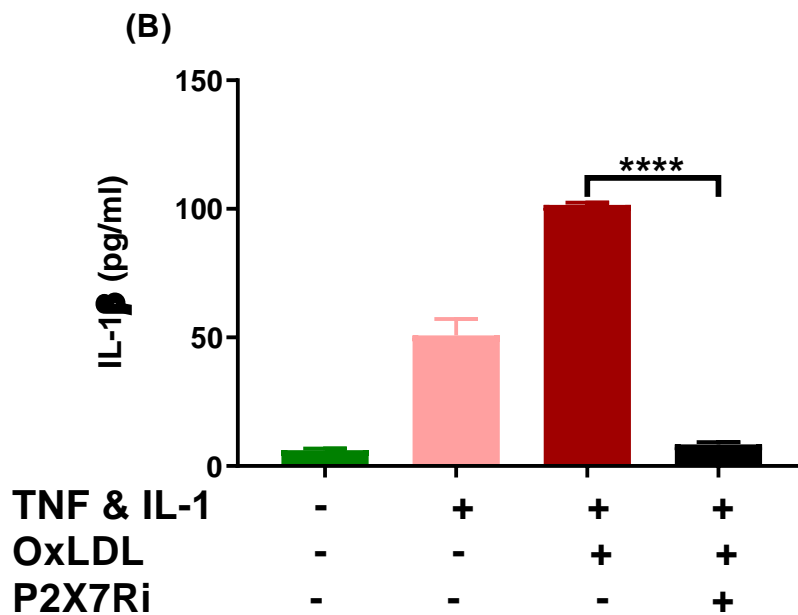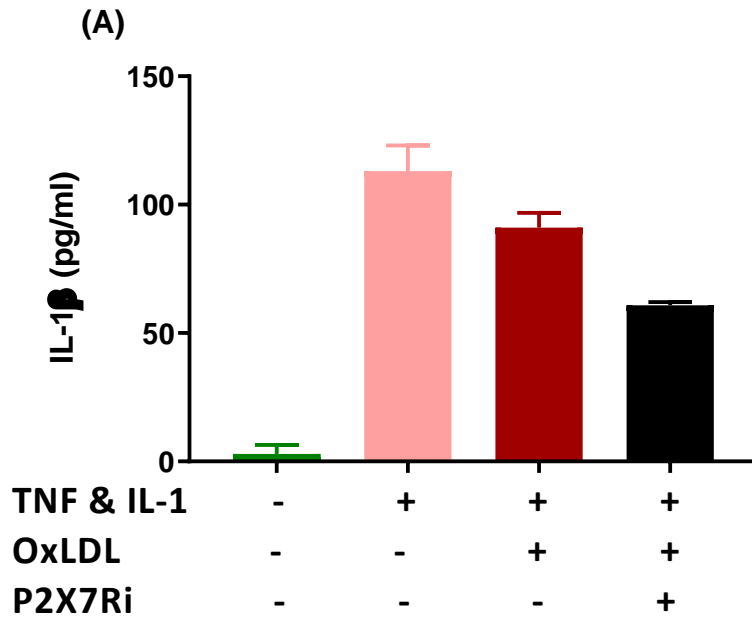
(Figure 5.5) Inhibition of the P2X7 receptor prevents OxLDL induced release of IL-1β from HCAECs: HCAECs stimulated with pro-inflammatory cytokines IL-1α and TNF-α (10 ng/ml for 48 hours) and treated with OxLDL (50 μg/ml for 6 hours) showed a slight non significant reduction of intracellular IL-1β in lysates (A). Released IL-1β in supernatants (B), showed an approximate reduction of 92% following P2X7 receptor inhibition. n=3 independent donors, data are expressed as mean ± SEM, analysed by one-way ANOVA followed by Bonferroni post hoc test, ****$P<0.0001$.

5.3.2.2 Inhibition of the P2X7 receptor, but not Caspase-1 or NLRP3 inhibits the intracellular expression of proIL-1β and reduces inactive caspase-1 expression, following OxLDL treatment in primed HCAECs

Having shown that inhibition of caspase-1, NLRP3 and P2X7 receptor led to inhibition of IL-1β release into HCAECs supernatants after priming and OxLDL treatment, I wished to study the protein expression of IL-1β and procaspase-1 inside and potentially outside cells. The latter proved very difficult and, after many months of trying to detect IL-1β outside cells, I concluded that this was not possible due to a lack of antibody sensitivity. I performed a serial dilution experiment (See figure 7.1 in Appendix IIII) and determined that the lowest amount of active IL-1β detectable in my system was 1.25 μg/ml. My supernatant samples contained significantly less than this lower limit and, even with 10-fold concentration of cell supernatants, I was not able to detect any bands in my samples. Therefore, I concentrated on the analysis of lysates during my studies.

HCAECs express proIL-1β (31kD) and proCaspase-1 (50kD) intracellularly after stimulation with the pro-inflammatory cytokine combination IL-1α and TNF-α (10 ng/ml for 48 hours) (Section 2.2.2). By Western blot, I was not able to detect any bands representing other forms of IL-1β, including 17kD. The data show that P2X7 receptor inhibition reduced the expression of proCaspase-1 and proIL-1β in primed HCAECs only following OxLDL treatment (Figure 5.6). Expression of both pro forms of these proteins was consistent between different samples.
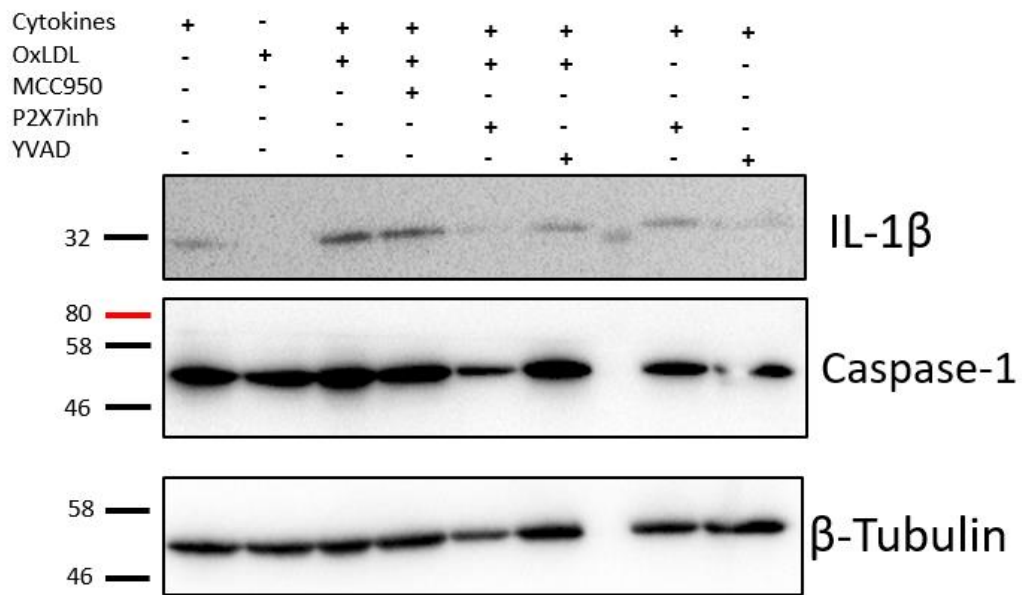
(Figure 5.6) Inhibition of the P2X7 receptor reduces the expression of inactive Caspase-1 and proIL-1β from HCAECs: Western Blotting analysis of cell lysates of primed HCAECs (stimulated with pro-inflammatory cytokines IL-1α and TNF-α (10 ng/ml for 48 hours)) and treated with OxLDL (50 μg/ml for 6 hours) in the presence of inhibitors of either Caspase-1, NLRP3 or the P27X receptor inhibitor. Reduced expression of both pro forms is seen, secondary to P2X7 receptor inhibition and OxLDL treatment. B-Tubulin was used as a house keeping protein to ensure equal loading of samples.

5.3.2.3 HCAECs Uptake of OxLDL is regulated via the P2X7 receptor

The Western blot data in the previous section, especially when using the P2X7Ri, suggested a possible connection between OxLDL and the P2X7 receptor, since only when these were present in the cells and milieu was the production of proIL-1β and proCaspase-1 reduced. Since activation of the P2X7 receptor leads to opening of a dye permeable pore involved in cellular trafficking (Qu and Dubyak, 2009, Karasawa et al., 2017). I hypothesised that the P2X7 receptor could also be involved in lipid uptake by HCAECs, similar to scavenger receptors.

157

Bright-field microscopy showed that P2X7 receptor inhibition prevents the uptake of OxLDL by HCAECs (Figure 5.7B) compared to OxLDL treated, cytokine stimulated cells, where OxLDL is clearly seen inside the cells (Figure 5.7A). Inhibiting the NLRP3 inflammasome by MCC950, did not prevent the OxLDL uptake and crystal-like structure formation, figures (5.7C and 5.7D). These data highlight the novel, early role of the P2X7 receptor in regulating entry of OxLDL into HCAECs which thereafter leads to Caspase-1/NLRP3 pathway activation. It also, potentially, explains why P2X7Ri leads to a reduction in released IL-1β if the entry of OxLDL as a second priming step for HCAECs is prevented.

(More detailed large images and high-resolution images for this experiment can be found in (Appendix A.3.3))
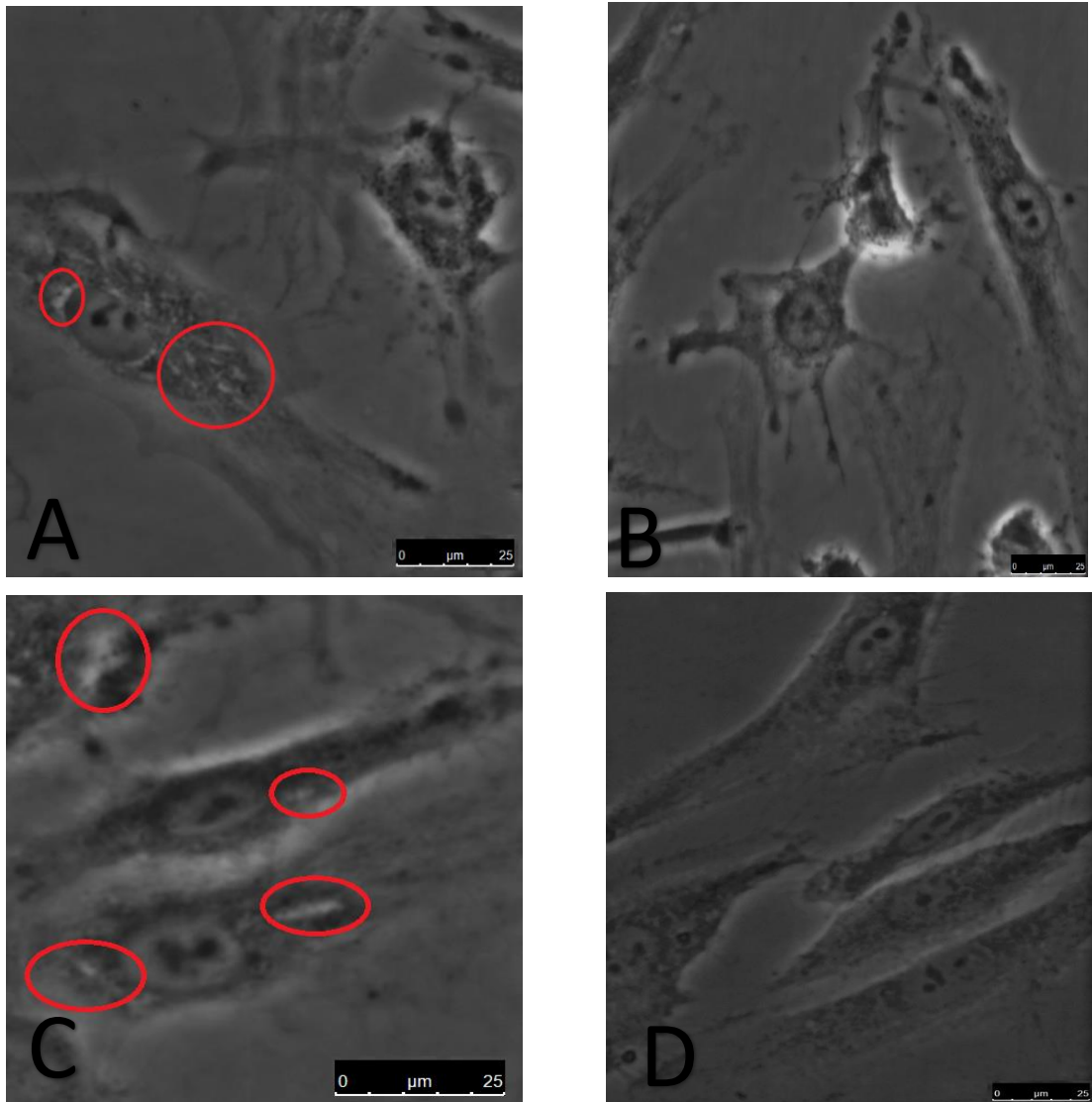
(Figure 5.7) Inhibition of the P2X7 receptor prevents the OxLDL uptake by HCAECs: HCAECs stimulated with pro-inflammatory cytokines IL-1α and TNF-α (10 ng/ml for 48 hours) and treated with OxLDL (50 µg/ml for 6 hours) without any inhibitor, shows OxLDL droplets within the cells. Positive control cells without any inhibitor treatment showing OxLDL droplets inside cells (A), P2X7 receptor inhibited cells with no OxLDL droplets visible (B), Caspase-1 inhibited cells showing OxLDL droplets/particles visible (C). Image (D) is the cytokine only stimulated control. OxLDL droplets/particles are highlighted in red circles. Images were taken by bright-field phase contrast Leica© microscope, scale bar 25 µm. Images have been cropped and modified to fit for this comparison figure. More images of this experiment, higher resolution and original size uncropped images can be found in Appendix (III) section A.3.3.

5.3.3 The OxLDL release of IL-1β from HCAEC is via a lysosomal destabilisation-pyroptosis pore-formation pathway

As previously described (section 1.5), the NLRP3 inflammasome can be activated by several mechanisms of which lysosomal destabilisation appears to be prominent (Lima et al., 2013, Niemi et al., 2011, Karasawa and Takahashi, 2017a).

To investigate whether the HCAECs-OxLDL activation of the NLRP3 inflammasome is also associated with release of mature activated (25-26 kDa) cathepsin B (section 1.5, introduction), lysates and supernatants were analysed by western blotting and a cathepsin B antibody was used to investigate expression of cathepsin B isoforms.

5.3.3.1 Heavy chain cathepsin B is expressed in Cytokine stimulated HCAECs and released into culture supernatants, only following OxLDL treatment.

HCAECs (stimulated with IL-1α and TNF-α 10 ng/ml for 48 hours, only) did not express the heavy chain (25-26 kDa) or procathepsin B (43 kDa) in either the lysate (figure 5.8A) or supernatant (figure 5.8B). In contrast, primed and OxLDL treated HCAECs (50 μg/ml for 6 hours), had high expression of the heavy chain cathepsin B isoform inside the cells, regardless of Caspase-1 or NLRP3 inflammasome inhibition, with lower expression of procathepsin B. Heavy chain cathepsin B was detected in OxLDL treated primed HCAECs with reduced expression after inhibition of Caspase-1 or NLRP3 inflammasome. NE which has a different mechanism of inflammasome activation which is caspase-1 independent (Alfaidi et al., 2015), did not induce cathepsin B release, nor cause activation intracellularly in primed HCAECs.

160
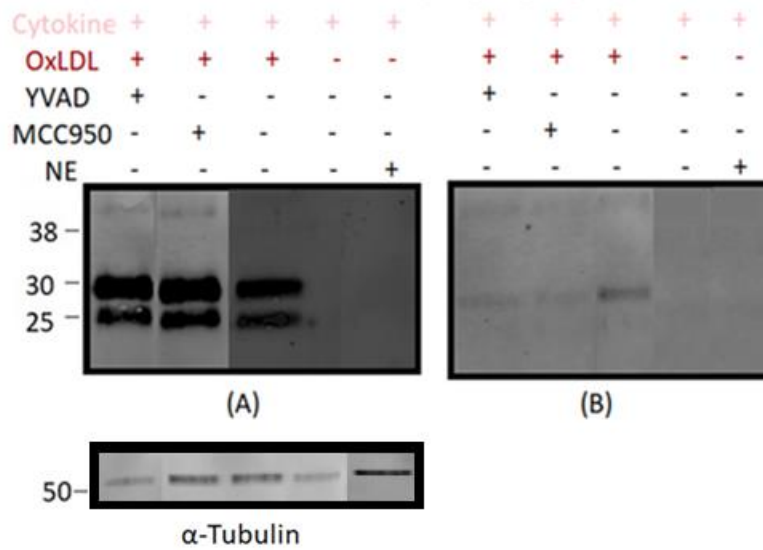
(Figure 5.8) OxLDL induces cathepsin B activation and secretion in primed HCAECs: Representative western blot of cell lysates (A) shows heavy chain cathepsin B (25-26 kDa), expressed in OxLDL treated (50 µg/ml for 6 hours), cytokine stimulated HCAECs (IL-1α and TNF-α 10 ng/ml for 48 hours), regardless of Caspase-1 or NLRP3 inhibition. Cytokine only stimulated lysates did not express either pro and mature forms. Secretion of activated cathepsin B in cell supernatants (B), was only found in OxLDL treated primed cells, with minimal expression after inhibition of Caspase-1 and NLRP3 inflammasome. Western blot was repeated 3 times. α-Tubulin was used as a house keeping protein to ensure equal loading of lysate samples (shown). Culture supernatants were equally loaded, further details and full blots can be seen in (Appendix VI (A.6.3))

5.3.3.2 OxLDL induced release of IL-1β is associated with GSDMD activation and cleavage, triggering pyroptosis.

The actual mechanism of release/exit of IL-1β from HCAECs was still elusive, but recent papers (Evavold et al., 2018, Kayagaki et al., 2015) suggested that pyroptosis, a highly inflammatory cell state which may precede cell death, uses intracellularly generated pores produced by a pore effector protein called gasdermin D (Shi et al., 2015). I hypothesised that IL-1β may exit twice primed HCAECs using gasdermin generated pores.

Western blot analysis for GSDMD isoforms in HCAECs, showed that primed HCAECs (stimulated with pro-inflammatory cytokines IL-1α and TNF-α at concentration of 10 ng/ml for 48 hours) express the full-length GSDMD (FL-GSDMD) protein (Figure 5.9). OxLDL treated (50 μg/ml for 6 hours), primed HCAECs show low expression of the cleaved C-terminal (22kDa) fragment. Both N-terminal and C-terminal fragments were not expressed after Caspase-1 or P2X7 receptor inhibition.

These results suggest that OxLDL-induced release of IL-1β from primed HCAECs is via programmed pyroptosis of these cells, and that OxLDL initiates programmed pyroptosis to facilitate release of IL-1β, but only after uptake of OxLDL and activation of the Caspase-1/NLRP3 inflammasome.
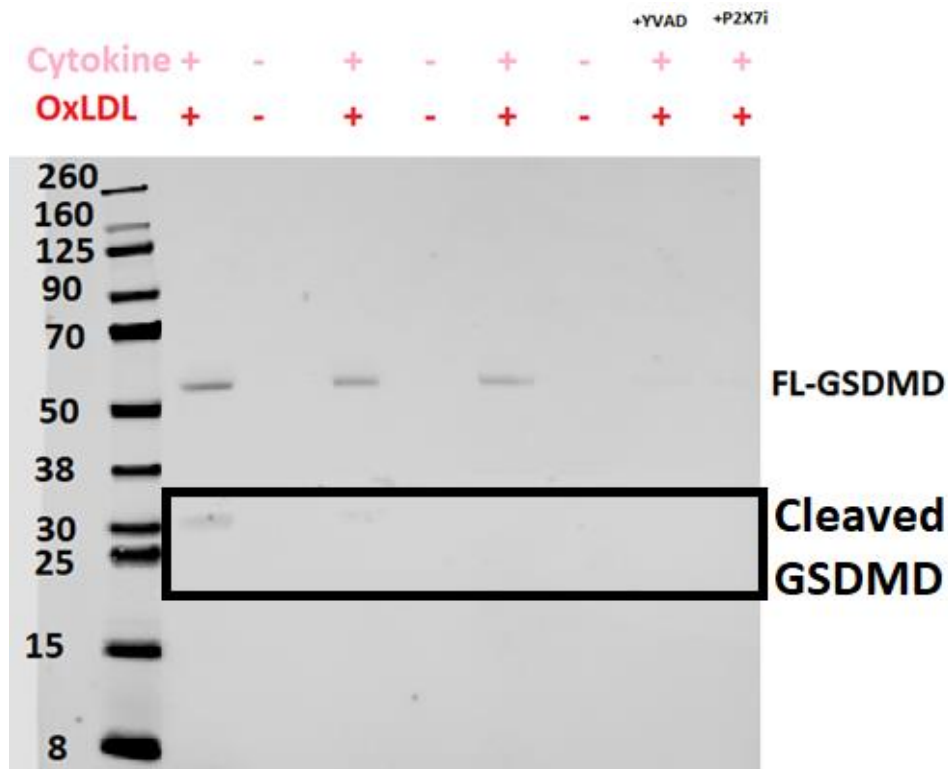
(Figure 5.9) OxLDL induces GSDMD activation and cleavage in primed HCAECs: Western blot analysis of cell lysates shows FL-GSDMD (50 kDa), expressed in primed HCAECs (cytokine stimulated HCAECs with IL-1α and TNF-α at concentrations of 10 ng/ml for 48 hours). Cleaved GSDMD was only expressed in OxLDL treated (50 μg/ml for 6 hours), cytokine stimulated HCAECs. Caspase-1 or P2X7 receptor inhibited cells, only expressed the FL-GSDMD. Western blot was repeated 3 times.

5.3.4 Summary of Results

In this chapter, I was able to show, for the first time, that cytokine stimulated HCAECs treated with OxLDL, release IL-1β via a caspase-1/NLRP3 inflammasome activation pathway. The uptake of OxLDL occurs via a P2X7 receptor regulated mechanism. The release of IL-1β is via a destabilisation of lysosomes leading to a pyroptosis, GSDMD regulated pore-forming mechanism. Key findings from this chapter to support this are:

1- Inhibition of caspase-1 significantly reduces release of bioactive IL-1β into culture supernatants.

163

2- Inhibition of the NLRP3 inflammasome prevents the processing of proIL-1β and significantly prevents release of IL-1β from the primed HCAECs.

3- OxLDL treatment, without priming, induces caspase-1 activity in HCAECs.

4- Inhibition of the P2X7 receptor inhibits OxLDL induced release from primed HCAECs, and inhibits cellular uptake of OxLDL.

5- Heavy chain cathepsin B and C terminal GSDMD (weak expression) are only expressed following the two-step priming and OxLDL treatment in HCAECs.

5.4 Discussion

The aim of this chapter was to understand the mechanism of OxLDL-induced release of IL-1β from HCAECs. Data presented support the hypothesis that a caspase-1/NLRP3 inflammasome activation pathway is involved in IL-1β release, and that this mechanism of release is similar to that studied in macrophages.

There is a well-established understanding that the protease caspase-1 is activated by the NLRP3 inflammasome, this activation cleaves proIL-1β intracellularly to a mature active IL-1β and controls the secretion of this active form extracellularly from the cell, via a highly inflammatory programmed cell death known as pyroptosis (Schneider et al., 2017).

Ac-YVAD-cmk (YVAD), was chosen in my study based on previous work that showed it is a strong peptide-based inhibitor of caspase-1, and considered an efficient reducer of IL-1β cleavage, as shown in macrophages and HCAECs (Gross et al., 2012, Broz et al., 2010, Alfaidi et al., 2015). Although, in my

experiments, there was a significant reduction of the OxLDL-induced release of IL-1β from HCAECs into cell supernatants after caspase-1 inhibition by YVAD, this appeared to be inactive proIL-1β as assessed by western blot. I was unable to detect active IL-1β by western blot due to sensitivity issues, as well as the possibility that no active IL-1β was in fact present. This finding (section 5.3.1.2) is in agreement with previous work showing that YVAD inhibition results in secretion of uncleaved IL-1β from nigericin-treated, primed macrophages (Schneider et al., 2017). These data, alongside mine confirm that the mechanism of release of IL-1β from macrophages and vascular endothelial cells are similar.

To further identify the mechanistic pathway, I used MCC950 as an NLRP3 inflammasome inhibitor, chosen because it is a potent and selective inhibitor of the NLRP3 inflammasome that does not inhibit NLRP1 or NLRC4 (Coll et al., 2015). In addition to being highly selective, it has been shown to block the release of active IL-1β by inhibiting the effect of several strong activators of the NLRP3 inflammasome such as nigericin and ATP in macrophages, by preventing the oligomerisation of ASC (Guo et al., 2015).

In my work, MCC950 significantly blocked the release of IL-1β from OxLDL treated HCAECs, which confirms that the IL-1β release mechanism is via a Caspase-1/NLRP3 activation pathway. Furthermore, there was no release of proIL-1β detected as a result of the NLRP3 inflammasome inhibition, unlike YVAD-induced caspase-1 inhibition. This is likely due to the role of MCC950 in the prevention of oligomerization of ASC (Coll et al., 2015, Swanson et al.,

2019, Guo et al., 2015), which prevented caspase-1 activation; while in caspase-1 inhibited cells, OxLDL may have partially activated the inflammasome, resulting in minimal release. This could have been tested using an ASC oligomerization assay (Mambwe et al., 2019), although I studied caspase-1 activation as a more robust assay. These data direct attention towards MCC950 and NLRP3 inflammasome inhibitors as important targets for inflammation control.

Although I expected to observe that OxLDL increased the activity of caspase-1 in primed HCAECs, it was also interesting that OxLDL significantly induced caspase-1 activity in unstimulated HCAECs. Furthermore, the levels of caspase-1 activity in non-primed cells were higher than that of primed cells, and this was consistent in analysis of caspase-1 activity in both supernatants and lysates.

Since the caspase assay used measures the activity of caspase-1 and other cross-reacting caspases including Caspase-11 and Caspase-8 (as mentioned in the product sheet), it is likely that this increase in unprimed cells is due to multiple inflammatory effects that OxLDL elicit on HCAECs, which may result in promoting the activity of multiple caspases (Xu et al., 2019, Yu et al., 2019, Schroeter et al., 2001). Other studies have reported that priming cells (macrophages, HUVECs and HCAECs) with the same proinflammatory cytokine combination (IL-1α and TNF-α) used in my study results in strong caspase-1 specific regulation (Franchi et al., 2009, Di Paolo and

Shayakhmetov, 2016, Alfaidi et al., 2015, Wilson et al., 2007). These findings also add further evidence to the inflammatory properties of OxLDL.

After demonstrating that OxLDL treatment induced release of IL-1β from HCAECs via a caspase-1/NLRP3 mechanism, I continued investigating the likely upstream and downstream pathways.

In terms of upstream pathways, the plasma membrane receptor (known as P2R) most involved in immunity and inflammation is the P2X7 receptor, which is expressed by most adaptive and innate immune (Di Virgilio et al., 2017) and endothelial cells (Subauste, 2019, Platania et al., 2019). The P2X7 receptor is an ATP-gated plasma membrane ion channel that, upon stimulation, generates a pore (Giuliani et al., 2017).

Since the P2X7 receptor is a major agonist of the NLRP3 inflammasome (Tschopp and Schroder, 2010) studied in context to OxLDL and foam cell formation in macrophages (Schroder et al., 2010, Niemi et al., 2011), studying its effects on ameliorating the release of IL-1β from HCAECs was novel and likely important. The P2X7 receptor inhibitor used was A-438079-hydrochloride, reported to be a strong P2X7 receptor antagonist by blocking the potassium ion efflux from cells, resulting in inhibition of the NLRP3 inflammasome and inhibiting the secretion of IL-1β in cells such as murine and human neutrophils (Karmakar et al., 2016). Indeed, blocking the P2X7 receptor in primed HCAECs resulted in inhibition of IL-1β secretion, but it was also interesting to note reduced intracellular levels of both procaspase-1 and proIL-1β. This further validated the sequence of cascades in the

167

pathway showing that potassium ion efflux is one of the main initiators of the NLRP3 inflammasome, and that loss of activation of the NLRP3 inflammasome results in the absence of intracellular processing of both procaspase-1 and proIL-1β. This also suggests, for the first time, that the P2X7 receptor is a very important early target of activation of inflammatory responses in HCAECs.

It was interesting to investigate the morphological changes of HCAECs in response to these inhibitors. Although no significant changes in cell appearance and extent of OxLDL intracellular crystal/particle formation were noted as a result of Casapse-1 and NLRP3 inflammasome inhibition, it was very clear indeed that inhibition of the P2X7 receptor resulted in a complete absence of intracellular OxLDL. This suggests that the P2X7 receptor is crucial for OxLDL uptake and that it is possibly involved early on as a regulator in the process of OxLDL uptake and induced release of IL-1β in HCAECs. This finding agrees with a recent study conducted on podocytes, showing that blocking the P2X7 receptor (with the same inhibitor used in my project) results in inhibition of OxLDL uptake and, therefore, stops OxLDL-induced apoptosis of podocytes (Zhu et al., 2019). The study also stated that absence of uptake led to inhibition of IL-1β secretion, primarily due to the inhibitor's role in blocking potassium ion efflux which resulted in inactivation of the NLRP3 inflammasome (Zhu et al., 2019). Another study by (Dewi et al., 2012) showed that P2X7 receptor inhibitor (AZ11645373) reduced OxLDL induced secretion of IL-8 and MCP-1 as well as preserving morphology changes in human macrophages. The role of the P2X7 receptor in direct

168

regulation of the uptake of OxLDL in HCAECs was shown for the first time in my project.

Another major feature of inflammasome regulation is lysosomal destabilisation, accompanied by release of mature heavy chain cathepsin B from cells and considered the single most effective upstream regulator for the NLRP3 inflammasome activation. This has been extensively reported in cholesterol crystal induced NLRP3 inflammasome activation pathway in macrophages (Lima et al., 2013, Niemi et al., 2011, Karasawa and Takahashi, 2017a, Schroder et al., 2010), and therefore, I analysed cathepsin B isoforms. Cathepsin B heavy chain was observed in OxLDL-treated, primed HCAECs only, regardless of Caspase-1 or NLRP3 inflammasome inhibition. This is in agreement with previous studies conducted on macrophages, which showed that cholesterol crystals activate the NLRP3 inflammasome by lysosomal destabilisation and subsequent cathepsin B activation and release (Moore et al., 2013, Oury, 2014, Rajamaki et al., 2010). This also indicates that lysosomal destabilisation takes place after uptake of OxLDL, which then leads to inflammasome activation. Hence, this explains why mature cathepsin B was seen regardless of caspase-1 or NLRP3 inflammasome inhibition in this current study, since I have shown that inhibition of either did not inhibit uptake or OxLDL crystal-like particle formation. These findings also suggest that OxLDL intracellular particles, which were reported in my study, behave similarly to cholesterol crystals. As discussed in (section 4.4.1), to further prove the nature of the OxLDL particles I imaged, I would need to use techniques such as electron microscopy and optical coherence

169

tomography, or stochastic optical reconstruction microscopy (STORM) such as that developed by (Varsano et al., 2018).

To determine whether cathepsin B was activated and expressed in HCAECs following OxLDL treatment only (Caspase-1 dependent), or via any secondary stimulus (that could elicit IL-1β and isn't caspase-1 dependent), NE was used as a stimulus, because it is known to induce the release of IL-1β from primed HCAECs via a caspase-1 independent pathway (Alfaidi et al., 2015). NE treated HCAECs did not induce activation of mature cathepsin B, suggesting that this cathepsin B activation is due to the inflammatory properties of OxLDL and its downstream roles.

OxLDL activates the NLRP3 inflammsome, in a similar mechanism to its function in macrophages (introduction, sections 1.4 and 1.5), and leads to cathepsin B activation and secretion, via lysosomal destabilisation.

The next stage was to consider how IL-1β exited the cell and under which cellular process. Recent studies on macrophages have suggested pyroptosis (section 1.5.3), a process which is associated with increased expression and release of caspase-1-activated GSDMD protein. This area of study is not well understood and caspase-1 has been shown to be involved in both GSDMD dependent and independent pyroptosis pathways (Shi et al., 2015, Kayagaki et al., 2015, Tsuchiya et al., 2019).

In my study, although it was very clear that primed HCAECs expressed the full-length GSDMD protein regardless of Caspase-1 or P2X7 receptor inhibition, the C-terminal activated GSDMD was only observed in the non-

inhibited cells, indicating that a pyroptotic activity was triggered. Despite multiple repetition of the western blotting analysis, the bands observed in this study were faint. The reason behind this is likely because of the 6-hour treatment period used in my project, as other studies used longer treatment durations (minimum of 16 hours of OxLDL treatment) to show GSDMD C terminal band (Evavold et al., 2018, Zhaolin et al., 2019). However, this duration of time in serum free media would have led to significant HCAECs death by apoptosis which could potentially confound the results (King et al., 2003).

The low expression level was also consistent with the relatively low levels of LDH released from HCAECs after a 6-hour treatment with OxLDL. Furthermore, given that HCAECs are primary human cells, the expression levels of proteins such as GSDMD and IL-1β are lower than that reported in many studies that used cell lines.

In addition to GSDMD expression, LDH release from cells is also considered an important factor associated with pyroptosis and studies have shown that LDH release occurs during pyroptosis (Bergsbaken et al., 2009, Evavold et al., 2018). My study showed LDH release was associated with OxLDL release in HCAECs (Section 4.3.8.4) without cell loss or cell death. It is also important to point that this release of LDH was in direct proportion to the release of IL-1β from HCAECs, and that the optimised concentration of 50 μg/ml which with the highest inducing release of IL-1β, was also the highest inducing concentration for LDH release.

The gasdermin data, together with LDH release as a result of OxLDL treatment, support the hypothesis that OxLDL induces the release of IL-1β via a pyroptotic mechanism. Activation of GSDMD results in membrane pore formation, and this activation and cleavage of GSDMD is enough to create membrane pores, which act as secretion windows for inflammatory molecules (de Rivero Vaccari et al., 2014, Bergsbaken et al., 2009, Schneider et al., 2017, Evavold et al., 2018). Thus, IL-1β is released from HCAECs in response to cytokine stimulation and OxLDL, via an endothelial cell membrane pore formation mechanism. The pores appear to be temporary in this experimental setting since wide scale cell death/loss does not occur.

5.5 Conclusions and Summary of Chapter

In this chapter, I showed that the release of IL-1β from HCAECs, in response to OxLDL secondary to priming with cytokines, is via a Caspase-1/NLRP3 dependent mechanism, supporting the main project hypothesis.

I also showed that OxLDL induces the activity of caspase-1, with or without the presence of priming cytokines.

I have postulated a mechanism (figure 5.10). Briefly, the P2X7 receptor plays a key role in the initiation of the Caspase-1/NLRP3 cascade by regulating the uptake of OxLDL by primed HCAECs. This triggers lysosomal destabilisation, which activates the NLRP3 inflammasome and caspase-1, which cleaves proIL-1β into mature IL-1β and cleaves GSDMD into a mature C-terminal GSDMD. The active GSDMD creates a sufficient number of membrane pores,

which allow IL-1β to exit the cell along with other inflammatory proteins and

cytokines by initiating pyroptosis (Figure 5.10).
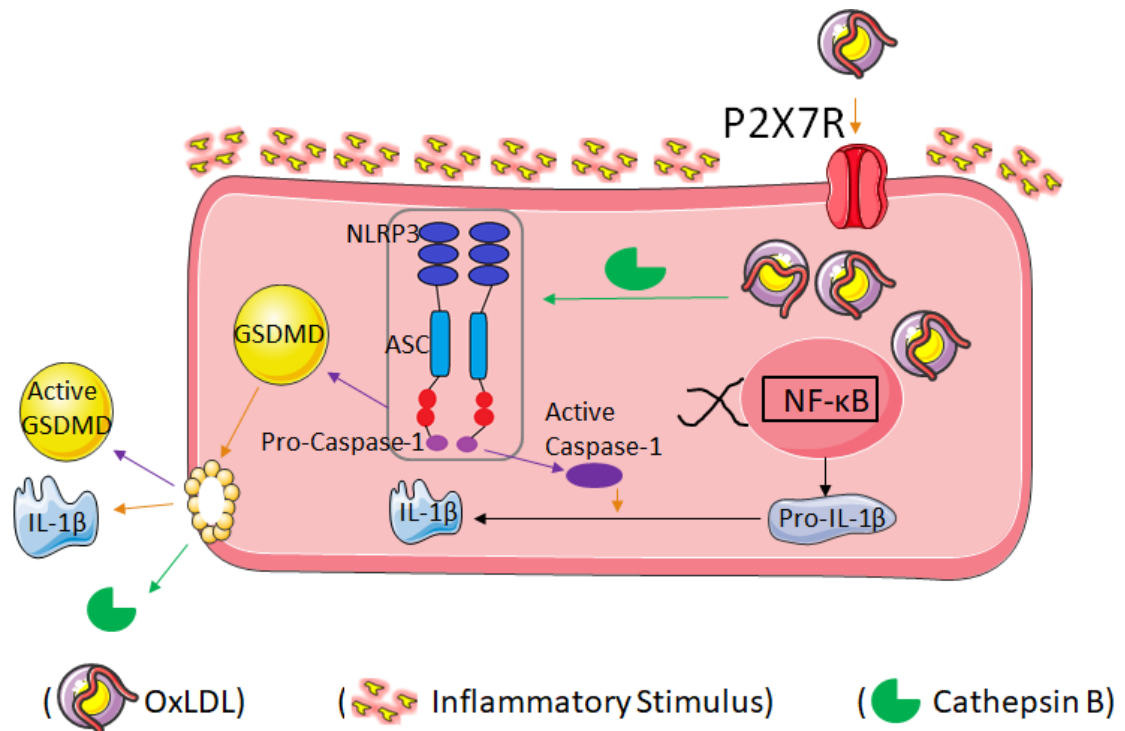
(Figure 5.10) Unravelling the mechanism of OxLDL induced release of IL-1β release from primed HCAECs: When vascular endothelial cells are inflamed, the innate immune system is activated which triggers the intracellular synthesis of proIL-1β and the first signal of the inflammasome activation via the NF-kB pathway. This leaves an inactive IL-1β and an inactive inflammasome, until a second danger/inflammatory signal is received by the cell. OxLDL, the second signal, enters to the cell via the P2X7 receptor, which triggers cascades of inflammasome activation pathways primarily lysosomal destabilisation and activation of cathepsin B, which thereafter activates the inflammasome via oligomerization of ASC. This results in the release of active caspase-1, which cleaves proIL-1β into bioactive mature IL-1β and cleaves GSDMD into mature C-terminal GSDMD, which triggers a pyroptotic cell response and creates membrane pores. The created membrane pore allows IL-1β to be secreted freely from the cell.

(Chapter 6) Final Discussion, Summary, Limitations and Future Work

6.1 Overview of final discussion and relevance of the study

There is a well-established understanding that atherosclerosis is a disorder that begins with structural changes to the arterial wall, leading to life threatening cardiovascular events, and that this process is driven by two important factors: inflammation and lipid accumulation (Glanz et al., 2020). This understanding was established after decades of studies providing evidence that inflammation is associated with atherosclerosis development, and is equally important to hyperlipidaemia in this process (Section 1.3).

In 2005, robust evidence showed the direct relationship between hsCRP levels and ACS disease progression and cardiovascular complications (Ridker et al., 2005). Ridker also showed that statins have a favourable effect on prognosis in CVD and ACS patients by lowering inflammation, independent of lowering LDL (Ridker et al., 2008, Ridker et al., 2005).

These studies were conducted in parallel with multiple clinical trials, all of which aimed to investigate to what extent inhibition of inflammation can be promising in prevention of atherosclerosis development. These include: the CANTOS trial (NCT01900600), which used a monoclonal L-1β antibody (canakinumab) and the CIRT (Cardiovascular inflammation reduction trial) (NCT01594333) which targeted inflammation using Low dose methotrexate. However, after an average follow up of 27 months, the CIRT trial was stopped, as methotrexate did not significantly reduce adverse CVD events, mainly due to the absence of its effect on lowering L-1β, IL-6 and hsCRP levels (Ridker et al., 2019, Le Bras, 2019).

In addition, (Sabatine et al., 2017) showed that LDL reduction using Evolocumab (a PCSK9 inhibitor), alone, without the administration of an anti-inflammatory agent, led to a 12.6% reduction in the risk of adverse cardiovascular events (MI, cardiovascular death, stroke, coronary revascularisation or hospitalisation due to unstable angina). This study also showed that the risk reduction increased to nearly 19% after the first year of administrating the treatment. Interestingly, the CANTOS trial showed that the anti-inflammatory treatment (in particular IL-1β inhibition), using canakinumab, without a LDL lowering agent, led to 15-17% reduction in the same end points (Ridker et al., 2017).

Surprisingly, the range of risk reduction of both approaches in CVD endpoints is similar, and raise attention towards the association between LDL and inflammation in atherosclerosis development, without focusing on one of them as a single target to ameliorate atherosclerosis. The data suggest that both are equally important targets. My understanding is that there is a strong positive interaction between LDL and inflammation, and the combined effect drives the pathophysiological development of plaques and CVDs thereafter. This is in agreement with the study conducted by (Bohula et al., 2015), which was among the first trials to use the combined LDL-lowering plus inflammation-lowering approach. The main objective of this trial (which is also known as the IMPROVE-IT Trial NCT00202878), was to evaluate the clinical outcome of using an LDL lowering agent as well as a pleotropic inflammatory lowering agent at the same time. Bohula et al., showed that using simvastatin and ezetimibe (inhibitor of cholesterol

176

absorption) combined, results in strong LDL and inflammation reduction, and that this combined effect is more efficient in reaching target hsCRP and LDL-C levels, and, therefore, results in better outcomes for the patients with significantly fewer CVD complications and events (Bohula et al., 2015). In particular, achieving both target levels of hsCRP and LDL-C with both simvastatin and ezetimibe combined reduced the relative risk of the primary endpoints by 29%, compared to achieving neither target by either of the drugs alone. This study highlighted the importance of the dual target approach for future drugs and atheroprotective agents, and has inspired many studies, including my project.

Two years after the IMPROVE-IT study, the CANTOS trial was published. This reignited interest in IL-1β in particular, and in the mechanism of its release from vascular cells. Specifically, CANTOS showed that there was a 31% reduction in CVD mortality and all-cause mortality among the trial participants, as a result of the robust inhibition of inflammatory response, by inhibiting IL-1β. There was also a 35-40% reduction in serum hsCRP and IL-6, with no change in LDL-C (Ridker, 2018).

Thus, there remains a need to develop a therapeutic/preventative system that targets both inflammation and cholesterol, and can potentially limit the residual inflammation and residual cholesterol risk and become more efficient than the recently proposed agents. The complexity of IL-1β release is well known. However, there are unanswered questions regarding what causes its release, how it is released and via which mechanism(s), which

could be targetable in future. This thesis has highlighted, for the first time, that OxLDL leads to the release of mature bioactive IL-1β, from the vascular endothelium, via a caspase-1/NLRP3 inflammasome, GSDMD-D-pyroptosis pathway, triggered by P2X7 mediated uptake of OxLDL (Figure 5.10). Thus, the research presented highlights the potential importance of inhibitors for the NLRP3 inflammasome, the P2X7 receptor and GSDMD, as potential atheroprotective targets, reducing inflammation and cholesterol entry to cells to ameliorate atherosclerosis development.

6.2 Summary of the study, limitations and future perspective

LDL is present in the arterial wall in different forms, such as OxLDL, and the highly inflammatory environment of atherosclerotic lesions with the presence of oxidising agents and free radicals alters the structure of these molecules and changes their forms (Valko et al., 2007, Stocker and Keaney, 2004, Steinberg, 1997). Therefore, studying the effect of different types of modified cholesterols on the propensity of the vascular endothelium to become inflamed adds to the overall understanding of atherosclerosis and early detection of pathological changes. Despite this, *in vitro* models of atherosclerosis, in context to IL-1β release and expression, have been primarily focused on macrophages and HVSMCs, with less focus on endothelial cells.

The endothelium is the inner most layer of the artery, and, therefore, it is the layer that is in continuous contact with the blood stream. Thus, studying the endothelium is important if we want to understand the early changes to the vasculature that leads to atherosclerosis development. As inflammation

also plays a key role in atherosclerosis, the changes that occur to the expression of IL-1β in human vascular endothelial cells in response to different types of LDL molecules is the core of my study.

In all experiments, cytokine-stimulated versus non-cytokine stimulated cells, in the presence or absence of LDL (as controls), were investigated. This was crucial to tease out the mechanisms involved in release of IL-1β when exposed to LDL. Non-stimulated cells showed that modified LDLs (such as OxLDL or AcLDL) are not sufficient to cause release of this inflammatory cytokine, in an inactive endothelium. Only when an endothelial cell has been exposed to inflammatory stimuli, is IL-1β released, and this release is dependent on a second stimulus: in this case, modified LDL.

I began my study using HUVECs, then followed that by HCAECs, using multiple forms of LDL (water-soluble cholesterol, OxLDL, AcLDL, AgLDL and Native LDL) with treatment time of 6 hours. This time was chosen as it has previously been shown to be the optimum time for IL-1β release, following two-step stimulation (Alfaidi et al., 2015). Furthermore, it has been shown that the 6-hour treatment with OxLDL, in particular, was sufficient for THP-1 macrophages to take up OxLDL and to elicit inflammatory effects (Munteanu et al., 2006). My studies showed that HCAECs can engulf and allow infiltration of modified LDL (not unmodified native LDL), and this was only if the cells were inflamed (primed or stimulated by inflammatory stimulus). Similarly, HCAECs only released IL-1β following these two-step stimuli. water-soluble cholesterol, AcLDL and OxLDL all were found to cause

IL-1β release from primed HCAECs. However, AgLDL and native LDL did not cause release, probably because neither of these types of LDL were taken up by the cells. AgLDL is thought to be too large for the cells to engulf, and native LDL lacks the modification needed to cause uptake.

After optimising the in *vitro* model to elicit the maximum release of IL-1β: using IL-1α and TNF-α stimulated HCAECs treated with OxLDL, I used these conditions alone to investigate the mechanisms involved.

Primed HCAECs released significant amounts of IL-1β after incubation with OxLDL. This was concentration dependent and was recorded to release the maximum levels of IL-1β at a concentration of 50 μg/ml. Stimulated HCAECs do not release IL-1β without this second stimulus of OxLDL. Similarly, unstimulated (un-primed) HCAECs do not release IL-1β. This confirms the two-step process that is crucial for the mechanism of IL-1β release in a priming step to produce proIL-1β followed by a second signal to initiate the cleavage of and release of mature IL-1β.

I have shown that primed HCAECs engulf OxLDL via the P2X7 receptor, creating OxLDL crystal like particles inside the cell. Inhibition of the P2X7 receptor inhibits the uptake of OxLDL and the release of IL-1β.

I have also shown that OxLDL induces the release of IL-1β from HCAECs via a caspase-1/NLRP3 pathway, and that this mechanism is contingent on the OxLDL uptake by HCAECs. Furthermore, OxLDL increases caspase-1 activity in HCAECs, indicating its highly inflammatory properties. The uptake of OxLDL is enough to activate the inflammasome via lysosomal destabilisation

180

and release of active cathepsin B. The activated NLRP3 inflammasome releases active caspase-1, which cleaves proIL-1β into mature IL-1β and cleaves GSDMD into active GSDMD creating membrane pores that allow the exit of mature IL-1β.

Understanding the inflammatory pathways that lead to developing life affecting diseases (such as atherosclerosis) helps significantly in discovering new techniques and methods to prevent these diseases by altering or completely inhibiting such pathways. In particular, data from this study suggests the importance of inhibitors (such as the NLRP3 inflammasome inhibitors and P2X7 receptor inhibitors) in ameliorating the inflammatory responses, which lead to development of atherosclerosis, and therefore preventing IHDs and ACS.

This study has several limitations that could be addressed in future investigations. Most imaging protocols require the cells to be fixed with chemicals and/or wax, which could potentially dissolve the cholesterol inside tissue. Frozen sections are generally used to image crystals in cells, which can lead to potential errors caused by ice-crystal formation when freezing tissue. However, this study focussed on cells alone, rather than tissue, and cells were imaged following formalin fixation alone, which does not affect crystal formation.

The focus of the study was to observe the changes that occur in release and production as well as the expression of IL-1β, and this study concentrated on investigations using a 6-hour incubation. Investigating the effects of

181

prolonged treatments could add more to the understanding of the mechanisms of IL-1β release from HCAECs.

At the time of this study, human GSDMD inhibitors were not well established and therefore GSDMD expression was visualised using western blotting. Although weak active GSDMD was detected, I was unable to confirm the role of GSDMD by use of an inhibitor. The current available inhibitors such as Necrosulfonamide (NSA) (Rathkey et al., 2018, Sun et al., 2012), Bay 11-7082 (McKenzie et al., 2020) and disulfiram (Li et al., 2019), are not GSDMD specific (McKenzie et al., 2020), and inhibit caspase or NF-κB, which also inhibit GSDMD cleavage, as part of their downstream pathways.

HCAECs released levels of IL-1β that fall below the detection limit of western blotting see (Appendix A.4). Therefore, I was unable to confirm that only active IL-1β was being detected in the ELISA relied on during the study. However, information from the supplier stated that the detection of proIL-1β, although possible, is rare.

To continue this project, given time, the effects of longer and shorter periods of OxLDL treatment on HCAECs, would be investigated to confirm the time scale involved in OxLDL action. Investigating the effects of human GSDMD inhibitors once well established and available commercially would also be an interesting avenue. In addition to HCAECs, investigating the effects of OxLDL on HVSMCs, and comparing the effects with HCAECs, could add more understanding to the pathway of atherosclerosis lesion development.

Another promising direction to take this project could also be to investigate whether the release of IL-1β from endothelial cells is luminal or abluminal, using methods such as transwell plates. This would potentially answer the question of which direction endothelial cells release IL-1β: to the luminal side, or abluminally towards SMC? Knowing this would add more understanding to the release mechanism and approaches to inhibit IL-1β release.

In context of the mechanistic study, adding more pathway specific inhibitors such as ASC, cathepsin B and scavenger receptor inhibitors such as CD36, could also more clearly define the pathway and show other possible ways of inhibiting IL-1β release caused by OxLDL particles.

6.3 Concluding remarks

Due to the complexity of cardiovascular disease development, the amelioration of atherosclerosis by one therapeutic agent has proven, so far, to be difficult. The current available agents and medications are costly, and there is uncertainty about the side effects of long term use associated with them. Atherosclerosis is usually asymptomatic, and the medications and management are usually started when it becomes symptomatic. Thus, there is still a need to develop a preventative agent, rather than a therapeutic, to stop and potentially reverse atherosclerosis lesion formation in the early development phases, rather than the late phases.

My study highlights potential targets that could potentially be developed as future preventive and therapeutic agents. The oxidation of LDL within blood vessels is a major event triggered by a complex inflammatory pathway involving the high expression of multiple inflammatory cytokines. I speculate that, in addition to the approach of lowering LDL-C and inflammation, specific inhibition of the NLRP3 inflammasome and P2X7 receptors could add further specificity to target residual inflammation and residual LDL-C risk, and, therefore, limit, and potentially reverse, atherosclerosis lesion formation and prevent life threatening events.

References

All references were written in accordance to the Harvard format managed

by the reference manager EndNote version 8.0.2.

ABDELHAMID, A. S., BROWN, T. J., BRAINARD, J. S., BISWAS, P., THORPE, G. C., MOORE, H. J., DEANE, K. H., ALABDULGHAFOOR, F. K., SUMMERBELL, C. D., WORTHINGTON, H. V., SONG, F. & HOOPER, L. 2018. Omega-3 fatty acids for the primary and secondary prevention of cardiovascular disease. *Cochrane Database Syst Rev,* 7**,** CD003177.

ABDUL-MUNEER, P. M., ALIKUNJU, S., MISHRA, V., SCHUETZ, H., SZLACHETKA, A. M., BURNHAM, E. L. & HAORAH, J. 2017. Activation of NLRP3 inflammasome by cholesterol crystals in alcohol consumption induces atherosclerotic lesions. *Brain Behav Immun,* 62**,** 291-305.

ABE, K. & MATSUKI, N. 2000. Measurement of cellular 3-(4,5-dimethylthiazol-2-yl)-2,5-diphenyltetrazolium bromide (MTT) reduction activity and lactate dehydrogenase release using MTT. *Neurosci Res,* 38**,** 325-9.

ABELA, G. S. 2010. Cholesterol crystals piercing the arterial plaque and intima trigger local and systemic inflammation. *J Clin Lipidol,* 4**,** 156-64.

ABELA, G. S. & AZIZ, K. 2005. Cholesterol crystals cause mechanical damage to biological membranes: a proposed mechanism of plaque rupture and erosion leading to arterial thrombosis. *Clin Cardiol,* 28**,** 413-20.

ABELA, G. S. & AZIZ, K. 2006. Cholesterol crystals rupture biological membranes and human plaques during acute cardiovascular events--a novel insight into plaque rupture by scanning electron microscopy. *Scanning,* 28**,** 1-10.

ABELA, G. S., AZIZ, K., VEDRE, A., PATHAK, D. R., TALBOTT, J. D. & DEJONG, J. 2009. Effect of cholesterol crystals on plaques and intima in arteries of patients with acute coronary and cerebrovascular syndromes. *Am J Cardiol,* 103**,** 959-68.

ADAMS, M. R., KINLAY, S., BLAKE, G. J., ORFORD, J. L., GANZ, P. & SELWYN, A. P. 2000. Pathophysiology of atherosclerosis: development, regression, restenosis. *Curr Atheroscler Rep,* 2**,** 251-8.

AHSAN, A., HAN, G., PAN, J., LIU, S., PADHIAR, A. A., CHU, P., SUN, Z., ZHANG, Z., SUN, B., WU, J., IRSHAD, A., LIN, Y., PENG, J. & TANG, Z. 2015. Phosphocreatine protects endothelial cells from oxidized low-density lipoprotein-induced apoptosis by modulating the PI3K/Akt/eNOS pathway. *Apoptosis,* 20**,** 1563-76.

AKESON, A. L., SCHROEDER, K., WOODS, C., SCHMIDT, C. J. & JONES, W. D. 1991. Suppression of interleukin-1 beta and LDL scavenger receptor expression in macrophages by a selective protein kinase C inhibitor. *J Lipid Res,* 32**,** 1699-707.

ALFAIDI, M., WILSON, H., DAIGNEAULT, M., BURNETT, A., RIDGER, V., CHAMBERLAIN, J. & FRANCIS, S. 2015. Neutrophil elastase promotes interleukin-1beta secretion from human coronary endothelium. *J Biol Chem,* 290**,** 24067-78.

ANDREI, C., DAZZI, C., LOTTI, L., TORRISI, M. R., CHIMINI, G. & RUBARTELLI, A. 1999. The secretory route of the leaderless protein interleukin 1beta involves exocytosis of endolysosome-related vesicles. *Mol Biol Cell,* 10, 1463-75.

ARENAS DE LARRIVA, A. P., ALONSO, A., NORBY, F. L., ROETKER, N. S. & FOLSOM, A. R. 2019. Circulating ceruloplasmin, ceruloplasmin-associated genes and the incidence of venous thromboembolism in the Atherosclerosis Risk in Communities study. *J Thromb Haemost,* 17**,** 818-826.

ASMIS, R., BEGLEY, J. G., JELK, J. & EVERSON, W. V. 2005. Lipoprotein aggregation protects human monocyte-derived macrophages from OxLDL-induced cytotoxicity. *J Lipid Res,* 46**,** 1124-32.

AVIRAM, M. 1993. Modified forms of low density lipoprotein and atherosclerosis. *Atherosclerosis,* 98**,** 1-9.

AVIRAM, M., MAOR, I., KEIDAR, S., HAYEK, T., OIKNINE, J., BAR-EL, Y., ADLER, Z., KERTZMAN, V. & MILO, S. 1995. Lesioned low density lipoprotein in atherosclerotic apolipoprotein E-deficient transgenic mice and in humans is oxidized and aggregated. *Biochem Biophys Res Commun,* 216**,** 501-13.

BACH, R. G., CANNON, C. P., GIUGLIANO, R. P., WHITE, J. A., LOKHNYGINA, Y., BOHULA, E. A., CALIFF, R. M., BRAUNWALD, E. & BLAZING, M. A. 2019. Effect of Simvastatin-Ezetimibe Compared With Simvastatin Monotherapy After Acute Coronary Syndrome Among Patients 75 Years or Older: A Secondary Analysis of a Randomized Clinical Trial. *JAMA Cardiol*.

BADIMON, L., PADRÓ, T. & VILAHUR, G. 2012. Atherosclerosis, platelets and thrombosis in acute ischaemic heart disease. *Eur Heart J Acute Cardiovasc Care,* 1**,** 60-74.

BADIMON, L. & VILAHUR, G. 2012. LDL-cholesterol versus HDL-cholesterol in the atherosclerotic plaque: inflammatory resolution versus thrombotic chaos. *Ann N Y Acad Sci,* 1254**,** 18-32.

BASATEMUR, G. L., JØRGENSEN, H. F., CLARKE, M. C. H., BENNETT, M. R. & MALLAT, Z. 2019. Vascular smooth muscle cells in atherosclerosis. *Nat Rev Cardiol,* 16**,** 727-744.

BASELET, B., SONVEAUX, P., BAATOUT, S. & AERTS, A. 2019. Pathological effects of ionizing radiation: endothelial activation and dysfunction. *Cell Mol Life Sci,* 76**,** 699-728.

BAUERNFEIND, F. G., HORVATH, G., STUTZ, A., ALNEMRI, E. S., MACDONALD, K., SPEERT, D., FERNANDES-ALNEMRI, T., WU, J., MONKS, B. G., FITZGERALD, K. A., HORNUNG, V. & LATZ, E. 2009. Cutting edge: NF-kappaB activating pattern recognition and cytokine receptors license NLRP3 inflammasome activation by regulating NLRP3 expression. *J Immunol,* 183**,** 787-91.

BAUMER, Y., MCCURDY, S., JIN, X., WEATHERBY, T. M., DEY, A. K., MEHTA, N. N., YAP, J. K., KRUTH, H. S. & BOISVERT, W. A. 2019. Ultramorphological analysis of plaque advancement and cholesterol crystal formation in Ldlr knockout mouse atherosclerosis. *Atherosclerosis,* 287**,** 100-111.

BENDITT, E. P. 1977. The origin of atherosclerosis. *Sci Am,* 236**,** 74-85.

BENTZON, J. F., OTSUKA, F., VIRMANI, R. & FALK, E. 2014. Mechanisms of plaque formation and rupture. *Circ Res,* 114**,** 1852-66.

BERGSBAKEN, T., FINK, S. L. & COOKSON, B. T. 2009. Pyroptosis: host cell death and inflammation. *Nat Rev Microbiol,* 7**,** 99-109.

BIASUCCI, L. M., LIUZZO, G., FANTUZZI, G., CALIGIURI, G., REBUZZI, A. G., GINNETTI, F., DINARELLO, C. A. & MASERI, A. 1999. Increasing levels of interleukin (IL)-1Ra and IL-6 during the first 2 days of hospitalization in unstable angina are associated with increased risk of in-hospital coronary events. *Circulation,* 99**,** 2079-84.

BIRDWELL, C. R., GOSPODAROWICZ, D. & NICOLSON, G. L. 1978. Identification, localization, and role of fibronectin in cultured bovine endothelial cells. *Proc Natl Acad Sci U S A,* 75**,** 3273-7.

BLACK, R. A., KRONHEIM, S. R., MERRIAM, J. E., MARCH, C. J. & HOPP, T. P. 1989. A pre-aspartate-specific protease from human leukocytes that cleaves pro-interleukin-1 beta. *J Biol Chem,* 264**,** 5323-6.

BOBRYSHEV, Y. V. 2006. Monocyte recruitment and foam cell formation in atherosclerosis. *Micron,* 37**,** 208-22.

BOHULA, E. A., GIUGLIANO, R. P., CANNON, C. P., ZHOU, J., MURPHY, S. A., WHITE, J. A., TERSHAKOVEC, A. M., BLAZING, M. A. & BRAUNWALD, E. 2015. Achievement of dual low-density lipoprotein cholesterol and high-sensitivity C-reactive protein targets more frequent with the addition of ezetimibe to simvastatin and associated with better outcomes in IMPROVE-IT. *Circulation,* 132**,** 1224-33.

BRAGANHOL, E., KUKULSKI, F., LÉVESQUE, S. A., FAUSTHER, M., LAVOIE, E. G., ZANOTTO-FILHO, A., BERGAMIN, L. S., PELLETIER, J., BAHRAMI, F., BEN YEBDRI, F., FONSECA MOREIRA, J. C., BATTASTINI, A. M. & SÉVIGNY, J. 2015. Nucleotide receptors control IL-8/CXCL8 and MCP-1/CCL2 secretions as well as proliferation in human glioma cells. *Biochim Biophys Acta,* 1852**,** 120-30.

BROUGH, D., TYRRELL, P. J. & ALLAN, S. M. 2011. Regulation of interleukin-1 in acute brain injury. *Trends Pharmacol Sci,* 32**,** 617-22.

BROWN, A. J., MANDER, E. L., GELISSEN, I. C., KRITHARIDES, L., DEAN, R. T. & JESSUP, W. 2000. Cholesterol and oxysterol metabolism and subcellular distribution in macrophage foam cells. Accumulation of oxidized esters in lysosomes. *J Lipid Res,* 41**,** 226-37.

BROWN, M. S. & GOLDSTEIN, J. L. 1983. Lipoprotein metabolism in the macrophage: implications for cholesterol deposition in atherosclerosis. *Annu Rev Biochem,* 52**,** 223-61.

BROZ, P., VON MOLTKE, J., JONES, J. W., VANCE, R. E. & MONACK, D. M. 2010. Differential requirement for Caspase-1 autoproteolysis in pathogen-induced cell death and cytokine processing. *Cell Host Microbe,* 8**,** 471-83.

BUCCI, B., MISITI, S., CANNIZZARO, A., MARCHESE, R., RAZA, G. H., MICELI, R., STIGLIANO, A., AMENDOLA, D., MONTI, O., BIANCOLELLA, M., AMATI, F., NOVELLI, G., VECCHIONE, A., BRUNETTI, E. & DE PAULA, U. 2006. Fractionated ionizing radiation exposure induces apoptosis through caspase-3 activation and reactive oxygen species generation. *Anticancer Res,* 26**,** 4549-57.

BURNS, K., MARTINON, F. & TSCHOPP, J. 2003. New insights into the mechanism of IL-1beta maturation. *Curr Opin Immunol,* 15**,** 26-30.

BURZYNSKI, L. C., HUMPHRY, M., BENNETT, M. R. & CLARKE, M. C. 2015. Interleukin-1α Activity in Necrotic Endothelial Cells Is Controlled by Caspase-1 Cleavage of Interleukin-1 Receptor-2: IMPLICATIONS FOR ALLOGRAFT REJECTION. *J Biol Chem,* 290**,** 25188-96.

BYFIELD, F. J., ARANDA-ESPINOZA, H., ROMANENKO, V. G., ROTHBLAT, G. H. & LEVITAN, I. 2004. Cholesterol depletion increases membrane stiffness of aortic endothelial cells. *Biophys J,* 87**,** 3336-43.

CAMEJO, G., HURT-CAMEJO, E., WIKLUND, O. & BONDJERS, G. 1998. Association of apo B lipoproteins with arterial proteoglycans: pathological significance and molecular basis. *Atherosclerosis,* 139**,** 205-22.

CAMPOS, H., BLIJLEVENS, E., MCNAMARA, J. R., ORDOVAS, J. M., POSNER, B. M., WILSON, P. W., CASTELLI, W. P. & SCHAEFER, E. J. 1992. LDL particle size distribution. Results from the Framingham Offspring Study. *Arterioscler Thromb,* 12**,** 1410-9.

CASSEL, S. L., JOLY, S. & SUTTERWALA, F. S. 2009. The NLRP3 inflammasome: a sensor of immune danger signals. *Semin Immunol,* 21**,** 194-8.

CENERI, N., ZHAO, L., YOUNG, B. D., HEALY, A., COSKUN, S., VASAVADA, H., YAROVINSKY, T. O., IKE, K., PARDI, R., QIN, L., TELLIDES, G., HIRSCHI, K., MEADOWS, J., SOUFER, R., CHUN, H. J., SADEGHI, M. M., BENDER, J. R. & MORRISON, A. R. 2017. Rac2 Modulates Atherosclerotic Calcification by Regulating Macrophage Interleukin-1β Production. *Arterioscler Thromb Vasc Biol,* 37**,** 328-340.

CERLETTI, C., DE GAETANO, G. & LORENZET, R. 2010. Platelet - leukocyte interactions: multiple links between inflammation, blood coagulation and vascular risk. *Mediterr J Hematol Infect Dis,* 2**,** e2010023.

CHAMBERLAIN, J., EVANS, D., KING, A., DEWBERRY, R., DOWER, S., CROSSMAN, D. & FRANCIS, S. 2006. Interleukin-1beta and signaling of interleukin-1 in vascular wall and circulating cells modulates the extent of neointima formation in mice. *Am J Pathol,* 168**,** 1396-403.

CHAMBERLAIN, J., FRANCIS, S., BROOKES, Z., SHAW, G., GRAHAM, D., ALP, N. J., DOWER, S. & CROSSMAN, D. C. 2009. Interleukin-1 regulates multiple atherogenic mechanisms in response to fat feeding. *PLoS One,* 4**,** e5073.

CHAMPAIBOON, C., POOLGESORN, M., WISITRASAMEEWONG, W., SA-ARD-IAM, N., RERKYEN, P. & MAHANONDA, R. 2014. Differential inflammasome activation by Porphyromonas gingivalis and cholesterol crystals in human macrophages and coronary artery endothelial cells. *Atherosclerosis,* 235**,** 38-44.

CHAN, A. H. & SCHRODER, K. 2020. Inflammasome signaling and regulation of interleukin-1 family cytokines. *J Exp Med,* 217.

CHANG, T. Y., CHANG, C. C., OHGAMI, N. & YAMAUCHI, Y. 2006. Cholesterol sensing, trafficking, and esterification. *Annu Rev Cell Dev Biol,* 22**,** 129-57.

CHAPPELL, D. C., VARNER, S. E., NEREM, R. M., MEDFORD, R. M. & ALEXANDER, R. W. 1998. Oscillatory shear stress stimulates adhesion molecule expression in cultured human endothelium. *Circ Res,* 82**,** 532-9.

CLARKE, M. C., TALIB, S., FIGG, N. L. & BENNETT, M. R. 2010. Vascular smooth muscle cell apoptosis induces interleukin-1-directed inflammation: effects of hyperlipidemia-mediated inhibition of phagocytosis. *Circ Res,* 106**,** 363-72.

CLINTON, S. K., UNDERWOOD, R., HAYES, L., SHERMAN, M. L., KUFE, D. W. & LIBBY, P. 1992. Macrophage colony-stimulating factor gene expression in vascular cells and in experimental and human atherosclerosis. *Am J Pathol,* 140**,** 301-16.

COLL, R. C., ROBERTSON, A. A., CHAE, J. J., HIGGINS, S. C., MUÑOZ-PLANILLO, R., INSERRA, M. C., VETTER, I., DUNGAN, L. S., MONKS, B. G., STUTZ, A., CROKER, D. E., BUTLER, M. S., HANEKLAUS, M., SUTTON, C. E., NÚÑEZ, G., LATZ, E., KASTNER, D. L., MILLS, K. H., MASTERS, S. L., SCHRODER, K., COOPER, M. A. & O'NEILL, L. A. 2015. A small-molecule inhibitor of the NLRP3 inflammasome for the treatment of inflammatory diseases. *Nat Med,* 21**,** 248-55.

COSTALES, P., FUENTES-PRIOR, P., CASTELLANO, J., REVUELTA-LOPEZ, E., CORRAL-RODRÍGUEZ, M., NASARRE, L., BADIMON, L. & LLORENTE-CORTES, V. 2015.

K Domain CR9 of Low Density Lipoprotein (LDL) Receptor-related Protein 1 (LRP1) Is Critical for Aggregated LDL-induced Foam Cell Formation from Human Vascular Smooth Muscle Cells. *J Biol Chem,* 290**,** 14852-65.

CUNNINGHAM, K. S. & GOTLIEB, A. I. 2005. The role of shear stress in the pathogenesis of atherosclerosis. *Lab Invest,* 85**,** 9-23.

D'ELIOS, M. M., VALLESE, F., CAPITANI, N., BENAGIANO, M., BERNARDINI, M. L., ROSSI, M., ROSSI, G. P., FERRARI, M., BALDARI, C. T., ZANOTTI, G., DE BERNARD, M. & CODOLO, G. 2017. The Helicobacter cinaedi antigen CAIP participates in atherosclerotic inflammation by promoting the differentiation of macrophages in foam cells. *Sci Rep,* 7**,** 40515.

DAI, J., TIAN, J., HOU, J., XING, L., LIU, S., MA, L., YU, H., REN, X., DONG, N. & YU, B. 2016. Association between cholesterol crystals and culprit lesion vulnerability in patients with acute coronary syndrome: An optical coherence tomography study. *Atherosclerosis,* 247**,** 111-7.

DAI, Y., SU, W., DING, Z., WANG, X., MERCANTI, F., CHEN, M., RAINA, S. & MEHTA, J. L. 2013. Regulation of MSR-1 and CD36 in macrophages by LOX-1 mediated through PPAR-gamma. *Biochem Biophys Res Commun,* 431**,** 496-500.

DAUB, K., SEIZER, P., STELLOS, K., KRÄMER, B. F., BIGALKE, B., SCHALLER, M., FATEH-MOGHADAM, S., GAWAZ, M. & LINDEMANN, S. 2010. Oxidized LDL-activated platelets induce vascular inflammation. *Semin Thromb Hemost,* 36**,** 146-56.

DAVIES, J. R., RUDD, J. H., WEISSBERG, P. L. & NARULA, J. 2006. Radionuclide imaging for the detection of inflammation in vulnerable plaques. *J Am Coll Cardiol,* 47**,** C57-68.

DAVIGNON, J. & GANZ, P. 2004. Role of endothelial dysfunction in atherosclerosis. *Circulation,* 109**,** III27-32.

DE NIGRIS, F., LERMAN, A., IGNARRO, L. J., WILLIAMS-IGNARRO, S., SICA, V., BAKER, A. H., LERMAN, L. O., GENG, Y. J. & NAPOLI, C. 2003. Oxidation-sensitive mechanisms, vascular apoptosis and atherosclerosis. *Trends Mol Med,* 9**,** 351-9.

DE RIVERO VACCARI, J. P., DIETRICH, W. D. & KEANE, R. W. 2014. Activation and regulation of cellular inflammasomes: gaps in our knowledge for central nervous system injury. *J Cereb Blood Flow Metab,* 34**,** 369-75.

DEN HARTIGH, A. B. & FINK, S. L. 2018. Detection of Inflammasome Activation and Pyroptotic Cell Death in Murine Bone Marrow-derived Macrophages. *J Vis Exp*.

DESTEFANO, J. G., WILLIAMS, A., WNOROWSKI, A., YIMAM, N., SEARSON, P. C. & WONG, A. D. 2017. Real-time quantification of endothelial response to shear stress and vascular modulators. *Integr Biol (Camb),* 9**,** 362-374.

DEWBERRY, R., HOLDEN, H., CROSSMAN, D. & FRANCIS, S. 2000. Interleukin-1 receptor antagonist expression in human endothelial cells and atherosclerosis. *Arterioscler Thromb Vasc Biol,* 20**,** 2394-400.

DI PAOLO, N. C. & SHAYAKHMETOV, D. M. 2016. Interleukin 1α and the inflammatory process. *Nat Immunol,* 17**,** 906-13.

DI PIETRO, N., FORMOSO, G. & PANDOLFI, A. 2016. Physiology and pathophysiology of oxLDL uptake by vascular wall cells in atherosclerosis. *Vascul Pharmacol,* 84**,** 1-7.

DI VIRGILIO, F., DAL BEN, D., SARTI, A. C., GIULIANI, A. L. & FALZONI, S. 2017. The P2X7 Receptor in Infection and Inflammation. *Immunity,* 47**,** 15-31.

DIKALOV, S., ITANI, H., RICHMOND, B., VERGEADE, A., RAHMAN, S. M. J., BOUTAUD, O., BLACKWELL, T., MASSION, P. P., HARRISON, D. G. & DIKALOVA, A. 2019. Tobacco smoking induces cardiovascular mitochondrial oxidative stress, promotes endothelial dysfunction, and enhances hypertension. *Am J Physiol Heart Circ Physiol,* 316**,** H639-H646.

DINARELLO, C. A. 1991. Interleukin-1 and interleukin-1 antagonism. *Blood,* 77**,** 1627-52.

DINARELLO, C. A. 2005. Blocking IL-1 in systemic inflammation. *J Exp Med,* 201**,** 1355-9.

DINARELLO, C. A. 2009. Immunological and inflammatory functions of the interleukin-1 family. *Annu Rev Immunol,* 27**,** 519-50.

DINARELLO, C. A., SIMON, A. & VAN DER MEER, J. W. 2012. Treating inflammation by blocking interleukin-1 in a broad spectrum of diseases. *Nat Rev Drug Discov,* 11**,** 633-52.

DINARELLO, C. A. & VAN DER MEER, J. W. 2013. Treating inflammation by blocking interleukin-1 in humans. *Semin Immunol,* 25**,** 469-84.

DORAN, A. C., MELLER, N. & MCNAMARA, C. A. 2008. Role of smooth muscle cells in the initiation and early progression of atherosclerosis. *Arterioscler Thromb Vasc Biol,* 28**,** 812-9.

DUEWELL, P., KONO, H., RAYNER, K. J., SIROIS, C. M., VLADIMER, G., BAUERNFEIND, F. G., ABELA, G. S., FRANCHI, L., NUNEZ, G., SCHNURR, M., ESPEVIK, T., LIEN, E., FITZGERALD, K. A., ROCK, K. L., MOORE, K. J., WRIGHT, S. D., HORNUNG, V. & LATZ, E. 2010. NLRP3 inflammasomes are required for atherogenesis and activated by cholesterol crystals. *Nature,* 464**,** 1357-61.

DUFF, G. L. 1951. The pathogenesis of atherosclerosis. *Can Med Assoc J,* 64**,** 387-94.

DYERBERG, J., BANG, H. O., STOFFERSEN, E., MONCADA, S. & VANE, J. R. 1978. Eicosapentaenoic acid and prevention of thrombosis and atherosclerosis? *Lancet,* 2**,** 117-9.

EHARA, S., UEDA, M., NARUKO, T., HAZE, K., ITOH, A., OTSUKA, M., KOMATSU, R., MATSUO, T., ITABE, H., TAKANO, T., TSUKAMOTO, Y., YOSHIYAMA, M., TAKEUCHI, K., YOSHIKAWA, J. & BECKER, A. E. 2001. Elevated levels of oxidized low density lipoprotein show a positive relationship with the severity of acute coronary syndromes. *Circulation,* 103**,** 1955-60.

ELHAGE, R., MARET, A., PIERAGGI, M. T., THIERS, J. C., ARNAL, J. F. & BAYARD, F. 1998. Differential effects of interleukin-1 receptor antagonist and tumor necrosis factor binding protein on fatty-streak formation in apolipoprotein E-deficient mice. *Circulation,* 97**,** 242-4.

ENOS, W. F., HOLMES, R. H. & BEYER, J. 1953. Coronary disease among United States soldiers killed in action in Korea; preliminary report. *J Am Med Assoc,* 152**,** 1090-3.

ESTRUCH, M., RAJAMÄKI, K., SANCHEZ-QUESADA, J. L., KOVANEN, P. T., ÖÖRNI, K., BENITEZ, S. & ORDOÑEZ-LLANOS, J. 2015. Electronegative LDL induces priming and inflammasome activation leading to IL-1β release in human monocytes and macrophages. *Biochim Biophys Acta,* 1851**,** 1442-9.

EVAVOLD, C. L., RUAN, J., TAN, Y., XIA, S., WU, H. & KAGAN, J. C. 2018. The Pore-Forming Protein Gasdermin D Regulates Interleukin-1 Secretion from Living Macrophages. *Immunity,* 48**,** 35-44.e6.

FANG, L., CHOI, S. H., BAEK, J. S., LIU, C., ALMAZAN, F., ULRICH, F., WIESNER, P., TALEB, A., DEER, E., PATTISON, J., TORRES-VÁZQUEZ, J., LI, A. C. & MILLER,

Y. I. 2013. Control of angiogenesis by AIBP-mediated cholesterol efflux. *Nature,* 498**,** 118-22.

FARB, A., BURKE, A. P., TANG, A. L., LIANG, T. Y., MANNAN, P., SMIALEK, J. & VIRMANI, R. 1996. Coronary plaque erosion without rupture into a lipid core. A frequent cause of coronary thrombosis in sudden coronary death. *Circulation,* 93**,** 1354-63.

FEIL, S., FEHRENBACHER, B., LUKOWSKI, R., ESSMANN, F., SCHULZE-OSTHOFF, K., SCHALLER, M. & FEIL, R. 2014. Transdifferentiation of vascular smooth muscle cells to macrophage-like cells during atherogenesis. *Circ Res,* 115**,** 662-7.

FOLCO, E. J., SUKHOVA, G. K., QUILLARD, T. & LIBBY, P. 2014. Moderate hypoxia potentiates interleukin-1beta production in activated human macrophages. *Circ Res,* 115**,** 875-83.

FOTEINOS, G., HU, Y., XIAO, Q., METZLER, B. & XU, Q. 2008. Rapid endothelial turnover in atherosclerosis-prone areas coincides with stem cell repair in apolipoprotein E-deficient mice. *Circulation,* 117**,** 1856-63.

FRANCHI, L., EIGENBROD, T. & NÚÑEZ, G. 2009. Cutting edge: TNF-alpha mediates sensitization to ATP and silica via the NLRP3 inflammasome in the absence of microbial stimulation. *J Immunol,* 183**,** 792-6.

FRANCIS, S. E., CAMP, N. J., DEWBERRY, R. M., GUNN, J., SYRRIS, P., CARTER, N. D., JEFFERY, S., KASKI, J. C., CUMBERLAND, D. C., DUFF, G. W. & CROSSMAN, D. C. 1999. Interleukin-1 receptor antagonist gene polymorphism and coronary artery disease. *Circulation,* 99**,** 861-6.

FRANK, J. S. & FOGELMAN, A. M. 1989. Ultrastructure of the intima in WHHL and cholesterol-fed rabbit aortas prepared by ultra-rapid freezing and freeze-etching. *J Lipid Res,* 30**,** 967-78.

FRIEDMAN, M. 1975. The pathogenesis of coronary plaques, thromboses, and hemorrhages: an evaluative review. *Circulation,* 52**,** III34-40.

FURUOKA, M., OZAKI, K., SADATOMI, D., MAMIYA, S., YONEZAWA, T., TANIMURA, S. & TAKEDA, K. 2016. TNF-α Induces Caspase-1 Activation Independently of Simultaneously Induced NLRP3 in 3T3-L1 Cells. *J Cell Physiol,* 231**,** 2761-7.

GAN, C., WANG, K., TANG, Q. & CHEN, Y. 2018. Comparative investigation on the sizes and scavenger receptor binding of human native and modified lipoprotein particles with atomic force microscopy. *J Nanobiotechnology,* 16**,** 25.

GARCIA-CALVO, M., PETERSON, E. P., LEITING, B., RUEL, R., NICHOLSON, D. W. & THORNBERRY, N. A. 1998. Inhibition of human caspases by peptide-based and macromolecular inhibitors. *J Biol Chem,* 273**,** 32608-13.

GARCIA-HERRERA, C. M. & CELENTANO, D. J. 2013. Modelling and numerical simulation of the human aortic arch under in vivo conditions. *Biomech Model Mechanobiol,* 12**,** 1143-54.

GENG, Y. J., PHILLIPS, J. E., MASON, R. P. & CASSCELLS, S. W. 2003. Cholesterol crystallization and macrophage apoptosis: implication for atherosclerotic plaque instability and rupture. *Biochem Pharmacol,* 66**,** 1485-92.

GHANEM, F., VODNALA, D., K KALAVAKUNTA, J., DURGA, S., THORMEIER, N., SUBRAMANIYAM, P., ABELA, S. & S ABELA, G. 2017. Cholesterol crystal embolization following plaque rupture: a systemic disease with unusual features. *J Biomed Res,* 31**,** 82-94.

GIACCO, F. & BROWNLEE, M. 2010. Oxidative stress and diabetic complications. *Circ Res,* 107**,** 1058-70.

GIANNOTTI, K. C., WEINERT, S., VIANA, M. N., LEIGUEZ, E., ARAUJO, T. L. S., LAURINDO, F. R. M., LOMONTE, B., BRAUN-DULLAEUS, R. & TEIXEIRA, C. 2019. A Secreted Phospholipase A. *Molecules,* 24.

GIMBRONE, M. A. & GARCÍA-CARDEÑA, G. 2016. Endothelial Cell Dysfunction and the Pathobiology of Atherosclerosis. *Circ Res,* 118**,** 620-36.

GIULIANI, A. L., SARTI, A. C., FALZONI, S. & DI VIRGILIO, F. 2017. The P2X7 Receptor-Interleukin-1 Liaison. *Front Pharmacol,* 8**,** 123.

GLANZ, V. Y., SOBENIN, I. A., GRECHKO, A. V., YET, S. F. & OREKHOV, A. N. 2020. The role of mitochondria in cardiovascular diseases related to atherosclerosis. *Front Biosci (Elite Ed),* 12**,** 102-112.

GOLDSTEIN, J. L., HO, Y. K., BASU, S. K. & BROWN, M. S. 1979. Binding site on macrophages that mediates uptake and degradation of acetylated low density lipoprotein, producing massive cholesterol deposition. *Proc Natl Acad Sci U S A,* 76**,** 333-7.

GOMEZ, J. P., GONÇALVES, C., PICHON, C. & MIDOUX, P. 2017. Effect of IL-1β, TNF-α and IGF-1 on trans-endothelial passage of synthetic vectors through an in vitro vascular endothelial barrier of striated muscle. *Gene Ther*.

GREBE, A. & LATZ, E. 2013. Cholesterol crystals and inflammation. *Curr Rheumatol Rep,* 15**,** 313.

GROSS, O., YAZDI, A. S., THOMAS, C. J., MASIN, M., HEINZ, L. X., GUARDA, G., QUADRONI, M., DREXLER, S. K. & TSCHOPP, J. 2012. Inflammasome activators induce interleukin-1α secretion via distinct pathways with differential requirement for the protease function of caspase-1. *Immunity,* 36**,** 388-400.

GRUNDY, S. M., CLEEMAN, J. I., MERZ, C. N., BREWER, H. B., JR., CLARK, L. T., HUNNINGHAKE, D. B., PASTERNAK, R. C., SMITH, S. C., JR., STONE, N. J., NATIONAL HEART, L., BLOOD, I., AMERICAN COLLEGE OF CARDIOLOGY, F. & AMERICAN HEART, A. 2004. Implications of recent clinical trials for the National Cholesterol Education Program Adult Treatment Panel III guidelines. *Circulation,* 110**,** 227-39.

GU, L., OKADA, Y., CLINTON, S. K., GERARD, C., SUKHOVA, G. K., LIBBY, P. & ROLLINS, B. J. 1998. Absence of monocyte chemoattractant protein-1 reduces atherosclerosis in low density lipoprotein receptor-deficient mice. *Mol Cell,* 2**,** 275-81.

GUO, H., CALLAWAY, J. B. & TING, J. P. 2015. Inflammasomes: mechanism of action, role in disease, and therapeutics. *Nat Med,* 21**,** 677-87.

HABERLAND, M. E., MOTTINO, G., LE, M. & FRANK, J. S. 2001. Sequestration of aggregated LDL by macrophages studied with freeze-etch electron microscopy. *J Lipid Res,* 42**,** 605-19.

HAN, C. Y. & PAK, Y. K. 1999. Oxidation-dependent effects of oxidized LDL: proliferation or cell death. *Exp Mol Med,* 31**,** 165-73.

HAN, X., KITAMOTO, S., LIAN, Q. & BOISVERT, W. A. 2009. Interleukin-10 facilitates both cholesterol uptake and efflux in macrophages. *J Biol Chem,* 284**,** 32950-8.

HASANALLY, D., EDEL, A., CHAUDHARY, R. & RAVANDI, A. 2017. Identification of Oxidized Phosphatidylinositols Present in OxLDL and Human Atherosclerotic Plaque. *Lipids,* 52**,** 11-26.

HASSAN, H. H., DENIS, M., KRIMBOU, L., MARCIL, M. & GENEST, J. 2006. Cellular cholesterol homeostasis in vascular endothelial cells. *Can J Cardiol,* 22 Suppl B**,** 35B-40B.

HAYDEN, M. S. & GHOSH, S. 2011. NF-κB in immunobiology. *Cell Res,* 21**,** 223-44.

HERRINGTON, W., LACEY, B., SHERLIKER, P., ARMITAGE, J. & LEWINGTON, S. 2016. Epidemiology of Atherosclerosis and the Potential to Reduce the Global Burden of Atherothrombotic Disease. *Circ Res,* 118**,** 535-46.

HOFF, H. F. & MORTON, R. E. 1985. Lipoproteins containing apo B extracted from human aortas. Structure and function. *Ann N Y Acad Sci,* 454**,** 183-94.

HURT-CAMEJO, E., CAMEJO, G. & SARTIPY, P. 2000. Phospholipase A2 and small, dense low-density lipoprotein. *Curr Opin Lipidol,* 11**,** 465-71.

HWANG, J., ING, M. H., SALAZAR, A., LASSEGUE, B., GRIENDLING, K., NAVAB, M., SEVANIAN, A. & HSIAI, T. K. 2003. Pulsatile versus oscillatory shear stress regulates NADPH oxidase subunit expression: implication for native LDL oxidation. *Circ Res,* 93**,** 1225-32.

IKONOMIDIS, I., LEKAKIS, J., REVELA, I., ANDREOTTI, F. & NIHOYANNOPOULOS, P. 2005. Increased circulating C-reactive protein and macrophage-colony stimulating factor are complementary predictors of long-term outcome in patients with chronic coronary artery disease. *Eur Heart J,* 26**,** 1618-24.

IOANNOU, G. N., VAN ROOYEN, D. M., SAVARD, C., HAIGH, W. G., YEH, M. M., TEOH, N. C. & FARRELL, G. C. 2015. Cholesterol-lowering drugs cause dissolution of cholesterol crystals and disperse Kupffer cell crown-like structures during resolution of NASH. *J Lipid Res,* 56**,** 277-85.

ITABE, H. 1998. Oxidized phospholipids as a new landmark in atherosclerosis. *Prog Lipid Res,* 37**,** 181-207.

JAFFE, E. A., NACHMAN, R. L., BECKER, C. G. & MINICK, C. R. 1973. Culture of human endothelial cells derived from umbilical veins. Identification by morphologic and immunologic criteria. *J Clin Invest,* 52**,** 2745-56.

JANG, Y., LINCOFF, A. M., PLOW, E. F. & TOPOL, E. J. 1994. Cell adhesion molecules in coronary artery disease. *J Am Coll Cardiol,* 24**,** 1591-601.

JIANG, W., LI, M., HE, F., ZHOU, S. & ZHU, L. 2017. Targeting the NLRP3 inflammasome to attenuate spinal cord injury in mice. *J Neuroinflammation,* 14**,** 207.

JUNG, Y. D., LIU, W., REINMUTH, N., AHMAD, S. A., FAN, F., GALLICK, G. E. & ELLIS, L. M. 2001. Vascular endothelial growth factor is upregulated by interleukin-1 beta in human vascular smooth muscle cells via the P38 mitogen-activated protein kinase pathway. *Angiogenesis,* 4**,** 155-62.

KARASAWA, A., MICHALSKI, K., MIKHELZON, P. & KAWATE, T. 2017. The P2X7 receptor forms a dye-permeable pore independent of its intracellular domain but dependent on membrane lipid composition. *Elife,* 6.

KARASAWA, T. & TAKAHASHI, M. 2017a. Role of NLRP3 Inflammasomes in Atherosclerosis. *J Atheroscler Thromb,* 24**,** 443-451.

KARASAWA, T. & TAKAHASHI, M. 2017b. The crystal-induced activation of NLRP3 inflammasomes in atherosclerosis. *Inflamm Regen,* 37**,** 18.

KARMAKAR, M., KATSNELSON, M. A., DUBYAK, G. R. & PEARLMAN, E. 2016. Neutrophil P2X7 receptors mediate NLRP3 inflammasome-dependent IL-1β secretion in response to ATP. *Nat Commun,* 7**,** 10555.

KATAYAMA, Y., TANAKA, A., TARUYA, A., KASHIWAGI, M., NISHIGUCHI, T., OZAKI, Y., MATSUO, Y., KITABATA, H., KUBO, T., SHIMADA, E., KONDO, T. & AKASAKA, T. 2020. Feasibility and Clinical Significance of In Vivo Cholesterol Crystal Detection Using Optical Coherence Tomography. *Arterioscler Thromb Vasc Biol,* 40**,** 220-229.

KATZ, S. S., SHIPLEY, G. G. & SMALL, D. M. 1976. Physical chemistry of the lipids of human atherosclerotic lesions. Demonstration of a lesion intermediate between fatty streaks and advanced plaques. *J Clin Invest,* 58**,** 200-11.

KATZ, S. S. & SMALL, D. M. 1980. Isolation and and partial characterization of the lipid phases of human atherosclerotic plaques. *J Biol Chem,* 255**,** 9753-9.

KAYAGAKI, N., STOWE, I. B., LEE, B. L., O'ROURKE, K., ANDERSON, K., WARMING, S., CUELLAR, T., HALEY, B., ROOSE-GIRMA, M., PHUNG, Q. T., LIU, P. S., LILL, J. R., LI, H., WU, J., KUMMERFELD, S., ZHANG, J., LEE, W. P., SNIPAS, S. J., SALVESEN, G. S., MORRIS, L. X., FITZGERALD, L., ZHANG, Y., BERTRAM, E. M., GOODNOW, C. C. & DIXIT, V. M. 2015. Caspase-11 cleaves gasdermin D for non-canonical inflammasome signalling. *Nature,* 526**,** 666-71.

KEDI, X., MING, Y., YONGPING, W., YI, Y. & XIAOXIANG, Z. 2009. Free cholesterol overloading induced smooth muscle cells death and activated both ER- and mitochondrial-dependent death pathway. *Atherosclerosis,* 207**,** 123-30.

KIM, I., MOON, S. O., KIM, S. H., KIM, H. J., KOH, Y. S. & KOH, G. Y. 2001. Vascular endothelial growth factor expression of intercellular adhesion molecule 1 (ICAM-1), vascular cell adhesion molecule 1 (VCAM-1), and E-selectin through nuclear factor-kappa B activation in endothelial cells. *J Biol Chem,* 276**,** 7614-20.

KIM, S. R., BAE, Y. H., BAE, S. K., CHOI, K. S., YOON, K. H., KOO, T. H., JANG, H. O., YUN, I., KIM, K. W., KWON, Y. G., YOO, M. A. & BAE, M. K. 2008. Visfatin enhances ICAM-1 and VCAM-1 expression through ROS-dependent NF-kappaB activation in endothelial cells. *Biochim Biophys Acta,* 1783**,** 886-95.

KING, A. R., FRANCIS, S. E., BRIDGEMAN, C. J., BIRD, H., WHYTE, M. K. & CROSSMAN, D. C. 2003. A role for caspase-1 in serum withdrawal-induced apoptosis of endothelial cells. *Lab Invest,* 83**,** 1497-508.

KIRII, H., NIWA, T., YAMADA, Y., WADA, H., SAITO, K., IWAKURA, Y., ASANO, M., MORIWAKI, H. & SEISHIMA, M. 2003. Lack of interleukin-1beta decreases the severity of atherosclerosis in ApoE-deficient mice. *Arterioscler Thromb Vasc Biol,* 23**,** 656-60.

KIYAN, Y., TKACHUK, S., HILFIKER-KLEINER, D., HALLER, H., FUHRMAN, B. & DUMLER, I. 2014. oxLDL induces inflammatory responses in vascular smooth muscle cells via urokinase receptor association with CD36 and TLR4. *J Mol Cell Cardiol,* 66**,** 72-82.

KLEEMANN, R., ZADELAAR, S. & KOOISTRA, T. 2008. Cytokines and atherosclerosis: a comprehensive review of studies in mice. *Cardiovasc Res,* 79**,** 360-76.

KOIDE, M., MATSUO, A., SHIMOO, S., TAKAMATSU, K., KYODO, A., TSUJI, Y., MERA, K., TSUBAKIMOTO, Y., ISODONO, K., SAKATANI, T., INOUE, K. & FUJITA, H. 2017. Cholesterol crystal depth in coronary atherosclerotic plaques: A novel index of plaque vulnerability using optical frequency domain imaging. *PLoS One,* 12**,** e0180303.

KOLOVOU, G., ANAGNOSTOPOULOU, K., MIKHAILIDIS, D. P. & COKKINOS, D. V. 2008. Apolipoprotein E knockout models. *Curr Pharm Des,* 14**,** 338-51.

KRISHNASWAMY, G., KELLEY, J., YERRA, L., SMITH, J. K. & CHI, D. S. 1999. Human endothelium as a source of multifunctional cytokines: molecular regulation and possible role in human disease. *J Interferon Cytokine Res,* 19**,** 91-104.

KRUTH, H. S. 2001. Lipoprotein cholesterol and atherosclerosis. *Curr Mol Med,* 1**,** 633-53.

KRUTH, H. S., JONES, N. L., HUANG, W., ZHAO, B., ISHII, I., CHANG, J., COMBS, C. A., MALIDE, D. & ZHANG, W. Y. 2005. Macropinocytosis is the endocytic pathway that mediates macrophage foam cell formation with native low density lipoprotein. *J Biol Chem,* 280**,** 2352-60.

KUBO, N., KIKUCHI, J., FURUKAWA, Y., SAKAI, T., OHTA, H., IWASE, S., YAMADA, H. & SAKURABAYASHI, I. 1997. Regulatory effects of aggregated LDL on

apoptosis during foam cell formation of human peripheral blood monocytes. *FEBS Lett,* 409**,** 177-82.

KUDA, O., PIETKA, T. A., DEMIANOVA, Z., KUDOVA, E., CVACKA, J., KOPECKY, J. & ABUMRAD, N. A. 2013. Sulfo-N-succinimidyl oleate (SSO) inhibits fatty acid uptake and signaling for intracellular calcium via binding CD36 lysine 164: SSO also inhibits oxidized low density lipoprotein uptake by macrophages. *J Biol Chem,* 288**,** 15547-55.

KUNNAS, T., MAATTA, K. & NIKKARI, S. T. 2015. NLR family pyrin domain containing 3 (NLRP3) inflammasome gene polymorphism rs7512998 (C>T) predicts aging-related increase of blood pressure, the TAMRISK study. *Immun Ageing,* 12**,** 19.

KUSHNER, I., BRODER, M. L. & KARP, D. 1978. Control of the acute phase response. Serum C-reactive protein kinetics after acute myocardial infarction. *J Clin Invest,* 61**,** 235-42.

LAMKANFI, M. & DIXIT, V. M. 2014. Mechanisms and functions of inflammasomes. *Cell,* 157**,** 1013-22.

LANGE, C., STORKEBAUM, E., DE ALMODOVAR, C. R., DEWERCHIN, M. & CARMELIET, P. 2016. Vascular endothelial growth factor: a neurovascular target in neurological diseases. *Nat Rev Neurol,* 12**,** 439-54.

LATZ, E., XIAO, T. S. & STUTZ, A. 2013. Activation and regulation of the inflammasomes. *Nat Rev Immunol,* 13**,** 397-411.

LE BRAS, A. 2019. No benefit of methotrexate on the risk of cardiovascular events. *Nat Rev Cardiol,* 16**,** 2-3.

LE MAY, C., BERGER, J. M., LESPINE, A., PILLOT, B., PRIEUR, X., LETESSIER, E., HUSSAIN, M. M., COLLET, X., CARIOU, B. & COSTET, P. 2013. Transintestinal cholesterol excretion is an active metabolic process modulated by PCSK9 and statin involving ABCB1. *Arterioscler Thromb Vasc Biol,* 33**,** 1484-93.

LEITINGER, N. 2005. Oxidized phospholipids as triggers of inflammation in atherosclerosis. *Mol Nutr Food Res,* 49**,** 1063-71.

LEONARDUZZI, G., GAMBA, P., GARGIULO, S., BIASI, F. & POLI, G. 2012. Inflammation-related gene expression by lipid oxidation-derived products in the progression of atherosclerosis. *Free Radic Biol Med,* 52**,** 19-34.

LEPEDDA, A. J. & FORMATO, M. 2020. Oxidative Modifications in Advanced Atherosclerotic Plaques: A Focus on. *Oxid Med Cell Longev,* 2020**,** 6169825.

LEVITAN, I., CHRISTIAN, A. E., TULENKO, T. N. & ROTHBLAT, G. H. 2000. Membrane cholesterol content modulates activation of volume-regulated anion current in bovine endothelial cells. *J Gen Physiol,* 115**,** 405-16.

LI, J. J. & FANG, C. H. 2004. Atheroscleritis is a more rational term for the pathological entity currently known as atherosclerosis. *Med Hypotheses,* 63**,** 100-2.

LI, S., WU, Y., YANG, D., WU, C., MA, C., LIU, X., MOYNAGH, P. N., WANG, B., HU, G. & YANG, S. 2019. Gasdermin D in peripheral myeloid cells drives neuroinflammation in experimental autoimmune encephalomyelitis. *J Exp Med,* 216**,** 2562-2581.

LIBBY, P. 2008. Role of inflammation in atherosclerosis associated with rheumatoid arthritis. *Am J Med,* 121**,** S21-31.

LIBBY, P. 2013. Mechanisms of acute coronary syndromes and their implications for therapy. *N Engl J Med,* 368**,** 2004-13.

LIBBY, P. 2015. How does lipid lowering prevent coronary events? New insights from human imaging trials. *Eur Heart J,* 36**,** 472-4.

LIBBY, P. & AIKAWA, M. 2002. Stabilization of atherosclerotic plaques: new mechanisms and clinical targets. *Nat Med,* 8**,** 1257-62.

LIBBY, P., PASTERKAMP, G., CREA, F. & JANG, I. K. 2019. Reassessing the Mechanisms of Acute Coronary Syndromes. *Circ Res,* 124**,** 150-160.

LIBBY, P., RIDKER, P. M. & MASERI, A. 2002. Inflammation and atherosclerosis. *Circulation,* 105**,** 1135-43.

LIMA, H., JACOBSON, L. S., GOLDBERG, M. F., CHANDRAN, K., DIAZ-GRIFFERO, F., LISANTI, M. P. & BROJATSCH, J. 2013. Role of lysosome rupture in controlling Nlrp3 signaling and necrotic cell death. *Cell Cycle,* 12**,** 1868-78.

LIMMON, G. V., ARREDOUANI, M., MCCANN, K. L., CORN MINOR, R. A., KOBZIK, L. & IMANI, F. 2008. Scavenger receptor class-A is a novel cell surface receptor for double-stranded RNA. *FASEB J,* 22**,** 159-67.

LIU, L., GAO, C., YAO, P. & GONG, Z. 2015. Quercetin Alleviates High-Fat Diet-Induced Oxidized Low-Density Lipoprotein Accumulation in the Liver: Implication for Autophagy Regulation. *Biomed Res Int,* 2015**,** 607531.

LIU, T., ZHANG, L., JOO, D. & SUN, S. C. 2017. NF-κB signaling in inflammation. *Signal Transduct Target Ther,* 2.

LIU, W., YIN, Y., ZHOU, Z., HE, M. & DAI, Y. 2014. OxLDL-induced IL-1 beta secretion promoting foam cells formation was mainly via CD36 mediated ROS production leading to NLRP3 inflammasome activation. *Inflamm Res,* 63**,** 33-43.

LIU, Y., JIA, S. D., YAO, Y., TANG, X. F., XU, N., JIANG, L., GAO, Z., CHEN, J., YANG, Y. J., GAO, R. L., XU, B. & YUAN, J. Q. 2020. Impact of high-sensitivity C-reactive protein on coronary artery disease severity and outcomes in patients undergoing percutaneous coronary intervention. *J Cardiol,* 75**,** 60-65.

LLORENTE-CORTÉS, V., OTERO-VIÑAS, M., HURT-CAMEJO, E., MARTÍNEZ-GONZÁLEZ, J. & BADIMON, L. 2002. Human coronary smooth muscle cells internalize versican-modified LDL through LDL receptor-related protein and LDL receptors. *Arterioscler Thromb Vasc Biol,* 22**,** 387-93.

LU, M. & GURSKY, O. 2013. Aggregation and fusion of low-density lipoproteins in vivo and in vitro. *Biomol Concepts,* 4**,** 501-18.

LUBRANO, V. & BALZAN, S. 2014. LOX-1 and ROS, inseparable factors in the process of endothelial damage. *Free Radic Res,* 48**,** 841-8.

LUNDBERG, B. 1985. Chemical composition and physical state of lipid deposits in atherosclerosis. *Atherosclerosis,* 56**,** 93-110.

LUNG, C. W., YANG, T. D., CRANE, B. A., ELLIOTT, J., DICIANNO, B. E. & JAN, Y. K. 2014. Investigation of peak pressure index parameters for people with spinal cord injury using wheelchair tilt-in-space and recline: methodology and preliminary report. *Biomed Res Int,* 2014**,** 508583.

MALEK, A. M., ALPER, S. L. & IZUMO, S. 1999. Hemodynamic shear stress and its role in atherosclerosis. *JAMA,* 282**,** 2035-42.

MAMBWE, B., NEO, K., JAVANMARD KHAMENEH, H., LEONG, K. W. K., COLANTUONI, M., VACCA, M., MUIMO, R. & MORTELLARO, A. 2019. Tyrosine Dephosphorylation of ASC Modulates the Activation of the NLRP3 and AIM2 Inflammasomes. *Front Immunol,* 10**,** 1556.

MAOR, I., HAYEK, T., HIRSH, M., IANCU, T. C. & AVIRAM, M. 2000. Macrophage-released proteoglycans enhance LDL aggregation: studies in aorta from apolipoprotein E-deficient mice. *Atherosclerosis,* 150**,** 91-101.

MARATHE, S., SCHISSEL, S. L., YELLIN, M. J., BEATINI, N., MINTZER, R., WILLIAMS, K. J. & TABAS, I. 1998. Human vascular endothelial cells are a rich and regulatable source of secretory sphingomyelinase. Implications for early

atherogenesis and ceramide-mediated cell signaling. *J Biol Chem,* 273**,** 4081-8.

MARTINON, F., BURNS, K. & TSCHOPP, J. 2002. The inflammasome: a molecular platform triggering activation of inflammatory caspases and processing of proIL-beta. *Mol Cell,* 10**,** 417-26.

MARTÍN-SÁNCHEZ, F., DIAMOND, C., ZEITLER, M., GOMEZ, A. I., BAROJA-MAZO, A., BAGNALL, J., SPILLER, D., WHITE, M., DANIELS, M. J., MORTELLARO, A., PEÑALVER, M., PASZEK, P., STERINGER, J. P., NICKEL, W., BROUGH, D. & PELEGRÍN, P. 2016. Inflammasome-dependent IL-1β release depends upon membrane permeabilisation. *Cell Death Differ,* 23**,** 1219-31.

MASON, J. C., YARWOOD, H., SUGARS, K. & HASKARD, D. O. 1997. Human umbilical vein and dermal microvascular endothelial cells show heterogeneity in response to PKC activation. *Am J Physiol,* 273**,** C1233-40.

MASTERS, S. L., MIELKE, L. A., CORNISH, A. L., SUTTON, C. E., O'DONNELL, J., CENGIA, L. H., ROBERTS, A. W., WICKS, I. P., MILLS, K. H. & CROKER, B. A. 2010. Regulation of interleukin-1beta by interferon-gamma is species specific, limited by suppressor of cytokine signalling 1 and influences interleukin-17 production. *EMBO Rep,* 11**,** 640-6.

MC NAMARA, K., ALZUBAIDI, H. & JACKSON, J. K. 2019. Cardiovascular disease as a leading cause of death: how are pharmacists getting involved? *Integr Pharm Res Pract,* 8**,** 1-11.

MCGEOUGH, M. D., WREE, A., INZAUGARAT, M. E., HAIMOVICH, A., JOHNSON, C. D., PEÑA, C. A., GOLDBACH-MANSKY, R., BRODERICK, L., FELDSTEIN, A. E. & HOFFMAN, H. M. 2017. TNF regulates transcription of NLRP3 inflammasome components and inflammatory molecules in cryopyrinopathies. *J Clin Invest,* 127**,** 4488-4497.

MCKENZIE, B. A., DIXIT, V. M. & POWER, C. 2020. Fiery Cell Death: Pyroptosis in the Central Nervous System. *Trends Neurosci,* 43**,** 55-73.

MESSNER, B. & BERNHARD, D. 2014. Smoking and cardiovascular disease: mechanisms of endothelial dysfunction and early atherogenesis. *Arterioscler Thromb Vasc Biol,* 34**,** 509-15.

MESTAS, J. & LEY, K. 2008. Monocyte-endothelial cell interactions in the development of atherosclerosis. *Trends Cardiovasc Med,* 18**,** 228-32.

MEZZASOMA, L., ANTOGNELLI, C. & TALESA, V. N. 2016. Atrial natriuretic peptide down-regulates LPS/ATP-mediated IL-1β release by inhibiting NF-kB, NLRP3 inflammasome and caspase-1 activation in THP-1 cells. *Immunol Res,* 64**,** 303-12.

MIAO, Q., XU, Y., ZHANG, H., XU, P. & YE, J. 2019. Cigarette smoke induces ROS mediated autophagy impairment in human corneal epithelial cells. *Environ Pollut,* 245**,** 389-397.

MILLAN, J., PINTÓ, X., BREA, A., BLASCO, M., HERNÁNDEZ-MIJARES, A., ASCASO, J., DIAZ, A., MANTILLA, T. & PEDRO-BOTET, J. 2018. Fibrates in the secondary prevention of cardiovascular disease (infarction and stroke). Results of a systematic review and meta-analysis of the Cochrane collaboration. *Clin Investig Arterioscler,* 30**,** 30-35.

MILLER, J. D. 2016. Arterial calcification: Conscripted by collagen. *Nat Mater,* 15**,** 257-8.

MONDAL, N. K., SORENSEN, E., HIIVALA, N., FELLER, E., GRIFFITH, B. & WU, Z. J. 2013. Oxidative stress, DNA damage and repair in heart failure patients after implantation of continuous flow left ventricular assist devices. *Int J Med Sci,* 10**,** 883-93.

MOORE, K. J., SHEEDY, F. J. & FISHER, E. A. 2013. Macrophages in atherosclerosis: a dynamic balance. *Nat Rev Immunol,* 13**,** 709-21.

MORTON, A. C., ROTHMAN, A. M., GREENWOOD, J. P., GUNN, J., CHASE, A., CLARKE, B., HALL, A. S., FOX, K., FOLEY, C., BANYA, W., WANG, D., FLATHER, M. D. & CROSSMAN, D. C. 2015. The effect of interleukin-1 receptor antagonist therapy on markers of inflammation in non-ST elevation acute coronary syndromes: the MRC-ILA Heart Study. *Eur Heart J,* 36**,** 377-84.

MULLEN, A., LOSCHER, C. E. & ROCHE, H. M. 2010. Anti-inflammatory effects of EPA and DHA are dependent upon time and dose-response elements associated with LPS stimulation in THP-1-derived macrophages. *J Nutr Biochem,* 21**,** 444-50.

MUNTEANU, A., TADDEI, M., TAMBURINI, I., BERGAMINI, E., AZZI, A. & ZINGG, J. M. 2006. Antagonistic effects of oxidized low density lipoprotein and alpha-tocopherol on CD36 scavenger receptor expression in monocytes: involvement of protein kinase B and peroxisome proliferator-activated receptor-gamma. *J Biol Chem,* 281**,** 6489-97.

NABEL, E. G. & BRAUNWALD, E. 2012. A tale of coronary artery disease and myocardial infarction. *N Engl J Med,* 366**,** 54-63.

NEWBY, A. C. 2016. Metalloproteinase production from macrophages - a perfect storm leading to atherosclerotic plaque rupture and myocardial infarction. *Exp Physiol,* 101**,** 1327-1337.

NIEMI, K., TEIRILÄ, L., LAPPALAINEN, J., RAJAMÄKI, K., BAUMANN, M. H., ÖÖRNI, K., WOLFF, H., KOVANEN, P. T., MATIKAINEN, S. & EKLUND, K. K. 2011. Serum amyloid A activates the NLRP3 inflammasome via P2X7 receptor and a cathepsin B-sensitive pathway. *J Immunol,* 186**,** 6119-28.

NIJM, J., WIKBY, A., TOMPA, A., OLSSON, A. G. & JONASSON, L. 2005. Circulating levels of proinflammatory cytokines and neutrophil-platelet aggregates in patients with coronary artery disease. *Am J Cardiol,* 95**,** 452-6.

NISHI, K., ITABE, H., UNO, M., KITAZATO, K. T., HORIGUCHI, H., SHINNO, K. & NAGAHIRO, S. 2002. Oxidized LDL in carotid plaques and plasma associates with plaque instability. *Arterioscler Thromb Vasc Biol,* 22**,** 1649-54.

NYMO, S., NIYONZIMA, N., ESPEVIK, T. & MOLLNES, T. E. 2014. Cholesterol crystal-induced endothelial cell activation is complement-dependent and mediated by TNF. *Immunobiology,* 219**,** 786-92.

OESTERLE, A., LAUFS, U. & LIAO, J. K. 2017. Pleiotropic Effects of Statins on the Cardiovascular System. *Circ Res,* 120**,** 229-243.

OKAJI, Y., TSUNO, N. H., KITAYAMA, J., SAITO, S., TAKAHASHI, T., KAWAI, K., YAZAWA, K., ASAKAGE, M., TSUCHIYA, T., SAKURAI, D., TSUCHIYA, N., TOKUNAGA, K., TAKAHASHI, K. & NAGAWA, H. 2004. A novel method for isolation of endothelial cells and macrophages from murine tumors based on Ac-LDL uptake and CD16 expression. *J Immunol Methods,* 295**,** 183-93.

OLIVIERI, F., LAZZARINI, R., RECCHIONI, R., MARCHESELLI, F., RIPPO, M. R., DI NUZZO, S., ALBERTINI, M. C., GRACIOTTI, L., BABINI, L., MARIOTTI, S., SPADA, G., ABBATECOLA, A. M., ANTONICELLI, R., FRANCESCHI, C. & PROCOPIO, A. D. 2013. MiR-146a as marker of senescence-associated pro-inflammatory status in cells involved in vascular remodelling. *Age (Dordr),* 35**,** 1157-72.

ONODY, A., CSONKA, C., GIRICZ, Z. & FERDINANDY, P. 2003. Hyperlipidemia induced by a cholesterol-rich diet leads to enhanced peroxynitrite formation in rat hearts. *Cardiovasc Res,* 58**,** 663-70.

OOI, B. K., GOH, B. H. & YAP, W. H. 2017. Oxidative Stress in Cardiovascular Diseases: Involvement of Nrf2 Antioxidant Redox Signaling in Macrophage Foam Cells Formation. *Int J Mol Sci,* 18.

OREKHOV, A. N. & SOBENIN, I. A. 2018. Modified lipoproteins as biomarkers of atherosclerosis. *Front Biosci (Landmark Ed),* 23**,** 1422-1444.

ORN, S., UELAND, T., MANHENKE, C., SANDANGER, O., GODANG, K., YNDESTAD, A., MOLLNES, T. E., DICKSTEIN, K. & AUKRUST, P. 2012. Increased interleukin-1beta levels are associated with left ventricular hypertrophy and remodelling following acute ST segment elevation myocardial infarction treated by primary percutaneous coronary intervention. *J Intern Med,* 272**,** 267-76.

OURY, C. 2014. CD36: linking lipids to the NLRP3 inflammasome, atherogenesis and atherothrombosis. *Cell Mol Immunol,* 11**,** 8-10.

OUWENEEL, A. B., VERWILLIGEN, R. A. F. & VAN ECK, M. 2019. Vulnerable plaque and vulnerable blood: Two critical factors for spontaneous atherothrombosis in mouse models. *Atherosclerosis,* 284**,** 160-164.

PACKER, D. L. 2000. Intermittent atrial fibrillation and stroke. *Rev Cardiovasc Med,* 1**,** 18-9.

PALINSKI, W., ROSENFELD, M. E., YLA-HERTTUALA, S., GURTNER, G. C., SOCHER, S. S., BUTLER, S. W., PARTHASARATHY, S., CAREW, T. E., STEINBERG, D. & WITZTUM, J. L. 1989. Low density lipoprotein undergoes oxidative modification in vivo. *Proc Natl Acad Sci U S A,* 86**,** 1372-6.

PAOLETTI, R., GOTTO, A. M. & HAJJAR, D. P. 2004. Inflammation in atherosclerosis and implications for therapy. *Circulation,* 109**,** III20-6.

PARTHASARATHY, S., SANTANAM, N., RAMACHANDRAN, S. & MEILHAC, O. 2000. Potential role of oxidized lipids and lipoproteins in antioxidant defense. *Free Radic Res,* 33**,** 197-215.

PASTERKAMP, G., DEN RUIJTER, H. M. & LIBBY, P. 2017. Temporal shifts in clinical presentation and underlying mechanisms of atherosclerotic disease. *Nat Rev Cardiol,* 14**,** 21-29.

PEARSON, T. A., MENSAH, G. A., ALEXANDER, R. W., ANDERSON, J. L., CANNON, R. O., 3RD, CRIQUI, M., FADL, Y. Y., FORTMANN, S. P., HONG, Y., MYERS, G. L., RIFAI, N., SMITH, S. C., JR., TAUBERT, K., TRACY, R. P., VINICOR, F., CENTERS FOR DISEASE, C., PREVENTION & AMERICAN HEART, A. 2003. Markers of inflammation and cardiovascular disease: application to clinical and public health practice: A statement for healthcare professionals from the Centers for Disease Control and Prevention and the American Heart Association. *Circulation,* 107**,** 499-511.

PEREZ, C., KÖHLER, M., JANSER, D., PARDON, E., STEYAERT, J., ZENOBI, R. & LOCHER, K. P. 2017. Structural basis of inhibition of lipid-linked oligosaccharide flippase PglK by a conformational nanobody. *Sci Rep,* 7**,** 46641.

PERSSON, J., NILSSON, J. & LINDHOLM, M. W. 2006. Cytokine response to lipoprotein lipid loading in human monocyte-derived macrophages. *Lipids Health Dis,* 5**,** 17.

PHILLIPS, M. C. 2014. Molecular mechanisms of cellular cholesterol efflux. *J Biol Chem,* 289**,** 24020-9.

PLATANIA, C. B. M., LAZZARA, F., FIDILIO, A., FRESTA, C. G., CONTI, F., GIURDANELLA, G., LEGGIO, G. M., SALOMONE, S., DRAGO, F. & BUCOLO, C. 2019. Blood-retinal barrier protection against high glucose damage: The role of P2X7 receptor. *Biochem Pharmacol,* 168**,** 249-258.

PRANDONI, P., BILORA, F., MARCHIORI, A., BERNARDI, E., PETROBELLI, F., LENSING, A. W., PRINS, M. H. & GIROLAMI, A. 2003. An association between atherosclerosis and venous thrombosis. *N Engl J Med,* 348**,** 1435-41.

PRANDONI, P., GHIRARDUZZI, A., PRINS, M. H., PENGO, V., DAVIDSON, B. L., SØRENSEN, H., PESAVENTO, R., IOTTI, M., CASIGLIA, E., ILICETO, S., PAGNAN, A. & LENSING, A. W. 2006. Venous thromboembolism and the risk of subsequent symptomatic atherosclerosis. *J Thromb Haemost,* 4**,** 1891-6.

QIAO, J. H., TRIPATHI, J., MISHRA, N. K., CAI, Y., TRIPATHI, S., WANG, X. P., IMES, S., FISHBEIN, M. C., CLINTON, S. K., LIBBY, P., LUSIS, A. J. & RAJAVASHISTH, T. B. 1997. Role of macrophage colony-stimulating factor in atherosclerosis: studies of osteopetrotic mice. *Am J Pathol,* 150**,** 1687-99.

QU, Y. & DUBYAK, G. R. 2009. P2X7 receptors regulate multiple types of membrane trafficking responses and non-classical secretion pathways. *Purinergic Signal,* 5**,** 163-73.

QUILLARD, T., FRANCK, G., MAWSON, T., FOLCO, E. & LIBBY, P. 2017. Mechanisms of erosion of atherosclerotic plaques. *Curr Opin Lipidol,* 28**,** 434-441.

RADER, D. J. 2012. IL-1 and atherosclerosis: a murine twist to an evolving human story. *J Clin Invest,* 122**,** 27-30.

RAJAMAKI, K., LAPPALAINEN, J., OORNI, K., VALIMAKI, E., MATIKAINEN, S., KOVANEN, P. T. & EKLUND, K. K. 2010. Cholesterol crystals activate the NLRP3 inflammasome in human macrophages: a novel link between cholesterol metabolism and inflammation. *PLoS One,* 5**,** e11765.

RANDLE, P. J., PRIESTMAN, D. A., MISTRY, S. & HALSALL, A. 1994. Mechanisms modifying glucose oxidation in diabetes mellitus. *Diabetologia,* 37 Suppl 2**,** S155-61.

RANDOLPH, G. J. 2014. Mechanisms that regulate macrophage burden in atherosclerosis. *Circ Res,* 114**,** 1757-71.

RATHKEY, J. K., ZHAO, J., LIU, Z., CHEN, Y., YANG, J., KONDOLF, H. C., BENSON, B. L., CHIRIELEISON, S. M., HUANG, A. Y., DUBYAK, G. R., XIAO, T. S., LI, X. & ABBOTT, D. W. 2018. Chemical disruption of the pyroptotic pore-forming protein gasdermin D inhibits inflammatory cell death and sepsis. *Sci Immunol,* 3.

REICH, L. M., FOLSOM, A. R., KEY, N. S., BOLAND, L. L., HECKBERT, S. R., ROSAMOND, W. D. & CUSHMAN, M. 2006. Prospective study of subclinical atherosclerosis as a risk factor for venous thromboembolism. *J Thromb Haemost,* 4**,** 1909-13.

RIDKER, P. M. 2018. Mortality Differences Associated With Treatment Responses in CANTOS and FOURIER: Insights and Implications. *Circulation,* 137**,** 1763-1766.

RIDKER, P. M., CANNON, C. P., MORROW, D., RIFAI, N., ROSE, L. M., MCCABE, C. H., PFEFFER, M. A., BRAUNWALD, E., PRAVASTATIN OR ATORVASTATIN, E. & INFECTION THERAPY-THROMBOLYSIS IN MYOCARDIAL INFARCTION, I. 2005. C-reactive protein levels and outcomes after statin therapy. *N Engl J Med,* 352**,** 20-8.

RIDKER, P. M., DANIELSON, E., FONSECA, F. A., GENEST, J., GOTTO, A. M., JR., KASTELEIN, J. J., KOENIG, W., LIBBY, P., LORENZATTI, A. J., MACFADYEN, J. G., NORDESTGAARD, B. G., SHEPHERD, J., WILLERSON, J. T., GLYNN, R. J. & GROUP, J. S. 2008. Rosuvastatin to prevent vascular events in men and women with elevated C-reactive protein. *N Engl J Med,* 359**,** 2195-207.

RIDKER, P. M., EVERETT, B. M., PRADHAN, A., MACFADYEN, J. G., SOLOMON, D. H., ZAHARRIS, E., MAM, V., HASAN, A., ROSENBERG, Y., ITURRIAGA, E., GUPTA, M., TSIGOULIS, M., VERMA, S., CLEARFIELD, M., LIBBY, P., GOLDHABER, S. Z., SEAGLE, R., OFORI, C., SAKLAYEN, M., BUTMAN, S., SINGH, N., LE MAY, M., BERTRAND, O., JOHNSTON, J., PAYNTER, N. P., GLYNN, R. J. & INVESTIGATORS, C. 2019. Low-Dose Methotrexate for the Prevention of Atherosclerotic Events. *N Engl J Med,* 380**,** 752-762.

RIDKER, P. M., EVERETT, B. M., THUREN, T., MACFADYEN, J. G., CHANG, W. H., BALLANTYNE, C., FONSECA, F., NICOLAU, J., KOENIG, W., ANKER, S. D., KASTELEIN, J. J. P., CORNEL, J. H., PAIS, P., PELLA, D., GENEST, J., CIFKOVA, R., LORENZATTI, A., FORSTER, T., KOBALAVA, Z., VIDA-SIMITI, L., FLATHER, M., SHIMOKAWA, H., OGAWA, H., DELLBORG, M., ROSSI, P. R. F., TROQUAY, R. P. T., LIBBY, P., GLYNN, R. J. & GROUP, C. T. 2017. Antiinflammatory Therapy with Canakinumab for Atherosclerotic Disease. *N Engl J Med,* 377**,** 1119-1131.

RIOS, F. J., KOGA, M. M., FERRACINI, M. & JANCAR, S. 2012. Co-stimulation of PAFR and CD36 is required for oxLDL-induced human macrophages activation. *PLoS One,* 7**,** e36632.

RIOUFOL, G., FINET, G., GINON, I., ANDRÉ-FOUËT, X., ROSSI, R., VIALLE, E., DESJOYAUX, E., CONVERT, G., HURET, J. F. & TABIB, A. 2002. Multiple atherosclerotic plaque rupture in acute coronary syndrome: a three-vessel intravascular ultrasound study. *Circulation,* 106**,** 804-8.

ROMANENKO, V. G., ROTHBLAT, G. H. & LEVITAN, I. 2002. Modulation of endothelial inward-rectifier K+ current by optical isomers of cholesterol. *Biophys J,* 83**,** 3211-22.

ROMANI, M., HOFER, D. C., KATSYUBA, E. & AUWERX, J. 2019. Niacin: an old lipid drug in a new NAD. *J Lipid Res,* 60**,** 741-746.

RONG, J. X., SHAPIRO, M., TROGAN, E. & FISHER, E. A. 2003. Transdifferentiation of mouse aortic smooth muscle cells to a macrophage-like state after cholesterol loading. *Proc Natl Acad Sci U S A,* 100**,** 13531-6.

ROSS, R. 1993. The pathogenesis of atherosclerosis: a perspective for the 1990s. *Nature,* 362**,** 801-9.

ROSS, R. 1999a. Atherosclerosis is an inflammatory disease. *Am Heart J,* 138**,** S419-20.

ROSS, R. 1999b. Atherosclerosis--an inflammatory disease. *N Engl J Med,* 340**,** 115-26.

ROSS, R. & AGIUS, L. 1992. The process of atherogenesis--cellular and molecular interaction: from experimental animal models to humans. *Diabetologia,* 35 Suppl 2**,** S34-40.

ROY, A., BANERJEE, S., SAQIB, U. & BAIG, M. S. 2019. NOS1-derived nitric oxide facilitates macrophage uptake of low-density lipoprotein. *J Cell Biochem*.

ROY, S., AXUP, J. Y., FORSYTH, J. S., GOSWAMI, R. K., HUTCHINS, B. M., BAJURI, K. M., KAZANE, S. A., SMIDER, V. V., FELDING, B. H. & SINHA, S. C. 2017. SMI-Ribosome inactivating protein conjugates selectively inhibit tumor cell growth. *Chem Commun (Camb),* 53**,** 4234-4237.

ROY, S., VEDALA, H. & CHOI, W. 2006. Vertically aligned carbon nanotube probes for monitoring blood cholesterol. *Nanotechnology,* 17**,** S14-8.

RUUTH, M., NGUYEN, S. D., VIHERVAARA, T., HILVO, M., LAAJALA, T. D., KONDADI, P. K., GISTERÅ, A., LÄHTEENMÄKI, H., KITTILÄ, T., HUUSKO, J., UUSITUPA, M., SCHWAB, U., SAVOLAINEN, M. J., SINISALO, J., LOKKI, M. L., NIEMINEN, M. S., JULA, A., PEROLA, M., YLÄ-HERTTULA, S., RUDEL, L., ÖÖRNI, A.,

201

BAUMANN, M., BARUCH, A., LAAKSONEN, R., KETELHUTH, D. F. J., AITTOKALLIO, T., JAUHIAINEN, M., KÄKELÄ, R., BORÉN, J., WILLIAMS, K. J., KOVANEN, P. T. & ÖÖRNI, K. 2018. Susceptibility of low-density lipoprotein particles to aggregate depends on particle lipidome, is modifiable, and associates with future cardiovascular deaths. *Eur Heart J,* 39**,** 2562-2573.

SABATINE, M. S., GIUGLIANO, R. P., KEECH, A. C., HONARPOUR, N., WIVIOTT, S. D., MURPHY, S. A., KUDER, J. F., WANG, H., LIU, T., WASSERMAN, S. M., SEVER, P. S., PEDERSEN, T. R. & INVESTIGATORS, F. S. C. A. 2017. Evolocumab and Clinical Outcomes in Patients with Cardiovascular Disease. *N Engl J Med,* 376**,** 1713-1722.

SAKAGUCHI, M., EHARA, S., HASEGAWA, T., MATSUMOTO, K., NISHIMURA, S., YOSHIKAWA, J. & SHIMADA, K. 2017. Coronary plaque rupture with subsequent thrombosis typifies the culprit lesion of non-ST-segment-elevation myocardial infarction, not unstable angina: non-ST-segment-elevation acute coronary syndrome study. *Heart Vessels,* 32**,** 241-251.

SAMSTAD, E. O., NIYONZIMA, N., NYMO, S., AUNE, M. H., RYAN, L., BAKKE, S. S., LAPPEGARD, K. T., BREKKE, O. L., LAMBRIS, J. D., DAMAS, J. K., LATZ, E., MOLLNES, T. E. & ESPEVIK, T. 2014. Cholesterol crystals induce complement-dependent inflammasome activation and cytokine release. *J Immunol,* 192**,** 2837-45.

SATOH, T., KAMBE, N. & MATSUE, H. 2013. NLRP3 activation induces ASC-dependent programmed necrotic cell death, which leads to neutrophilic inflammation. *Cell Death Dis,* 4**,** e644.

SATTERTHWAITE, G., FRANCIS, S. E., SUVARNA, K., BLAKEMORE, S., WARD, C., WALLACE, D., BRADDOCK, M. & CROSSMAN, D. 2005. Differential gene expression in coronary arteries from patients presenting with ischemic heart disease: further evidence for the inflammatory basis of atherosclerosis. *Am Heart J,* 150**,** 488-99.

SCHINDLER, R., MANCILLA, J., ENDRES, S., GHORBANI, R., CLARK, S. C. & DINARELLO, C. A. 1990. Correlations and interactions in the production of interleukin-6 (IL-6), IL-1, and tumor necrosis factor (TNF) in human blood mononuclear cells: IL-6 suppresses IL-1 and TNF. *Blood,* 75**,** 40-7.

SCHNEIDER, K. S., GROß, C. J., DREIER, R. F., SALLER, B. S., MISHRA, R., GORKA, O., HEILIG, R., MEUNIER, E., DICK, M. S., ĆIKOVIĆ, T., SODENKAMP, J., MÉDARD, G., NAUMANN, R., RULAND, J., KUSTER, B., BROZ, P. & GROß, O. 2017. The Inflammasome Drives GSDMD-Independent Secondary Pyroptosis and IL-1 Release in the Absence of Caspase-1 Protease Activity. *Cell Rep,* 21**,** 3846-3859.

SCHRODER, K., ZHOU, R. & TSCHOPP, J. 2010. The NLRP3 inflammasome: a sensor for metabolic danger? *Science,* 327**,** 296-300.

SCHROETER, H., SPENCER, J. P., RICE-EVANS, C. & WILLIAMS, R. J. 2001. Flavonoids protect neurons from oxidized low-density-lipoprotein-induced apoptosis involving c-Jun N-terminal kinase (JNK), c-Jun and caspase-3. *Biochem J,* 358**,** 547-57.

SCHUH, J., FAIRCLOUGH, G. F. & HASCHEMEYER, R. H. 1978. Oxygen-mediated heterogeneity of apo-low-density lipoprotein. *Proc Natl Acad Sci U S A,* 75**,** 3173-7.

SEKINE, N., CIRULLI, V., REGAZZI, R., BROWN, L. J., GINE, E., TAMARIT-RODRIGUEZ, J., GIROTTI, M., MARIE, S., MACDONALD, M. J. & WOLLHEIM, C. B. 1994. Low lactate dehydrogenase and high mitochondrial glycerol phosphate

dehydrogenase in pancreatic beta-cells. Potential role in nutrient sensing. *J Biol Chem,* 269**,** 4895-902.

SHAH, P. K. 2003. Mechanisms of plaque vulnerability and rupture. *J Am Coll Cardiol,* 41**,** 15S-22S.

SHAH, P. K. & LECIS, D. 2019. Inflammation in atherosclerotic cardiovascular disease. *F1000Res,* 8.

SHENDEROV, K., RITEAU, N., YIP, R., MAYER-BARBER, K. D., OLAND, S., HIENY, S., FITZGERALD, P., OBERST, A., DILLON, C. P., GREEN, D. R., CERUNDOLO, V. & SHER, A. 2014. Cutting edge: Endoplasmic reticulum stress licenses macrophages to produce mature IL-1beta in response to TLR4 stimulation through a caspase-8- and TRIF-dependent pathway. *J Immunol,* 192**,** 2029-33.

SHI, J., ZHAO, Y., WANG, K., SHI, X., WANG, Y., HUANG, H., ZHUANG, Y., CAI, T., WANG, F. & SHAO, F. 2015. Cleavage of GSDMD by inflammatory caspases determines pyroptotic cell death. *Nature,* 526**,** 660-5.

SHIMOKAWA, H. 1999. Primary endothelial dysfunction: atherosclerosis. *J Mol Cell Cardiol,* 31**,** 23-37.

SINGH, R., DEVI, S. & GOLLEN, R. 2015. Role of free radical in atherosclerosis, diabetes and dyslipidaemia: larger-than-life. *Diabetes Metab Res Rev,* 31**,** 113-26.

SINGH, R. K., BARBOSA-LORENZI, V. C., LUND, F. W., GROSHEVA, I., MAXFIELD, F. R. & HAKA, A. S. 2016. Degradation of aggregated LDL occurs in complex extracellular sub-compartments of the lysosomal synapse. *J Cell Sci,* 129**,** 1072-82.

SINGH, R. K., HAKA, A. S., ASMAL, A., BARBOSA-LORENZI, V. C., GROSHEVA, I., CHIN, H. F., XIONG, Y., HLA, T. & MAXFIELD, F. R. 2019. TLR4 (Toll-Like Receptor 4)-Dependent Signaling Drives Extracellular Catabolism of LDL (Low-Density Lipoprotein) Aggregates. *Arterioscler Thromb Vasc Biol***,** ATVBAHA119313200.

SMITH, J. D., TROGAN, E., GINSBERG, M., GRIGAUX, C., TIAN, J. & MIYATA, M. 1995. Decreased atherosclerosis in mice deficient in both macrophage colony-stimulating factor (op) and apolipoprotein E. *Proc Natl Acad Sci U S A,* 92**,** 8264-8.

SOBAL, G., MENZEL, J. & SINZINGER, H. 2000. Why is glycated LDL more sensitive to oxidation than native LDL? A comparative study. *Prostaglandins Leukot Essent Fatty Acids,* 63**,** 177-86.

SOTTERO, B., ROSSIN, D., POLI, G. & BIASI, F. 2018. Lipid Oxidation Products in the Pathogenesis of Inflammation-related Gut Diseases. *Curr Med Chem,* 25**,** 1311-1326.

SPAGNOLI, L. G., BONANNO, E., SANGIORGI, G. & MAURIELLO, A. 2007. Role of inflammation in atherosclerosis. *J Nucl Med,* 48**,** 1800-15.

STACY, M. R. 2019. Radionuclide Imaging of Atherothrombotic Diseases. *Curr Cardiovasc Imaging Rep,* 12.

STEFFEN, B. T., STEFFEN, L. M., ZHOU, X., OUYANG, P., WEIR, N. L. & TSAI, M. Y. 2015. n-3 Fatty acids attenuate the risk of diabetes associated with elevated serum nonesterified fatty acids: the multi-ethnic study of atherosclerosis. *Diabetes Care,* 38**,** 575-80.

STEINBERG, D. 1997. Lewis A. Conner Memorial Lecture. Oxidative modification of LDL and atherogenesis. *Circulation,* 95**,** 1062-71.

STEINBERG, D. 2009. The LDL modification hypothesis of atherogenesis: an update. *J Lipid Res,* 50 Suppl**,** S376-81.

STEWART, C. R., TSENG, A. A., MOK, Y. F., STAPLES, M. K., SCHIESSER, C. H., LAWRENCE, L. J., VARGHESE, J. N., MOORE, K. J. & HOWLETT, G. J. 2005. Oxidation of low-density lipoproteins induces amyloid-like structures that are recognized by macrophages. *Biochemistry,* 44**,** 9108-16.

STOCKER, R. & KEANEY, J. F. 2004. Role of oxidative modifications in atherosclerosis. *Physiol Rev,* 84**,** 1381-478.

STROWIG, T., HENAO-MEJIA, J., ELINAV, E. & FLAVELL, R. 2012. Inflammasomes in health and disease. *Nature,* 481**,** 278-86.

SUBAUSTE, C. S. 2019. The CD40-ATP-P2X. *Front Immunol,* 10**,** 2958.

SUN, L., WANG, H., WANG, Z., HE, S., CHEN, S., LIAO, D., WANG, L., YAN, J., LIU, W., LEI, X. & WANG, X. 2012. Mixed lineage kinase domain-like protein mediates necrosis signaling downstream of RIP3 kinase. *Cell,* 148**,** 213-27.

SUN, S. C., CHANG, J. H. & JIN, J. 2013. Regulation of nuclear factor-κB in autoimmunity. *Trends Immunol,* 34**,** 282-9.

SWANSON, K. V., DENG, M. & TING, J. P. 2019. The NLRP3 inflammasome: molecular activation and regulation to therapeutics. *Nat Rev Immunol,* 19**,** 477-489.

SZMITKO, P. E., WANG, C. H., WEISEL, R. D., DE ALMEIDA, J. R., ANDERSON, T. J. & VERMA, S. 2003. New markers of inflammation and endothelial cell activation: Part I. *Circulation,* 108**,** 1917-23.

TAK, P. P. & FIRESTEIN, G. S. 2001. NF-kappaB: a key role in inflammatory diseases. *J Clin Invest,* 107**,** 7-11.

TAMMINEN, M., MOTTINO, G., QIAO, J. H., BRESLOW, J. L. & FRANK, J. S. 1999. Ultrastructure of early lipid accumulation in ApoE-deficient mice. *Arterioscler Thromb Vasc Biol,* 19**,** 847-53.

THICHANPIANG, P., HARPER, S. J., WONGPRASERT, K. & BATES, D. O. 2014. TNF-α-induced ICAM-1 expression and monocyte adhesion in human RPE cells is mediated in part through autocrine VEGF stimulation. *Mol Vis,* 20**,** 781-9.

THIRUNAVUKKARASU, S. & KHADER, S. A. 2019. Advances in Cardiovascular Disease Lipid Research Can Provide Novel Insights Into Mycobacterial Pathogenesis. *Front Cell Infect Microbiol,* 9**,** 116.

THUM, T. & BORLAK, J. 2008. LOX-1 receptor blockade abrogates oxLDL-induced oxidative DNA damage and prevents activation of the transcriptional repressor Oct-1 in human coronary arterial endothelium. *J Biol Chem,* 283**,** 19456-64.

TOMKIN, G. H. & OWENS, D. 2017. Investigational therapies for hypercholesterolemia. *Expert Opin Investig Drugs,* 26**,** 603-617.

TOUTOUZAS, K., KARANASOS, A. & TOUSOULIS, D. 2016. Optical Coherence Tomography For the Detection of the Vulnerable Plaque. *Eur Cardiol,* 11**,** 90-95.

TSCHOPP, J. & SCHRODER, K. 2010. NLRP3 inflammasome activation: The convergence of multiple signalling pathways on ROS production? *Nat Rev Immunol,* 10**,** 210-5.

TSUCHIYA, K., NAKAJIMA, S., HOSOJIMA, S., THI NGUYEN, D., HATTORI, T., MANH LE, T., HORI, O., MAHIB, M. R., YAMAGUCHI, Y., MIURA, M., KINOSHITA, T., KUSHIYAMA, H., SAKURAI, M., SHIROISHI, T. & SUDA, T. 2019. Caspase-1 initiates apoptosis in the absence of gasdermin D. *Nat Commun,* 10**,** 2091.

VALKO, M., LEIBFRITZ, D., MONCOL, J., CRONIN, M. T., MAZUR, M. & TELSER, J. 2007. Free radicals and antioxidants in normal physiological functions and human disease. *Int J Biochem Cell Biol,* 39**,** 44-84.

VAN DEN HOOGEN, I. J., GIANNI, U., AL HUSSEIN ALAWAMLH, O., WIJERATNE, R., JINNOUCHI, H., FINN, A., EARLS, J. P., VIRMANI, R. & LIN, F. Y. 2019. What

atherosclerosis findings can CT see in sudden coronary death: Plaque rupture versus plaque erosion. *J Cardiovasc Comput Tomogr*.

VAN ROOY, M. J. & PRETORIUS, E. 2014. Obesity, hypertension and hypercholesterolemia as risk factors for atherosclerosis leading to ischemic events. *Curr Med Chem*, 21**,** 2121-9.

VAN TASSELL, B. W., TOLDO, S., MEZZAROMA, E. & ABBATE, A. 2013. Targeting interleukin-1 in heart disease. *Circulation*, 128**,** 1910-23.

VARSANO, N., BEGHI, F., ELAD, N., PEREIRO, E., DADOSH, T., PINKAS, I., PEREZ-BERNA, A. J., JIN, X., KRUTH, H. S., LEISEROWITZ, L. & ADDADI, L. 2018. Two polymorphic cholesterol monohydrate crystal structures form in macrophage culture models of atherosclerosis. *Proc Natl Acad Sci U S A*, 115**,** 7662-7669.

VENGRENYUK, Y., CARLIER, S., XANTHOS, S., CARDOSO, L., GANATOS, P., VIRMANI, R., EINAV, S., GILCHRIST, L. & WEINBAUM, S. 2006. A hypothesis for vulnerable plaque rupture due to stress-induced debonding around cellular microcalcifications in thin fibrous caps. *Proc Natl Acad Sci U S A*, 103**,** 14678-83.

VIRELLA, G., MUÑOZ, J. F., GALBRAITH, G. M., GISSINGER, C., CHASSEREAU, C. & LOPES-VIRELLA, M. F. 1995. Activation of human monocyte-derived macrophages by immune complexes containing low-density lipoprotein. *Clin Immunol Immunopathol*, 75**,** 179-89.

VIRMANI, R., BURKE, A. P., FARB, A. & KOLODGIE, F. D. 2006. Pathology of the vulnerable plaque. *J Am Coll Cardiol*, 47**,** C13-8.

WAKABAYASHI, T., TAKAHASHI, M., YAMAMURO, D., KARASAWA, T., TAKEI, A., TAKEI, S., YAMAZAKI, H., NAGASHIMA, S., EBIHARA, K. & ISHIBASHI, S. 2018. Inflammasome Activation Aggravates Cutaneous Xanthomatosis and Atherosclerosis in ACAT1 (Acyl-CoA Cholesterol Acyltransferase 1) Deficiency in Bone Marrow. *Arterioscler Thromb Vasc Biol*, 38**,** 2576-2589.

WALTHER, T. C. & FARESE, R. V., JR. 2012. Lipid droplets and cellular lipid metabolism. *Annu Rev Biochem*, 81**,** 687-714.

WANG, H., MAO, L. & MENG, G. 2013. The NLRP3 inflammasome activation in human or mouse cells, sensitivity causes puzzle. *Protein Cell*, 4**,** 565-8.

WARA, A. K., MITSUMATA, M., YAMANE, T., KUSUMI, Y. & YOSHIDA, Y. 2008. Gene expression in endothelial cells and intimal smooth muscle cells in atherosclerosis-prone or atherosclerosis-resistant regions of the human aorta. *J Vasc Res*, 45**,** 303-13.

WESTHORPE, C. L., DUFOUR, E. M., MAISA, A., JAWOROWSKI, A., CROWE, S. M. & MULLER, W. A. 2012. Endothelial cell activation promotes foam cell formation by monocytes following transendothelial migration in an in vitro model. *Exp Mol Pathol*, 93**,** 220-6.

WIERZBICKI, A. S. 2013. All at sea: new lipid-lowering drug trials continue to disappoint. *Int J Clin Pract*, 67**,** 595-8.

WILSON, H. L., VARCOE, R. W., STOKES, L., HOLLAND, K. L., FRANCIS, S. E., DOWER, S. K., SURPRENANT, A. & CROSSMAN, D. C. 2007. P2X receptor characterization and IL-1/IL-1Ra release from human endothelial cells. *Br J Pharmacol*, 151**,** 115-27.

WYBLE, C. W., HYNES, K. L., KUCHIBHOTLA, J., MARCUS, B. C., HALLAHAN, D. & GEWERTZ, B. L. 1997. TNF-alpha and IL-1 upregulate membrane-bound and soluble E-selectin through a common pathway. *J Surg Res*, 73**,** 107-12.

XIE, Z., WANG, X., LIU, X., DU, H., SUN, C., SHAO, X., TIAN, J., GU, X., WANG, H. & YU, B. 2018. Adipose-Derived Exosomes Exert Proatherogenic Effects by

Regulating Macrophage Foam Cell Formation and Polarization. *J Am Heart Assoc,* 7.

XU, K., YANG, Y., YAN, M., ZHAN, J., FU, X. & ZHENG, X. 2010. Autophagy plays a protective role in free cholesterol overload-induced death of smooth muscle cells. *J Lipid Res,* 51**,** 2581-90.

XU, Q. 2000. Biomechanical-stress-induced signaling and gene expression in the development of arteriosclerosis. *Trends Cardiovasc Med,* 10**,** 35-41.

XU, S., LUO, W., XU, X., QIAN, Y., XU, Z., YU, W., SHAN, X., GUAN, X., LUM, H., ZHOU, H. & WANG, Y. 2019. MD2 blockade prevents oxLDL-induced renal epithelial cell injury and protects against high-fat-diet-induced kidney dysfunction. *J Nutr Biochem,* 70**,** 47-55.

YAHAGI, K., KOLODGIE, F. D., OTSUKA, F., FINN, A. V., DAVIS, H. R., JONER, M. & VIRMANI, R. 2016. Pathophysiology of native coronary, vein graft, and in-stent atherosclerosis. *Nat Rev Cardiol,* 13**,** 79-98.

YAMAMOTO, K., SHIMIZU, N., OBI, S., KUMAGAYA, S., TAKETANI, Y., KAMIYA, A. & ANDO, J. 2007. Involvement of cell surface ATP synthase in flow-induced ATP release by vascular endothelial cells. *Am J Physiol Heart Circ Physiol,* 293**,** H1646-53.

YANG, S., LIU, L., MENG, L. & HU, X. 2019. Capsaicin is beneficial to hyperlipidemia, oxidative stress, endothelial dysfunction, and atherosclerosis in Guinea pigs fed on a high-fat diet. *Chem Biol Interact,* 297**,** 1-7.

YEBYO, H. G., ASCHMANN, H. E., KAUFMANN, M. & PUHAN, M. A. 2019. Comparative effectiveness and safety of statins as a class and of specific statins for primary prevention of cardiovascular disease: A systematic review, meta-analysis, and network meta-analysis of randomized trials with 94,283 participants. *Am Heart J,* 210**,** 18-28.

YI, H., BAI, Y., ZHU, X., LIN, L., ZHAO, L., WU, X., BUCH, S., WANG, L., CHAO, J. & YAO, H. 2014. IL-17A induces MIP-1alpha expression in primary astrocytes via Src/MAPK/PI3K/NF-kB pathways: implications for multiple sclerosis. *J Neuroimmune Pharmacol,* 9**,** 629-41.

YU, S., ZHANG, L., LIU, C., YANG, J., ZHANG, J. & HUANG, L. 2019. PACS2 is required for ox-LDL-induced endothelial cell apoptosis by regulating mitochondria-associated ER membrane formation and mitochondrial Ca. *Exp Cell Res,* 379**,** 191-202.

ZHANG, H., LIU, Q., LIN, J. L., WANG, Y., ZHANG, R. X., HOU, J. B. & YU, B. 2017. Recombinant Human Thioredoxin-1 Protects Macrophages from Oxidized Low-Density Lipoprotein-Induced Foam Cell Formation and Cell Apoptosis. *Biomol Ther (Seoul)*.

ZHANG, W. Y., GAYNOR, P. M. & KRUTH, H. S. 1997. Aggregated low density lipoprotein induces and enters surface-connected compartments of human monocyte-macrophages. Uptake occurs independently of the low density lipoprotein receptor. *J Biol Chem,* 272**,** 31700-6.

ZHANG, W. Y., ISHII, I. & KRUTH, H. S. 2000. Plasmin-mediated macrophage reversal of low density lipoprotein aggregation. *J Biol Chem,* 275**,** 33176-83.

ZHANG, Y., LIU, L., PENG, Y. L., LIU, Y. Z., WU, T. Y., SHEN, X. L., ZHOU, J. R., SUN, D. Y., HUANG, A. J., WANG, X., WANG, Y. X. & JIANG, C. L. 2014. Involvement of inflammasome activation in lipopolysaccharide-induced mice depressive-like behaviors. *CNS Neurosci Ther,* 20**,** 119-24.

ZHAO, B., HUANG, W., ZHANG, W. Y., ISHII, I. & KRUTH, H. S. 2004. Retention of aggregated LDL by cultured human coronary artery endothelial cells. *Biochem Biophys Res Commun,* 321**,** 728-35.

ZHAOLIN, Z., JIAOJIAO, C., PENG, W., YAMI, L., TINGTING, Z., JUN, T., SHIYUAN, W., JINYAN, X., DANGHENG, W., ZHISHENG, J. & ZUO, W. 2019. OxLDL induces vascular endothelial cell pyroptosis through miR-125a-5p/TET2 pathway. *J Cell Physiol,* 234**,** 7475-7491.

ZHENG, F., XING, S., GONG, Z. & XING, Q. 2013. NLRP3 inflammasomes show high expression in aorta of patients with atherosclerosis. *Heart Lung Circ,* 22**,** 746-50.

ZHOU, J., HU, G. & WANG, X. 2010. Repression of smooth muscle differentiation by a novel high mobility group box-containing protein, HMG2L1. *J Biol Chem,* 285**,** 23177-85.

ZHU, Y., LI, Q., XUN, W., CHEN, Y., ZHANG, C. & SUN, S. 2019. Blocking P2X7 receptor ameliorates oxidized LDL-mediated podocyte apoptosis. *Mol Biol Rep,* 46**,** 3809-3816.

208

Appendices

A.1 Appendix (I) Chemical Reagents, Concentrations and Supplier Companies

Chemical	Company	Catalogue Number	Concentrations
Recombinant Human IL-1α / IL1F1	R&D SYSTEMS a bio-techne brand R&D Systems, Inc.	200-LA-002	10 ng/ml
Neutrophil Elastase	SIGMA-ALDRICH Sigma-Aldrich	E8140	1 µg/ml
Tumour Necrosis factor-alpha (TNF-α).	CALBIOCHEM® Calbiochem	654205	10 ng/ml
Cholesterol–methyl-β-cyclodextrin (Cholesterol-Water Soluble)	SIGMA-ALDRICH Sigma-Aldrich	C4951	25, 50, 75, 100, 250 & 500 ug/ml
methyl-β-cyclodextrin	SIGMA-ALDRICH Sigma-Aldrich	C4555-1G	25, 50, 75, 100, 250 & 500 µg/ml
Collagenase A from Clostridium histolyticum	SIGMA-ALDRICH Sigma-Aldrich	C5138	1 µg/ml
Aggregated Low Density Lipoprotein from Human Plasma (agLDL)	SIGMA-ALDRICH Sigma-Aldrich	L8292	1 mg/ml Aggregated LDL in PBS
Low Density Lipoprotein From Human Plasma, Acetylated, Alexa Fluor™ 488	Thermo SCIENTIFIC ThermoFisher	L23380	10 µg/ml
CTB-555 Cholera Toxin Subunit B (Recombinant), Alexa Fluor™ 555 Conjugate	Thermo SCIENTIFIC ThermoFisher	C34776	10 µg/ml

Wheat Germ Agglutinin, Alexa Fluor™ 647 Conjugate	Thermo SCIENTIFIC ThermoFisher	W32466	1 µg/ml
Glutaraldehyde solution	SIGMA-ALDRICH Sigma-Aldrich	G7651	0.5% in 1 ml of 4% PFA for protocol in section 2.2.8
Pefabloc® AEBSF 4-(2-aminoethyl)-benzene-sulfonyl fluoride, aebsf, aminoethyl-benzene-sulfonyl fluoride, 4-2-, proteinase k inhibitor	SIGMA-ALDRICH Sigma-Aldrich	11429868001	1Mm in RIPA buffer
Ac-YVAD-cmk (Caspase-1 inhibitor)	InvivoGen InvivoGen	inh-yvad-178603-78-6	Solubility: 50 mg/ml (92.4 mM) in DMSO Working Concentration: 50 µM (27 µg/ml)
MCC950 (NLRP3-inflammasome inhibitor)	InvivoGen InvivoGen	inh-mcc-210826-40-7	Solubility: DMSO (10 mg/ml) Working concentration: 10 µM (4.04 µg/ml)
IL-1β Antibody (H-153) (Primary)	SANTA CRUZ BIOTECHNOLOGY SANTA CRUZ BIOTECHNOLOGY	899431-18-6 H-153-sc-7884	200 µg/ml
Polyclonal Goat Anti-Rabbit Immunoglobulins/HRP (Secondary antibody)	Dako Dako	P044801-2	(Used in western blotting as 1µl in 5 ml milk per each membrane)
P2X7 inhibitor (A 438079 hydrochloride competitive P2X7 antagonist)	TOCRIS TOCRIS	No. 2972-438079	5mM in H2O used as: 10µM (0.85 µg/ml)
Native Human Acetylated Low Density Lipoprotein (AcLDL)	BIO-RAD Bio-Rad	5685-3404	2.0 mg/ml used at multiple concentrations 10-200 µg/ml

Native Human Low Density Lipoprotein from Human Plasma NaLDL	MERCK	L8292-1	5mg used at multiple concentrations 10-200 µg/ml
Native Human Oxidized Low Density Lipoprotein (OxLDL)	Bio-Rad	5685-3557	2.0 mg/ml used at multiple concentrations 10-200 µg/ml
SIGMAFAST™ Protease Inhibitor Cocktail Tablets, EDTA-Free	Sigma-Aldrich	S8830-20TAB	One tablet per 100 ml of sterile deionised water
Anti-Gasdermin (Anti-GSDMD) Rabbit antibody (Primary)	Abcam	[EPR19829] (ab210070)	0.675 mg/ml Working dilution 1/1000 in milk
Skim Milk Powder	Sigma-Aldrich	70166-500G	Used at working concentration of 10% in distilled water
Odyssey® Blocking Buffer in TBS	LI-COR	927-50000	Used for membrane blocking and antibody dilution
Anti Cathepsin B Rabbit Antibody (Primary)	Abcam	Ab33538	Used at dilution of 1:250
Anti-IL-1β Rabbit Antibody (Primary)	Abcam	[EP408Y] (ab33774)	Used at 1:5000 Dilution
IRDye® 680RD Goat anti-Mouse IgG (H + L) (Secondary Antibody)	LICOR	926-68070	0.5 mg Used at 1:5000 Dilution
IRDye® 680RD Donkey anti-Rabbit IgG (H + L) (Secondary Antibody)	LICOR	926-68073	0.5 mg Used at 1:5000 Dilution
Tween20	VWR Chemicals	663684B	0.1% in TBS
Tris Buffered Saline (TBS)	Sigma-Aldrich	T6664-10	Used to dilute Tween20

A.2 Appendix (II) Solutions

A.2.1 Composition of solutions used in HUVECs tissue culture

(A.2.1.1) Minimum Essential Media (MEM)

MEM contains 500mL of EMEM (1x), 5mL of amphotecrin B, 5mL Penicillin-Streptomycin (10,000IU/ml), 10mL of 1M HEPES and 6ml of 7.5% sodium bicarbonate (0.20μm filtered).

(A.2.1.2) Serum Free Media (SFM):

SFM was prepared by adding 50mL M119 medium (10x), 5mL L-gultamine (100x) and 5mL Penicillin-Streptomycin (10,000IU/ml), to 450mL of sterile deionised water. As a colour detector, an amount of 10ml 7.5% sodium bicarbonate was added, to make up 500 ml of SFM.

(A.2.1.3) Complete growth media (CGM):

CGM contains SFM supplemented with 10% FBS (Foetal Bovine Serum), 10% NBCS (New-born Calf Serum), ECGS (Endothelial Cells Growth Factor) (10μg/mL) and heparin (90μg/mL).

(A.2.1.4) Gelatin:

10g of gelatin was dissolved in 500mL of sterile deionised water to make a stock solution of 2% (w/v) gelatin which was stored at 4°C after autoclaving. Stock solution was then diluted in sterile deionised water to make a working solution of 1%.

(A.2.1.5) Trypsin/EDTA:

1X in PBS without Magnesium, Calcium and without Phenol Red.

A.2.2 Composition of solutions used in HCAECs tissue culture

(A.2.2.1) Complete Endothelial Cell Growth Medium MV2

MV2 medium contains 500 ml of endothelial cells basal medium added with supplements at final concentrations as follows: Foetal Calf Serum 0.05 ml / ml, Human Recombinant Epidermal Growth Factor 5 ng/ml, Human Recombinant Basic Fibroblast Growth Factor 10 ng / ml, Insulin-like Growth Factor (Long R3 IGF) 20 ng/ml, Human Recombinant Vascular Endothelial Growth Factor 165 0.5 ng/ml, Ascorbic Acid 1 μg/ml and Hydrocortisone 0.2 μg/ml.

(A.2.2.2) Serum Free MV Medium

MV medium contains 500 ml of endothelial cells basal medium added with supplements at final concentrations as follows: Human Recombinant Epidermal Growth Factor 5 ng/ml, Human Recombinant Vascular Endothelial Growth Factor 165 0.5 ng/ml, and Hydrocortisone 0.2 μg/ml.

(A.2.2.3) Trypsin/EDTA:

1X in PBS without Magnesium, Calcium and without Phenol Red.

A.2.3 Composition of solutions used in HCASMCs tissue culture

(A.2.3.1) Complete Growth Media 311-500

Contains Molybdic Acid 4H2O (Ammonium), Copper (II) Sulfate / Cupric(II) Sulfate, Ferrous Sulfate, Manganese (II) Sulfate, Nickel Chloride, Sodium Selenite, Zinc Sulfate, Ammonium Metavanadate with added smooth muscle cell growth factors, supplements and components to promote optimal culture and growth of HCASMCs.

(A.2.3.2) Serum Free HCASMCs Media 310-500

Contains contents of Complete Growth Media (A.2.3.1) in previous section, excluding growth factors, supplements and serum.

(A.2.3.3) Hanks' Balanced Salt Solution H6648

Maintains osmotic balance and pH while providing vital inorganic ions and water to HCASMCs, contains sodium bicarbonate. Doesn't contain phenol red, magnesium sulfate and calcium chloride.

(A.2.3.4) Trypsin/EDTA

1X in PBS without Magnesium, Calcium and without Phenol Red.

A.2.4 Composition of solutions and materials used in Western Blotting and Pre-Western Blotting sample preparation

(A.2.4.1) Radioimmunoprecipitation assay buffer (RIPA buffer)

RIPA buffer was prepared freshly at time of use by adding 150Mm of Sodium Chloride (NaCl) to 1% Triton X-100, Sodium Deoxycholate 0.50%, SDS 0.10%, 50mM of Tris pH 8.0 and 1Mm of protease inhibitor AEBSF. RIPA buffer was used as a lysis buffer to collect cell lysates for analysis by Western Blotting.

(A.2.4.2) 4–15% Mini-PROTEAN® TGX™ Precast Protein Gels

4–15% precast western blotting polyacrylamide gels, with the following measurements 8.6 × 6.7 cm (W × L) for a volume of 15 μl per well. Bought from BIO-RAD #4561086.

(A.2.4.3) Laemmli Sample Buffer

Laemmli Sample Buffer is used for preparing the samples before loading them to the SDS PAGE. Bought from BIO-RAD #1610737.

(A.2.4.4) TBS-Tween

TBS-Tween was used for washing the nitrocellulose membrane and was composed by adding 1ml tween® to 1000ml of distilled water.

(A.2.5.1) Cell Fixating 10% Buffered Formalin Solution

Composed of Na $H_2 PO_4$, Concentrated Formaldehyde and sterile deionised

water.

A.3 Appendix (III) High-resolution images from thesis figures.

A.3.1 High-resolution images from (Figure 4.16):

Images were taken by bright-field phase contrast Leica© microscope scale bar 25 μm.

B

C

D

E
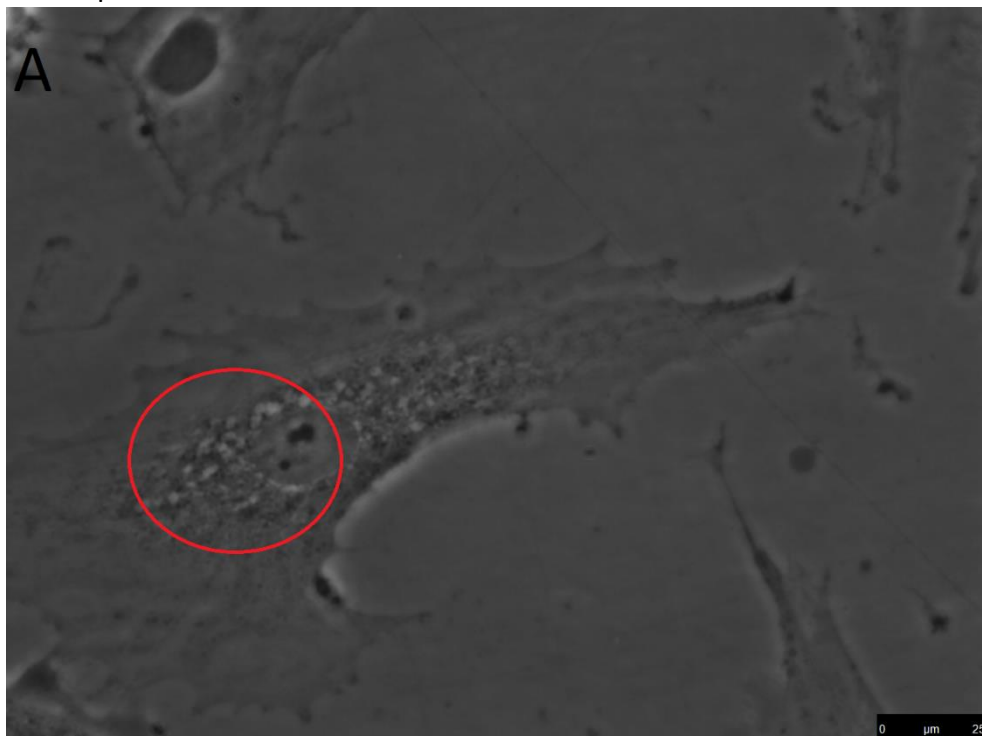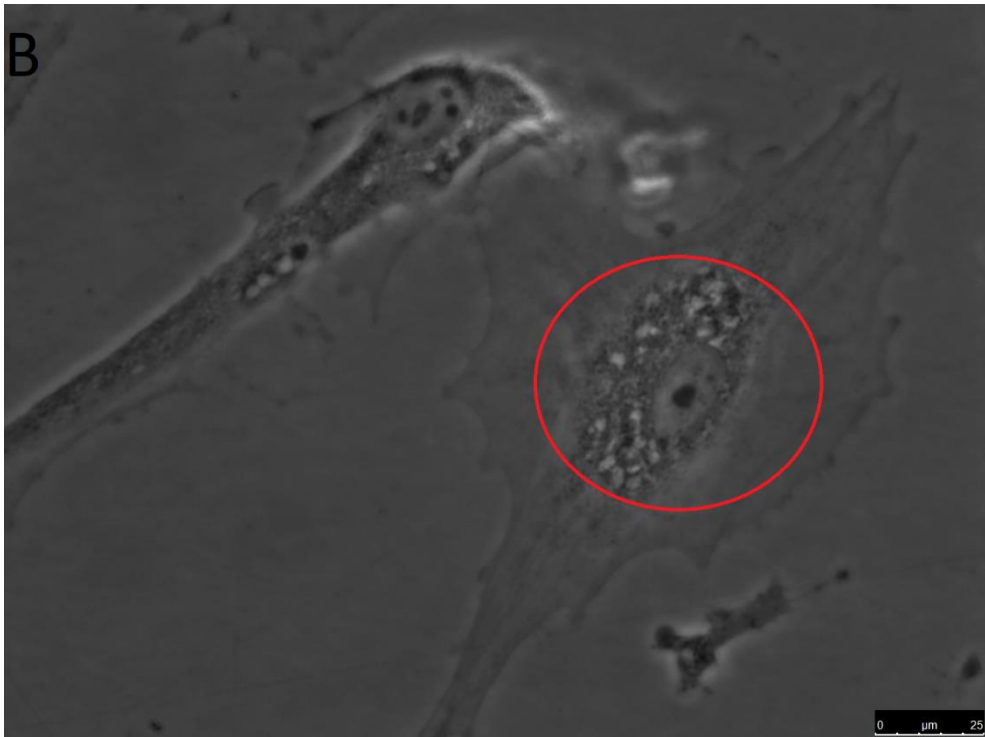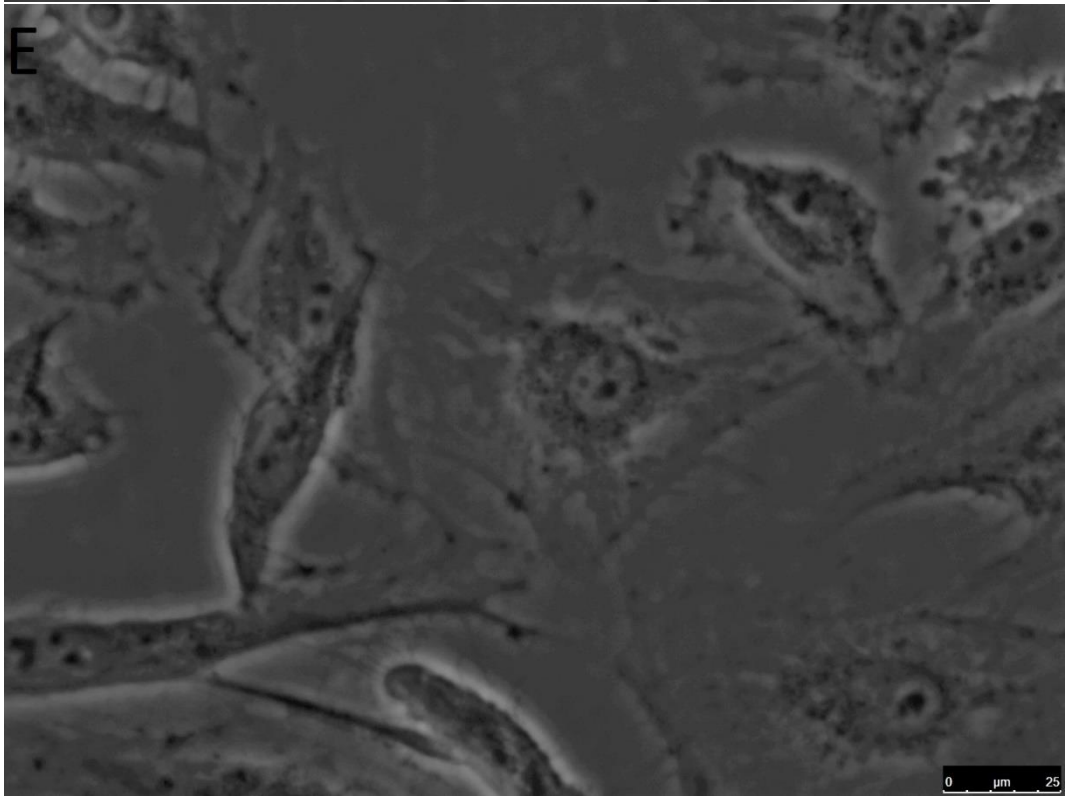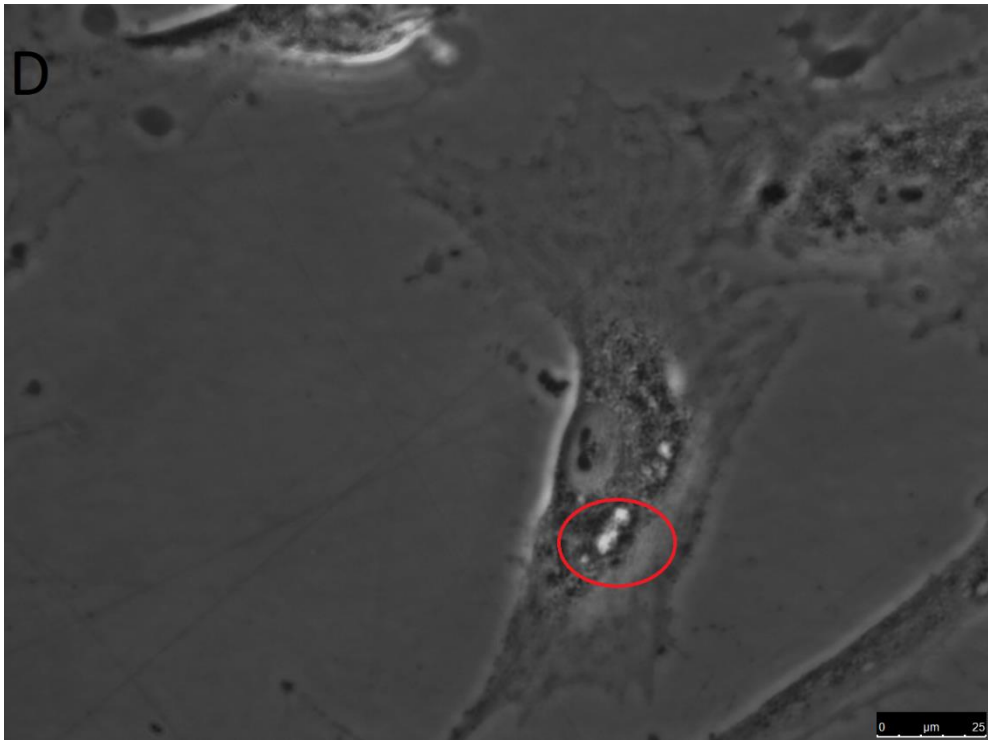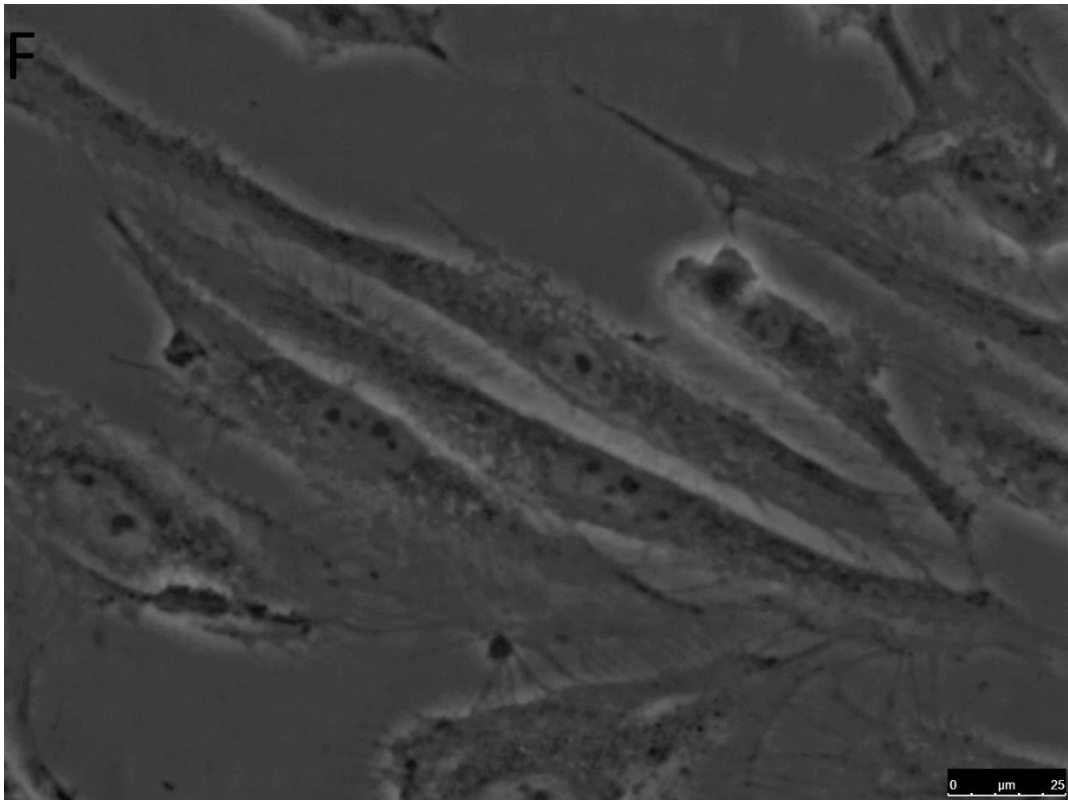
A.3.2 High-resolution images from (Figure 4.17):

Images were taken by bright-field phase contrast Leica© microscope scale
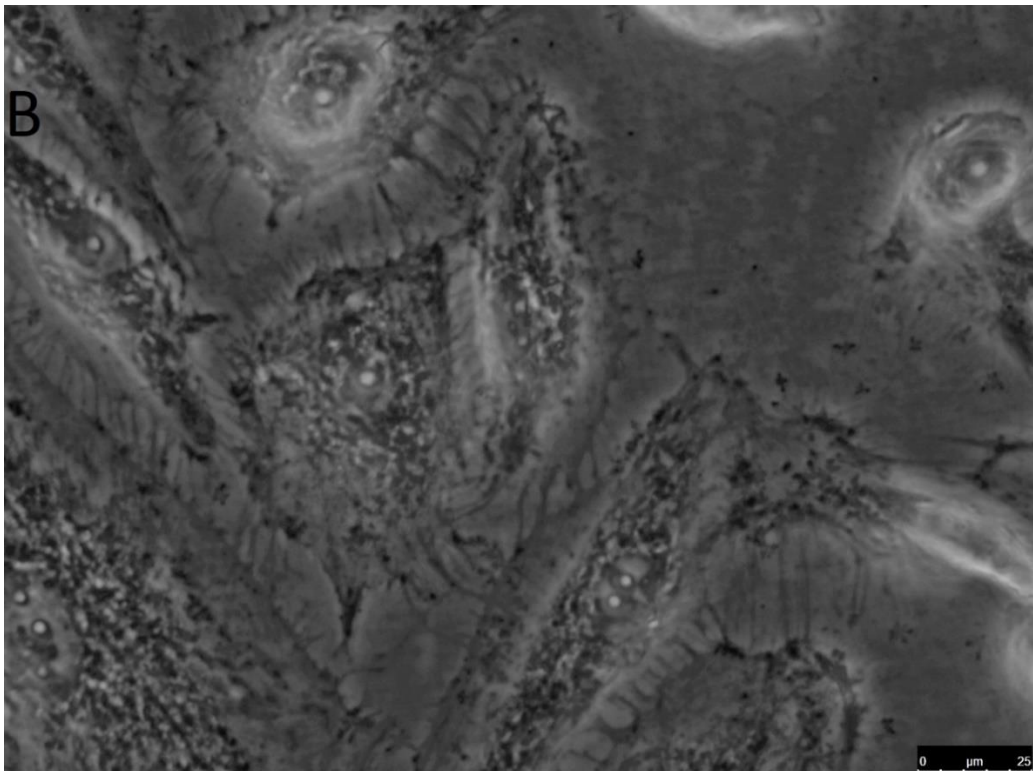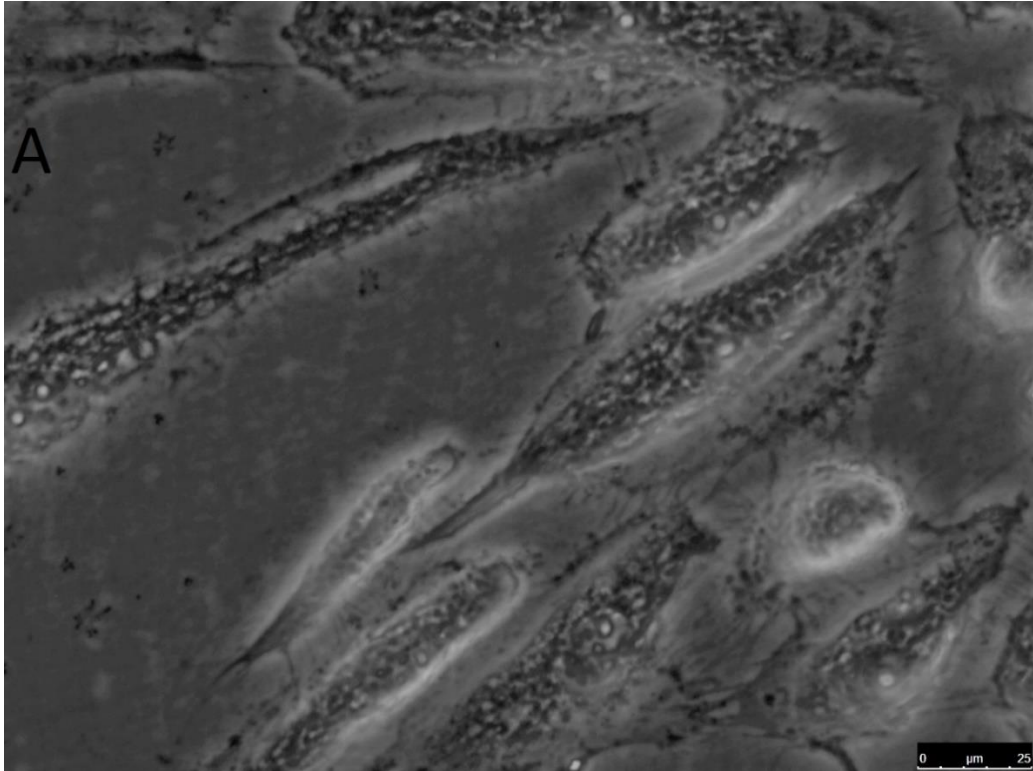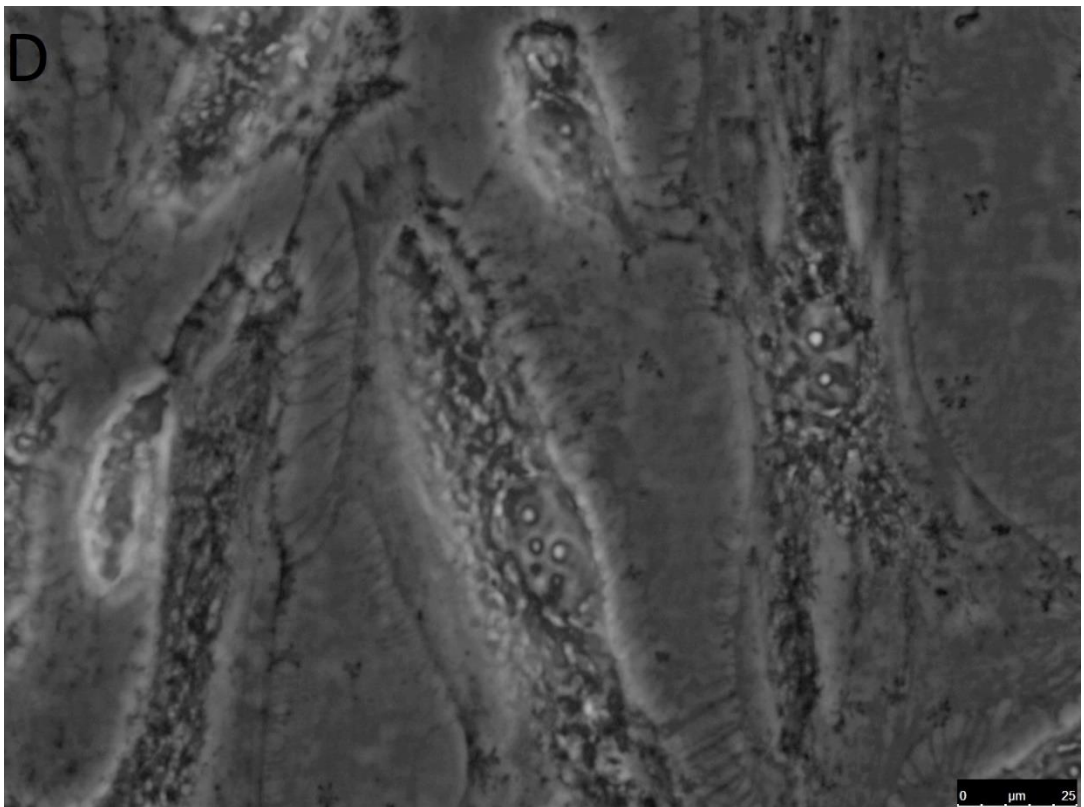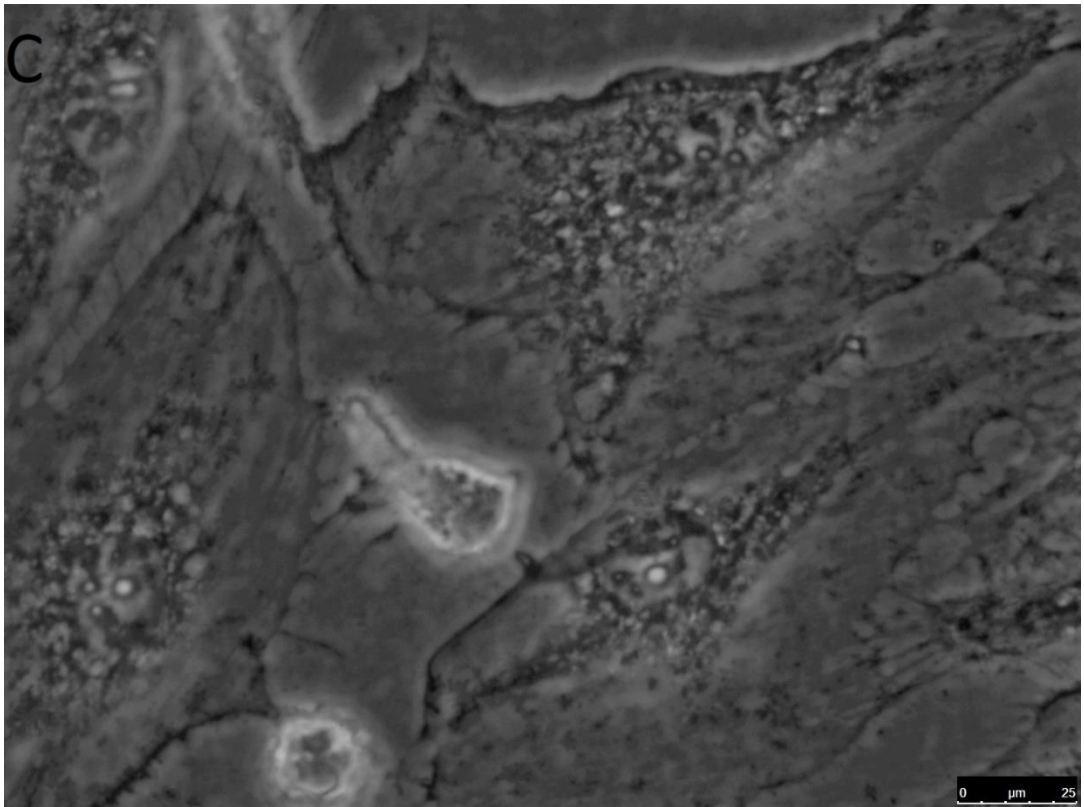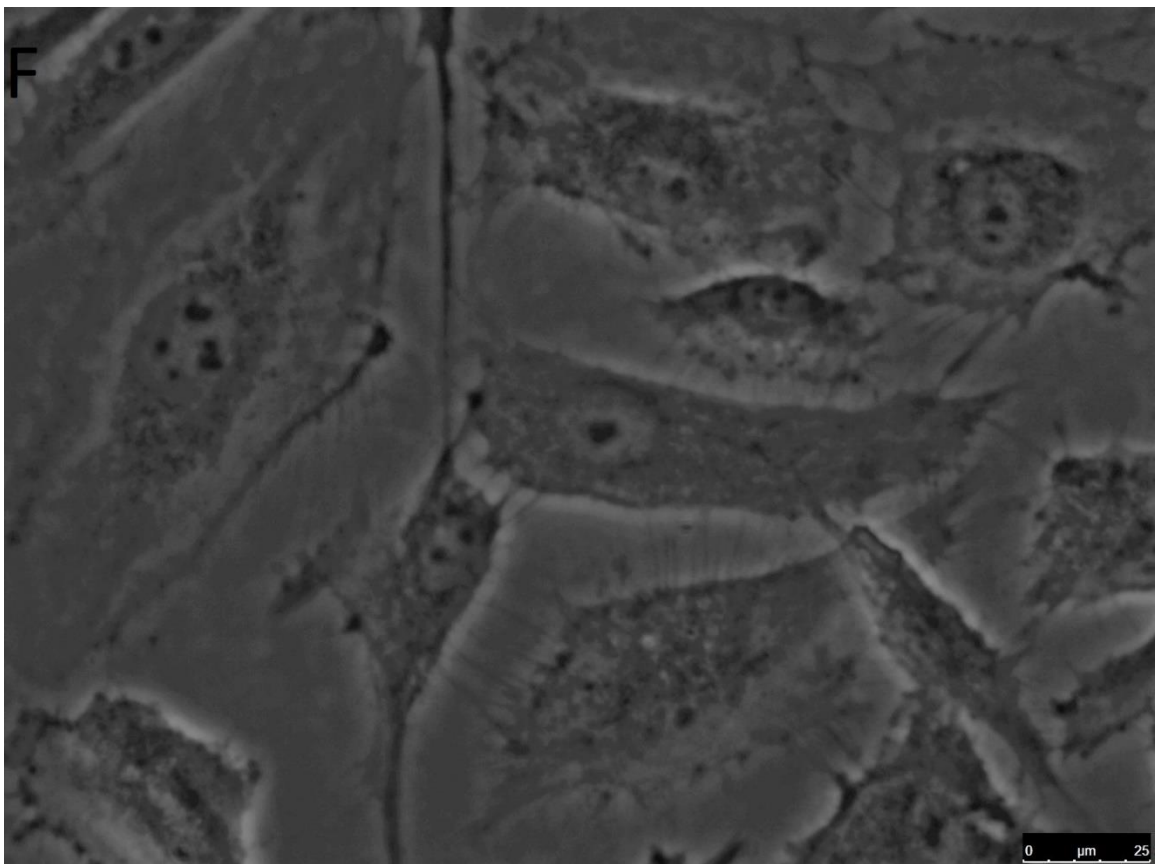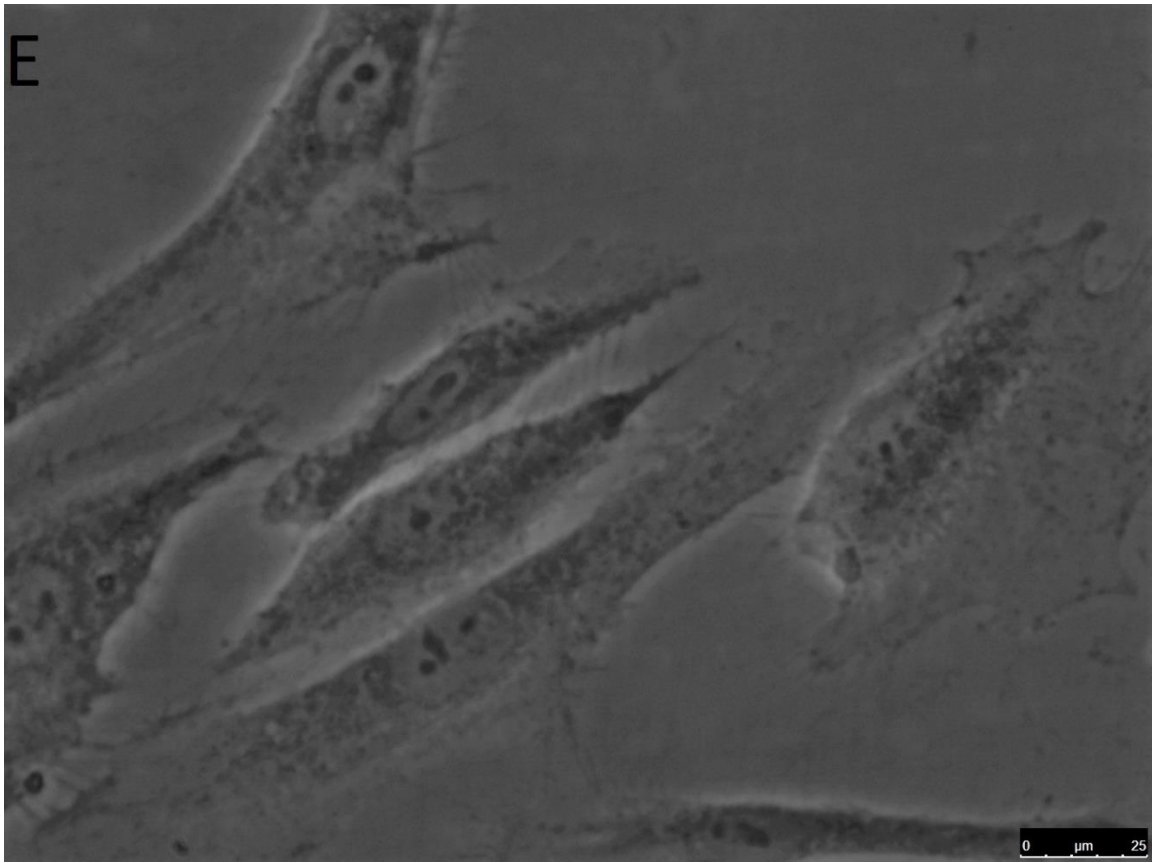
bar 25 μm.

C

D

Images were taken by bright-field phase contrast Leica© microscope scale

bar 25 µm. (Images 1-10 OxLDL treated (50 µg/ml for 6 hours), Cytokine

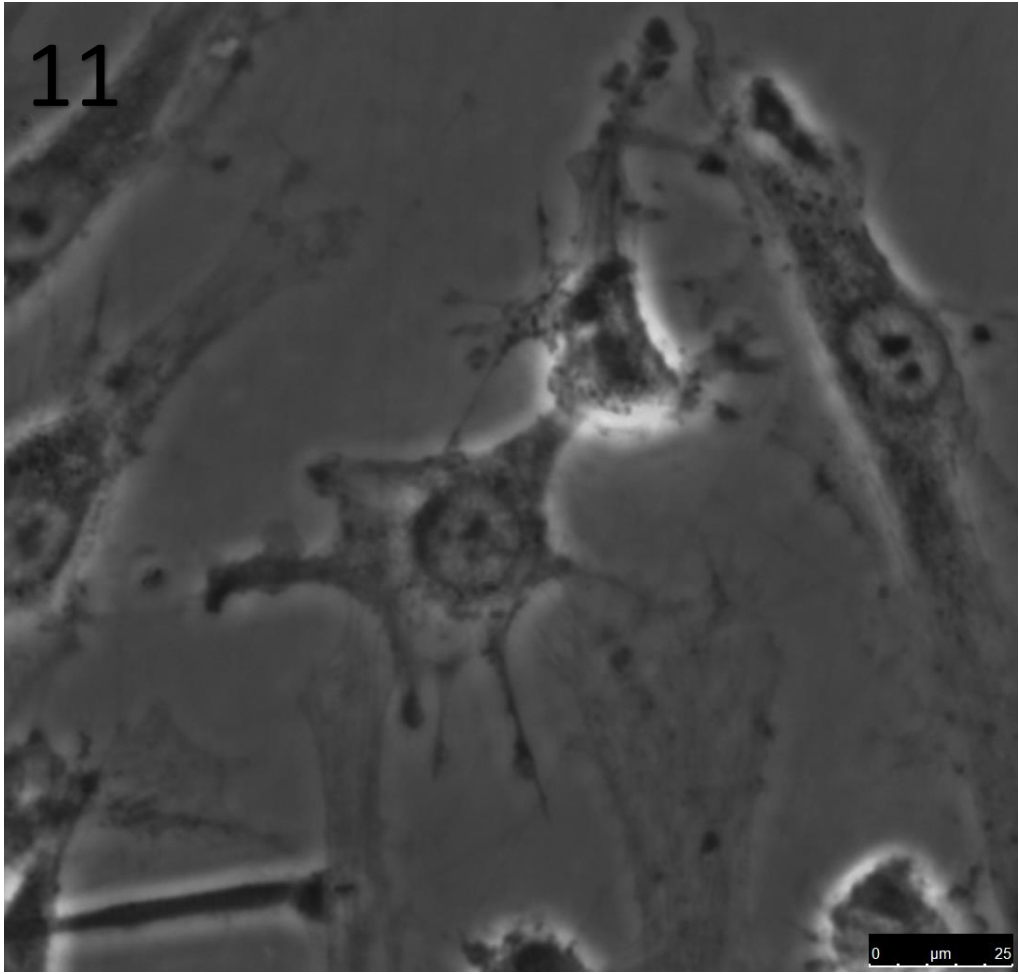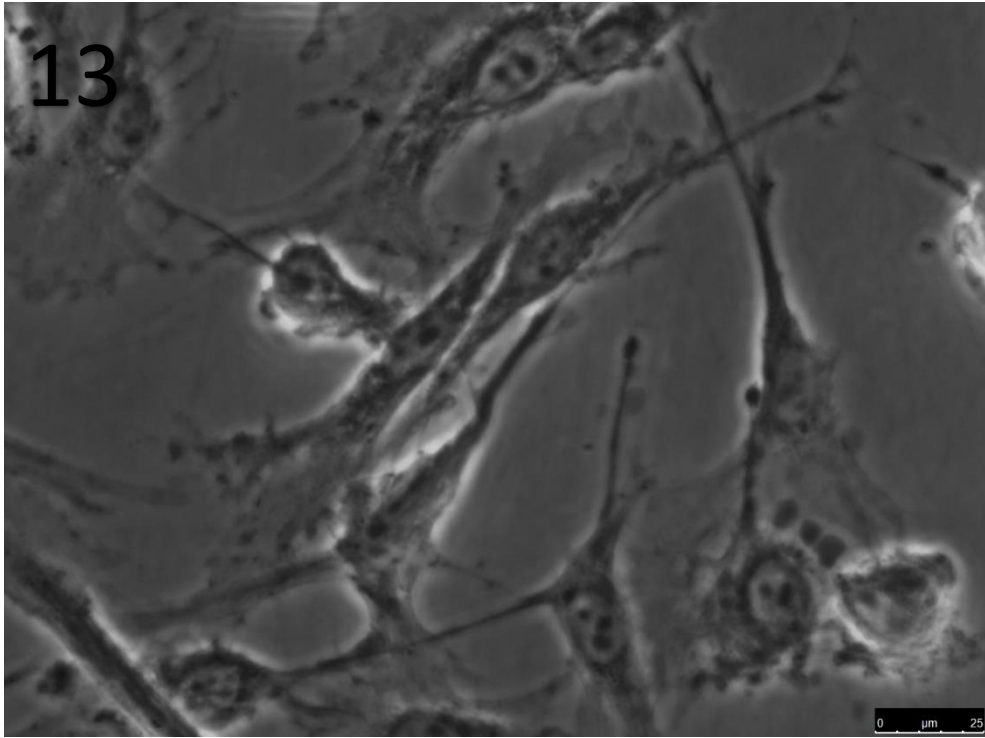stimulated HCAECs. Images 11-13 underwent P2X7 inhibition prior to OxLDL

treatment)

223

5

6

224

225

227
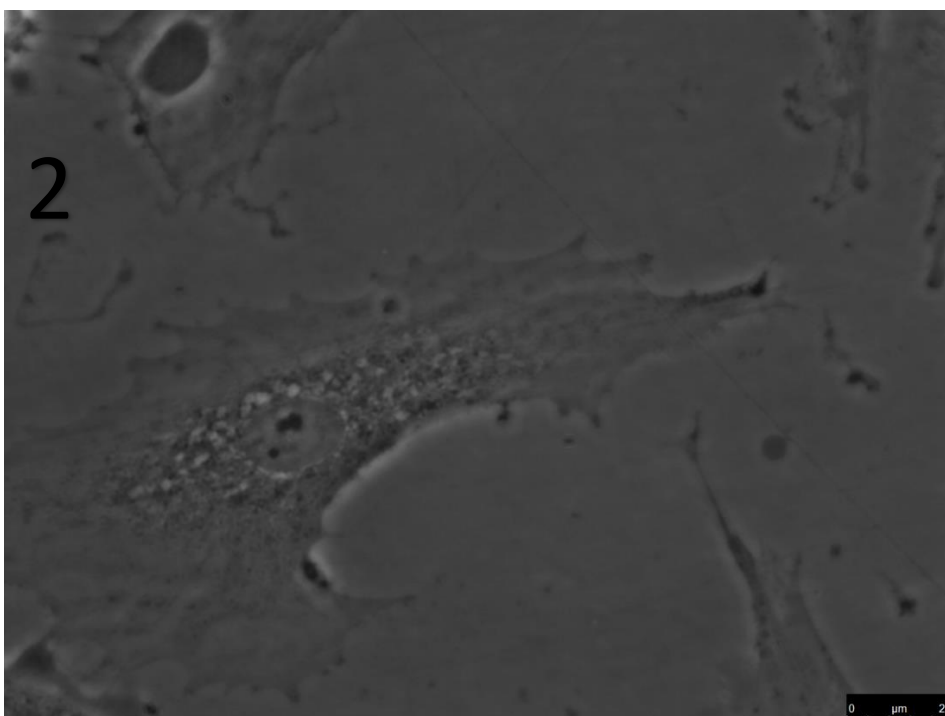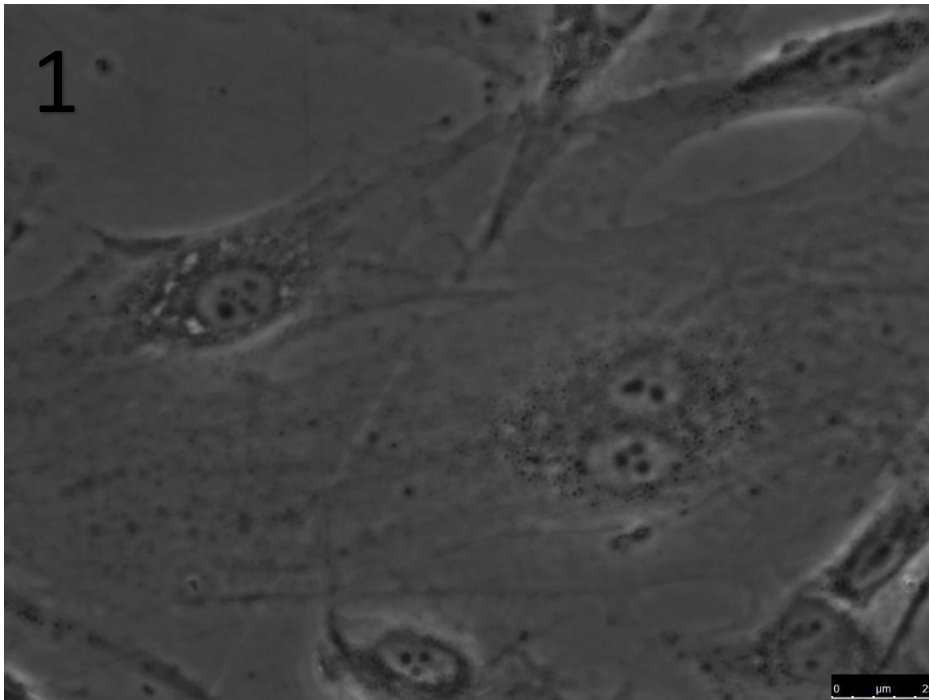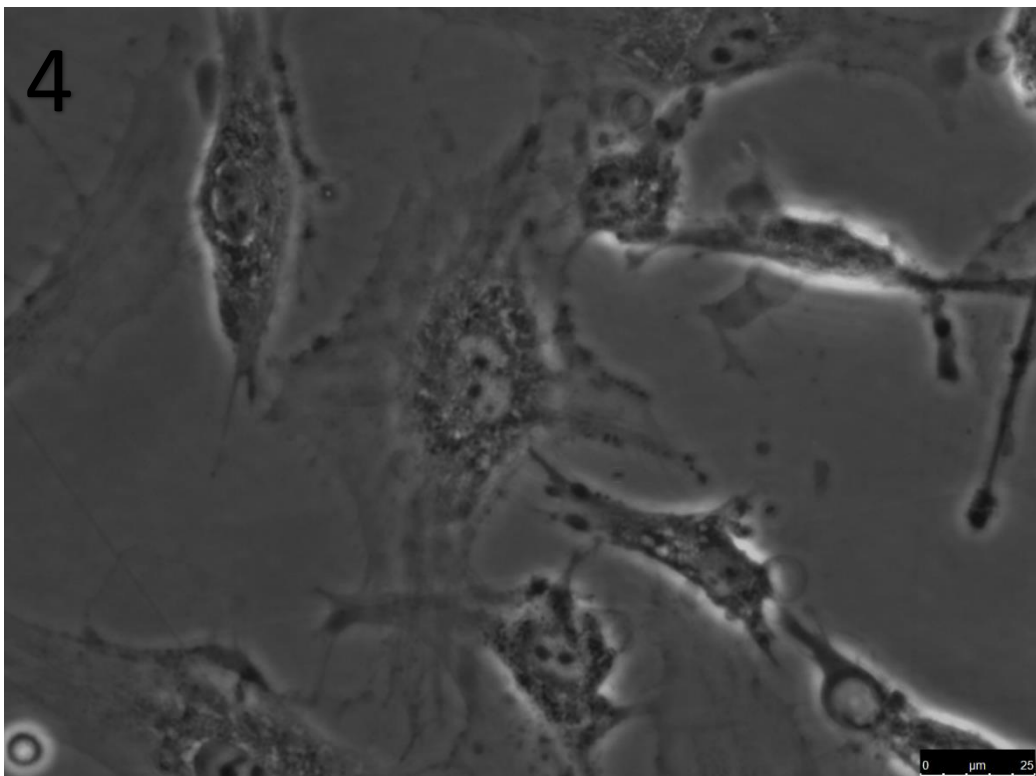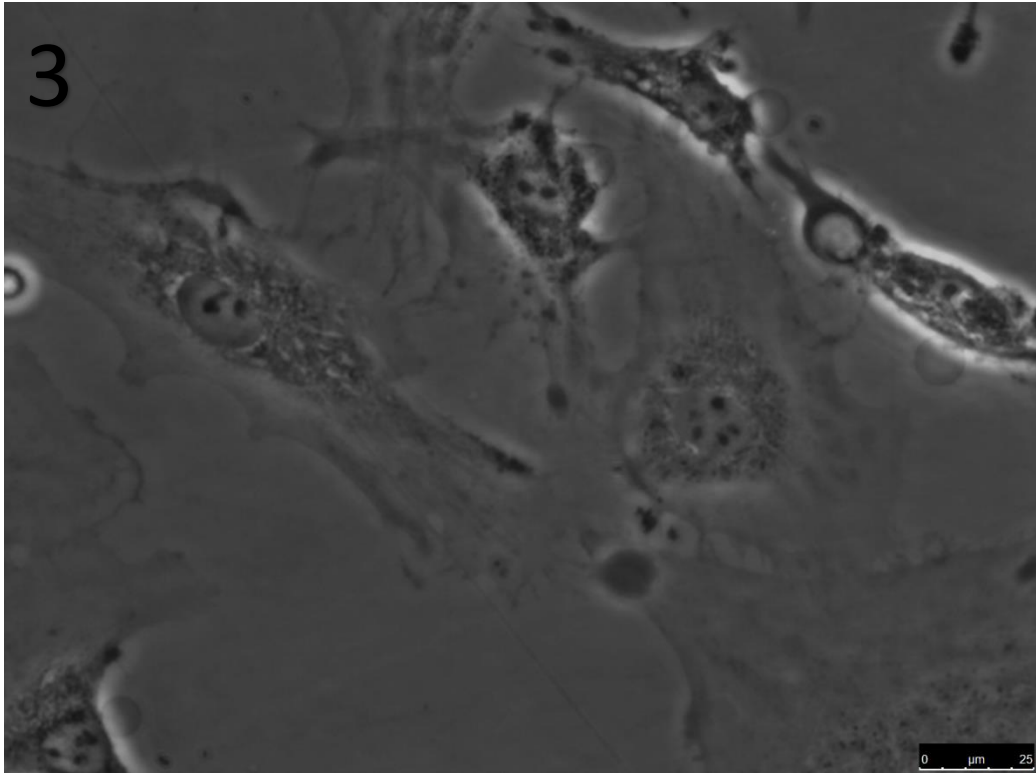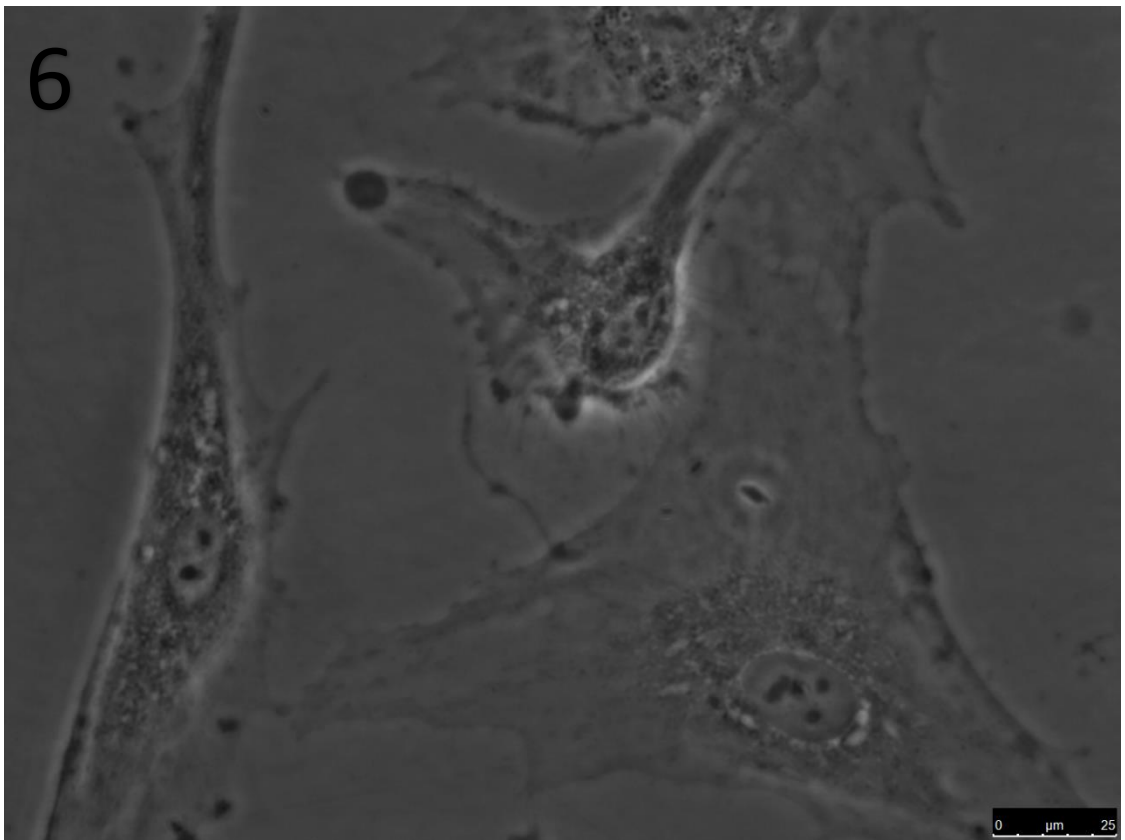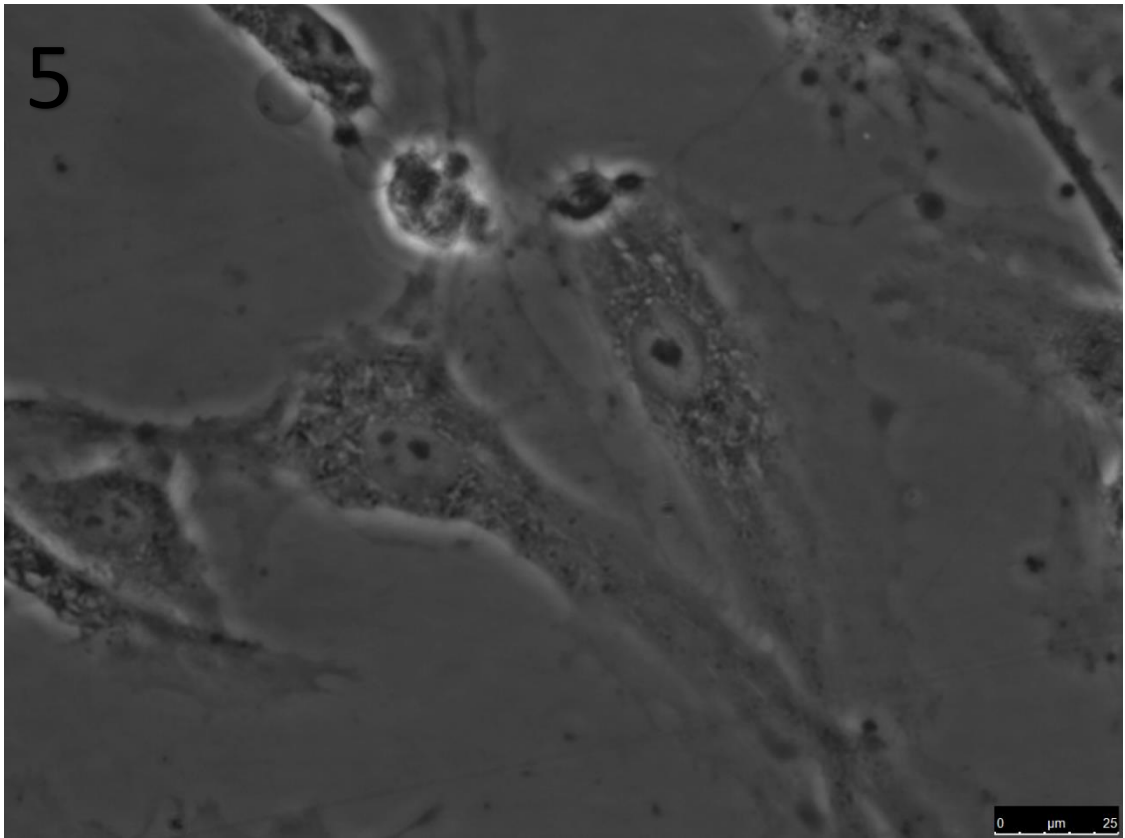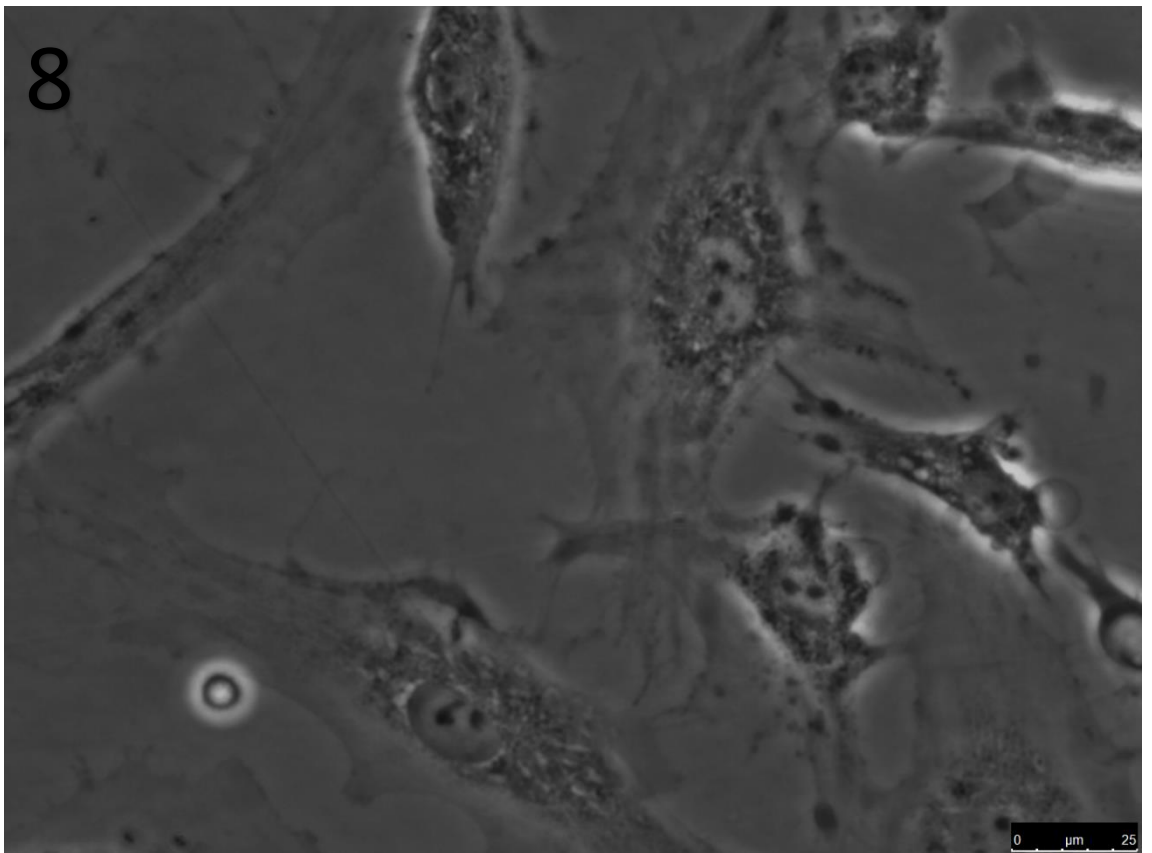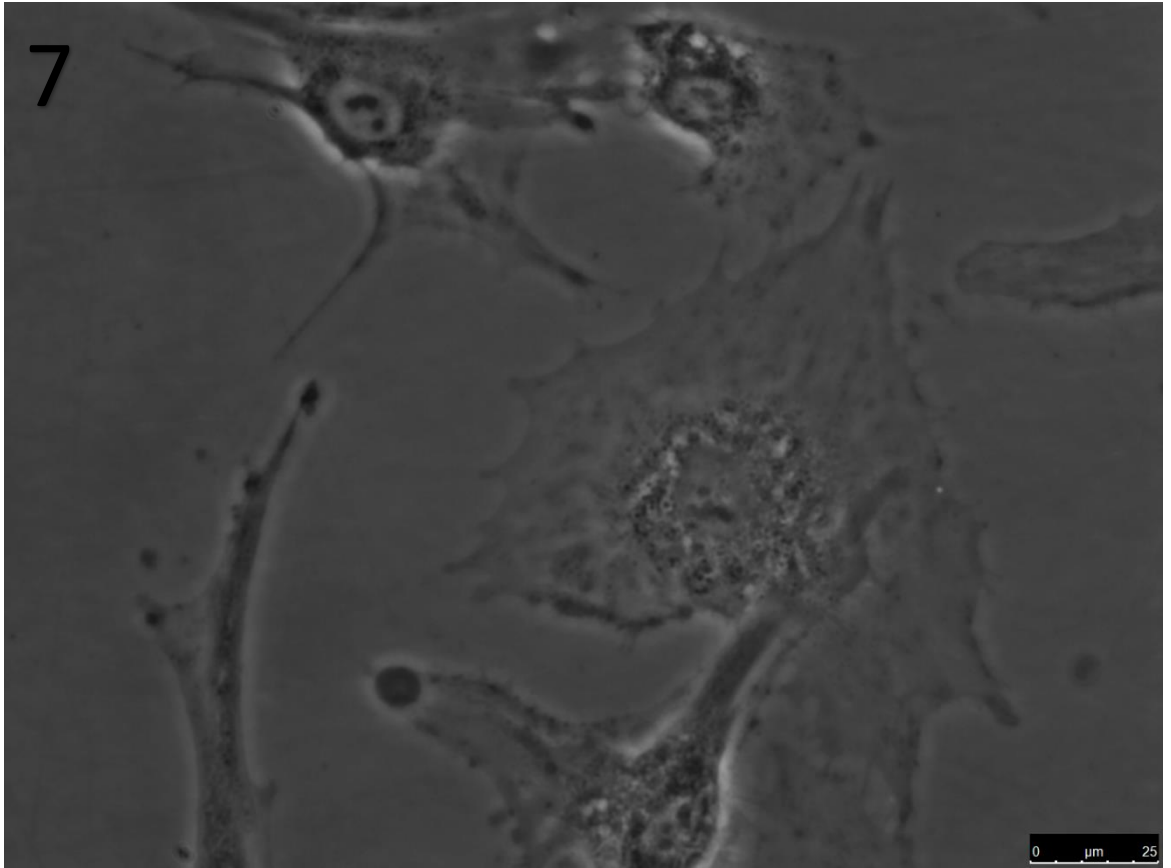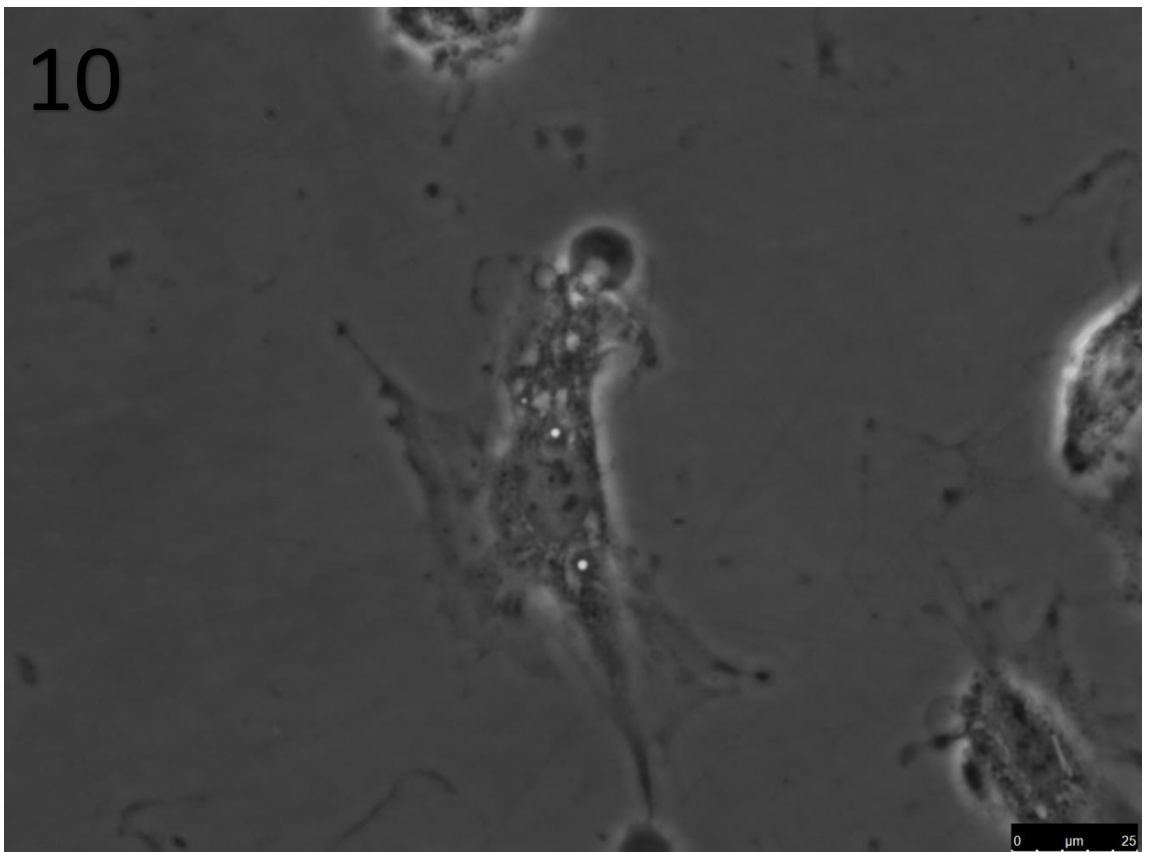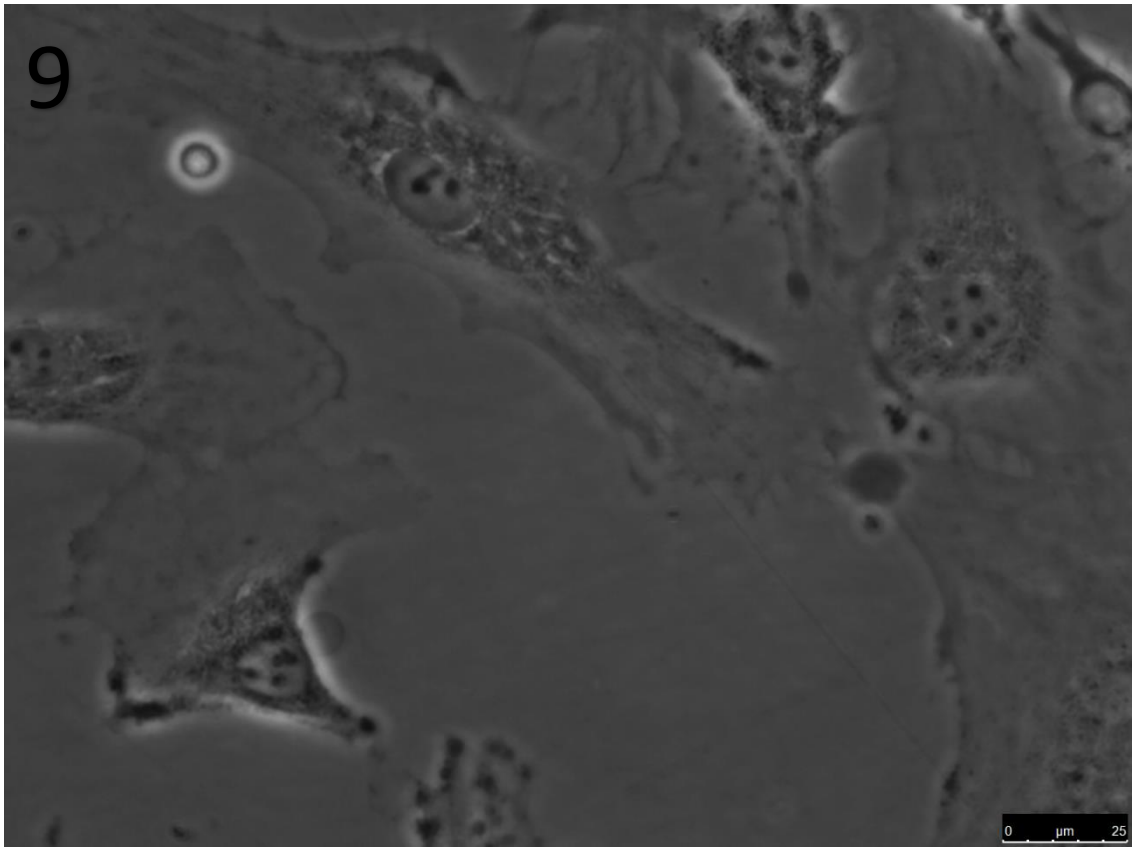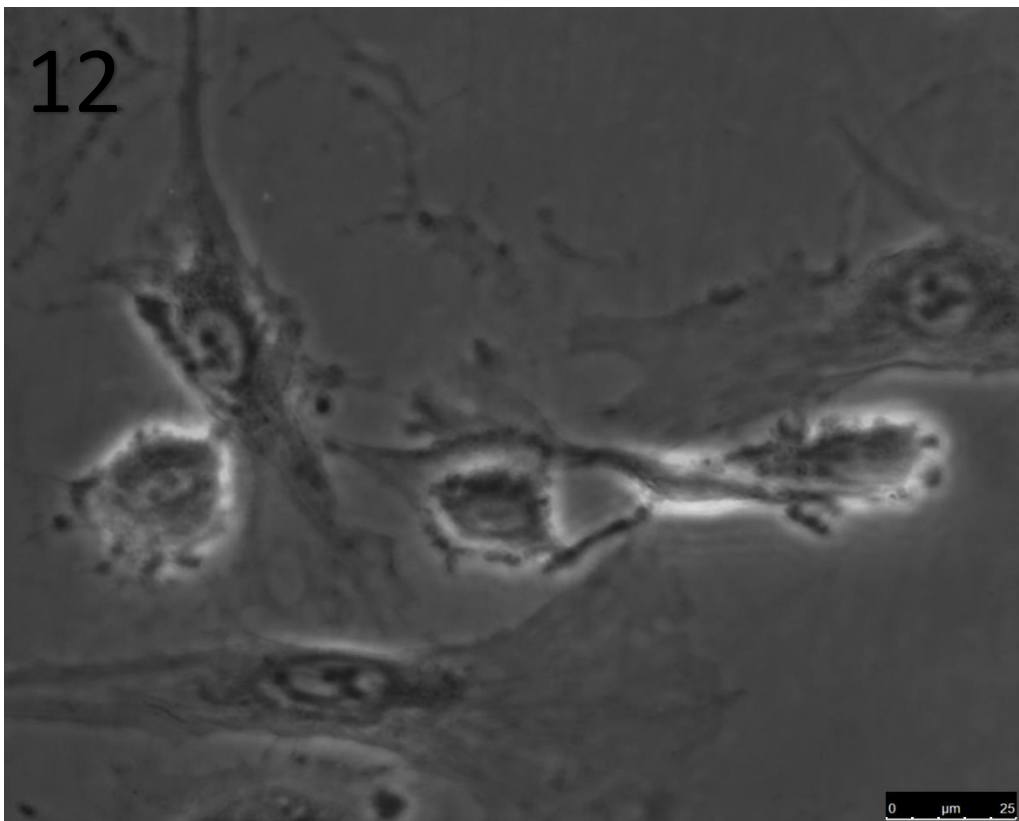
A.4 Appendix (IIII) IL-1β Antibody serial dilution

To further validate ELISA results and to show that primed HCAECs are releasing IL-1β in response to OxLDL treatment. An experiment was conducted to show the detection levels of the IL-1β antibody used (figure 7.1). results showed that the levels of secreted IL-1β fall below the detection limit of the antibody used ((ab33774) from Abcam antibodies), and therefore cannot be measured. However the detection limit of the ELISA is 3.9 pg/ml and quantification using ELISA was relied on through my study.
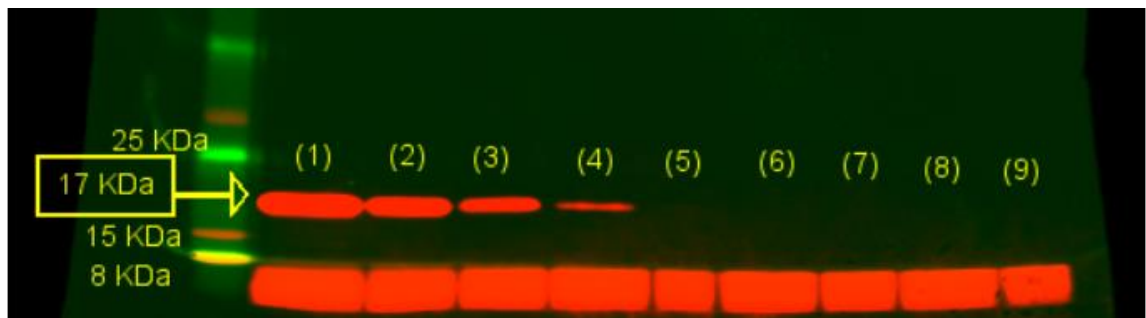
(Figure 7.1) Investigating the detection limit of IL-1β antibody : Western blot analysis of serial dilution performed on recombinant human mature IL-1β. This experiment was done to identify the detection limit of the IL-1β antibody (ab33774). Detectable concentrations: (1) 10 µg/ml (200,000 pg/20 µl), (2) 5 µg/ml (100,000 pg/20 µl), (3) 2.5 µg/ml (50,000 pg/20 µl), (4) 1.25 µg/ml (25,000 pg/20 µl). While undetectable concentrations were samples (5-6); (5) 0.625 µg/ml (12,500 pg/20 µl), (6) 0.3125 µg/ml (6,250 pg/20 µl), (7) 0.15625 µg/ml (3,125 pg/20 µl), (8) 0.0781 µg/ml (1562.5 pg/20 µl) and (9) 0.039 µg/ml (781.25 pg/20 µl). Concentrations in µg/ml and in pg/20 µl were both listed, because each well was loaded with 20 µl volume.

A.5 Appendix (V) NHS permission for the use of umbilical cords for the study of vascular cell research.

Ref: STH15599NO/NT

Sheffield Teaching Hospitals **NHS**

NHS Foundation Trust

18 March 2015

Prof Christopher Newman
Department of Cardiovascular Science
University of Sheffield
Medical School
Beech Hill Road
Sheffield
S10 2RX

Dear Prof Newman,

Change of Investigator

STH ref:	STH15599
NIHR CSP ref:	39601
REC ref:	10/H1308/25
MHRA ref:	CTA no.: N/A EudraCT no.: N/A
Study title:	Umbilical Cords for Vascular Cell Research
Principal Investigator:	Prof Christopher Newman
Sponsor:	STH NHS FT
Funder:	British Heart Foundation
Amendment ref:	New CI/PI – Prof Newman

Thank you for submitting the following documents:

Document	Version/date
Yorkshire & The Humber REC – Favourable ethical opinion	12 Mar 15
Notice of Substantial Amendment	17 Feb 15
Summary CV of Chief Investigator [Prof Christopher Newman]	No date

These have been reviewed by the Research Department who have no objection to the amendment and can confirm continued NHS permission for the study at STH.

Yours sincerely,

Professor S Heller
Director of R&D, Sheffield Teaching Hospitals NHS Foundation Trust
Telephone +44 (0) 114 22 65934
Fax +44 (0) 114 22 65937

CC: Charlotte Culver, Sheffield Teaching Hospital NHS Foundation Trust

In hospital and in the community
proud to make a difference

Chairman: Tony Pedder OBE   Chief Executive: Sir Andrew Cash OBE

Sheffield Hospitals Charity

A.6 Appendix VI full blots of western blot figures presented in chapter 5.

Western Blotting in my project was challenging considering the experimental setting and the nature of the cells and its low protein levels, as addressed in this thesis and as shown by the previous demonstration in Appendix (IIII). Original (unedited) blots of all western blot representative figures in chapter 5 are shown in this appendix to add further clarification to the bands shown in each figure.
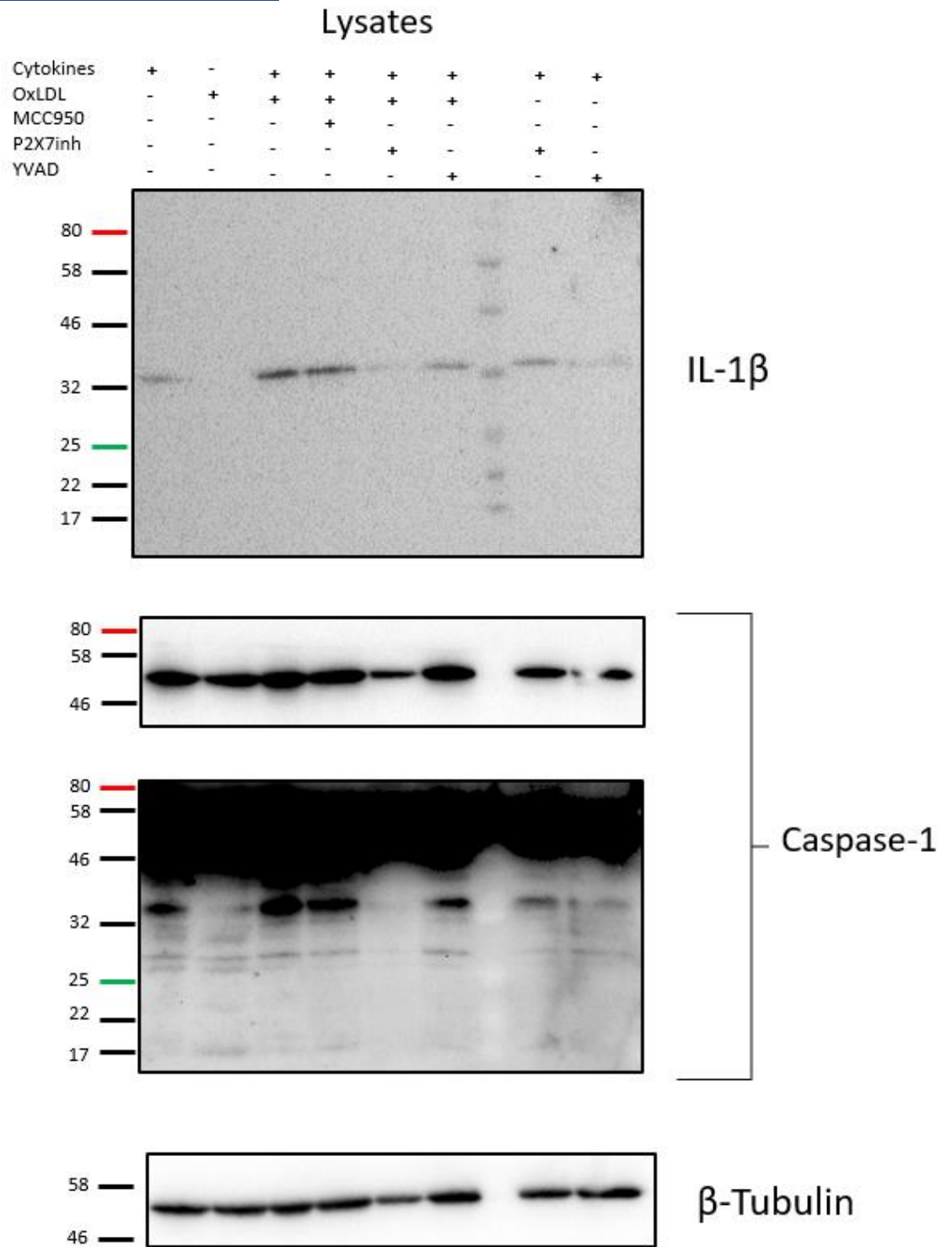
A.6.1 Full Blot of (Figure 5.2)
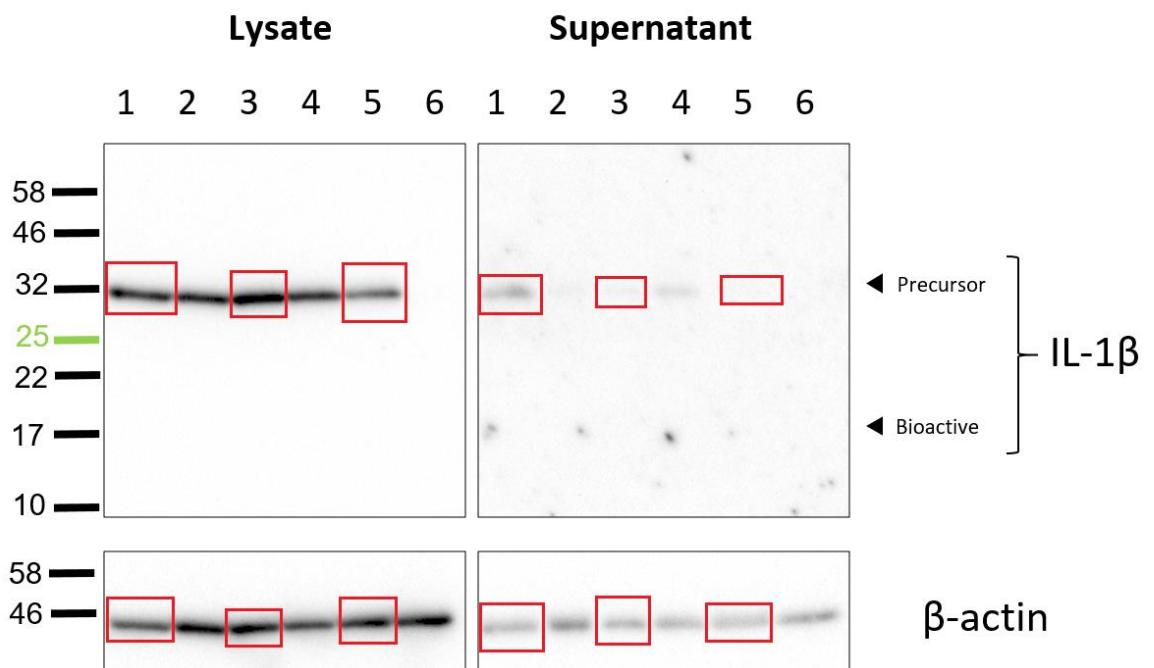
The bands used in the representative blot in (figure 5.2) are highlighted in red boxes. In this blot, all samples are HCAECs stimulated with the cytokine combination of TNFα and IL-1α (10 ng/ml each, for 48 hours) in different treatment conditions as follows:

1- + OxLDL + YVAD
2- + OxLDL + YVAD
3- + OxLDL
4- + AcLDL +YVAD
5- + YVAD
6- None (Stimulation only control)

231

A.6.2 Full blot of (figure 5.6)

A.6.3 Full blots used in the presentation of (figure 5.8)
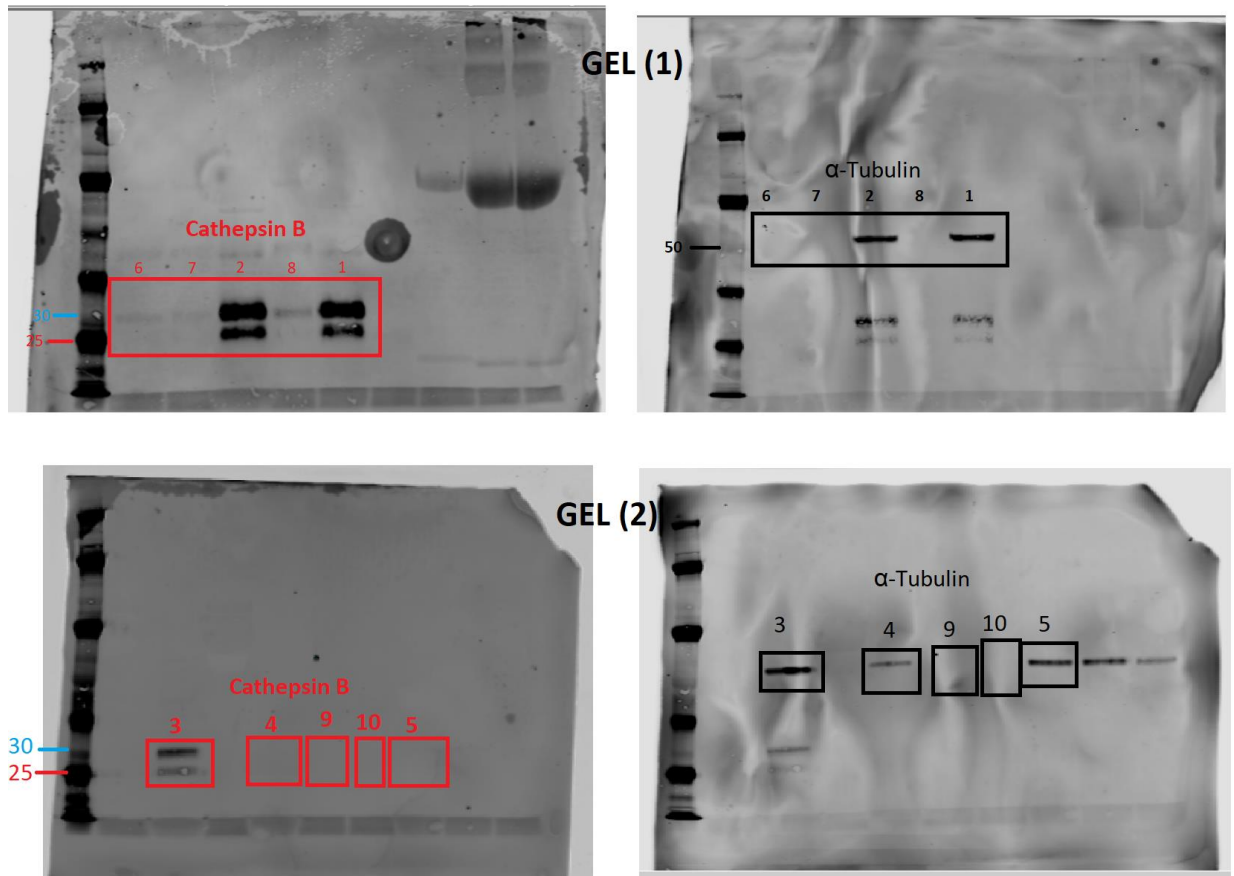
Samples are for HCAECs in the following conditions:

+Cytokine +OxLDL +YVAD (Lysate 1, Supernatant 6)

+Cytokine +OxLDL +MCC950 (Lysate 2, Supernatant 7)

+Cytokine +OxLDL (Lysate 3, Supernatant 8)

+Cytokine (Lysate 4, Supernatant 9)

+Cytokine +NE (Lysate 5, Supernatant 10)